CORROSION SCIENCE

An International Journal of the Science of Corrosion and Protection of Metals published under the auspices of the Corrosion Science Society and the Centre Belge d'Etude de la Corrosion

VOLUME 1, 1961

PERGAMON PRESS

LONDON . NEW YORK . PARIS . LOS ANGELES

CORROSION SCIENCE

An International Journal of the Science of Corrosion and Protection of Metals published under the auspices of the Corrosion Science Society and the Centre Belge d'Etude de la Corrosion

Publishing Offices: Headington Hill Hall, Oxford

Annual Subscription (including postage):

(A) For libraries, government establishments and research institutions £10 ($30.00).
(B) For individuals who write directly to the publisher certifying that the journal is for their personal use £3 10s. ($10.00).

PERGAMON PRESS LTD

4 & 5 FITZROY SQUARE, LONDON, W.1 122 EAST 55TH STREET, NEW YORK 22, N.Y

VOLUME I

NUMBER 1/2

AUTHOR INDEX TO VOLUME I

BLANK
PAGE

Corrosion Science, 1961, Vol. 1, p. 1. Pergamon Press Ltd. Printed in Great Britain

EDITORIAL NOTICE

CORROSION SCIENCE is an international journal and will contain original papers, short notes and critical reviews on every aspect of corrosion science. A discussion section will be included in the final issue of each volume and readers are invited to forward constructive comments and criticisms of papers to any of the Editors. It is published by the Pergamon Press Ltd. under the auspices of the Corrosion Science Society and the Centre Belge de l'Etude de la Corrosion, with the assistance of an international editorial board.

Papers in the field of corrosion science, including of course the science of all kinds of protective measures, may be submitted from any source, the sole criteria of suitability for publication being the quality and originality of their scientific content. Contributors can greatly assist the editors by submitting only papers prepared according to the Guide to Authors printed elsewhere in this issue; this will lighten editorial labour and allow rapid and efficient publication.

Chemical, metallurgical and engineering journals in many countries publish papers on corrosion; there are also several national publications dealing solely with corrosion and protection topics. Corrosion knowledge has thereby become widely diffused, and also—less happily—extremely diluted. We hope that the new international Journal will form a link between corrosion scientists the world over, and will come to provide each of them with a selection of the most interesting papers from the world's corrosion laboratories in concentrated form.

Corrosion Science, 1961, Vol. 1, pp. 2–20. Pergamon Press Ltd. Printed in Great Britain

THE DEVELOPMENT OF STRESS-CORROSION CRACKS IN AUSTENITIC Cr–Ni STEELS*

J. G. HINES
Imperial Chemical Industries, Billingham, Co. Durham, England

Abstract—Direct-loaded axially stressed specimens (0·160–0·635 cm dia.) of a variety of austenitic Cr–Ni steels were exposed to boiling 42 per cent $MgCl_2$ solution. The progress of cracking was followed by potential measurements and by removing specimens for examination after suitable periods of exposure. The results are comparable with those earlier obtained on 0·051 cm dia. specimens.

The life of a specimen can be divided into an induction period and a period of crack propagation; the latter consists of two stages. The cracks remain fine during the first stage, during which no change in potential can be detected; this stage is relatively more important the larger the specimen and the lower the applied stress, and so was not recognized previously. The cracks open up and become branched during the second stage, which is accompanied by a fall in potential. The relative duration of the induction period and the total period of crack propagation varies considerably with the experimental conditions, particularly the size and form of the specimen and the mode of stressing, but for fully softened axially-stressed cylindrical specimens the ratio of these periods is constant for a given specimen diameter. The practical significance of these observations is discussed briefly.

Sufficient corrosion current is available to account for crack-formation by purely electrochemical processes.

Résumé—On a exposé à une solution bouillante à 42 pourcent de $MgCl_2$, des échantillons de différents aciers austénitiques au chromenickel (diamètres 0,160 à 0,635 cm) et qui se trouvaient sous charge directe et sous pression axiale. La progression des fissures fut suivie par des mesures du potentiel et en retirant et examinant des échantillons après des temps d'exposition appropriés. Les résultats sont comparables à ceux obtenus ailleurs avec des échantillons de 0,051 cm de diamètre.

La vie d'un échantillon peut être divisée en une période d'induction et en une période de propagation des fissures. Celle-ci se compose de deux stades. Pendant le premier stade, les fissures restent minces; aucun changement de potentiel n'est décelable. Ce stade est, relativement, d'autant plus important que l'énchantillon est plus grand et la charge appliquée plus basse, ce qu'on n'avait pas reconnu autrefois. Pendant le deuxième stade, les fissures s'ouvrent et se ramifient, ce qui va de pair avec une chute du potentiel. La durée relative de la période d'induction et la période totale de la propagation des fissures présentent des variations considérables, en fonction des conditions d'essai, surtout de la grandeur et de la forme de l'échantillon ainsi que du mode de la charge; cependant, pour des échantillons cylindriques, complètement adoucis et sous charge axiale, la relation existant entre ces deux périodes est constante pour un diamètre donné de l'échantillon. L'importance pratique de ces observations est décrite succinctement.

Il y a un courant de corrosion suffisant qui permet d'expliquer la formation de fissures par des procédés purement électrochimiques.

Zusammenfassung—Direkt beanspruchte und unter Normalspannung stehende Proben von verschiedenen austenitischen Chromnickel-Stählen (Durchmesser 0,160–0,635 cm) werden einer kochenden, 42 Prozent-igen MgCl-Lösung ausgesetzt. Um den Ablauf des Reisvorganges zu verfolgen, wurden Potentialmessungen vorgenommen und einzelne Proben nach bestimmten Zeiten zur Untersuchung entnommen. Dir Ergebnisse sind mit den Resultaten vergleichbar, die früher an Proben zu 0,051 cm Durchmesser erzielt werden konnten.

Die Lebensdauer einer Probe lässt sich in eine Induktions-periode und in eine Periode der Rissfortpflanzung einteilen. Letztere besteht aus zwei Stadien. Während des ersten Stadiums bleiben die Risse fein, und eine Potentialänderung ist nicht festzustellen. Dieses Stadium ist relativ umso bedeutender, je grösser die Probe und je niedriger die angewendete Belastung, was früher nicht erkannt wurde. Während des zweite Stadiums, welches mit einem Potentialabfall einhergeht, öffnen sich die Risse und verzweigen sich. Die relative Dauer der Induktions-Periode und die Gesamtperiode der Rissfortpflanzung schwanken in weiten Grenzen, und zwar in Abhängigkeit von den Versuchsbedingungen, besonders aber in Abhängigkeit von Grösse und Form der Probe und von der Art der Belastung. Für vollenthärtete, axial belastete zylindrische Proben ist das Verhältnis zwischen diesen Perioden für einen gegebenen Durchmesser allerdings konstant. Dir praktische Bedeutung dieser Beobachtung wird kurz besprochen.

Es ist ein ausreichender Korrosionsstrom vorhanden, sodass Rissbildung rein durch elektrochemische Vorgänge denkbar ist.

*Manuscript received 5 October 1960.

INTRODUCTION

HOAR and Hines[1] divided the life of 0·051 cm dia. specimens of austenitic Cr–Ni steels direct-loaded in axial tension in hot concentrated chloride solutions into an induction period and a period of crack propagation. The latter was accompanied by a continual fall in potential and by accelerating extension of the specimen, and occupied only the final few minutes before fracture. The specimens used were small; other authors reported that cracks were present for much longer periods when larger specimens were used,[2, 3] but as the test conditions, in particular the mode of stressing, were very different from those used by Hoar and Hines it was not clear to what extent the difference in behaviour was due to specimen size.

Experiments have now been carried out on four further sizes of specimen (0·160, 0·320, 0·400 and 0·635 cm dia.) under conditions similar to those used on 0·051 cm dia. specimens. Some metallographic observations on the development of cracks in these specimens have been published elsewhere.[4]

EXPERIMENTAL DETAILS

The apparatus was essentially similar to that used previously[1, 5] except for modifications necessary to allow larger specimens to be handled and for recording corrosion potentials and/or external currents. The wire specimen is loaded by a lever system, and passes concentrically through the test cell and a reflux condenser; above the liquid level it is protected by a nitrogen sheath. A side tube leads to an Ag/AgCl/N NaCl reference electrode. The potentials here recorded were obtained by adding 250 mV to the experimental values; this converts them approximately to the hydrogen scale.[1]

Batches of specimens were cut from stock as required, straightened where necessary by straining *circa* 1 per cent in tension, and fully softened by heating in argon for 15 min at 1040–1060°C and quenching in water. They were then pickled, left in a desiccator for several days to allow a reproducible oxide film to develop,[6] and degreased in methanol and acetone immediately before testing. Some specimens were tested after being deformed plastically by straining in tension. This was done before pickling.

Most of the experiments described in this paper were carried out on 0·320 cm dia. specimens of an 18–8–Ti steel (steel H as used in other work[7]). A few experiments were made on 0·635 cm dia. specimens of the same alloy, and similar experiments have been carried out on other alloys using specimens of all four sizes. The results obtained were all consistent with those reported.

All of the experiments described were carried out in boiling (150–154°C) aqueous magnesium chloride solution (nominally 42% $MgCl_2$) made up from "pure crystals" of the hexahydrate and distilled water.

RESULTS AND INTERPRETATION

The effects of applied stress and plastic deformation

Regression analysis of data obtained on a variety of alloys tested after a number of thermal or mechanical treatments shows that the relation between applied stress, S, and time to fracture, t_f, is best represented by two straight-line plots of log t_f upon S intersecting at the 0·1 per cent proof stress measured at room temperature on similar

specimens.[7] This is also true of the data obtained previously on smaller specimens, although in the original papers the intersections were usually taken at a stress below the proof stress. However, the fit is never significantly worse, and is frequently better, if the lines are constrained to meet at the proof stress. This choice of the position of the intersection is convenient, and, as will be shown, it is less arbitrary than may first appear. Scheil[8] has also reported a linear relation between log t_f and S below the 0·1 per cent proof stress.

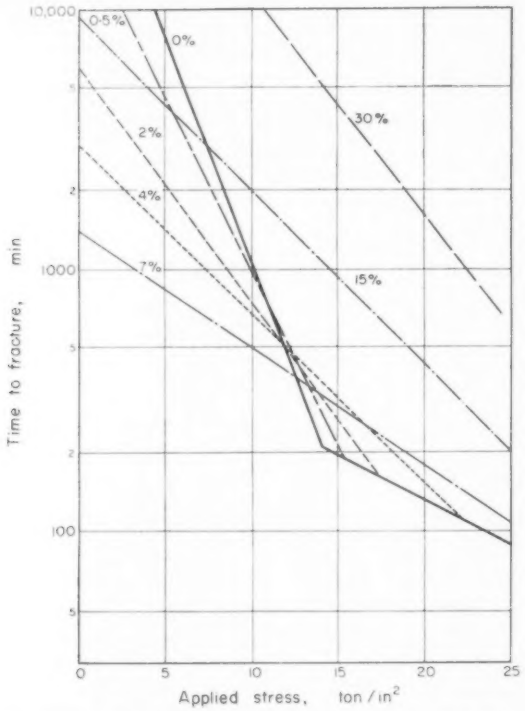

FIG. 1(a). Variation of time to fracture t_f with applied stress.
0·320 cm dia. specimens of steel H, fully softened or after various previous plastic deformations (0·5, 2, 4, 7, 15 and 30 per cent strain).

Fig. 1(a) shows a typical set of log t_f/S curves (obtained on 0·320 cm dia. specimens of steel H). For fully softened specimens the slope of the regression line at stresses below the proof stress is much larger than that at higher stress, but the slope of the lower stress line is reduced by plastic deformation involving strains of 0·5 per cent or more and passes through a minimum at about 8 per cent strain. Above the relevant proof stresses the data for fully softened and for plastically deformed specimens lie on the same line. This is not surprising, as there is no reason to suppose that plastic deformation at the test temperature (150°C) has effects different from those of deformation nominally at room temperature. The slope of this line is independent of composition,[7] whereas that of the lower stress line depends on composition as well

as on the amount of plastic strain. However, for a given strain the ratio of the slopes of the lower stress lines for plastically deformed and for fully softened specimens appears to be independent of composition (Fig. 1(b)).

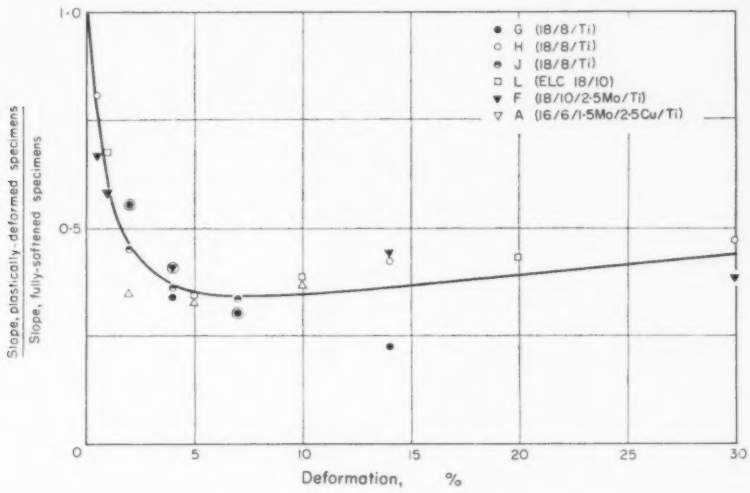

FIG. 1(b). Variation with the amount of plastic deformation of the ratio of the slopes of the log t_f/S lines below the proof stresses for plastically deformed and fully-softened specimens. Steels G and J are 18–8–Ti steels, L is an ELC 18–10 steel, F an 18–10–2·5 Mo–Ti steel and A a 16–6–1·5 Mo–2·5 Cu steel. Their analyses are given elsewhere.[7]

In a previous paper, stress-corrosion cracks in axially stressed cylindrical specimens were divided into two types; fine cracks that penetrate to a limiting depth and then spread sideways, and deeper, branched, open cracks that develop from the largest fine cracks.[4] The number of open cracks formed varies little with the experimental conditions, five to fifteen such cracks being usual. They are almost invariably confined to the immediate vicinity of the fracture, although isolated open cracks are occasionally formed at high stresses. The number and distribution of fine cracks, on the other hand, varies considerably. On fully softened specimens tested below the 0·1 per cent proof stress thirty to fifty such cracks are usually present, confined to a region 2–3 cm long which includes the point of final fracture; very occasionally groups of cracks are present elsewhere. In specimens deformed plastically before or during the test fine cracks are much more numerous and are distributed over the whole exposed length (*circa* 18 cm). The density of cracking is similar to that in the vicinity of the fracture on fully softened specimens. On both classes of specimen the number of fine cracks formed varies little with applied stress, except that at stresses below 5 ton/in^2 the number falls off somewhat; at these very low stresses the number of open cracks formed may also be unusually small, while at stresses above 25 ton/in^2 more open cracks than usual may form.

The major effect of plastic deformation appears to be to increase the number of fine cracks formed, presumably by increasing the number of sites from which cracks

can be initiated.[1, 9] It might be expected that the effect of stress on t_f would be less marked when such sites are plentiful than when they are relatively rare; this effect would explain both the change in slope of the log t_f/S curve for fully-softened specimens, and the effect of plastic deformation on the slope of the lower stress part of the line. Moreover, yielding at the crack tip is probably essential for crack propagation.[1, 3, 5, 9] More corrosion should therefore be necessary for localized yielding to begin at stresses below the proof stress than at higher stresses, so that a change of slope in the vicinity of the yield point would be expected even on plastically deformed specimens. A proof stress in an austenitic Cr–Ni steel does not correspond to a definite change in the behaviour of the material (unlike, for example, the yield point of annealed mild steel). However, the 0·1 per cent proof stress measured at room temperature corresponds to 0·3–0·4 per cent strain at 150°C and the effects of plastic deformation on the number of cracks formed and on the slope of the lower stress log t_f/S line become detectable at plastic strains between 0·2 per cent and 0·5 per cent. The choice of the 0·1 per cent proof stress as the position of the intersection is thus reasonable for fully softened specimens. It cannot be justified in this way for plastically deformed specimens, but in this case the change of slope is small.

Specimen size has little effect on the form of the log t_f/S curves or on the number of cracks produced. An increase in specimen size increases t_f at any stress, but the increase is small on specimens of diameter greater than 0·160 cm. The number and size of fine cracks formed increases somewhat with specimen size, but the density of cracking decreases; it appears that the total length of crack formed on unit area is

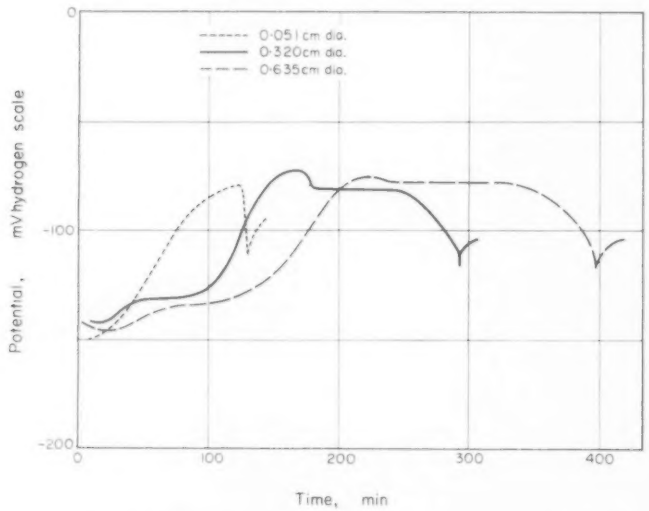

FIG. 2. Typical potential/time curves on 18–8–Ti steels at stresses near the 0·1 per cent proof stress.

0·051 cm dia. steel 18–8–Ti (b)[1]	12·1 ton/in.²
0·320 cm dia. steel H,	12·3 ton/in.²
0·635 cm dia. steel H,	12·0 ton/in.²

(The curves have been selected so that they are reasonably separated, and the apparent trend for the initial rise to be faster the smaller the specimen is not real.)

independent of specimen size. The 0·051 cm dia. specimens examined by Hoar and Hines were, however, unusual in that most of the cracks formed were open cracks, and that the time to fracture at a given stress was appreciably shorter than on larger specimens.

Potential/time curves

In the earlier work the progress of cracking was followed by observing the variation of corrosion potential with time and/or the variation of extension rate with time. The former was the more informative, as it also allowed study of the processes which precede the formation of cracks. Only a few extension measurements were made in the present work; these will not be described in detail as they yielded little information that was not obtained in other ways.

The potential/time curves (Fig. 2) obtained were very similar to those reported previously.[1, 5] They show the potential rise and fall which has been associated with a period of film-repair followed by localized film-breakdown and the onset of pitting,[10] and also a smooth continuous fall in potential before fracture. The duration of the final potential fall increases with specimen size (Fig. 3), but the increase is less than

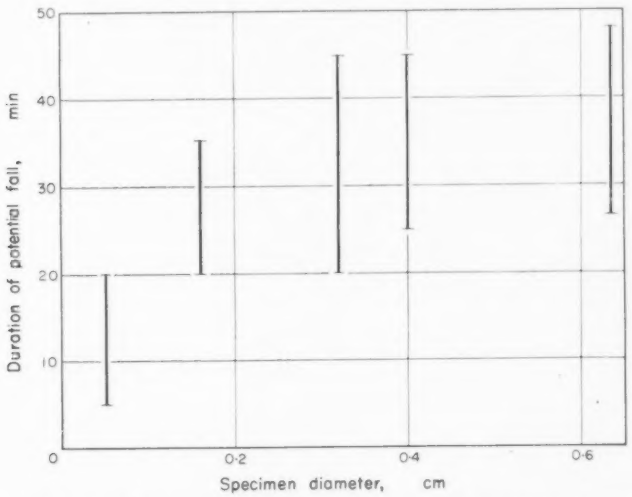

FIG. 3. Variation of the duration of the final potential fall with specimen size. The ranges indicated are the overall ranges obtained in all experiments on specimens of the size in question; replicate experiments give smaller ranges.

would be expected if cracks were present only during this stage and if the rate of propagation were independent of specimen size. The potential fall also begins at a later stage in the potential/time curve the larger the specimen. At stresses near the proof stress it began on 0·051 cm dia. specimens as soon as, if not before, the slight fall in potential associated with film-breakdown, whereas on similarly stressed 0·320 and 0·635 cm dia. specimens it is delayed for $\frac{1}{2}$–1 h and 1–2 h respectively.

The extension/time curves were also similar to those obtained previously. Slow creep at a decreasing rate occurred during the early stages, particularly at stresses

near or above the proof stress, and accelerating extension occurred during the period of the final potential fall. No change in extension rate could be detected before the start of the final potential fall.

The relation between the potential/time curves and the progress of cracking was studied by removing unbroken specimens from the apparatus after various periods of exposure. The specimens were washed, dried and broken in a tensile testing machine. The majority of the specimens removed before the start of the potential fall showed no sign of cracks under a low power microscope, and gave mechanical properties within the range of the control specimens. The remainder contained fine cracks (not always detected before they were opened-up during the tensile test) and had suffered some deterioration in properties. The deterioration and size of the biggest crack was greater the larger the number of cracks, showing that new cracks are formed as the original ones develop. The specimens removed after the start of the final potential fall contained open cracks, clearly visible before the tensile test, and their mechanical properties were greatly impaired.

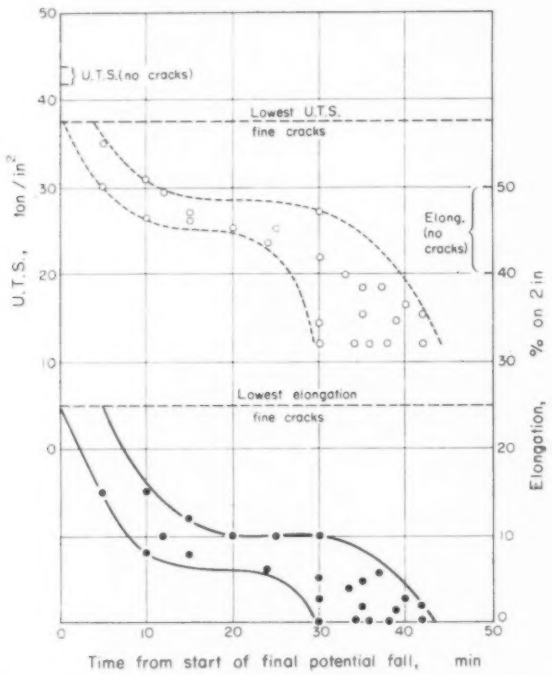

FIG. 4. Effect of exposure to stress-corrosion conditions on mechanical properties. Fully softened 0·320 cm dia. specimens of steel H tested at 12·3 ton/in.²

Fig. 4 shows data obtained in interrupted tests on sixty-two fully softened specimens heat treated as a single batch and tested at 12·3 ton/in². Very similar results were obtained on other smaller batches of fully-softened specimens tested at other stresses, and on batches of plastically deformed specimens. The size of the largest

crack was greater the lower the applied stress, and the appearance of open cracks after the tensile test was very similar to that of open cracks on undeformed specimens. These observations confirm that open cracks are formed from fine cracks when extensive yielding begins around the tip.

In the main experiments the potential difference measured was that between the 20 cm long specimen and the mouth of a side tube 2 cm away from it. This arrangement cannot be sensitive to small changes in corrosion current at points remote from the side tube. Experiments were therefore carried out in which four or more probes, 0·5 cm apart, were placed close to the surface of an 0·400 cm dia. specimen in a region 5 cm long which had been ground down to 0·320 cm dia. before softening. The probes were staggered round the specimen to minimize shielding. Cracking was confined to the immediate vicinity of the probes, but in no case was there any indication of a change in potential until the start of the final potential fall, at which stage open cracks could be seen. The curves obtained from the various probes and from the usual side tube were almost identical. It must be concluded that the formation of fine cracks is not associated with a change in potential greater than the limit of measurement, and that the use of a probe is an unnecessary refinement.

Evidently, the life of a specimen can be divided into an induction period and a period of crack-propagation, just as on smaller specimens,[1] but the period of crack-propagation itself consists of two stages which correspond to the stages of crack-development distinguished by examination of cracks.[4] Fine cracks are formed before a detectable change in potential or extension rate occurs, and the final potential fall corresponds to the second stage. This fall is clearly associated with a considerable increase in corrosion current, and it may readily be shown that the increase is more than adequate to account for the formation of the open cracks.[5] It is thus important to consider whether the current available during the first stage is sufficient to account for the formation of fine cracks.

The corrosion current associated with a crack may be divided into two parts, that flowing to the sides and that to the advancing edge of the crack. The current density on the crack sides must be small, as:—

(i) The sides show little sign of corrosion.

(ii) Estimates of the total extension of a specimen made from crack-geometry agree well with direct measurements, so that little of the gaping of a crack can be due to dissolution of its sides.

(iii) The corrosion current density on the (partly filmed) outer surface before crack-propagation begins is 20–50μA/cm^2,[2,5] which may be compared with an estimate of 100–150μA/cm^2 made from anodic polarization data on non-yielding metal in acidified solutions such that no film can be present.[11] The current density on the crack sides should be intermediate between these limits; it is probably nearer the lower limit, as the potential within the crack is lower than that at the open surface.

A value of 50μA/cm^2 will therefore be assumed for the current density on the crack sides. The current required for propagation of unit length of the advancing edge will be taken as that required for uniform dissolution of a strip 0·01μ wide; it has been shown elsewhere that crack-propagation is possible with a smaller current than this.[9]

On a 0·320 cm dia. specimen tested at 12·3 ton/in^2, the largest fine crack is less

than 0·05 cm deep and extends round almost one third of the circumference, and the duration of the first stage of crack-propagation is about 60 min (see below). If the crack is formed by anodic dissolution of metal of mean density 7·8 to form ions of mean equivalent weight 28 the average current required is

$$\frac{7{\cdot}8 \times 96{,}500 \times 10^{-6} \times 3{\cdot}142}{28 \times 3{,}600 \times 3}\{0{\cdot}160^2-0{\cdot}110^2\}\ \text{A}, \simeq 0{\cdot}01\mu\text{A}.$$

The current flowing to the sides of a crack of this size is

$$\frac{2 \times 5 \times 10^{-5} \times 3{\cdot}142}{3}(0{\cdot}160^2-0{\cdot}110^2)\ \text{A}, \simeq 1{\cdot}2\mu\text{A},$$

which is considerably greater than the current associated with propagation. The surface (cathode) area of the specimens was 17–18 cm², and <100 fine cracks were formed. Hence, if an average crack is half as big as the largest, the cathodic current density associated with cracks at the end of the first stage is about 3·5μA/cm².

At the end of the induction period the cathodic current density is in the range of 20–50μA/cm², and it is known that a current density of 20–30μA/cm² can be supplied to an external anode without a significant change in potential.[5] Clearly, the current required for the first stage of crack propagation could be obtained without a detectable change in potential.

Similar calculations have been made for fully softened specimens tested at other stresses, and for plastically deformed specimens. In no case was the estimated cathodic current density required at the end of the first stage greater than 15μA/cm².

The duration of the stages of stress-corrosion cracking

If the picture of the overall stress-corrosion process proposed by Hoar and Hines[1] is modified to include two stages of crack-propagation, the sequence of events is as follows.

(i) Anodic reaction occurs at weak spots in the initial air-formed film, leading to film repair by precipitation or direct formation of hydroxides and/or oxides. The concomitant increase in anodic acidity leads to film-breakdown at some of these points, and localized corrosion begins. These reactions are only slightly affected by stress.

(ii) Fine cracks are initiated from bare metal surface exposed during the induction period and develop, first in depth and then sideways, until the reduction in cross section caused by one or more cracks is sufficient for widespread yielding to begin.

(iii) The cracks then open up, and develop rapidly until final mechanical failure occurs.

Five times are thus of interest: the induction period, t_i, and the period of film repair, t_r; the two periods of crack-propagation, t_{c_1} and t_{c_2}; and the time to fracture, t_f. These times are shown schematically in Fig. 5. t_f is easily determined, and t_i and t_{c_2} can be obtained from recorded potential/time curves; t_r is the time to the maximum potential and t_{c_2} the duration of the final potential fall. The specimen must, however, be destroyed to detect the first fine cracks, so that t_i and t_{c_1} can only be estimated using data from interrupted tests. The most effective method was found to be as follows. The specimens are divided into groups according to the period of exposure, the group inter-

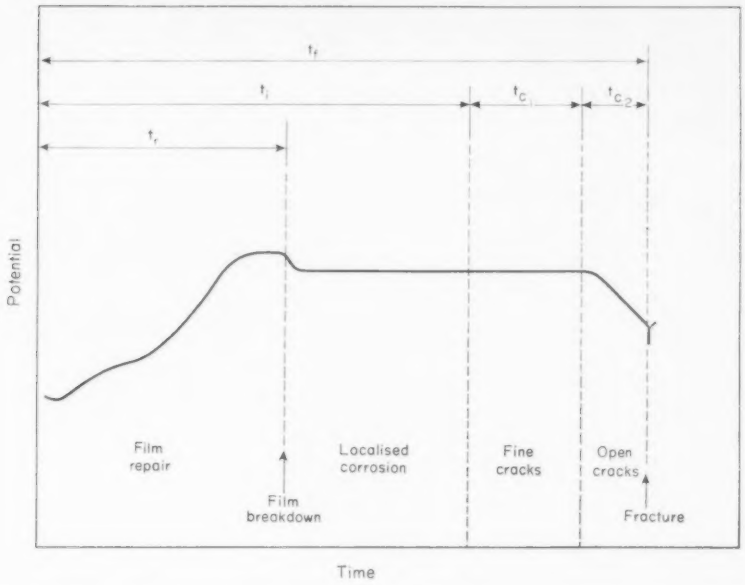

FIG. 5. Relation of t_f, t_r, t_i, t_{c_1}, and t_{c_2} to the progress of stress corrosion and an idealized potential/time curve.

val being selected so that at least three groups contain seven or more specimens. The proportions in each group of specimens containing cracks of any sort and of specimens containing open cracks (including any broken specimens) were then plotted on arithmetical probability paper.* Each set of points may be represented by a straight line. The times corresponding to 50 per cent probability for the two lines are the average induction period and the average time to the formation of open cracks; the difference between these times is the average period during which only fine cracks are present, which is t_{c_1}. It is found that the slopes of the two lines are approximately equal, showing that t_{c_1} is independent of t_i. Increased precision can therefore be obtained by fitting two parallel lines. Fig. 6 shows an example of the use of this technique on data obtained in sixty-two interrupted tests on fully-softened 0·320 cm dia. specimens of steel H tested at 12·3 ton/in². A suitable group interval was 25 min, and the estimated value of t_{c_1} was 60 min. Fewer data were available in other cases, so that the estimates made are less accurate.

Examination of potential/time curves shows that t_{c_2} is also independent of t_i, and a line representing t_f could thus be drawn parallel to the other two. Unusually long or short values of t_r are also associated with corresponding values of t_f, and hence t_i, but the difference $(t_i - t_r)$ also varied in the same way; the line representing t_r would thus have a steeper slope than the other three. It appears that the reactions occurring

*t_f is usually found to be distributed lognormally. The normal distribution (and hence arithmetical probability paper) is preferred for the present purpose as it gives two parallel lines; there is, in any case, little to choose between the two distributions as regards the fit obtained in the centre of the range, where the data are concentrated.

in the later stages of the induction period are controlled by the factors which determine t_r, but that these factors do not influence the rate of crack-propagation; there is, of course, no reason to expect crack-propagation to be controlled by the same factors as the surface reactions occurring during the induction period.

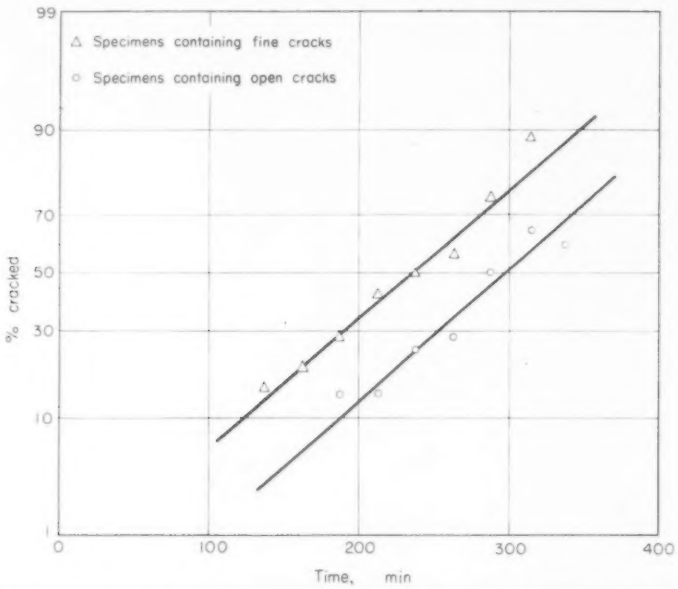

FIG. 6. Proportions of specimens containing fine cracks or open cracks after various exposure periods.
Fully softened 0·320 cm dia. specimens of steel H tested at 12·3 ton/in.²

Fully softened 0·320 cm dia. specimens

Table 1 summarizes data obtained from various experiments in the range 5–25 ton/in². The values of t_f listed are the points on the regression lines in Fig. 1(a) corresponding to the stress in question, and those of t_{c_2} are (arithmetic) mean values based on potential/time curves recorded during the experiments on which the lines

TABLE 1. DURATIONS OF THE STAGES OF THE STRESS-CORROSION CRACKING PROCESS ON FULLY SOFTENED 0·32 CM DIA. SPECIMENS OF STEEL H. THE SYMBOLS ARE DEFINED IN THE TEXT.

Applied Stress (ton/in²)	Period (min)							Ratios		
	t_r	t	t_{c_1}	t_{c_2}	t_f	$t_f-(t_{c_1}+t_{c_2})$	$t_f-t_{c_1}$	$t_i : t_f$	$t_t : (t_{c_1}+t_{c_2})$	$t_r : t_f$
0·0	174	—	—	—	—	—	—	—	—	—
5·0	150	—	>1440	25	6210	<4745	6185	—	0·76	0·02
7·8	210	1150	600	37	1920	1300	1880	0·60	0·67	0·11
10·0	152	460	180	35	750	545	715	0·61	0·73	0·20
12·3	148	225	60	38	295	197	258	0·86	0·67	0·50
15·9	82	100	20	36	126	70	90	0·79	0·56	0·65
19·6	55	—	—	30	90	—	60	—	—	0·61
24·8	35	—	—	25	60	—	35	—	—	0·58

are based. Individual values of t_{c_2} were in the range 30–45 min over the range 7–20 ton/in², and there is no indication of an effect of stress in this range. t_{c_2} is, however, less at higher or lower stresses. Interrupted tests were carried out at 7·8, 10·0, 12·3 and 15·9 ton/in², so that values of t_{c_1} and t_i are available for these stresses. An estimate of t_i may also be made using the identity $t_i = t_f - (t_{c_1} + t_{c_2})$. However, t_i, t_{c_1} and t_{c_2} are arithmetical means, whereas t_f, being the antilogarithm of a mean value of log t_f, is a geometric mean; furthermore, the values of t_f and t_{c_2} were obtained from a different batch of specimens from those on which t_i and t_{c_1} were based. The two estimates of the induction period (t_i and $(t_f - (t_{c_1} + t_{c_2}))$ would not be expected to be equal even if there were no real differences in behaviour between the two batches. Interrupted tests were not carried out at 5·0 ton/in², so no estimate of t_i is available. However, large fine cracks (visible because they opened up elastically) were observed 18–20 h before fracture occurred; smaller cracks must have been present before this, and t_{c_1} was probably more than 24 h.

Like t_f, t_r is distributed approximately log-normally, and the values quoted are geometric means based on potential/time curves recorded during both interrupted tests and tests continued to final fracture. At low stresses, t_r appears to be independent of applied stress, but at higher stresses film-breakdown occurs sooner (Fig. 7). At stresses only a little above the proof stress the form of the potential/time curve is

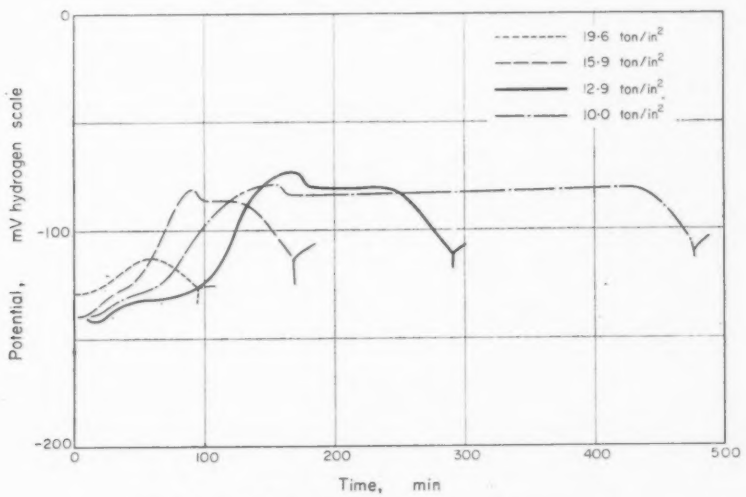

FIG. 7. Effect of applied stress on potential/time curves.
Fully softened 0·320 cm dia. specimens of steel H.
(The curves have been selected because they give values of t_r near the centre of the range for each stress.)

similar to those obtained at lower stresses. Such specimens extend considerably when the load is applied shortly before the start of the test, and the effective film thickness is probably less than at lower stresses; it is known that film breakdown occurs sooner on thin films.[1,10] At very high stresses the final potential fall begins as soon as the maximum potential is reached, and the maximum is lower than at lower stresses; these

curves are, in fact, very similar to those obtained on 0·051 cm dia. specimens at corresponding stresses.[1] These specimens creep appreciably throughout the tests, and it may well be that cracks are initiated at points where the film is damaged by this process, so that electrochemical film breakdown is unnecessary.

At stresses below the 0·1 per cent proof stress, the ratio $t_i : t_f$ is approximately independent of stress, and a log t_i/S line can be drawn parallel to the corresponding log t_f/S line (Fig. 8(a)). Estimates of the induction period are available only at a single stress above the 0·1 per cent proof stress. However, in this case cracks were initiated as soon as film breakdown occurred, and if this is also the case at higher stresses a combined log t_i/S and log t_r/S curve may be drawn. In this range the ratio t_r: t_f is approximately independent of stress, and its value is similar to that of the ratio t_i: t_f at lower stresses. In the absence of a better criterion, the combined line in Fig. 8(a) has been drawn so that the ratio t_i: t_f has the same value over the whole stress range; it is apparent that this line fits the data adequately.

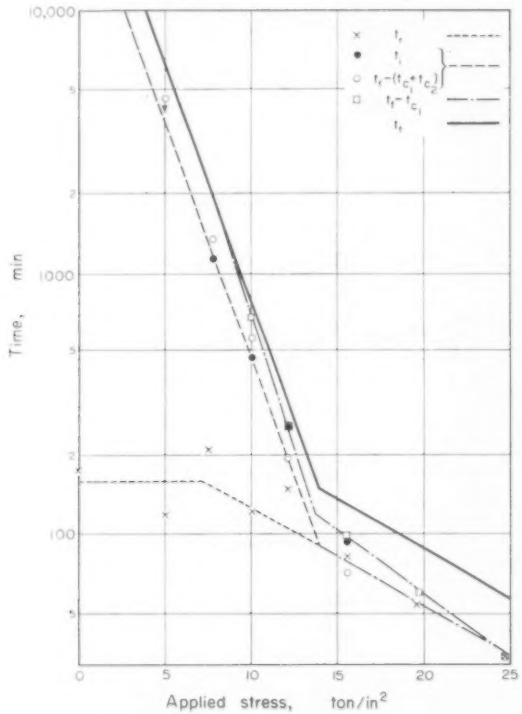

FIG. 8(a). Effect of applied stress on the stages of the stress-corrosion process using fully softened 0·320 cm dia. specimens of steel H.

The form of the log t_r/S curve at stresses below the proof stress is not well defined because the scatter is considerable. It seems reasonable to assume that at low stresses t_r is independent of stress, but as some localized yielding occurs at stresses below the 0·1 per cent proof stress it may well be that t_r decreases with increasing stress at

stresses just below the proof stress as well as at higher stresses. The combined log t_r/S and log t_i/S curve in Fig. 8(a) has been tentatively extended to meet a line drawn parallel to the stress axis through the mean value of log t_r at stresses below 10 ton/in².

Plastically deformed 0·320 cm dia. specimens

Data obtained in tests on specimens extended plastically by 4 per cent before testing at lower stresses is shown in Fig. 8(b). The log t_f/S lines are the regression lines in Fig. 1, and the values of $(t_f - t_{c_2})$ and t_r plotted are taken from potential/time curves

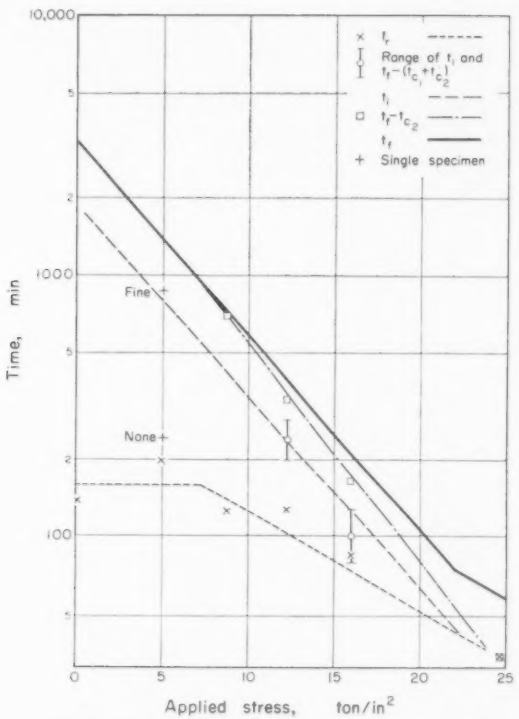

FIG. 8. (b) plastically deformed (4·0 per cent strain) 0·320 cm dia. specimens of steel H.

recorded during the experiments on which the lines were based. The values of t_r are clearly very similar to those obtained on fully softened specimens, and the log t_r/S curve in Fig. 8(b) is the same as in Fig. 8(a). A few interrupted tests were carried out at 12·4 and 16·0 ton/in²; these were not primarily intended to give an estimate of t_{c_1} and hence of $t_f-(t_{c_1}+t_{c_2})$, but they do lead to approximate limits for these quantities. At both stresses t_{c_1} is greater than on fully softened specimens. At 12·4 ton/in² it is $1\frac{1}{2}$–$3\frac{1}{2}$ h, compared to 60 min at 12·3 ton/in² on fully softened specimens, while at 16·0 ton/in² it is $\frac{3}{4}$–2 h, compared to about 20 min at 15·9 ton/in². At low stresses, on the other hand, t_{c_1} must be less than on fully softened specimens at 5·0 ton/in²; t_f for plastically deformed specimens is less than t_{c_1} for fully softened specimens. The

results of two interrupted tests at this stress are indicated on Fig. 8(b); these are consistent with a value of t_{c_1} in the range 6–18 h. The data are, of course, by no means sufficient to define a log t_i/S curve, but a line drawn parallel to the log t_f/S curve and meeting the log t_r/S curve at the proof stress appears eminently reasonable.

At stresses near the 0·1 per cent proof stress for fully softened specimens, the density of fine cracks in the vicinity of the fracture is similar in the two classes of specimen, but a higher stress is required to cause yielding in plastically deformed specimens. The development of fine cracks must therefore proceed further on plastically deformed specimens than on fully softened specimens. Moreover, the available current must be shared between a greater total number of cracks on plastically deformed specimens. Both factors would increase t_{c_1}. At low stresses, on the other hand, open cracks on a fully softened specimen usually form from a single fine crack, whereas several fine cracks are involved in plastically deformed specimens. t_{c_1} would thus be expected to be less on plastically deformed specimens.

Effects of alloy composition and specimen size

Tests to fracture have been carried out on a variety of alloys using 0·160, 0·320 and 0·400 cm dia. specimens; the results are described elsewhere[7]. Potential/time curves were recorded during most of these experiments. Similar tests were done on 0·635 cm dia. specimens of steel H and a few interrupted tests were made on these specimens and on 0·320 and 0·400 cm dia. specimens of other steels. Many data are thus available on the effects of composition and size on t_f, t_r and t_{c_2}, but reliable estimates of t_i and t_{c_1} cannot be made. It is clear, however, that the sequence of events discussed above is generally applicable.

The effects on t_f of variations in alloy composition within the usual limits of the 18–8 type Cr–Ni steels are complex and relatively small. Within these ranges t_{c_2} is independent of composition, and the only clear effect on t_r is that it is a little shorter on molybdenum-bearing steels than on other steels, probably because the initial air-formed film is thinner. Considerable increases in t_f are, however, produced by substantial increases in nickel content or by reducing the carbon content below 0·03 per cent. These changes have no significant effect on t_{c_2}, and little effect on t_r; the few data available show that t_{c_1} is apparently unaffected. The major effect of alloy composition is thus on the duration of the part of the induction that follows film breakdown, the initiation of cracks being greatly delayed in the more resistant alloys.

Comparison of data obtained on specimens of different sizes shows that:—

(i) t_f is considerably less on 0·051 cm dia. specimens than on 0·320 cm dia. specimens of similar composition, but it increases only slightly with further increase in size.

(ii) The slopes of the log t_f/S curves are not significantly altered by variations in specimen size.[7]

(iii) At stresses near the proof stress cracks are initiated as soon as, or shortly after, film breakdown occurs on 0·051, 0·320 and 0·400 cm dia. specimens. t_r was shorter on the fully softened and pickled 0·051 cm dia. specimens used by Hines and Hoar[6] than on the larger specimens of the present work. However, the difference is less than the range produced by treatments which influence the initial condition of the film,[1] and it is probably due to differences

in the methods of specimen preparation. In this stress range t_i is thus independent of specimen size.

(iv) At stresses appreciably below the proof stress, t_i is not significantly altered by increase in specimen size from 0·320 to 0·400 cm dia. No information on t_i in this stress range was obtained on 0·051 cm dia. specimens.

It seems reasonable to assume that at any stress cracks are initiated at the same stage (as indicated by the potential/time curve) on specimens of any size. The effect of specimen size may thus be represented by a family of log t_f/S curves parallel to each other and to a common log t_i/S curve (Fig. 9).

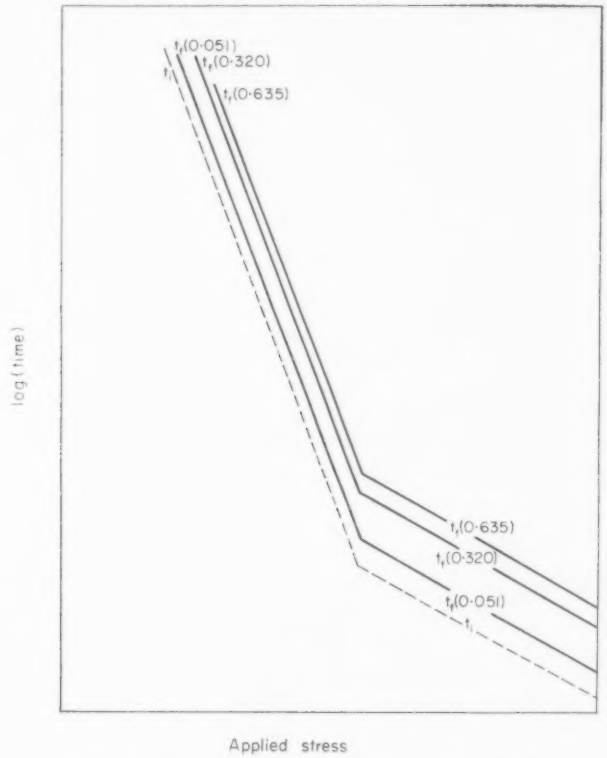

FIG. 9. Idealized log t_f/S and log t_i/S curves for fully softened specimens of different sizes.

The limiting depth for fine cracks is 0·03–0·04 cm,[4] so that on 0·051 cm dia. specimens at stresses near the proof stress open cracks will form shortly after the first crack is formed. t_{c_1} is thus very short, and it is not surprising that the two stages of crack propagation were not distinguished. This effect probably also explains why these specimens contained fewer fine cracks and more open cracks than did the larger specimens. At similar stresses on larger specimens, extensive sideways spreading of fine cracks is necessary before an open crack can form, so that t_{c_1} is considerable. On 0·320 cm dia. specimens open cracks usually formed from a single fine crack, whereas

on larger specimens most open cracks formed from two or more cracks on adjacent parallel planes, and it is thus not surprising that t_{c_1} increases only slightly with specimen size in this range.

At very high stresses (20–25 ton/in^2), t_{c_1} is very short even on 0·320 cm dia. specimens, and these specimens contain more open cracks than do those tested at lower stresses. They behave, in fact, in a similar way to 0·051 cm dia. specimens at stresses near the 0·1 per cent proof stress.

The rate of crack propagation

On a given specimen size the lower the applied stress the further fine cracks spread round the circumference before open cracks form. At low stresses an open crack therefore develops on a longer front than at higher stresses, and the distance which it must penetrate before final fracture occurs is almost independent of stress, except that at very high or very low stresses it is less than at intermediate stresses. It is thus not surprising that t_{c_2} varies little with applied stress; it varies only slightly with specimen size for a similar reason. The average rate of propagation of open cracks is in the range 0·1–0·4 cm/h, and examination of specimens from interrupted tests shows that it varies little with time.

The rate of propagation of fine cracks, however, varies considerably. Initially the whole advancing edge develops at 0·1–0·4 cm/h, and this rate is maintained during sideways spreading of the extremities until the crack extends more than half way round the circumference; this stage is reached only on fully softened specimens at very low stresses. The rate of penetration falls off markedly once the limiting depth is reached, and it is probable that the presence of uncracked material near the point of initiation reduces the stress at the extremities of a large crack and so causes the reduction in the rate of propagation.

DISCUSSION

These results are generally in harmony with those obtained by Hoar and Hines, and provide additional information that supports the electrochemical mechanism of crack propagation proposed by them. The theoretical implications of these results are discussed in detail elsewhere,[9] and will not, therefore, be considered here. It may be noted, however, that a crack model based on electrochemical crack propagation leads to a surprisingly good quantitative explanation of the mode of development of fine cracks.

The effect of variations in the experimental conditions on the relative duration of the induction period and the stages of crack propagation are of considerable importance. t_i is sensitive to the temperature[1] and composition[13, 14, 15] of the environment, to the initial surface condition of the metal[1, 2, 8] and to the rate and direction of heat transfer across the metal/solution interface; at low stresses it also depends on the metallurgical condition of the alloy. The major effect of alloy composition is on the induction period, which is, however, independent of specimen size, and is probably not very sensitive to specimen form. Nevertheless, it might be expected to be smaller on specimens with sharp corners or with roughly abraded surfaces, since such factors tend to accelerate film breakdown.[16]

The duration of the total period of crack propagation, $(t_{c_1} + t_{c_2})$, is not altered significantly by most changes in the environmental conditions, (although temperature has a small effect[1]) and it is probably also independent of alloy composition. t_{c_2} is only slightly influenced by specimen size or form, applied stress or the metallurgical condition of the alloy, but t_{c_1} is very sensitive to these variables, mainly because of the mode of development of fine cracks. t_{c_1} should be greater on sheet specimens than on cylindrical specimens of similar cross-sectional area. Finally, the duration of one or both stages of crack propagation will be prolonged, possibly indefinitely, if the mode of stressing is such that the formation of a crack relieves the stress; the slowing down of sideways spreading of large fine cracks discussed above is an example of a rather similar effect.

The relative durations of the various stages may thus vary considerably with the experimental conditions, the limits being, on the one hand, the case where cracks are present for almost all of the life of a specimen and, on the other hand, that where the induction period is only a little shorter than the life. There are two important consequences of this fact.

(i) In practice complete mechanical failure of a component is rare, so that t_f is not the most important measure of the resistance of an alloy; the quantity required is the induction period. With fully softened specimens tested by the method used in the present work, the induction period is proportional to time to fracture for a given alloy, and the difference between these quantities is essentially independent of alloy composition. t_f is thus a reasonable basis for comparison, but this may not be the case if other test methods are used.

(ii) Differences in the relative durations of the stages observed under different experimental conditions are *not* evidence of differences in the mechanism of the process, as has been suggested.[2, 3]

CONCLUSIONS

(i) On axially stressed cylindrical specimens of diameters in the range 0·160–0·635 cm the life of a specimen of austenitic Cr–Ni steel in hot concentrated chloride solution can be divided into an induction period and a period of crack propagation, which correspond to the stages recognized by Hoar and Hines on 0·051 cm dia. specimens.[1] The period of crack propagation may itself be divided into two parts, corresponding to two stages previously distinguished metallographically. The first of these is very short on 0·051 cm dia. specimens and was not noted at first.[1]

(ii) The second stage of crack propagation is accompanied by a fall in potential and by accelerating extension, but no detectable change in potential or extension rate occurs during the first stage. However, sufficient corrosion current is available to account for both stages of crack formation by purely electrochemical processes.

(iii) The duration of the induction period is mainly controlled by alloy composition and applied stress, the effect of stress depending on the metallurgical condition of the alloy. (It is also known to be sensitive to environmental conditions.) The duration of the second stage of crack propagation depends on specimen size as well as on the mode of stressing, while the duration of the first stage is very sensitive to applied stress, the metallurgical condition of the alloy and specimen size or form. The relative duration of the various stages can thus vary considerably with the conditions.

(iv) The induction period is the most satisfactory measure of the resistance of an alloy, but with direct loaded axially stressed cylindrical specimens the time to fracture (which is much easier to measure) is also a reasonable measure.

Acknowledgement—I am grateful to Messrs. M. Bartle, R. W. Hugill and R. C. Williamson, who carried out most of the experimental work.

REFERENCES

1. T. P. HOAR and J. G. HINES, *J. Iron St. Inst.* **182,** 124 (1956).
2. H. H. UHLIG and M. LINCOLN, *J. Electrochem Soc.* **104,** 167C (1957).
3. H. L. LOGAN and R. J. SHERMAN, *Welding J. N.Y.* **35,** 389 (1956).
4. J. G. HINES and R. W. HUGILL, *Physical Metallurgy of Stress-Corrosion Fracture*, p. 193. Interscience, New York (1959).
5. T. P. HOAR and J. G. HINES, *Proc. 8th Meeting C.I.T.C.E. Madrid* 1956, p. 273. Butterworths, London (1958).
6. J. G. HINES and T. P. HOAR, *J. Iron St. Inst.* **184,** 166 (1956).
7. J. G. HINES and E. R. W. JONES, *Corros. Sci.* **1,** (1961). In press.
8. M. A. SCHEIL, *Symposium on Stress-Corrosion Cracking*, p. 435. A.I.M.E./A.S.T.M. Philadelphia (1945).
9. J. G. HINES, *Corros. Sci.* **1,** 21 (1961).
10. T. P. HOAR, *Trans Faraday Soc.* **45,** 683 (1949).
11. T. P. HOAR and J. M. WEST, *Proc. Roy. Soc.* A. In press.
12. C. EDELEANU, *J. Iron St. Inst.* **173,** 140 (1953).
13. C. EDELEANU and P. P. SNOWDEN, *J. Iron St. Inst.* **186,** 406 (1957).
14. P. P. SNOWDEN, *J. Iron St. Inst.* **194,** 181 (1960).
15. J. G. HINES, Unpublished Work.
16. U. R. EVANS, *Symposium on Properties of Metallic Surfaces*, p. 253. Inst. Met., London (1953).

Corrosion Science, 1961, Vol. 1, pp. 21–48. Pergamon Press Ltd. Printed in Great Britain

ON THE PROPAGATION OF STRESS-CORROSION CRACKS IN METALS *

J. G. HINES
Imperial Chemical Industries Limited,
Billingham Division, Billingham, Co. Durham, England.

Abstract—Mechanisms which have been proposed for the propagation of stress-corrosion cracks are reviewed, and it is concluded that the simplest are the electrochemical mechanisms proposed by Logan and by Hoar and Hines. These attribute crack formation to yielding at the crack tip, which leads to concentration of attack at that point. Mechanisms that involve mechanical stages of crack propagation provide a satisfactory explanation of a number of cases in which there is evidence that, or where it may plausibly be argued that, paths that are mechanically weak exist in the material. These mechanisms are less satisfactory in cases where the cracks do not follow pre-existing paths in the material, as it is difficult to explain why localized brittle failure should occur.

The conditions under which the two electrochemical mechanisms are applicable are discussed in terms of a simple crack model, and it is shown that most, if not all, of the facts concerning stress-corrosion cracks in austenitic Cr–Ni steels can be explained qualitatively in this way; in some cases reasonable quantitative agreement is obtained. Logan's mechanism, which assumes that yielding at the crack tip merely prevents formation of a passive film, cannot be applied in this case, but it may well operate in cases where more active metals are involved. The Hoar/Hines mechanism, according to which yielding reduces the activation polarization for anodic dissolution at the crack tip, is satisfactory, and it is concluded that this is the best available explanation.

Other cases of stress-corrosion cracking are discussed.

Résumé—L'auteur étudie les méchanismes proposés pour l'élucidation de la propagation de fissures dues à la corrosion de charge. Il en découle que les méchanismes les plus simples sont les méchanismes électrochimiques proposés par Logan et par Hoar et Hines. Ces auteurs attribuent la formation de fissures à un phénomène de relâchement observé à la pointe de la fissure ce qui conduit à une concentration des attaques à ce même point. Les méchanismes qui englobent des stades méchaniques de la propagation des fissures donnent une explication satisfaisante pour certains cas où il y a respectivement où il paraît y avoir, dans le matériau, des cours faibles au point de vue méchanique. Ces méchanismes sont moins satisfaisants dans les cas où les fissures ne suivent pas des cours préexistants dans le matériau, parce qu'il n'est pas aisé de s'expliquer le fait pourquoi il y aurait des fautes localisées de fragilité.

A l'aide d'un modèle simple de fissure, les conditions sous lesquelles les deux méchanismés électrochimiques sont applicables, sont indiquées; il est démontré que la plupart des facteurs concernant les fissures dues à la corrosion de charge, voire même tous ces facteurs, peuvent être expliques qualitativement de cette manière, pourvu qu'il s'agisse d'aciers austénitiques au chrome-nickel. Dans certains cas, on a obtenu une correspodance quantitative raisonnable. Le méchanisme de Logan, selon lequel le relâchement à la pointe de la fissure prévient seulement la formation d'un film passif, ne peut pas être appliqué en ce cas, mais il semble être approprié dans les cas où des métaux plus actifs sont en jeu. Le mèchanisme de Hoar-Hines, selon lequel le relâchement réduit la polarisation d'activation pour une dissolution à la pointe de la fissure, est satisfaisant. On en arrive à la conclusion que c'est là la meilleure explication qu'on puisse apporter actuellement.

D'autres cas de fissures par corrosion de charge sont étudiés.

Zusammenfassung—Es werden die Mechanismen besprochen, mit welchen man sich die Fortpflanzung von Belastungs-Korrosions-Rissen erklärt. Man kommt zu dem Schluss, dass die von Logan und von Hoar und Hines ausgearbeiteten elektrochemischen Mechanismen als die einfachsten anzusprechen sind. Diese Mechanismen schreiben die Rissbildung der Tatsache zu, dass an der Rissspitze ein Nachgeben erfolgt, wodurch es zu einem konzentrierten Angriffl an dieser Stelle kommt. Mechanismen, die mechanische Stadien der Rissbildung einschliessen, geben eine befriedigende Erklärung in einer Anzahl von Fällen, in welchen Anzeichen dafür vorliegen, oder in denen man plausiblerweise vermuten kann, dass in dem Material mechanisch schwache Bahnen vorhanden sind. Diese Mechanismen geben aber weniger befriedigende Erklärungen für die Fälle, wo die Risse nicht den bereits vorhandenen

*Manuscript received 5 July 1960; part of the paper was presented at the first meeting of the Corrosion Science Society, London, April 4th-5th, 1960.

Bahnen folgen, da man sich nur schwer erklären kann, wieso in einem Material lokalisierte Sprödigkeitsfehler auftreten sollen.

Die Bedingungen, unter denen die beiden elektrochemischen Mechanismen anwendbar sind, werden an Hand eines einfachen Rissmodells besprochen, und es wird nachgewiesen, dass die meisten, um nicht zu sagen alle die auf Belastungs-Korrosions-Risse in austenitischen Chromnickel-Stählen bezüglichen Faktoren auf diese Weise qualitativ gedeutet werden können. In einigen Fällen lässt sich eine angemessene quantitative Übereinstimmung erzielen. Der Logan'sche Mechanismus, der davon ausgeht, dass ein Nachgeben an der Rissspitze lediglich die Bildung eines passiven Films verhindert, ist in diesem Falle nicht anwendbar, kann aber in Fällen, wo aktivere Metalle beteiligt sind, gut geeignet sein. Der Hoar-Hines-Mechanismus, laut welchem das Nachgeben die Aktivierungs-Polarisation an der Rissspitze bei anodischer Auflösung herabsetzt, gibt eine befriedigende und die derzeit wohl beste Erklärung des Problems.

Andere Fälle von Rissbildung durch Belastungs-Korrosion werden besprochen.

INTRODUCTION

FOUR features of the development of stress-corrosion cracks are particularly striking:

(i) Stress-corrosion cracks are formed only under the joint action of a tensile stress and corrosion; they cannot be produced by the consecutive action of these agencies.

(ii) The rate of penetration is much greater (by at least a factor of 10^3) than the rate of attack on the crack sides, and the reaction at the crack tip is very localized. It appears, therefore, that the processes responsible for crack propagation are self-sustaining and self-stimulating.

(iii) In many cases cracks advance slowly or at a rate of the order of 1 cm/h; faster rates than this have only been observed in a few cases which may be considered exceptional for other reasons. There appears to be a characteristic rate of about 1 cm/h, which varies surprisingly little with variations in the experimental conditions.

(iv) The conditions under which stress-corrosion cracking can occur are often very specific. The specificity is only partly explained by the requirement that the rate of attack on the crack sides and outer surface must be fairly small if fine cracks are to be formed, as environments which produce similar corrosion damage in the absence of stress do not always cause stress-corrosion cracking.

Any mechanism of stress-corrosion cracking must provide an explanation of these four features. There are also numerous other facts, often relating to a particular case, which must be explained; these will be considered later.

MECHANISMS THAT HAVE BEEN PROPOSED

A rate of 1 cm/h is considerably greater than is usual for corrosion processes, but rates of dissolution of this order have been obtained under conditions such that stifling does not occur. The conditions within a crack may well be less favourable to stifling than those near a flat surface dissolving uniformly, as yawning of the crack tends to draw fresh solution into the crack, but the concentration of attack on the narrow front that is needed to form a fine crack cannot be explained in this way. On the other hand, the extensive deformation associated with mechanical tearing does not occur, and cracks advance much more slowly than is usual for brittle cracking. Moreover, there is abundant evidence that electrochemical processes play some part in crack propagation and are not responsible merely for the initiation of the crack. The simple view that stress-corrosion cracks are mechanical failures triggered by corrosion on the surface is thus, in general, untenable.

The mechanisms that have been proposed may be divided into two classes, in which crack propagation occurs by purely electrochemical processes or by alternate fast mechanical and slow electrochemical stages.* The main features of the first group are the explanations of the concentration of attack at the crack tip and of the rate of propagation. The second group bring in the complication of a mechanical stage to explain how these characteristics can be obtained even though the current density at the crack tip is only a little, if any, greater than elsewhere.

Electrochemical mechanisms

Dix[1, 2] suggested that cracks were formed by preferential dissolution of susceptible paths in the material, the function of stress being to open up the cracks and so reduce stifling. The susceptibility was attributed to segregation or precipitation at grain or sub-grain boundaries, and later authors suggested that in cases where no such path exists previously a susceptible path might be produced by a strain-initiated transformation ahead of the crack.[3, 4, 5] In either case it is difficult to understand how the observed rates of propagation could be obtained unless the phases concerned have very different electrochemical properties; evidence that this is so does not usually exist. It also seems unlikely that the high strain energy at the crack tip, or the fact that the material in that region has been cold worked, could provide a sufficient concentration of attack to form a deep, fine crack;[5, 6] neither effect causes a marked acceleration in other corrosion processes.

Logan[7, 8] and Hoar and Hines[9, 10] suggested that the attack is concentrated at the tip because the metal at that point is continually yielding; the yielding is maintained because the metal is dissolving. Logan considered that yielding prevented the formation of passive films, whereas Hoar and Hines thought that it also directly assisted the removal of cations from the lattice. Recently Hoar and West[11] have shown that the activation polarization of anodic dissolution of austenitic Cr–Ni steels in hot, concentrated chloride solution is markedly reduced when the metal is simultaneously yielding rapidly. These alloys suffer stress-corrosion cracking in this medium, and the observation thus supports the suggestion of Hoar and Hines for this case.

Alternate mechanical/electrochemical mechanisms

Keating[12] and Evans[13] suggested that a crack advances by fast mechanical stages re-initiated by corrosion whenever an obstacle is encountered. A path of mechanical weakness, and probably also of susceptibility to corrosion, is required. This mechanism leads to a reasonably satisfactory explanation of many cases of intergranular stress-corrosion cracking. Several attempts have been made to devise mechanisms that do not require a pre-existing weak path. These are necessarily complicated by the fact that transgranular cracking occurs in alloys (such as the austenitic Cr–Ni steels and copper alloys) that do not normally behave in a brittle manner even if sharp notches are present; it is thus necessary to explain how corrosion can cause embrittlement. It seems unlikely that hydrogen produced near the crack tip could be responsible, as transgranular cracking of this type occurs most frequently in face-centred cubic

*Cases in which cracking is believed to be due to general embrittlement by cathodic hydrogen are not considered. There is considerable doubt whether these should be counted as true stress-corrosion cracking.

alloys (which are not very sensitive to hydrogen) at relatively noble potentials.[9, 10, 15] The first difficulty might be resolved if a phase transformation occurred in the highly strained region but the second is not easily overcome.

Forty[16] has proposed a mechanism for α–brass in which preferential dissolution of zinc causes local embrittlement, and a crack initiated in this region runs into the adjacent ductile material because yielding is inhibited by hardening caused by short-range ordering. Swann and Nutting[17] suggested that yielding is induced in the surrounding material as a result of preferential corrosion of a stacking fault, and that short mechanical cracks are caused by the piling-up of dislocations against the stacking fault. Both suggestions were based on observations on copper alloys and depend on special properties of the alloys in question; it may, however, be possible to adapt them for other cases.

It is unfortunately very difficult to determine directly and unambiguously whether mechanical cracking plays any part in crack propagation unless the stages are very obvious. A decision between the possibilities can thus be made only by determining which gives the best (i.e. the simplest and most complete) explanation of the facts. The electrochemical mechanisms suggested by Logan and by Hoar and Hines are essentially simpler than those involving mechanical stages, and it thus seems logical to consider these in detail first; if they are satisfactory the additional complication of an embrittlement process is unnecessary.

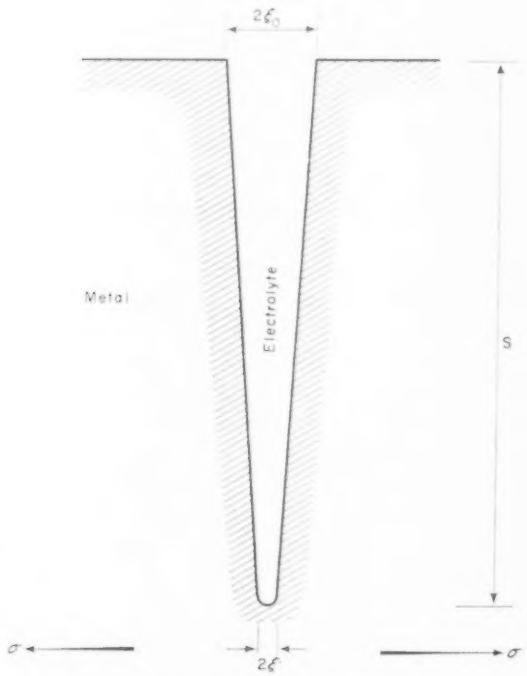

FIG. 1. General form of crack model.

ELECTROCHEMICAL CRACK-PROPAGATION

It is assumed that dissolution is concentrated at the crack tip because of the effects of yielding at that point, and that the cathodic reaction occurs only on the surface of the specimen.

Stress-corrosion cracks are approximately wedge-shaped in section, and if the metal at the tip is yielding the tip must be rounded (Fig. 1). Roesler[18] points out that in general the stress at the tip of a crack exceeds the yield stress and that the tip must widen until its width is approximately equal to the diameter of the region in which the yield point is exceeded. This suggestion leads to an expression for the radius of the crack tip, ξ, in terms of the crack depth, s, the applied stress, σ, and the "effective yield stress" at the crack tip, Σ.* This is

$$\xi = s\frac{\sigma^2}{\Sigma^2} = s\,k_1^2 \text{ (where } k_1 = \frac{\sigma}{\Sigma}) \qquad (1)^*$$

The width of the tip is thus greater the higher the applied stress and increases as the crack deepens. Σ cannot possibly be greater than the shear strength of the perfect lattice and a lower limit for ξ can therefore be obtained; it may be shown that a deep, narrow crack (i.e. one seen as a single line under the optical microscope) can only be formed at low stresses, and that a deep crack formed at a high stress must appear blunt ended; these points appear to be equally applicable to other types of cracks, and they have not always been appreciated.

It follows from equation (1) that

$$\frac{d\xi}{dt} = \frac{ds}{dt}\,k_1^2 \qquad (2)$$

i.e. that the rate at which the tip widens is independent of crack depth, so that the ratio $k_2 = \frac{s}{\xi_0}$ (where $2\xi_0$ is the width of the crack at its mouth) is constant for a given value of k_1 as long as the crack is relatively shallow (so that the average stress over the remaining cross-section is not very different from the nominal).

The tip of a propagating crack may be pictured as in Fig. 2. In the austenitic Cr–Ni steels the activation polarization for anodic dissolution decreases with increasing strain rate,[11] and similar behaviour would be expected whenever activation polarization is reduced by yielding; alternatively, the damage to a surface film will clearly increase with strain rate. The strain rate is zero at the crack sides, and dissolution will thus be concentrated near the centre of the tip. Moreover, even partial dissolution of the surface layer will weaken it, increasing the strain rate in the region where dissolution is concentrated, while the strain rate at the crack sides will be further reduced if a surface film forms in that region. The section of the tip will thus be an arch, the true advancing edge being the region of the cusp. Even in this region the current density will be smaller than would be expected if it were assumed that each layer exposed dissolved completely, as yielding of a partially dissolved surface helps to expose the underlying metal. Propagation is probably possible if only a single row of atoms is dissolved; it is, of course, unlikely that dissolution is as restricted as this, but at a given rate of propagation the current associated with unit length of an advancing edge is probably small and almost independent of the size of the crack.

*The equation is derived and Σ explained in Appendix I.

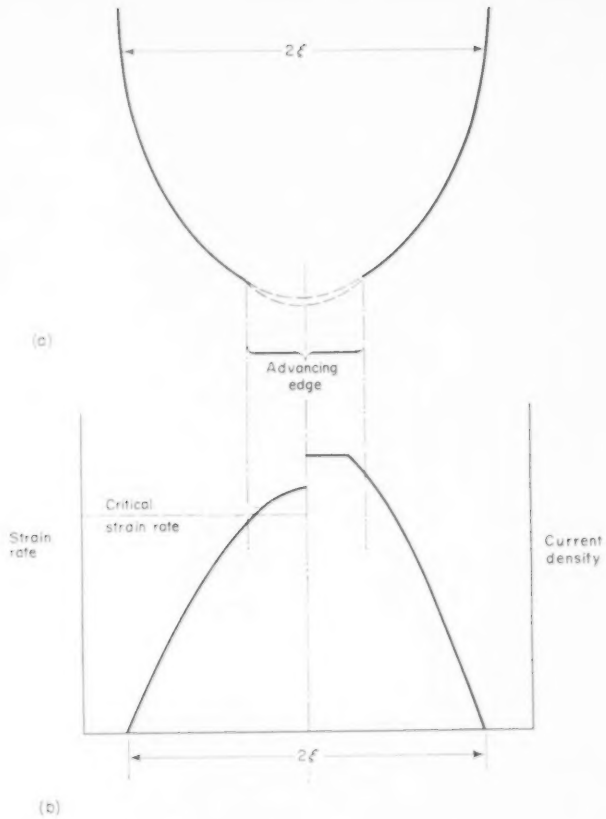

FIG. 2. (a) Section of the tip of a propagating crack.
(b) Variation of strain rate and current density over crack tip.

In any cell, the sum of the ohmic potential drops round the circuit and the polarization at both electrodes must equal the difference between the two reversible potentials. It will be shown that electrochemical crack propagation can occur only if the potential at the mouth of the crack (usually equal to the measured corrosion potential) lies in a relatively narrow range, so that the difference, E, between this potential and the anodic reversible potential is a characteristic of the stress-corrosion crack; it may be considered as the "available e.m.f.". The corrosion current available at a given value of the potential at the mouth of the crack is controlled by the cathodic polarization, and by ohmic effects in the metal, the bulk of the solution and any surface film on the cathodes. These factors determine the number of cracks formed, but they do not influence the behaviour of an individual crack, and therefore need not be considered in a treatment of a single crack.

The anodic polarization may be divided into three parts: activation polarization at a bare metal surface (η_A); concentration polarization due to a limitation of the supply of solvating or complexing species or the removal of soluble anodic products

(η_C); and the polarization caused by the presence of a surface film (η_F). The total polarization ($\eta_A + \eta_C + \eta_F$) must be equal the available e.m.f. less the ohmic potential drop down the crack, V. Hence if curves are plotted representing the variation of ($\eta_A + \eta_C + \eta_F$) and of (E–V) against current density at the advancing edge, they intersect at the current density available for crack-propagation under the conditions in question. It is convenient to refer to the second curve as the "load line", by analogy with the concept used in certain electrical calculations. The current density at the advancing edge is proportional to the rate of propagation. The current density on the crack sides may be obtained similarly; for the present purposes it is sufficient to use the load line appropriate to the advancing edge, although strictly a separate load line should be used for each part of the crack sides.

It may be shown (Appendix 2) that the ohmic potential drop down the crack is approximately

$$V = \rho s k_2 \left[I - \left\{ \frac{i}{2s} - I k_1^2 k_2 \right\} ln\ k_1^2 k_2 \right], \tag{3}$$

where ρ is the specific resistance of the electrolyte within the cracks, I is the anodic current density on the crack sides, and i the current required for propagation of unit length of the advancing edge. I is generally small, so that in a shallow crack V depends mainly on i unless k_2 is also small; in the latter case V can usually be neglected. In a deep crack the current to the sides is more important and V is almost independent of i.

η_A and η_F are determined by the strain rate. The mean strain rate at the crack tip is given by

$$\frac{1}{\xi} \cdot \frac{d\xi}{dt} = \frac{1}{s} \cdot \frac{ds}{dt} \qquad \text{(from 1 and 2)} \tag{4}$$

and is thus independent of ξ and k_1; at a given rate of propagation it is inversely proportional to the depth of the crack. η_C is determined by the rate at which solvating species can reach and/or solvated cations leave the anode surfaces. Both factors depend to some extent on crack geometry. If the current responsible for propagation is independent of the conditions, the ratio (volume of solution within the crack)/(volume of metal dissolved to form the crack) will decrease as the crack deepens. On the other hand, stirring due to the yawning of the crack will be less effective the deeper and the finer the crack, and in a deep, fine crack the contribution from anodic action on the crack sides may well be significant. η_C should, therefore, first decrease and then increase as the crack deepens. Nielsen[19] reports that deep, fine cracks often contain considerable quantities of corrosion product, whereas this is not present in shallower or wider cracks.

However, at current densities of the order of 1 A/cm^2 much of the concentration polarization probably arises in transport between the anode surface and the solution near the outside of the double layer, and this contribution is independent of crack geometry. It may be, therefore, that η_C is only slightly influenced by the form and size of the crack, except in the case of very deep, fine cracks.

Consider first the case where no surface film can form in the crack (i.e. $\eta_F = 0$) and η_A is reduced by yielding. η_A is small at the advancing edge when the crack is advancing rapidly despite the high current density at that point, but as the rate of propagation is reduced η_A increases although the current density at the advancing

edge becomes smaller. At low current densities η_A decreases again. On the other hand, η_C increases with current density over the whole range, the increase being very fast at high current densities. Hence if η_C is relatively small, $(\eta_A + \eta_C)$ passes through a minimum at a high current density (Curve I, Fig. 3a) whereas if η_C is large the minimum does not occur (Curve II). On the sides of the crack η_A does not decrease at high current densities and the polarization curves are thus of the form of Curves IA and IIA. Fig. 3(b) shows load lines corresponding to two levels of applied e.m.f. and two "crack resistances", and Fig. 3(c) the results of combining the polarization curves of Fig. 3(a) with the load lines of Fig. 3(b). An intersection at high current densities is possible—i.e. rapid propagation can occur if and only if η_C and V are small compared to E (*A* & *C* on Fig. 3(c)). The current density at the sides of the crack can be small only if the available e.m.f. is not large compared to η_A on a surface which is not yielding (Fig. 3(d)). A stress-corrosion crack can be formed only if these conditions are met and if activation polarization at the advancing edge is reduced by yielding.

If the conditions in the crack are such that a film can form on the crack sides the picture is similar, except that the total polarization on the advancing edge at low rate of propagation, and that on the sides of the crack are increased (Fig. 4(a)). These effects are more marked the more complete the film. A crack can be formed with a higher e.m.f. than if no film is formed, and η_C and V could be larger. This is the case originally considered by Hoar and Hines.[9]

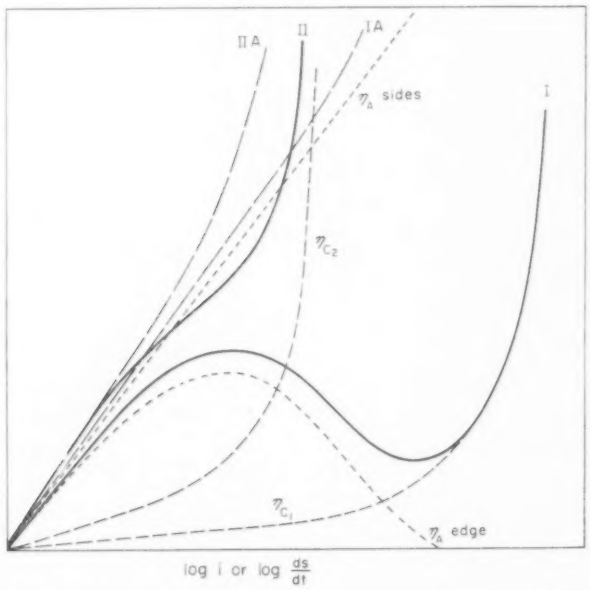

FIG. 3. Polarization curves and load lines for stress-corrosion cracks formed under conditions such that film-formation cannot occur. η_A is assumed to be reduced by yielding. (a) Activation (η_A), concentration (η_C) and total ($\eta_A + \eta_C$) polarization curves. Curves I and IA are total polarization curves for the advancing edge and crack sides respectively when η_C is small, and curves II and IIA are the corresponding curves when η_C is large.

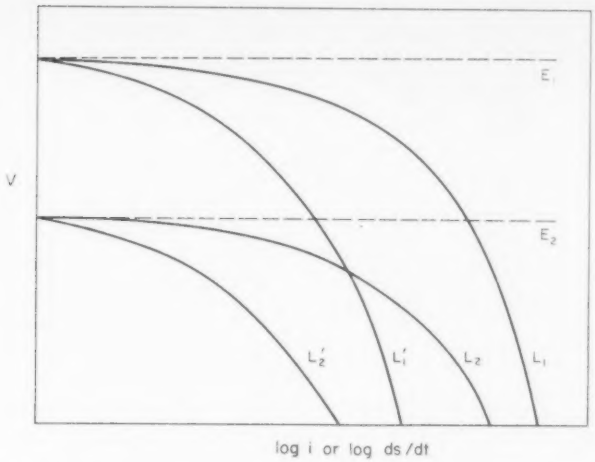

FIG. 3. (b) Load lines for large and small available e.m.f.'s and crack resistances.
$L_1 = E_1 - V_1$, $L_2 = E_2 - V_1'$, $L_1' = E_1 - V'$, $L_2' = E_2 - V$ when $E_1 > E_2$, $V' > V$.

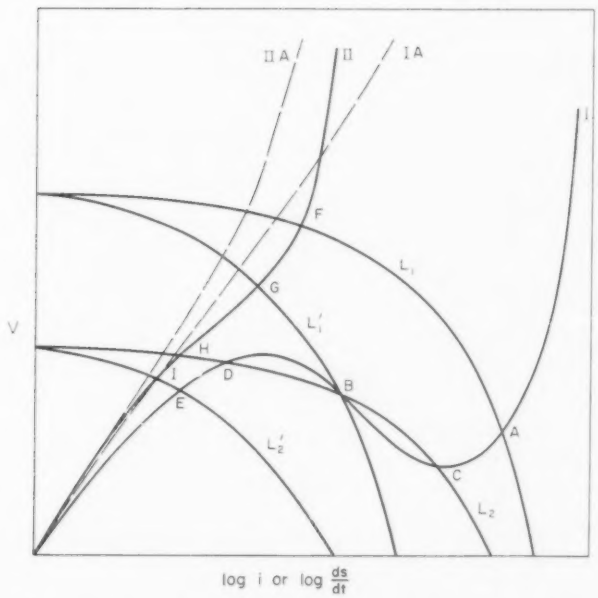

FIG. 3. (c) Combination of total polarization curves and load lines from (a) and (b).

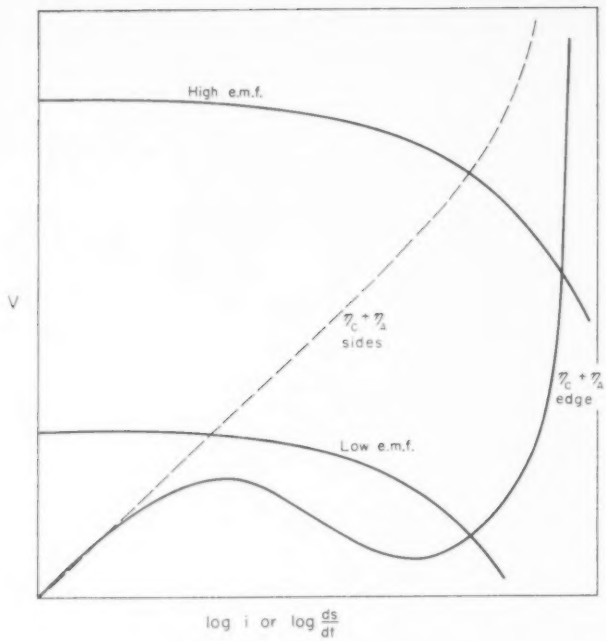

FIG. 3. (d) Total polarization curves for advancing edge and crack sides and load line corresponding to a normal and a very high e.m.f. The current density at the crack sides is not small compared to that at the advancing edge if E is relatively large.

Total polarization curves of the form of those in Fig. 3(a) can also be obtained if the sides of the crack are filmed and yielding has no effect on η_A but merely disrupts the film at the advancing edge. At the advancing edge, η_F decreases as the rate of propagation increases. (Fig. 4(b).) In this case, which is that considered by Logan,[7] rapid propagation is possible only when the available e.m.f. is large compared with $(\eta_A + \eta_C)$, and the current density on the sides can therefore be small only if the conditions in the crack are such that the film is maintained in a state of complete, or almost complete, repair—i.e. if η_F is also large. The condition of the film on the crack sides is much more important than in the previous case.

Three other important features are common to all three cases:

(i) In general, crack propagation must either be fast or very slow—i.e. the curves intersect at current densities much, or only a little, greater than those occurring on the crack sides. Under certain conditions two stable intersections are possible, one fast and one slow; the intermediate case (e.g. B, Fig. 3(c)) is unstable. Moreover, η_C is not very sensitive to crack geometry, so that the rate of rapid propagation should vary little with the conditions.

(ii) The mean strain rate at the crack tip decreases as the crack deepens, and the total polarization curve thus changes as indicated in Fig. 5. As the crack deepens a point is reached where rapid propagation is no longer possible and the rate of propagation falls rapidly to a low value. The mean strain rate is independent of other factors

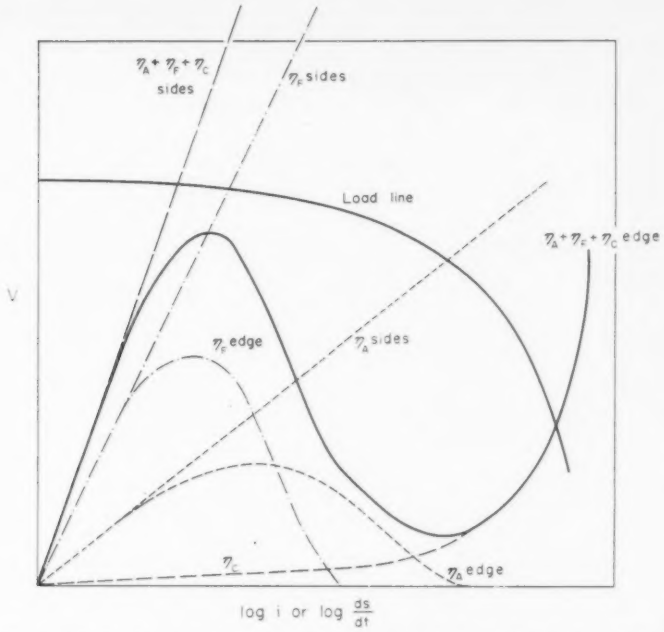

FIG. 4. Total polarization curves and load lines for a crack formed under conditions such that a film can form on the crack sides.
(a) If both η_F and η_A are reduced by yielding.

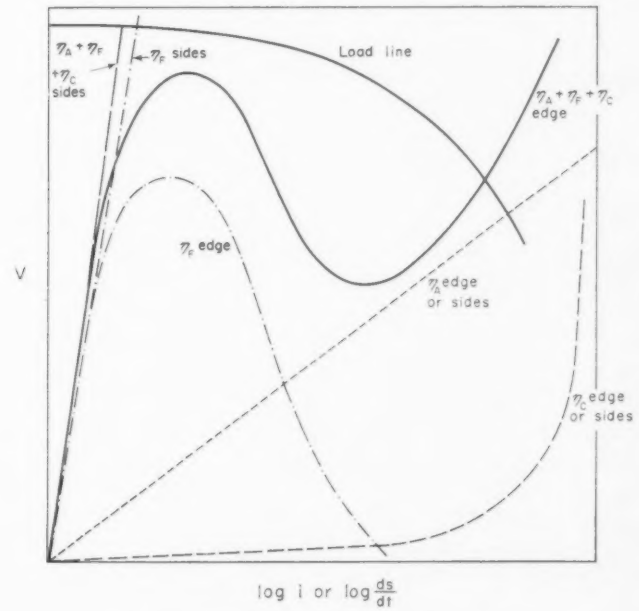

(b) If only η_F is reduced by yielding.

such as the crack form and the applied stress; hence a limiting depth should be obtained which varies little with the conditions.

(iii) Cracks can be formed only if E lies within a relatively narrow range, so that the total length of advancing edge is determined by the current available at a given value of E.* Mild polarization of the specimen as a whole using an external electrode

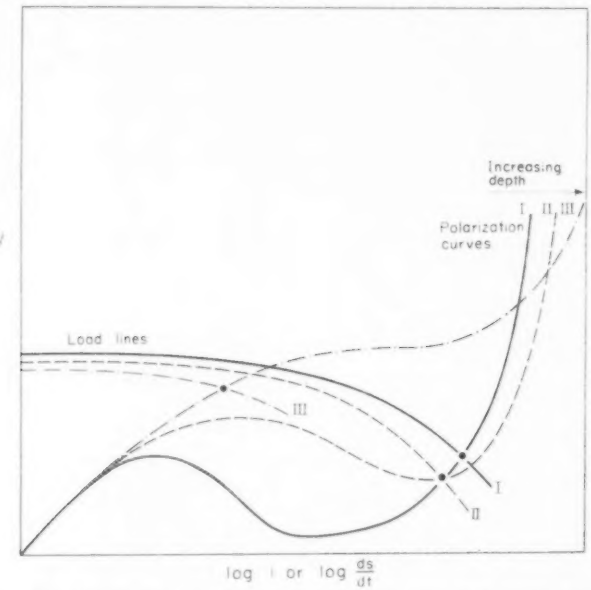

FIG. 5. Variation of total polarization curves and load lines with crack depth. Rapid propagation becomes impossible below a limiting depth (between curves II and III). The case considered is that of Fig. 3, but a similar situation arises if a film is present.

should alter the number of cracks formed and/or the extent to which branching occurs, but have little or no effect on the rate of propagation; more extensive polarization, either anodic or cathodic, should make crack formation impossible. Changes in the environment which alter cathodic polarization (e.g. addition of oxidizing agents) should have similar effects.

CRACK PROPAGATION IN AUSTENITIC Cr–Ni STEELS

The behaviour of the proposed crack-model is generally consistent with the features of crack propagation listed above, and it is thus desirable to consider a particular case in detail. The development of stress-corrosion cracks in austenitic Cr–Ni steels in chloride solutions has been extensively examined, and the electrochemical factors involved have also been studied in more detail than in other cases; this is therefore the best example for detailed consideration. The more important observations are as follows:

(i) Crack development can be divided into two stages, whose relative duration

*Note added in Proof. Since this paper was written, BRENNART (*Jernhonter Ann.* **144**, 560 (1960)) has obtained evidence which confirms this prediction for the case of austenitic Cr-Ni steels.

varies with the specimen size and form and the type of loading.[20, 21] Initially the crack is fine and shows little tendency to branch. Penetration is rapid at first, but its rate falls off sharply once a depth of 0·03–0·04 cm is reached. Sideways spreading continues, however, and the crack develops to a uniform depth over much of the periphery of a cylindrical specimen; slow penetration continues during this stage, and at low stresses fine unbranched cracks may eventually extend to much greater depths. The second stage is the development from the largest fine cracks of open, branched cracks with a markedly "Vee-shaped" section, which advance rapidly until complete fracture occurs. Only a few open cracks are formed, and the development of fine cracks ceases completely shortly after the appearance of the first open crack.[20, 21] Other workers have also noted an apparent limiting depth of 0·03–0·05 cm[8, 22, 23] on both cylindrical and sheet specimens.

(ii) The tip of a fine crack is much narrower than that of an open crack of similar depth, and an open crack forms from a fine crack at the depth at which the latter is a little more than 0·5μ wide. The values of the effective yield stress, Σ, calculated using equation (1) for open cracks, show reasonable agreement with the bulk properties of the material. Values calculated for fine cracks are much larger than would be expected from the bulk properties (Appendix III).

(iii) The first stage, the development of fine cracks, is not accompanied by a detectable change in corrosion potential, but the potential falls continuously during the second stage.[21] Anodic action ceases at —150 mV (approx., hydrogen scale);[10, 11, 24] this is not a true reversible potential and may be called the "zero-current" potential. The measured potential near the specimen surface is 50–80 mV more noble than this value during the first stage but the difference may be as little as 20–30 mV shortly before final fracture.

The corrosion currents flowing during crack propagation have been estimated by two independent methods which agree well,[10, 21, 23] and the current available is more than adequate to amount for crack-formation.

(iv) The overall rate of propagation during the second stage is almost invariably in the range 0·1–0·4 cm/h, but the rate of propagation of fine cracks varies considerably with time and between different parts of the crack; it appears, however, that it is either 0·1–0·4 cm/h or much less.[21] Several other workers have observed rates of propagation in the range 0·1–0·5 cm/h using a variety of experimental techniques,[8, 23, 25, 28] and the rate of propagation is apparently unaltered when the potential of the surface is altered by mild polarization (either anodic[23] or cathodic[29, 30]) *before* cracking begins; such polarization merely alters the number of cracks formed. The rate of propagation is apparently unaltered by variations in alloy composition that may have a considerable effect on the crack-initiation process.[21]

(v) The potential/time curves are smooth even when sensitive instruments with a fast response are used[28] and there is thus no evidence of the large, transient increases in corrosion current which have been observed during crack-propagation in other systems.[31–34] These marked increases in current are probably due to the exposure of considerable areas of fresh (unpolarized) metal surface by mechanical cracking. The extension of the specimens during crack propagation is also smooth.[28, 30*] It

*The discontinuous extension reported by Hoar and Hines was due to "stick-slip" in the measuring system.

follows that mechanical cracking is confined to very short jumps if it occurs at all. There is some evidence that the progress of the end of a crack trace is jerky;[35] however, such evidence must be interpreted with caution, particularly if tunnelling occurs.[20]

(vi) The path taken by a crack bears no apparent relation to metallographic features, and cracks do not usually follow a single simple crystallographic plane for long distances.[20]

The behaviour of the crack model is obviously consistent with many of the above facts. It is, therefore, desirable to discuss the application of the model in some detail.

Electrochemical considerations

The available e.m.f. is less than 100 mV, and η_A on a non-yielding surface in acidified 42% $MgCl_2$ solution (in which the surface film must be almost entirely destroyed) is 100–200 mV at a current density of the order of 1 A/cm² [11, 30] (which corresponds to penetration by uniform anodic dissolution at about 0·2 cm/h). Thus crack-propagation would be impossible unless η_A was reduced by yielding—i.e. Logan's mechanism cannot be applied to the present case. The surface film is probably largely destroyed even in non-acidified hot concentrated chloride solutions, so that crack-propagation in austenitic Cr–Ni steels in chloride solutions is an example similar to the first case discussed above (that in Fig. 3) rather than to the case originally considered by Hoar and Hines (Fig. 4(a)).

Three stages of crack development are of particular interest: the initial rapid penetration of fine cracks; the subsequent slower penetration of fine cracks, and the final rapid propagation of open cracks. If the values of Σ for fine and open cracks are respectively taken as 400 and 150 ton/in² (Appendix III), and if it is assumed that the largest fine crack is about 0·5μ wide, the values of tip radius ξ, the mean strain rate at the tip, $\frac{1}{\xi} \cdot \frac{d\xi}{dt}$, and the ohmic potential drop down the crack, V, shown in Table 1 may be calculated. These values show how these quantities vary with crack depth and applied stress for the two types of crack.

Rapid propagation of fine cracks

At about 0·5–1·0 A/cm² η_A becomes negligible at a microscopic strain rate of about 0·1 per cent/sec[11] but the true critical strain rate for a small area is probably a little larger than this, say 0·5 per cent/sec. In the early stages of development of a fine crack the average strain rate at the tip is of the order of the critical strain rate when the rate of propagation is about 0·2 cm/h, and η_A will be small. The ohmic potential drop down a shallow crack is also small. It seems, therefore, that the major part of the available e.m.f. is dissipated in overcoming concentration polarization. Hoar and West found that η_C was of the order of 500 mV for a surface dissolving anodically at a current density of *circa* 0·5 A/cm². The stirring produced by the yawning of the crack draws fresh solution into the crack, and the average current density at the advancing edge is less than that required for uniform dissolution at a rate equal to the rate of propagation, so that a value of about 50 mV for η_C at the advancing edge is reasonable. This value suggests that η_C is beginning to increase rapidly with current density, and the configuration of total polarization curves and load lines is probably similar to that indicated in Fig. 6(a) (Curves I and II). Rapid

TABLE 1. CALCULATED VALUES OF THE TIP RADIUS, THE MEAN STRAIN RATE AT THE CRACK TIP AND THE OHMIC POTENTIAL DROP FOR TYPICAL STRESS-CORROSION CRACKS IN AUSTENITIC CR–NI STEELS. THE VALUES ARE CALCULATED USING EQUATIONS (1), (3) AND (4).

Crack depth, s, (cm)	0·01	0·03	0·05	0·07	0·10	0·30	0·50
Mean radius of Crack Tip, ξ, (4) and Potential drop down crack, V, (mV).							
Fine Cracks (1)							
Stress 15 ton/in². ξ. (3)	0·14	0·42	0·70	—	—	—	—
V. (10)	0·35	0·50	0·65	—	—	—	—
Stress 10 ton/in². ξ. (4)	0·06	0·19	0·31	0·44	—	—	—
V. (9)	0·20	0·61	1·03	1·44	—	—	—
V. (10)	0·93	1·3	1·7	2·2	—	—	—
V. (11)	1·7	2·1	2·5	2·9	—	—	—
5 ton/in². ξ. (5)	0·016	0·047	0·078	0·11	0·16	0·47	—
V. (10)	2·8	3·8	4·9	5·9	7·5	18	—
Open Cracks (2)							
15 ton/in². ξ. (6)	—	3·0	5·0	7·0	10	30	50
V. (10)	—	0·05	0·07	0·08	0·11	0·27	0·43
10 ton/in². ξ. (7)	—	—	2·2	3·1	4·4	13	22
V. (9)			0·10	0·15	0·22	0·66	1·10
V. (10)			0·19	0·23	0·29	0·70	1·13
V. (11)			0·28	0·33	0·39	0·80	1·19
5 ton/in². ξ. (8)					1·1	3·3	5·5
V. (10)					0·8	1·9	3·1
Mean strain rate at crack tip, $\frac{1}{\xi}\frac{d\xi}{dt}$, (%/sec.)							
Rate of propagation 0·4 cm/h	1·11	0·37	0·22	0·16	0·11	0·037	0·022
$\frac{ds}{dt}$ 0·2 cm/h	0·56	0·18	0·11	0·078	0·056	0·019	0·011
0·1 cm/h	0·28	0·092	0·056	0·040	0·028	0·009	0·006
0·01 cm/h	0·028	0·009	0·006	0·004	0·003	0·001	0·001

NOTES: (1) Σ = 400 ton/in² (2) Σ = 150 ton/in²
(3) k_2 = 100, (4) k_2 = 300,
(5) k_2 = 700, (6) k_2 = 10,
(7) k_2 = 30, (8) k_2 = 70,
(9) $\frac{ds}{dt}$ = 0·0 (10) $\frac{ds}{dt}$ = 0·2 cm/h
(11) $\frac{ds}{dt}$ = 0·4 cm/h

In calculations of V, based on equation (3), the following values are assumed:
$I = 5 \times 10^{-5}$ A/cm²; $i = 0{\cdot}72 \frac{ds}{dt} \times 10^{-6}$ A/cm^{-2}; $\rho = 2\ \Omega$ cm

crack-propagation should therefore cease at a depth such that the critical strain rate is just not reached at the advancing edge—i.e. such that η_A is beginning to increase as the crack deepens. If the rate of propagation is taken as 0·2 cm/h, the critical strain rate as 0·5 per cent/sec and the maximum strain rate at the crack tip as twice the average, the limiting depth for fine cracks should be about 0·025 cm, which is astonishingly close to the observed value.

If η_C is considerable in a fine crack and the e.m.f. available is just sufficient to overcome it, the development of fine cracks should cease once open cracks have formed and the available e.m.f. is reduced. This is what is observed experimentally.

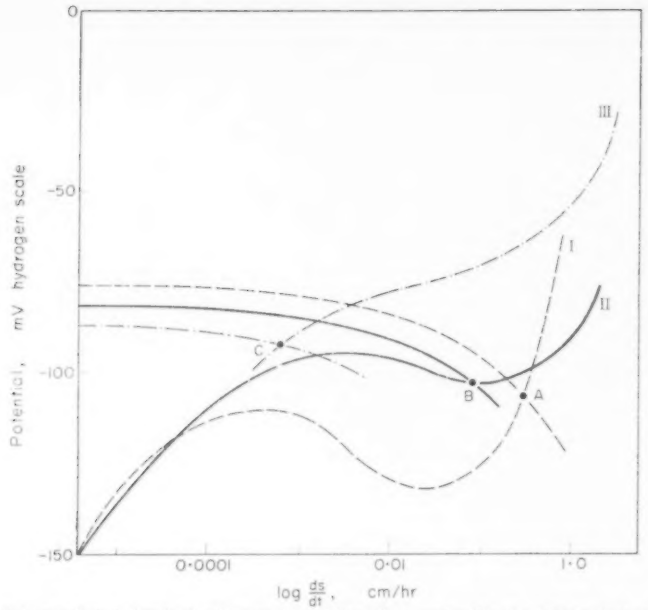

FIG. 6. Schematic total polarization and load lines for austenitic Cr–Ni steels in chloride solutions. η_F is assumed to be zero. The scales quoted are only approximate.
(a) Fine cracks. I and II represent conditions during the initial stage of rapid propagation and III the slow propagation once the limiting depth is reached, assuming that the crack advances uniformly during this stage.

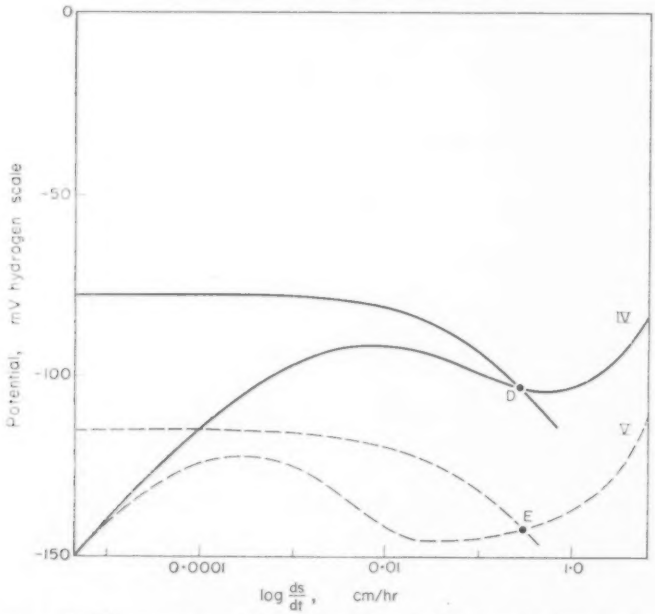

(b) Open cracks. IV represents uniform propagation and V a crack advancing in a series of short bursts.

Slow propagation of fine cracks

In a deep fine crack the ohmic potential drop is large and almost independent of the rate of propagation, the maximum strain rate at the crack tip cannot be very much greater than the average, and the average strain rate must be much smaller than the critical strain rate unless the rate of propagation is much greater than 0·5 cm/h. Moreover, the concentration of anodic reaction products is large and stirring due to yawning cannot be very effective. Hence the total polarization must be high and the ohmic potential drop considerable, and rapid crack propagation is thus impossible (Fig. 6(a), Curve III).

Cracks of this type could advance by local bursts of rapid propagation rather than by slow continuous propagation. A burst could be initiated either because slow corrosion at the crack tip exposes a weak region in the metal or because development of other parts of the crack raises the stress at part of the crack tip and so induces yielding. Stress-corrosion cracks develop in tongues or lobes which can penetrate for considerable distances,[20] and it may well be that a similar effect occurs on a much smaller scale. This type of behaviour is consistent with the mode of yielding of austenitic Cr–Ni steels, in which slip is almost completely confined to a few planes; it might be expected that at any instant yielding would occur more easily at some parts of the crack tip than at others.

Rapid propagation over short distances of small parts of the crack tip would involve a smaller ohmic potential drop than would uniform penetration at the same, or even a lower rate. Moreover, local rapid yielding might well produce a greater stirring effect than slower general yielding, particularly if solid corrosion products are present;[19] it may be that fresh solution can reach the region of the tip only if propagation occurs in bursts.

Rapid propagation of open cracks

When an open crack forms the tip widens and the ratio k_2 is reduced, so that the ohmic potential drop down the crack and the ratio (volume of solution within the crack)/(volume of metal dissolved) are reduced and the efficiency of stirring is increased; η_C is thus also reduced. The total polarization curve is of the form of curve IV, of Fig. 6(b) and rapid propagation is possible with a reduced available e.m.f. However, during the later stages of the development of open cracks the available e.m.f. and the mean strain rate at the crack tip is very small, and rapid propagation is unlikely if the maximum strain rate at the tip is only a little greater than the mean. It seems probable, therefore, that particularly rapid yielding occurs at points of weakness at the crack tip, which is no longer narrow compared to the spacing of defects in the lattice. The fact that the tip is wide also helps to achieve a high strain rate over a reasonable width even though the mean strain rate is low. Rapid propagation could occur in this way even if the potential of the cathode fell considerably.

It is quite possible that the cracks advance by a succession of local bursts occurring at points where rapid yielding can occur most easily. The instantaneous rate of propagation must be appreciably higher than the average of 0·1–0·5 cm/h, but as particularly rapid local yielding is involved, stirring may locally be very violent and η_C correspondingly reduced. Indeed, it may well be that intermittent very rapid local

propagation is energetically preferable to slower, more uniform propagation, and that this is the normal mode of propagation.

The path taken by cracks

In an austenitic steel, slip is normally confined to a relatively small number of {111} planes (1–5μ apart), cross slip being almost impossible because of the very low stacking fault energy;[36] the amount of slip which can occur on a single plane is limited by piling-up of dislocations. The tip of a fine crack is $<1\mu$ wide, and it is probable that only a single slip plane is operating. (The observed strain rate is equivalent to a dislocation flux of 10–20/sec on a plane at 45° to the direction of propagation, and this is by no means an impossibly high value.) Slip on a plane of this type could not, however, account for all of the yielding at the tip, some of which is in a direction perpendicular to the slip plane, and it may be that localized cross slip occurs in the immediate vicinity of the surface or that the surface layers, weakened by partial dissolution, yield without the assistance of dislocations. Either process would require a higher stress than would normal slipping, and would thus account for the high effective yield stress that is observed.

The maximum strain rate should be in the immediate vicinity of the slipping plane and the crack should advance down this plane. Slip on a single plane can continue for only a limited period because piles-up form, but the crack would change to an intersecting plane on which slip can occur more easily; this process would be assisted by the removal (by dissolution) of the stress field associated with dislocations on the original plane. A rate of propagation of 0·2 cm/h (*circa* 0·5μ/sec) implied that about forty dislocations must be formed on a plane when the crack advances 1 μ, and as up to 10^3 dislocations can occur in a single pile-up, the crack need not change to an intersecting plane at the first opportunity; it is indeed, unlikely that it would do so unless the two sets of planes are approximately symmetrically arranged with respect to the stress system. In material that has been plastically deformed before cracking begins, some slip planes are not available as they have already operated, and cracks might follow a single plane for longer distances than in fully softened specimens.

The cracks should thus follow a zig-zag path made up of segments little more than 1 μ long in softened specimens; the segments may be longer in cold worked material. However, yielding at the crack tip, dissolution on the crack sides, and the effects of polishing and etching during preparation of a metallographic section will all tend to obscure the zig-zag nature of the crack path. The apparent crack path will thus bear no obvious relation to the crystal lattice in fully softened specimens, although some "crystallographic" segments may be distinguishable in cold worked specimens. These predictions agree well with experimental observations on fine grained material.[20] In specimens containing very large grains, cracks do not, in general, follow simple crystallographic planes, but Denhard[37] found that a minority of cracks follow {111} planes for relatively long distances. More slip might well occur on a single plane in a large than in a small grain. Denhard also reports that the portion of a crack immediately behind the tip often lies on a {111} plane, and Nielsen has observed small steps at intervals of 1–5 μ on fracture surfaces;[19] these observations may be direct evidence that the crack path is made up of short segments each of which is on a {111} plane.

The tip of an open crack is relatively wide, and it is noteworthy that branching,

which is rare in fine cracks, usually occurs at the same time as a crack opens up. This suggests that the tip of an open crack intersects slip planes of at least two systems, and it is not surprising that the effective yield stress is consistent with the bulk property.

Crack initiation

Cracks are initiated from corrosion damage on a microscopic scale at "active sites" on slip bands,[38] the number of sites is markedly increased by cold working,[21, 39] and the major effect of changes of alloy composition is on the duration of the induction period, not on the rate of crack-propagation.[21] It also appears that crack initiation is controlled by elastic strain energy and that yielding plays no part in the rate-controlling stage, since the variation of the stress dependence of the induction period with alloy composition is much simpler if comparisons are based on true stress than if account is taken of plastic properties, by, for example, representing stress as a fraction of the yield stress.[40]

Crack initiation requires a transition between surface corrosion and true crack propagation. The above facts suggest that preferential dissolution of some feature forms a notch similar in form to a crack (a deep narrow trench rather than an etch-pit) and that true crack propagation begins when the stress at the tip of the notch becomes sufficient for appreciable yielding to occur. Preferential corrosion of even highly strained material would not be expected to produce a concentration of attack of the order required for crack-propagation: it seems more likely that an intermediate stage involving some slow yielding is necessary.

Any identification of the features from which cracks are initiated can only be tentative. It seems reasonable to assume, however, that they are essentially two dimensional and steeply inclined to the surface. One possibility is a suitably orientated dislocation pile-up. In this case the first stage is, presumably, preferential dissolution of the highly strained region at the head of the pile-up; this process might well be controlled by elastic strain energy. This dissolution will, however, tend to destroy the barrier against which the dislocations are piled up and in suitable cases the dislocations may run out at the surface, assisting in the formation of a deep narrow trench. This process differs from the process of crack-propagation in that, although movement of dislocations is involved, the operation of a dislocation source is not required.

Other features which might act as starting points are stacking faults. The energy density associated with these defects is much less than that at piles-up, so that crack initiation from a stacking fault seems the less likely; however, marked preferential corrosion of stacking faults has been reported in some copper-base alloys.[17]

Effects of alloy composition

Variations in alloy composition have little effect on the rate of crack propagation;[21] this supports the view that the rate depends on concentration polarization, and it may be evidence that the rate-determining stage is transport of anions to the anode surface. On the other hand, the duration of the induction period is greatly altered by some compositional changes, and the effects cannot be explained by variations in the reactions in the original surface film (which may be followed by potential measurements[9]). The onset of crack propagation is thus delayed by some variations in composi-

tion, either because crack propagation is more difficult or because features from which cracks can be initiated easily are absent.

Although several effects of composition on stress-corrosion cracking resistance have been established, there are few data on the corresponding effects on other properties. However, interesting correlations appear to exists in two cases. Ferritic stainless steels, and δ–ferrite and martensite present in some "austenitic" steels, are much more resistant to stress-corrosion cracking than is austenite containing 16–20% Cr and 6–12% Ni, and the resistance of austenitic steels is increased by an increase in nickel content; alloys containing more than 50% Ni appear immune.[41] Cross slip occurs more easily and the slip separation is finer in both classes of resistant material than in 18–8 steels, indicating that the stacking fault energy is higher. Moreover, Hoar and West[11] found that mild steel and nickel, which have similar slip characteristics to the resistant materials, did not suffer a reduction in activation polarization on yielding.

Three possible explanations of the resistance of the ferritic steels and of the high-nickel alloys are:

(i) Piles-up are confined to a single plane to a much greater extent and are more widely spaced in 18–8 steels than in alloys of higher stacking fault energy, and large stacking faults are more numerous. Crack initiation is therefore unusually easy in 18–8 type steels.

(ii) According to the crack model, electrochemical crack propagation can occur only if a high strain rate is maintained at the advancing edge; this may well be possible only if yielding is concentrated, in this case because it is confined to relatively few planes.

(iii) In Fe–Cr–Ni alloys it seems that electrochemical crack-propagation is possible only if activation polarization is reduced by yielding. Hoar and West's evidence indicates that this condition may not be met in the resistant alloys.

It is tempting to suggest that these approaches are equivalent—i.e. that they are all consequences of the low stacking fault energy of the 18–8 type steels. As yet, however, it is by no means certain that this is the case; further experimental work would clearly be of considerable interest.

DISCUSSION

Crack propagation in austenitic Cr–Ni steels

A model based on the assumption that stress-corrosion cracks are formed by the dissolution of rapidly yielding material at the crack tip can explain qualitatively, and in some cases quantitatively, most if not all of the known facts on the development and properties of stress-corrosion cracks in austenitic Cr–Ni steels. Some of the features readily explained by the electrochemical mechanism are difficult to interpret if crack propagation is predominantly mechanical; this is particularly true of the limiting depth at which rapid propagation of fine cracks ceases. The electrochemical mechanism also leads to possible explanations of the marked susceptibility of these alloys; explanations which are plausible and capable of being checked by experiment. In this case, the simple film-rupture mechanism proposed by Logan must be rejected in favour of the Hoar/Hines mechanism; indeed the original picture considered by Hoar and Hines appears to be slightly incorrect as surface films probably play no part in the process.

Other cases of stress-corrosion cracking

Electrochemical crack propagation of the type discussed above may well occur in other cases of stress-corrosion cracking. The essential conditions are:

(i) the current density at the crack tip is greater than that at the sides of the crack and on the specimen surface.

(ii) concentration polarization at the advancing edge and the ohmic potential drop down the crack are relatively small, and

(iii) that yielding is concentrated either because cross-slip is difficult or because of the distribution of a precipitate.

The first condition can be met only if relatively little corrosion occurs in the absence of stress. With an active metal in an environment which produces almost complete passivity, Logan's film-rupture mechanism might be applicable; possible cases are titanium, aluminium or magnesium alloys, and, less likely, mild and low-alloy steels. In more noble alloys it is probably essential that activation polarization is reduced by yielding at the advancing edge, although even in these cases some film-formation may be necessary on the crack sides.

Stress-corrosion cracks might be formed electrochemically even if yielding at the tip (which must necessarily occur) plays no part other than to open the crack up. If, for example, paths of material susceptible to corrosion exist in a matrix which is essentially immune, a fine crack could be formed, but the rate of propagation would

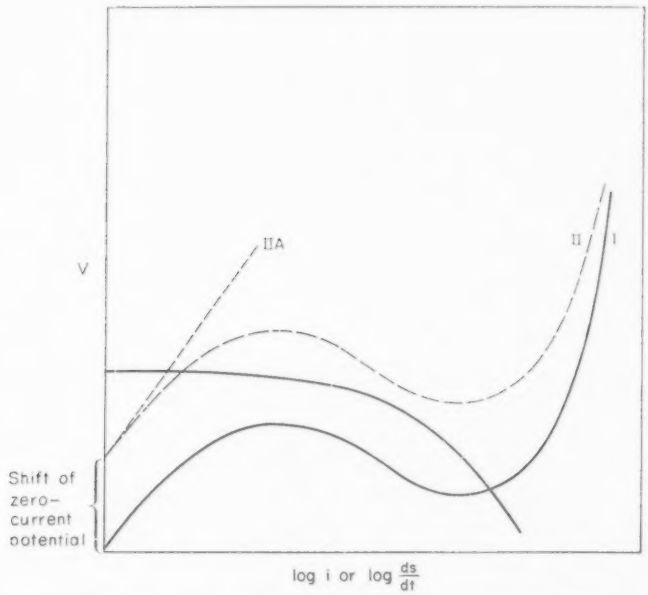

FIG. 7. Hypothetical case where rapid propagation is possible only if the anodic zero-current potential at the crack tip is lower than that at the crack-sides.
I total polarization of advancing edge.
IIA total polarization at crack sides.
II total polarization at advancing edge if no shift of the zero-current potential occurred.

probably be rather low. The conditions required for this type of attack have been discussed by Graf.[42–44] Local differences in electrochemical activity might also be important in cases where electrochemical crack-propagation occurs predominantly by the mechanisms discussed above. It is conceivable that a lowering of the effective anodic zero-current potential at the crack tip could allow crack-propagation by the Logan or Hoar/Hines mechanisms under conditions such that it could not otherwise occur (Fig. 7).

The condition that the ohmic potential drop down the crack be small is probably not very important, for it is greatly reduced by the inevitable yawning of the crack. The same may be true of the condition that concentration polarization be small. There is, in fact, little variation in the form of cracks from one system to another, and it may be that concentration polarization also varies only slightly—this would account for the fact that very similar rates of propagation have been reported in a number of systems. However, many cases of stress-corrosion cracking involve chloride or hydroxyl ions, which readily form solvated or complexed cations and are also highly polarizable.[45] These properties may be essential if current densities of the order of 1 A/cm^2 are to be maintained with limited concentration polarization. (There is strong evidence that mechanical cracking is important in nitrate cracking, which is the most prominent example in which chloride or hydroxyl ions appear unimportant.)

In the f.c.c. Fe–Cr–Ni and copper-base alloys susceptibility to transgranular stress-corrosion cracking seems to be associated with an unusually low stacking-fault energy, and this may also be true in other cases where cracks do not follow microstructural features. In age-hardening aluminium alloys cracking is usually intergranular, and it is therefore interesting that Thomas and Nutting[46] observed that yielding is confined to the immediate vicinity of the grain boundaries when the alloy is near to the condition of maximum hardness, which is also the condition of maximum susceptibility to stress-corrosion cracking. Thomas and Nutting suggested that the concentration of yielding was responsible for the susceptibility to stress-corrosion cracking.

This evidence suggests strongly that concentration of yielding is an essential condition for electrochemical crack propagation, and that the path taken by cracking depends on the mode of yielding. Cracks are transgranular when yielding is confined to relatively few planes within the grain, and intergranular when it is concentrated at the grain boundaries by the distribution of a precipitate, or possibly, of tesselated stresses. The concentration of yielding is probably the most general of the three reasons advanced above for the susceptibility of 18–8 type steels. Cracks could probably be initiated at features other than piles-up or stacking faults, and in other systems electrochemical crack-propagation might occur if yielding does not reduce activation polarization.

It is not, of course, suggested that stress-corrosion cracks always advance electrochemically. In some aluminium alloys after certain heat treatments rates of propagation at least of 1 cm/sec have been recorded,[33] and in other cases where the average rate of propagation is lower the evidence for mechanical cracking is very strong – e.g. when large transient increases in corrosion current and sudden extensions occur simultaneously.[31, 34] These effects have, however, been reported only in cases where cracking is intergranular and there is at least a plausible explanation for grain-

boundary weakness. In cases where the evidence for mechanical cracking is less strong, it seems logical to accept the simpler electrochemical mechanism. This course does not rule out the possibility that a little mechanical cracking occurs even when cracking is predominantly electrochemical – e.g. two parts of the crack formed electrochemically may join up mechanically.[20]

CONCLUSIONS

1. Stress-corrosion cracks can be formed only if the rate of penetration of the tip is much greater than the rate of attack on the crack sides or the rest of the surface. This condition can be obtained whether crack-propagation occurs by purely electrochemical processes or mechanical stages are involved. The former provides the simpler process in many cases, as unless the reason for localized mechanical failure is obvious, attempts to explain it leads to considerable complication.

2. Electrochemical crack-propagation is possible if—
   (a) the total polarization at the crack tip is much less than that at the crack sides. This condition can be met if activation polarization for anodic dissolution is reduced by the yielding that necessarily occurs at the crack tip or if this yielding disrupts a passive film present on the crack sides.
   (b) the polarization at the crack sides is large compared to difference between the anodic zero-current potential and the potential near the external cathodes (the corrosion potential).
   (c) yielding at the crack tip is concentrated either because cross slip is difficult or because yielding is localized by the distribution of stress or a precipitate near a grain boundary.
   (d) concentration polarization at the crack tip in the crack and the ohmic potential drop down the crack are relatively small. This condition may not be important, for these quantities are greatly reduced by the yawning of the crack associated with yielding at the tip. It is possible, however, that a low concentration polarization can be obtained only if certain anions are present.

3. In the case of the austenitic Cr–Ni steels in chloride solutions, most, if not all, of the known facts concerning crack development can be explained in terms of electrochemical crack propagation in which the attack is concentrated at the crack tip because the activation polarization for anodic dissolution is reduced by yielding. Surface films probably play little part. There is no evidence that mechanical cracking plays an important part in crack propagation and the electrochemical mechanism, which is essentially that proposed by Hoar and Hines, must be regarded as the most satisfactory available mechanism.

4. Similar mechanisms may apply in other cases of stress-corrosion cracking if the conditions in (2) above are met. It is clear, however, that mechanical cracking does play an important part in some cases of crack propagation, and in a few cases cracking probably occurs predominantly by mechanical processes; some electrochemical action is essential in all cases.

Acknowledgements—I am very grateful to Dr. F. C. Roesler for a suggestion which led to an important part of the basis of this paper, and to Mr. E. R. W. Jones for many stimulating and fruitful discussions.

REFERENCES

1. E. H. DIX, *Trans. Amer. Inst. Met. Engrs.* **137,** 11 (1940).
2. R. B. MEARS, R. H. BROWN and E. H. DIX, *Symposium on Stress-Corrosion Cracking*, 323. A.I.M.M.E./A.S.T.M. Philadelphia (1945).
3. J. T. WABER, *Theory of Stress-Corrosion Cracking of Mild Steel*, p. 80. Corrosion Publishing Co., Pittsburgh, Pa. (1947).
4. H. H. UHLIG, M. LINCOLN and A. WHITE, *Acta Met.* **5,** 473 (1957).
5. H. H. UHLIG, *Physical Metallurgy of Stress-Corrosion Fracture*, p. 1. Interscience, New York (1959).
6. D. K. PRIEST, *J. Electrochem. Soc.* **106,** 358 (1959).
7. H. L. LOGAN, *J. Res. Nat. Bur. Stand.* **48,** 99 (1952).
8. H. L. LOGAN and R. J. SHERMAN, *Welding J. N.Y.* **35,** 389 (1956).
9. T. P. HOAR and J. G. HINES, *J. Iron St. Inst.* **182,** 124 (1956).
10. T. P. HOAR and J. G. HINES, Proceedings of 8th Meeting, C.I.T.C.E., Madrid (1956), p. 273. Butterworths, London (1958).
11. T. P. HOAR and J. M. WEST, *Proc. Roy. Soc.* A, In press.
12. F. H. KEATING, *International Stresses in Metals and Alloys*, p. 311. *Inst. Met. Lond.* (1948)
13. U. R. EVANS, *Internal Stresses in Metals and Alloys*, p. 291. *Inst. Met. Lond.* (1948): *Corrosion* **7,** 238 (1951).
14. U. R. EVANS, *Stress-Corrosion Cracking and Embrittlement*, p. 158. Wiley, New York (1956).
15. T. P. HOAR and C. J. BOOKER, Work reported at 1st Meeting of the Corrosion Science Society, London, 1960.
16. A. J. FORTY, *Physical Metallurgy of Stress-Corrosion Fracture*, p. 99. Interscience, New York (1959).
17. R. P. SWANN and J. NUTTING, *J. Inst. Met.* **88,** 478 (1960).
18. F. C. ROESLER, Private Communication, 1959.
19. N. A. NIELSEN, *Physical Metallurgy of Stress-Corrosion Fracture*, p. 121. Interscience, New York (1959).
20. J. G. HINES and R. W. HUGILL, *Physical Metallurgy of Stress-Corrosion Fracture*, p. 193. Interscience, New York (1959).
21. J. G. HINES, *Corros. Sci.* **1,** 2 (1961).
22. D. BIRCHON, Private Communication, 1958.
23. H. H. UHLIG and M. LINCOLN, *J. Electrochem. Soc.* **104,** 167C (1957).
24. J. G. HINES and T. P. HOAR, *J. Appl. Chem.* **8,** 764 (1958).
25. C. EDELEANU, *J. Iron St. Inst.* **173,** 124 (1953).
26. C. EDELEANU, *Physical Metallurgy of Stress-Corrosion Fracture*, p. 126. Interscience, New York (1958).
27. W. W. KIRK, F. H. BECK and M. G. FONTANA, *Physical Metallurgy of Stress-Corrosion Fracture*, p. 227. Interscience, New York (1958).
28. D. VAN ROOYAN, Private Communication, 1959.
29. J. G. HINES, Unpublished Work, 1956–7.
30. J. M. WEST, Thesis. University of Cambridge, 1958.
31. H. A. GILBERT and S. E. HADDEN, *J. Inst. Met.* **77,** 237 (1950).
32. R. N. PARKINS, *Stress-Corrosion Cracking and Embrittlement*, p. 140. Wiley, New York (1956).
33. H. K. FARMERY, Thesis. University of Cambridge, 1954.
34. H. J. ENGELL and A. BAUMEL, *Physical Metallurgy of Stress-Corrosion Fracture*, p. 341. Interscience, New York (1958).
35. T. P. HOAR and J. C. SCULLY, Private Communication, 1959.
36. P. B. HIRSCH, *J. Inst. Met.* **87,** 406 (1959).
37. E. E. DENHARD, Thesis. John Hopkins University, 1957: *Physical Metallurgy of Stress-Corrosion Fracture*, p. 224. Interscience, New York (1958).
38. K. W. LEU and J. N. HELLE, *Corrosion* **14,** 249 (1958).
39. J. G. HINES and T. P. HOAR, *J. Iron St. Inst.* **184,** 166 (1956).
40. J. G. HINES and E. R. W. JONES. *Corros. Sci.* **1,** (1961). In press.
41. H. R. COPSON, *Physical Metallurgy of Stress-Corrosion Fracture*, p. 247. Interscience, New York (1958).
42. L. GRAF, *Z. Metallk.* **38,** 193 (1947).
43. L. GRAF and J. BUDKE, *Z. Metallk.* **46,** 378 (1955).
44. L. GRAF, *Stress-Corrosion Cracking and Embrittlement*, p. 48. Wiley, New York (1956).
45. J. M. WEST, Private Communication, 1960.
46. G. THOMAS and J. NUTTING, *J. Inst. Met.* **88,** 81 (1959).

APPENDIX I

THE WIDTH OF THE TIP OF A CRACK AND DERIVATION OF EQUATION (1)

Consider the fine parallel-sided slit shown in Fig. 8(a). If the metal in which it is situated is stressed, there will be a considerable stress concentration at its tip and in general the yield stress will be exceeded in a region extending up to a distance ξ from the tip. The slit must, therefore, open up until its width is approximately equal to the diameter (2ξ) of the region in which the yield stress is exceeded (Fig. 8(b)). If the slit is an advancing crack the region in which the yielding occurs becomes larger and the crack must become wider as the crack deepens; the crack thus becomes wedge-shaped in section.

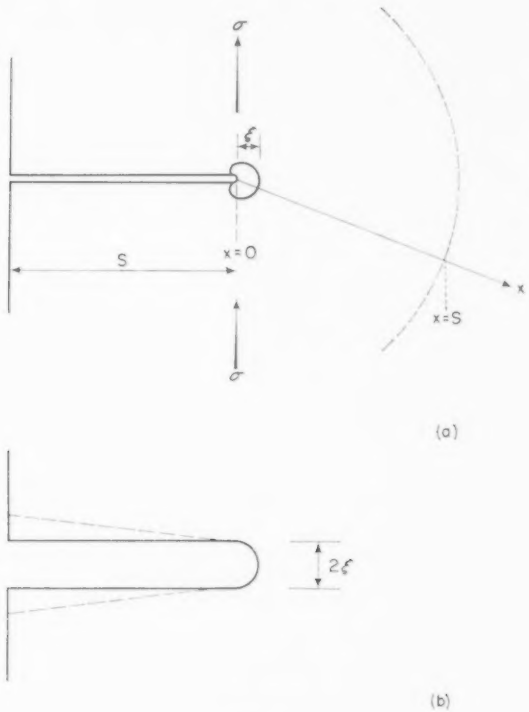

FIG. 8.

The elastic stress in the vicinity of the crack tip, σ', may be taken as proportional to x, where $\sqrt{x}$ is the distance from the tip.* Now for $x = s$, $\sigma' \geqslant \sigma$, where σ is the average applied stress.

It follows, therefore, that $\sigma' \geqslant \sigma\left(\frac{s}{x}\right)^{\frac{1}{2}}$.

Hence, if Σ is the effective yield stress at the crack tip,

$$\Sigma \geqslant \sigma\left(\frac{s}{\xi}\right)^{\frac{1}{2}},$$

whence $\xi > s\left(\frac{\sigma}{\Sigma}\right)^2$.

The lower limit of ξ is thus given by

$$\xi = s\left(\frac{\sigma}{\Sigma}\right)^2 = sk_1^2. \qquad \text{Equation (1)}$$

*Relations of this form have been derived for a number of cases by several authors, e.g. A. W. MAUE, *Z. Naturf.* **7a**, 387 (1952).

The true value of ξ is close to this limit as long as s is small compared to the diameter of the specimen. When this is not the case ξ is larger than the value given by equation (1); this may be accounted for by increasing σ.

APPENDIX II

THE OHMIC POTENTIAL DROP DOWN A STRESS-CORROSION CRACK

It is assumed that the cathodic reaction occurs only on the specimen surface outside the crack. A rigorous treatment is difficult, but an estimate can be made if it is assumed that:

(i) the current density on the sides of the crack is constant;

(ii) the equipotential surfaces within the crack are perpendicular to the axis of the crack. This is a reasonable assumption if the crack is fine; the ohmic potential drop is very small in an open crack so that in this case the error is not serious.

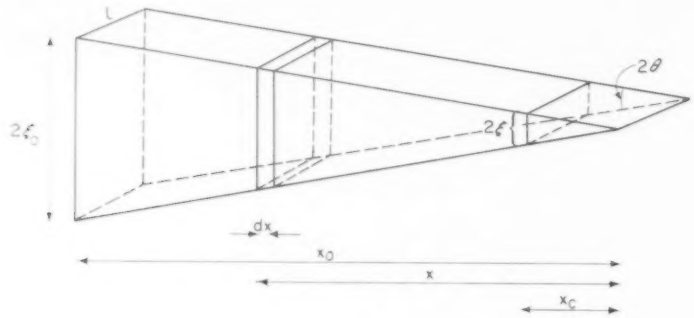

FIG. 9

Consider the crack shown in Fig. 9. The resistance of the element,

$$dR = \frac{\rho}{2l \tan \theta} \cdot \frac{dx}{x}.$$

Then if the current flowing to unit length of the advancing edge of the crack (i.e. the current responsible for propagation) is i, the current flowing to the advancing edge is il, and the potential drop over the element due to this current is

$$dV_1 = \frac{\rho i}{2 \tan \theta} \cdot \frac{dx}{x}.$$

If the current density on the crack sides is I, the current flowing to the sides of the crack below the element is $\dfrac{2Il\,(x - x_c)}{\cos \theta}$

and the potential drop over the element is

$$dV_2 = \frac{I\rho\,(x - x_c)}{\cos \theta \tan \theta} \cdot \frac{dx}{x} = I\rho \left(\frac{x - x_c}{\sin \theta}\right) \cdot \frac{dx}{x}.$$

The potential drop down the crack,

$$V = \int_{x_c}^{x_0} dV_1 + \int_{x_c}^{x_0} dV_2$$

$$= \frac{\rho i}{2 \tan \theta} ln \frac{x_0}{x_c} + \frac{\rho I}{\sin \theta}\left[x_0 - x_c - x_c\, ln \frac{x_0}{x_c}\right].$$

Now $x_0 - x_c = s$,

$\dfrac{x_0}{x_c} = \dfrac{\xi_0}{\xi} = \dfrac{\xi_0}{k_1^2} = \dfrac{1}{k_1^2 k_2}$ (as $\dfrac{\xi_0}{s} = \dfrac{1}{k_2}$, by definition),

$\sin \theta \simeq \tan \theta = \dfrac{\xi_0}{x_0} \simeq \dfrac{\xi_0}{s} = \dfrac{1}{k_2}$ (for small angles, and as $x_0 \gg x_c$),

and $x_c = \dfrac{\xi}{\tan\theta} = sk_1{}^2k_2$.

Hence $V = \dfrac{\rho ik_2}{2} ln \dfrac{1}{k_1{}^2k_2} + \rho Ik_2 \left[s - sk_1{}^2k_2 ln \dfrac{1}{k_1{}^2k_2} \right]$

$$= \rho k_2 s \left[\mathrm{I} - \left(\frac{i}{2s} - \mathrm{I}\, k_1{}^2k_2 \right) ln\, k_1{}^2k_2 \right],$$

which is equation (3).

APPENDIX III—SOME EXPERIMENTAL RESULTS

Most of the facts used in this paper have been published or will be published shortly. One important piece of evidence has not previously been published, and it is thus necessary to describe the results briefly here.

THE FORM OF STRESS-CORROSION CRACKS IN AUSTENITIC CR–NI STEELS

Measurement of cracks in metallographic sections shows that the ratio of depth to width at the mouth is much smaller for open cracks than for fine cracks, that for each class the ratio is smaller the higher the applied stress, and that at a given stress the ratio is approximately constant for a given type of crack. There is, however, some indication that the ratio is smaller in a very deep crack than in shallower cracks. These points are illustrated in Table 2. The observations are consistent with equations (1) and (2) above, if it is assumed that the effective yield stress, Σ, is greater for fine than for open cracks. In a very deep crack the applied stress is considerably increased by the reduction in cross section, and the ratio k_1 is thus larger and the ratio k_2 smaller than in a shallower crack.

The width of the crack tip is of particular importance, and it is unfortunate that it is very difficult to measure this quantity on a fine crack. These cracks are often narrower than the limit of resolution of an optical microscope and it is not easy to strip a replica for electron-microscope examination from a cracked region. Moreover, even where the two sides can be resolved the width is uncertain because of smearing during polishing or rounding during etching; these errors are not important with larger cracks. The values in Table 2 were determined with an optical microscope on specimens polished carefully using diamond dust (to minimize smearing) and lightly etched. The limit of resolution was taken as 0·4μ. It is clear from these values that the tip of a fine crack is much narrower than that of an open crack of similar depth, and that an open crack forms from a fine crack at the depth where the latter is a little more than 0·5μ wide.

If the tip radii in Table 2 are used to calculate the effective yield stress, Σ, the values obtained for open cracks are in the range 150–200 ton/in^2, whereas those for fine cracks are much larger, in the range 350–400 ton/in^2; this is consistent with the observed difference in the ratios k_2. If it is assumed that the yield stress at the tip of a crack is about three times that in simple uniaxial tension, a value of Σ of 150 ton/in^2 corresponds to a yield point in simple tension of about 50 ton/in^2, which implies that the material near the tip has undergone 20–30 per cent plastic strain. This seems reasonable, and is thus evidence that the assumption on which equation (1) is based is sound (i.e. that the width of the crack tip is approximately equal to the diameter of the region in which the yield stress is exceeded). There is no reason to believe that fine cracks are different from open cracks in this respect, and it must be concluded that the yield stress at the tip of a fine crack is considerably greater than the normal bulk property. The value of Σ of 400 ton/in^2 is, however, less than that corresponding to a perfect lattice. The shear strength of a perfect lattice is about $G/30$ (where G is the shear modulus) —i.e. about 450 ton/in^2. The corresponding value of Σ should be about 1400 ton/in^2.

TABLE 2. DIMENSIONS OF STRESS-CORROSION CRACKS IN FULLY SOFTENED SPECIMENS OF 18–8 TYPE AUSTENITIC CR–NI STEELS.

Type	Applied Stress (σ) (ton/in^2)	Depth, (s) cm	Ratio k_2	Tip radius (ξ), (μ)	Σ calculated ton/in^2
Fine	6·8	0·010	>500	< 0·2	>150
		0·016	530	< 0·2	>190
		0·040	480	< 0·2	>304
		0·078	500	0·30	350
		0·106	530	0·31	400
	8·6	0·011	370	< 0·2	>200
		0·015	430	< 0·2	>240
		0·019	380	< 0·2	>265
		0·031	420	< 0·2	>340
		0·048	350	0·30	350
	12·3	0·010	250	< 0·2	>270
		0·013	320	< 0·2	>310
		0·016	270	< 0·2	>380
		0·025	280	0·28	365
		0·035	250	0·33	400
	16·6	0·011	220	< 0·2	>390
		0·012	170	< 0·2	>400
		0·022	180	0·41	380
		0·023	150	0·40	395
Open	6·8	0·125	90	2·0	170
	8·6	0·075	60	2·2	160
		0·104	45	2·4	180
	12·3	0·036	85	1·4	190
		0·039	30	1·6	180
		0·061	25	3·5	160
		0·142	24	9·0	155
	16·6	0·028	55	2·1	190
		0·033	25	2·4	200
		0·060	20	4·8	185
		0·105	23	11·2	160
		0·132	18	15·0	150

Corrosion Science, 1961, Vol. 1, pp. 49–61. Pergamon Press Ltd. Printed in Great Britain

THE ANODIC CHARACTERISTICS OF MILD STEEL IN DILUTE AQUEOUS SOIL ELECTROLYTES*

T. P. HOAR and T. W. FARRER†
Department of Metallurgy, University of Cambridge, England.

Abstract—A study has been made of the relationship of anode current density with electrode potential for mild steel, in dilute solutions of soil electrolytes and under conditions simulating the natural corrosion of metal buried in soil. The results allow the estimation of the increase in corrosion rate resulting from the (measurable) change in electrode potential of buried steel structures that may be caused by adjacent cathodic protection or other electrical installations.

The logarithm of the anode current density i A/cm² in the range 10^{-5}–10^{-4} A/cm² is related approximately rectilinearly to the anode potential E; the increase of potential for a tenfold increase of current density, $dE/d\log i$, is between 40–65 mV in most conditions. Thus a change of potential of +10 mV produces about a 40 per cent increase of anode current density under the most favourable conditions and about an 80 per cent increase under the least; and a change of +20 mV produces about a two-fold increase under the most favourable conditions and a three-fold increase under the least. The presence of active sulphate-reducing bacteria or of *small* amounts of sulphide tends to give the smallest, least favourable, values of $dE/d\log i$. Film-forming solutions, including those containing *large* amounts of sulphide, tend to give the highest, most favourable values (exceptionally, much higher than 65 mV). The theoretical and practical significance of the results is discussed.

Résumé—On a étudié les relations existant entre la densité du courant anodique et le potentiel des électrodes, en ce qui concerne l'acier doux. Ces recherches ont été effectuées dans des solutions diluées d'electrolytes du sol, et sous des conditions rappellant celles existant lors de la corrosion naturelle de métaux enterrés. Les résultats permettent de déterminer l'augmentation de la corrosion résultant d'un changement (mesurable) du potentiel des électrodes de l'acier de structures enterrées, changement qui pourrait être déclenché par une protection cathodique avoisinante ou par n'importe quelle autre installation électrique.

Lorsque le logarithme de la densité du courant anodique i A/cm² est de l'ordre de grandeur de 10^{-5}–10^{-4} A/cm², il se trouve dans une relation rectiligne avec le potentiel anodique E. Lorsque la densité du courant ($dE/d\log i$) est portée à dix fois sa valeur initiale, l'augmentation du potentiel est de l'ordre de 40 à 65 mV le plus souvent. Un changement du potentiel de +10 mV déclenche donc, dans les conditions les plus favorables, une augmentation d'env. 40 pourcent de la densité du courant anodique, alors que l'augmentation est de 80 pourcent dans les conditions les moins favorables. Un changement de +20 mV la fait monter deux fois dans les conditions les plus favorables, et trois fois dans les conditions les moins favorables. La présence de bactéries sulfa-to-réductrices actives ou d'une petite quantité de sulfure comporte la tendance à l'obtention des valeurs $dE/d\log i$ les plus basses et défavorables. Les solutions qui forment des films, les solutions contenant de larges quantités de sulfure y comprises, donnent les valeurs les plus élevées et favorables (dépassant exceptionnellement de loin 65 mV). La signification théorique et pratique de ces résultats est passée en revue.

Zusammenfassung—Es werden die Beziehungen untersucht, welche für Weichstahl in verdünnten Lösungen von Erd-Elektrolyten zwischen Anodenstromdichte und Elektrodenpotential bestehen. Die Versuchsbedingungen ähnelten dabei der natürlichen Korrosion von in den Erdboden eingebetteten Metallen. Die Ergebnisse ermöglichen die Bestimmung der Zunahme der Korrosions-Geschwindigkeit, wir sie aus den (messbaren) Veränderungen des Elektrodenpotentials eingegrabener Stahlkonstruktionen resultiert, wobei diese Veränderungen durch benachbarten Kathodenschutz oder sonstige elektrische Anlagen hervorgerufen werden.

Der Logarithmus der Dichte des Anodenstroms i A/cm² steht, wenn er im Bereich 10^{-5}–10^{-4} A/cm² liegt, in annähernd geradlinigem Verhältnis mit dem Anodenpotential E. Der Potentialanstief ($dE/d\log i$) liegt unter den meisten Bedingungen zwischen 40 und 65mV, wenn die Stromdichte auf das Zehnfache anwächst. Eine Potentialänderung um +10 mV ergibt unter den günstigsten Bedingungen etwa eine 40 Prozent-ige Zunahme der Anodenstromdichte, und unter den ungünstigsten Bedingungen eine etwa 80 Prozent-ige Zunahme. Eine Veränderung um +20 mV ergibt unter den günstigsten Bedingungen etwa eine doppelte Zunahme, unter den ungünstigsten Bedingungen eine Zunahme um etwa das Dreifache. Bei Vorhandensein von aktiven, sulfatreduziereden Bakterien oder einer geringen Sulfidmenge ist die Tendenz zu erkennen, dass sich die niedrigsten, ungünstigsten Werte von $dE/d\log i$ einstellen. Filmbildende Lösungen, einschliesslich der Lösungen mit einem hohen Sulfidgehalt, haben die Tendenz, die höchsten, günstigsten Werte zu ergeben (ausnahmsweise weit über 65 mV). Die theoretische und praktische Bedeutung dieser Resultate wird besprochen.

*Manuscript received 2 January 1961.

†Dr. Farrer met his death in a tragic accident at sea in April, 1961. He was responsible for the experimental work in this paper, and had approved the final draft.

INTRODUCTION

WHEN cathodic protection is applied to a buried steel structure by the impressed e.m.f. system, or (on occasion) by the reactive anode system, nearby unprotected steel structures may accept some of the current flowing through the soil. Parts of such a structure are cathodic and receive positive current from the soil, consequently receiving some protection, but other parts are anodic and pass positive current to the soil, with consequent increase in corrosion rate. Although it is scarcely practical to measure the current densities involved, it is relatively simple to measure the structure/soil electrode potential. The current-density/electrode-potential relationship has hitherto been known only qualitatively for ferrous materials in soil electrolytes. We have therefore investigated the relationship between anode current density and electrode potential for steel and iron under various conditions simulating natural soil environments, in order to estimate the probable increase in corrosion rate resulting from changes of structure/soil potential in the positive direction. From the results we may estimate the change of potential—which is measurable (see later)—that can be regarded as indicating a reasonably small and acceptable increase of corrosion rate in installations adjacent to cathodic protection or other electrical systems.

EXPERIMENTAL TECHNIQUE

Modified Piontelli cells[1] were used, Figs. 1 and 2, to provide uniform current distribution on the metal under examination. A glass cylinder, 2·5 cm internal

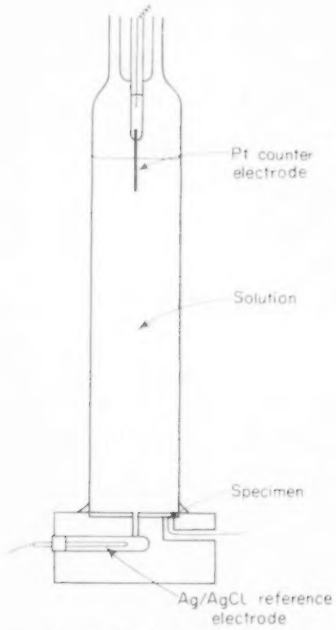

FIG. 1. Experimental cell.

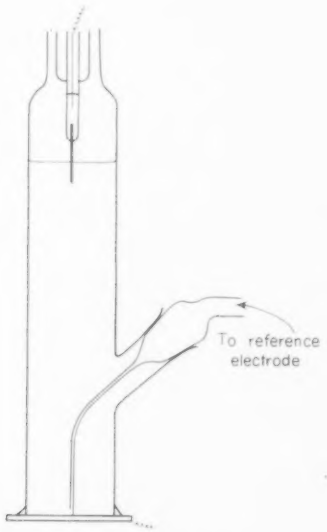

FIG. 2. Modified cell.

diameter, fitted exactly over the metal specimen mounted in unplasticized polymethylmethacrylate. A platinum wire sealed through the head of the cylinder served as counter electrode. For potential measurements in solutions containing chloride ion, a silver/silver-chloride reference electrode was arranged in the specimen mount as shown in Fig. 1, with a communicating polythene capillary through the specimen. For potential measurements in chloride-free solutions, and in those in which contaminating sulphide was added or formed *in situ*, an external silver/silver-chloride or a calomel electrode was arranged as shown in Fig. 2. The simplicity of the cells permitted the presence, if required, of natural soil solids resting on the metal under examination, and the accumulation of electrode products on the metal surface. Furthermore, the arrangement shown in Fig. 2 was readily adaptable for use with solutions or soils containing sulphate-reducing bacteria.

Current through the cells was provided from accumulators with conventional coarse and fine rheostat control. The cells were covered with polythene bags to exclude liquid water, placed in a thermostat bath and allowed to reach steady temperature, usually 25°C, before readings were begun.

Metals. Mild steel cold-rolled strip (C, 0·12; S, 0·016; P, 0·028; Si, 0·28; Mn, 0·51%) was used for most experiments. Armco iron rolled strip (C, 0·012; S, 0·017; P, 0·005; Si, 0·017; Mn, 0·07%) was used in a few experiments. All electrodes were prepared by anodic etching *in situ* in the cell, at $1{\cdot}5 \times 10^{-4}$ A/cm² for 1 h before measurements were begun.

Solutions. A.R. quality chemicals and Pyrex-condensed water were used. Oxygen-free solutions were prepared by boiling under reduced pressure with a stream of oxygen-free hydrogen passing over immersed platinum foil. The solution was transferred to the experimental cells under a stream of hydrogen. To avoid contamination with grease, polytetrafluorethylene sleeves were used on all joints. Solutions containing active sulphate-reducing bacteria must contain suitable bacterial nutrients: such solutions used in the present work, based on the conventional Baars'[2] medium,* were prepared as described in Appendix I.

Soils. 100 g of the soil sample was thoroughly mixed with 100 ml of freshly boiled and cooled distilled water. The mixture was saturated with hydrogen in the same way as the plain electrolyte solutions, but without any heating, and was then transferred to the experimental cell. The coarsest soil particles were not carried into the cell, and the additional water was necessary to allow manipulation of the soil. Thus, the soil and extract examined was somewhat different from natural undisturbed soil. However, disturbances to natural soil occur during the installation of buried structures, and frequent alterations in soil water occur in nature through rain and seasonal fluctuations in the water-table; thus the experiments probably simulated practical conditions to a reasonable extent.

In the cells, the soluble organic plant leachates in the soils were diluted, and the particulate organic matter was the last to settle, so that little organic matter was initially in contact with the metal. Also, the coarser inorganic particulate matter

*Sodium lactate (70% soln.), 5 g; K_2HPO_4, 0·5 g; NH_4Cl, 1 g; $CaSO_4$, 1 g; $MgSO_4.7H_2O$, 2 g; $Fe(NH_4)_2(SO_4)^6.6H_2O$, 0·5 g; mains water to 1 l. pH 8·3, sterilize for 20 min. (autoclave 20 lb/in²), pH after sterilizing 7·3. This is a heterotrophic medium; for an autotrophic medium, the sodium lactate is omitted.

naturally settled first. In soils containing active sulphate-reducing bacteria these effects may have rendered the activity of the bacteria near to the anode surface somewhat lower than it would have been in nature; however, although sulphide formation in such soils was frequently observed to begin at the soil/water interface, it rapidly spread throughout the cell.

Procedure. After the initial anodic etch (see above, and later discussion), a controlled current-density of 10^{-5} A/cm² was passed through the cell for 20 min, and the anode potential, which had become nearly steady, was then recorded. The current-density was then increased successively to 2, 4, 6, 8 and 10×10^{-5} A/cm², the potential being recorded after 20 min at each current-density. Further similar readings at decreasing current-densities were then made. In all cases the usual "hysteresis" was observed, as shown by the typical plot of Fig. 3(a). Since the "increasing" and

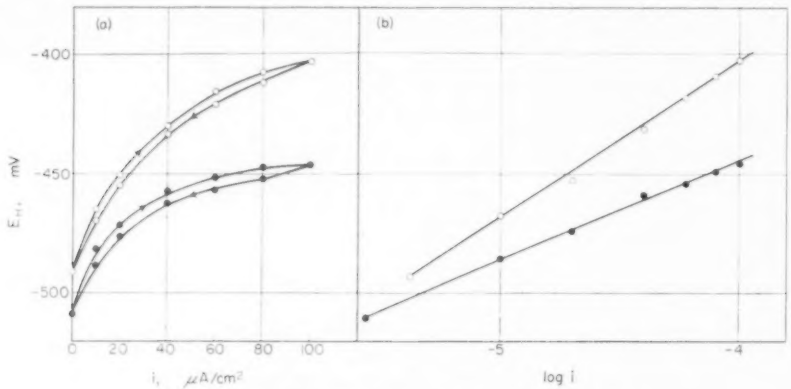

Fig. 3. Typical potential/current-density relationships.
(a) E_H vs. i, showing experimental points and "hysteresis".
(b) E_H vs. log i, using mean points and showing extrapolation to open-circuit potential.
○ 0·001 M K_2SO_4 0·0001 M KCl (run 2).
● Clay soil extract (run 60).

"decreasing" values of potential generally differed by no more than 10 mV, the averaged values have been used to plot E_H/log i diagrams such as Fig. 3(b).* This procedure provides results of sufficient accuracy for the present purpose of obtaining a wide survey of the current-density/anode-potential relationships to be expected under practical conditions.

EXPERIMENTAL RESULTS

Table 1 summarizes the results of 27 typical runs in various simple electrolyte solutions and culture media. In each run curves qualitatively similar to those shown in Fig. 3(a) and (b) were obtained, the E_H/log i plots being straight lines within experimental deviation over the range studied. Smoothed values for E_H (10^{-5} A/cm²) and E_H (10^{-4} A/cm²) and the mean dE/d log i are therefore recorded,* together with the open-circuit potential where this was measured.

* In certain cases the values of E_H (potential of the electrode on the normal hydrogen scale) may be in systematic error owing to error in the reference electrode; but the mean values of $dE/d\log i$ are not thereby affected.

TABLE 1. SUMMARIZED ANODIC BEHAVIOUR OF MILD STEEL IN VARIOUS OXYGEN-FREE ELECTROLYTE SOLUTIONS AND MEDIA.
Temp. 25°C. Iron = *circa* 0·0003 M dissolved anodically before start of run.

Run	Solution	Potential, E_H, mV			$dE_H/d \log i$, mV
		Open Circuit	For 10^{-5} A/cm²	For 10^{-4} A/cm²	
1	0·001 M Na_2SO_4, 0·0001 M KCl	−492	−470	−411	59
2	0·001 M K_2SO_4, 0·0001 M KCl	−492	−468	−403	65
3	0·001 M $CaSO_4$, 0·0001 M KCl	−492	−464	−405	59
4	0·001 M $FeSO_4$, 0·0001 M KCl	−492	−465	−404	61
5	0·001 M $Fe(NH_4)_2(SO_4)_2$, 0·0001 M KCl	−492	−456	−392	64
6	0·0001 M $Ca(HCO_3)_2$, 0·0001 M KCl	−492	−469	−408	61
7	0·001 M $NaHCO_3$, 0·0001 M KCl	ND	−487	−430	57
8	0·001 M NaCl	−504	−492	−428	64
9	0·01 M NaCl	ND	−479	−421	58
10	0·001 M KCl	−504	−490	−429	61
11	0·001 M $CaCl_2$	−520	−508	−442	66
12	0·01 M $CaCl_2$	ND	−489	−429	60
13	0·1 M $CaCl_2$	ND	−495	−433	62
14	0·001 M $MgCl_2$	−519	−498	−439	59
15	0·01 M $MgCl_2$	ND	−492	−433	59
16	0·012 M $NaNO_3$, 0·0001 M KCl	ND	−390*	−297*	93
17	0·01 M KNO_3, 0·0001 M KCl	ND	−347*	−275*	72
18	0·0025 M NaOH	ND	−373	−311	62
19	0·0025 M NaOH (after standing 24 h)	ND	−373	−218	155
20	0·001 M Na_2S	ND	−480	−410	70
21	0·013 M Na_2S	ND	−480	− 50	430
22	0·135 M KCl, 0·00013 M Na_2S	ND	−425	−384	41
23	0·135 M KCl, 0·0013 M Na_2S	ND	−433	−286	147
24	0·135 M KCl, 0·013 M Na_2S	ND	−430	−183	247
25	Autotrophic medium, sterile†	−487	−460	−405	55
26	Autotrophic medium, inoculated†	−501	−477	−477	36
27	Heterotrophic medium, inoculated†	−501	−473	−438	35

ND Not determined *Poorly reproducible †After Baars[2]; see footnote, p. 51.

Runs 1–15, for solutions that produced even dissolution of the anode, gave an overall mean $dE/d \log i$ of 61 mV. No large differences were found in solutions containing the cations Na^+, K^+, NH_4^+, Mg^{2+}, Ca^{2+} and Fe^{2+}, or the anions SO_4^{2-}, Cl^- or HCO_3^-, nor was there any significant trend caused by change of electrolyte concentration in the range examined. Since the solutions were unbuffered, with an initial pH of around 7, some of the dissolved iron appeared as flocculent $Fe(OH)_2$, especially when cathodically produced alkali became mixed with the anode product; but no indication of any passivation or film formation was observed.

Runs 16–21 and 23–24 exemplify the higher potentials and increased values of $dE_H/d \log i$ observed in solutions tending to give film formation at the anode, the result in the more concentrated sodium sulphide solution (run 21) being especially striking. Since sulphide ion is often a stimulator of the iron anodic reaction—for instance when it is present in *small* concentrations,[3] when the medium is *acid*,[4] and often when the sulphide is produced by bacterial activity (see later)—it is well to emphasize its evident inhibiting effect when it is present in such relatively high concentration that visible

compact films of ferrous sulphide form on the anode. Run 22 does, in fact, indicate the stimulating effect of a small concentration of sulphide, insufficient to cause film formation; here a given increase of E_H leads to a considerably greater increase of i than in the sulphide-free solutions of runs 1–15.

Runs 25–27 are typical of many experiments done with culture media. The sterile medium of run 25 led to results very similar to those of runs 1–15. The inoculated media of runs 26 and 27 led to E_H/log i lines of smaller slopes. Here, the final anode product was precipitated ferrous sulphide, typical of "bacterial corrosion", and no compact film was formed. It is interesting that the inoculated medium appears to be inimical to the formation of ferrous sulphide in the compact, inhibitory form noted above.

Table 2 summarizes the results of runs with 33 typical soil samples, of which the source, type, anion qualitative analysis, pH and bacterial activity (the "Activity

TABLE 2. SUMMARIZED ANODIC BEHAVIOUR OF MILD STEEL EXPOSED TO SOIL AND ADDED DISTILLED WATER.

Temp. 25°C. Iron = *circa* 0·0003 M dissolved anodically before start of run.
H = High, P = Present, T = Trace, N = Nil

Run	Soil							Potential, E_H, mV			
	Source	Type	SO_4^{2-}	Cl^-	CO_3^{2-}	pH	Activity Index	Open Circuit	For 10^{-5} A/cm²	For 10^{-4} A/cm²	$\frac{dE_H}{\log t}$, mV
28	Gog-Magog Hills, Cambs.	Chalk	H	T	H	8·9	0	−494	−474	−417	57
29	,,	,,	T	T	H	8·4	0	−572	−492	−432	60
30	,,	,,	T	T	H	8·4	1	−514	−492	−434	58
31	Kinlochewe, W. Ross	Peat	T	T	N	5·7	0	−497	−475	−437	38
32	Inver Alligin, W. Ross	,,	T	T	T	5·3	0	−507	−481	−425	54
33	Torridon, W. Ross	,,	T	T	N	5·8	0	−503	−480	−421	59
34	Slaterdale, Ross & Crom.	,,	T	T	N	5·5	0	−513	−482	−421	61
35	Wicken Fen, Cambs.	,,	T	T	N	6·9	2	−512	−484	−418	66
36	,,	,,	T	T	T	6·6	3	−508	−485	−425	60
37	Grantchester, Cambs.	,,	T	T	T	6·8	6	−575	−482	−421	61
38	Durness, Sutherland	Sand	T	H	H	6·9	0	−489	−475	−422	53
39	,,	,,	T	H	P	6·2	1	−502	−486	−420	66
40	,,	,,	T	H	P	6·5	2	−507	−489	−430	59
41	Armthorpe, Yorks	Sandy-loam	T	T	T	6·1	0	−513	−493	−432	61
42	,,	,,	T	T	T	6·4	1	−501	−488	−435	53
43	,,	,,	T	T	T	6·8	2	−504	−495	−429	64
44	,,	,,	T	T	T	6·0	3	−502	−482	−432	50
45	Wicken Fen, Cambs	Clay-loam	T	T	T	6·6	0	−506	−484	−421	63
46	,,	,,	T	T	T	6·6	4	−512	−484	−420	64
47	Guildford, Surrey	,,	T	T	P	6·6	1	−503	−485	−423	62
48	,,	,,	T	T	T	6·8	2	−515	−489	−424	65
49	,,	,,	T	T	T	7·2	3	−507	−489	−427	62
50	Saxilby, Lincs.	Clay	T	T	T	6·2	0	−506	−485	−428	57
51	,,	,,	T	T	T	6·8	1	−504	−482	−429	53
52	,,	,,	T	T	T	6·8	2	−504	−482	−427	55
53	Grantchester, Cambs.	,,	P	T	P	7·2	3	−515	−489	−440	49
54	,,	,,	P	T	P	7·5	4	−505	−477	−419	58
55	Rudston, Yorks	,,	P	T	H	7·9	5	−501	−481	−439	42
56	,,	,,	T	T	H	8·0	6	−510	−490	−445	45
57	,,	,,	T	T	H	7·7	7	−503	−478	−435	43
58	Thorne, Yorks	,,	T	T	T	6·5	8	−506	−481	−442	39
59	,,	,,	T	T	T	6·8	9	−505	−484	−445	39
60	,,	,,	T	T	T	6·6	10	−509	−486	−445	41

Index", see Appendix II) are indicated. E_H/log i curves qualitatively similar to those of Fig. 3(a) and (b) were obtained in every case.

Runs 28–49, for a series of chalk, sand, sandy-loam and clay-loam soils, all save one (run 37) showing low bacterial activity, gave remarkably similar results, with no significant difference except the low dE/d log i found in run 31. The results of the other 21 runs can be expressed by an average E_H/log i line, somewhat below the range found

for plain electrolyte solutions, and with the same slope of *circa* 60 mV. Runs 50–52, for clay soils showing low bacterial activity, may be averaged to give a line with a slope of 55 mV; it is scarcely significantly different from the average of runs 28–49 (omitting 31).

Runs 53–60, for a series of clay soils of increasing bacterial activity, gave results showing generally a decrease of $dE_H/d \log i$ to around 39 mV. The more active of this group (*Activity Index* (Appendix II) 5–10) gave $dE_H/d \log i$ results very similar to those of the typical inoculated media of runs 26 and 27, and there can be little doubt that the overall anode process, with final production of non-protective ferrous sulphide, was the same.

A few of the runs were repeated at 12° and 0°C. $dE_H/d \log i$ decreased slightly with decrease of temperature, but even at 0°C never by more than the 8 per cent or so to be expected (since on theoretical grounds the slope is proportional to absolute temperature). Consequently the 25°C results for $dE_H/d \log i$ can be applied without significant practical error to steel/soil systems at most ordinary temperatures.

Several runs, using simple electrolyte solutions, inoculated culture media and soil-water fluids, were repeated with the "pure" iron. No significant difference from those given by the fairly "clean" mild steel, used for most of the experiments, were found.

DISCUSSION

Fundamental considerations

The initial anodic etch already mentioned, $1{\cdot}5 \times 10^{-4}$ A/cm² for 1 h produced dissolved ferrous iron equivalent to *circa* 0·0003 M in the supernatant fluid over the anode in the cell, if complete mixing is assumed; although no attempt at other than "natural" mixing was made, since it was desired to simulate the conditions of stagnant waterlogged soil, it is likely that considerable convectional mixing occurred in the plain electrolyte solutions, and indeed also in the fluids containing soil particles. For the solutions of low ionic strength used in the present work, the activity coefficient of Fe^{2+}_{aq} is around 0·82[6], so that we calculate the reversible Fe/Fe^{2+}_{aq} potential ($E^{\circ}_H = -0{\cdot}441$ V) in 0·0003 M Fe^{2+}_{aq} solution as $-0{\cdot}548$ V (E_H).

We can now consider the experimental $E_H/\log i$ lines of Fig. 3, and their extrapolation to the open-circuit potentials, in more detail.

(a) *Simple electrolyte solutions.* In the $E_H/\log i$ plots exemplified by Fig. 3, the current density is, of course, the measured external current density, i_e. This is a sufficiently good approximation to the true anode current density i_a only if the local cathode current density i_c is small, since $i_a = i_e + i_c$. The only possible cathodic processes in the plain *de-aerated* solutions are $Fe^{2+}_{aq} + 2e \rightarrow Fe$ and $2H^+ + 2e \rightarrow H_2$. Since the reversible potential for the process $Fe \rightleftarrows Fe^{2+}_{aq} + 2e$, in the present solutions, is $-0{\cdot}548$ V (E_H) for uncomplexed Fe^{2+}_{aq}, and lower if complexing ions such as chloride are present, rough extrapolation of the experimental $E_H/\log i$ relationships shows that the exchange current-density at $-0{\cdot}548$ V (E_H) is between 10^{-7} and 10^{-6} A/cm², so that the back (cathode) current density at the experimental potentials, even that for open-circuit conditions, is completely negligible. Any local cathodic action is thus to be accounted for entirely by hydrogen-ion reduction, which may be appreciable at the present experimental potentials which are considerably more negative than the reversible hydrogen potential at pH 7, $-0{\cdot}414$ V (E_H).

When the experimental E_H/log i_e relationships are extrapolated to the experimental open-circuit potentials, where $i_a = i_c$, the open-circuit or corrosion current densities so found all lie in the range 10^{-6}–10^{-5} A/cm², with a mean around 4×10^{-6} A/cm². The extrapolation is, of course, justifiable only if i_e is a sufficiently good approximation to i_a over the experimental range of 10^{-5}–10^{-4} A/cm². Fig. 4 shows schematically that this is indeed so for a corrosion current density of 4×10^{-6} A/cm² and an assumed Tafel slope for the hydrogen-ion discharge reaction of 118 mV, the Tafel slope for the anode reaction being taken as 59 mV (the experimental mean was 61 mV); for such conditions, i_e is evidently a reasonable approximation to i_a except at the extreme lower end of the 10^{-5}–10^{-4} A/cm² range, and the extrapolation is in little error. It may also be noted that in the scheme of Fig. 4 an external current density of 10^{-5} A/cm² requires a polarization of *circa* 28 mV above the open-circuit potential; Table 1 shows that the experimental electrodes usually required a polarization of between 20 and 30 mV to give this current density.

The E_H/log i results for the simple electrolyte solutions may therefore be regarded, with little error, as representing the true anode polarization curves over the range 10^{-4}–10^{-5} A/cm².

(b) *Culture media and soil extracts.* The E_H/log i relationships for sterile media and for soils containing no active sulphate-reducing bacteria are similar to those for simple electrolyte solutions (Tables 1 and 2), and may be similarly interpreted. As before, the relationships represent the true anode E_H/log i_a relationships with little error, and extrapolation to the open-circuit potentials gives the approximate corrosion current density, which is also around 4×10^{-6} A/cm².

In the present media and soil extracts, bacterially stimulated sulphate reduction is thermodynamically possible as a local cathodic process,

$$SO_4^{2-} + 4H_2O + 8e \rightarrow S^{2-} + 8OH^-.$$

From the several free energies of formation given by Latimer[5] (SO_4^{2-}, — 176·1; H_2O, — 56·69; S^{2-}, 23·42; OH^-, — 37·59 kcal/mole), we find for the above process at $E_H = 0, \Delta G^\circ = 125{\cdot}6$ kcal, so that $E_H^\circ = -0{\cdot}680$ V, E_H° (pH 7) $= -0{\cdot}266$ V, and for pH 7, $a_{SO_4^{2-}} = 10^{-3}$ M, $a_{S^{2-}} = 10^{-12}$ M (reasonable values for an "active" soil), $E_H = -0{\cdot}002$ V. Cathodic reduction of sulphate is thus thermodynamically possible at *circa* — 0·5 V(E_H).

If the present media and soil extracts as examined in fact supported cathodic sulphate reduction, the open-circuit corrosion current density would have been quite large. Fig. 4 shows a scheme similar to that already discussed, but with an assumed corrosion current density ten times larger, 4×10^{-5} A/cm². In the absence of any knowledge of the Tafel slope for the sulphate-reduction process, 118 mV is assumed, but the following argument applies equally to any other remotely possible value. The E_H/log i line for i_e between 10^{-5} and 10^{-4} A/cm² is now, of course, no longer any sort of approximation for the E_H/log i_a relationship. Its average slope is much lower, and at first sight it might be thought that the lower slopes of the experimental E_H/log i relationships found in active soils could be accounted for by regarding them as E_H/log i_e lines. Consideration of the experimental data, Fig. 3(a) and (b), shows however that this would be wrong. Not only is there no sign of the concave-upwards curvature suggested by Fig. 4 for an E_H/log i_e line; but an i_e of 10^{-5} A/cm² requires a polarization of between 20–28 mV above the open-circuit potential, instead of the 4 mV suggested

by Fig. 4. We may conclude that the open-circuit corrosion current is in fact well below 10^{-5} A/cm², and that the experimental E_H/log i lines for active soils, including the extrapolations to the open-circuit potentials, are as valid E_H/log i_a relationships as those previously discussed. This in turn implies that whatever cathodic process is

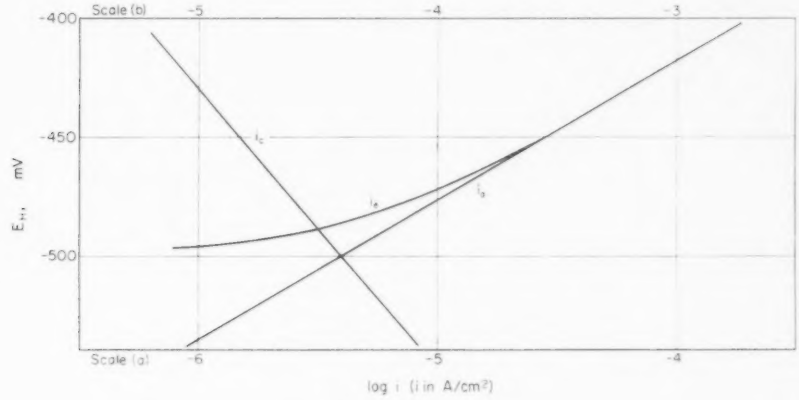

FIG. 4. Schematic i_a, i_c and i_e.
(a) For corrosion current-density of 4×10^{-6} A/cm² at −500 mV (E_H), showing $i_e \sim i_a$ over the experimental range of i_e 10^{-5}–10^{-4} A/cm².
(b) For corrosion current/density of 4×10^{-5} A/cm² at −500 mV (E_H), showing $i_e \neq i_a$ over the experimental range of i_e 10^{-5}–10^{-4} A/cm².

operating, it is no faster than the hydrogen-ion reduction previously considered for the plain electrolyte solutions and "inactive" soils. Evidently, cathodic reduction of sulphate ion is substantially absent.

Special experiments showed that the strain of *Desulphovibrio desulphuricans* obtained from mud at Byron's Pool, Grantchester (Appendix I), after 20–30 days' growth when the population had become almost stationary, induced no sulphate reduction at steel deliberately made cathodic—the cathodic polarization curves in the presence of bacteria were experimentally unaltered when the bacteria were killed. Quite probably the bacteria in all the media and soils as examined in the present work (*after* bacterial growth had become very slow) were similarly inactive as cathodic stimulators, although they had been active in producing sulphide to stimulate anodes. We understand, however, that other strains under other conditions—especially during the rapid period of bacterial growth—are active cathodic stimulators;[7] in such cases, measured values of i_e might be poor approximations to i_a on account of the large values of local i_c.

The average value of *circa* 60 mV obtained for dE/d log it in the overall process $Fe \rightarrow Fe^{2+}_{aq} + 2e$ in all the present sulphide-free, non-film-forming solutions of pH *circa* 7 leads to a transfer coefficient α of 0·5 in the Tafel equation

$$E_H = \frac{2{\cdot}3\,RT}{\alpha z F} \log i + a,$$

since $z = 2$ for the 2-electron reaction. Such a slope is in harmony with the simplest kinetic model for the dissolution, that of one Fe entity undergoing a rate-determining

2-electron transfer without intermediate steps, as discussed by one of us elsewhere.[8] The lower slopes found in the conditions giving non-film-forming sulphide require a more complex mechanism. Slopes of 30 mV have been found in acid media by Bonhoeffer and Heusler,[9] Hoar and Hurlen,[10] and Hoar and Sedzimir;[11] such slopes have been interpreted[9–11] as due to hydroxyl-bearing intermediates containing more than one Fe entity. In the present case, similar hydrosulphide-bearing intermediates are quite possible; future work on the very complex iron-dissolution process should certainly consider these.

Practical significance of the data

From a knowledge of shift of anode potential in the positive direction, the coefficient of increase of anode current, that is, of corrosion rate, can at once be calculated from $dE_H/d \log i_a$. For convenience, coefficients of i_a corresponding to potential shifts, ΔE, of 1, 5, 10 and 20 mV, for several values of $dE_H/d \log i_a$, are set out in Table 3. Our present results for $dE_H/d \log i_a$ lead to the following conclusions:

TABLE 3. COEFFICIENTS OF ANODE CURRENT-DENSITY FOR VARIOUS CHANGES OF ANODE POTENTIAL

$dE_H/d \log i$ (mV)	Coefficient of i_a for ΔE:			
	1 mV	5 mV	10 mV	20 mV
200	1·01	1·10	1·12	1·26
70	1·02	1·18	1·39	1·93
65		1·19	1·43	2·03
60	1·04	1·21	1·47	2·15
55		1·23	1·52	2·31
50	1·05	1·26	1·58	2·51
45		1·29	1·67	2·78
40	1·06	1·33	1·78	3·16
35		1·39	1·93	3·73

1. In simple electrolyte solutions and in extracts from inactive soils giving $dE_H/d \log i_a$ averaging 60 mV, a steel/solution potential shift ΔE of 10 mV in the positive direction indicates a 47 per cent increase in corrosion rate, and $\Delta E = 20$ mV indicates a 115 per cent increase. Since the average $dE_H/d \log i_a$ includes experimental values (Table 2) in the range 50–66 mV, these increases can be expected to lie in the respective ranges 42–58 per cent and 105–151 per cent.

2. In media and soil extracts containing small amounts of sulphide and giving $dE_H/d \log i_a$ averaging 40 mV (range say 35–45 mV), $\Delta E = 10$ mV indicates a 78 per cent (range 67–93 per cent) increase in corrosion rate, and $\Delta E = 20$ mV indicates a 216 per cent (range 178–273 per cent) increase.

3. In environments giving high values of $dE_H/d \log i_a$ (see Table 1), ΔE of 10 or 20 mV may indicate very much smaller increases of corrosion rate.

4. $\Delta E = 1$ mV indicates negligible increases of corrosion rate (6 per cent) under all conditions; $\Delta E = 5$ mV indicates increases never more than about 40 per cent.

In cathodic protection practice, a shift of "structure/soil potential" of "not more than 10 (or 20) mV in the positive direction" has often been used as a criterion of a

"safe" increase of corrosion rate of an unprotected structure, where it passes positive current to the soil, when the cathodic protection scheme is switched on. The present results, on superficial consideration, suggest that even a 10 mV shift is a very doubtful criterion of corrosion "safety". However, it must be borne in mind that the practical measurement of structure/soil potential is ordinarily made with a reference half-cell making liquid junction to a point (usually on the soil surface) "as near as possible" to the structure concerned—*not*, as in the standard laboratory practice used in the present work to measure ΔE, to a point *adjacent to the metal anode*. Consequently, the shift as measured may include a substantial potential drop caused by the electrolytic resistance of the current-carrying soil between the structure anode surface and the point where the reference half-cell makes liquid junction; thus a "10 mV shift" as measured may mean a very much smaller value of ΔE, especially in soils of high specific resistivity, or in situations where the half-cell junction has perforce to be at a substantial distance from the structure anode.

To measure ΔE in the field, it would be necessary to insert a probe—for example a stiff plastic tube—into the soil so that its end was as near as possible, say 0·1–0·2 cm, from the structure anode surface, and to make liquid contact from the soil at this point to the reference half-cell. This could, indeed, be contained within the plastic tube near the lower end, a silver/silver chloride half-cell being perhaps preferable to a copper/copper sulphate to avoid contamination of the structure with copper. Such an arrangement would be quite practical except in very hard, stony soils, and in selected cases could well supplement the conventional surface reference half-cell.

Alternatively, in some cases it may be possible to calculate the ohmic "error" in the conventional measurements if the soil resistivity and the geometry of the system are well enough known, although such an estimation would probably be very rough; comparison of such calculated results with experimental measurements such as those just suggested would be of interest.

Provided that ΔE can be measured or calculated, the broad practical implication of our conclusions (1) to (4) is, of course, that $\Delta E = 10$ mV is a doubtful criterion of corrosion "safety" even in inactive soils, and an indication of a nearly doubled corrosion rate in active soils. A ΔE of 20 mV is a far too liberal criterion under all conditions, and one of 1 mV is too conservative. If a general criterion giving a reasonable balance between restrictive and over-free conditions is needed, $\Delta E \gtrsim 5$ mV might be suitable.

These broad implications, however, require interpretation for each special case. In particular, the "natural" corrosion rate in the absence of extra anodic current may well determine how much extra can be tolerated—a structure corroding at say 2 mil/yr (*circa* $4{\cdot}4 \times 10^{-6}$ A/cm² for steel) might perhaps tolerate a doubled rate of attack, whereas one corroding at say 10 mil/yr (*circa* 22×10^{-6} A/cm²) could not. "Active" soils, leading to low values of $dE_H/d \log i_a$, will often (though by no means always*) be those that give the fastest rates of "natural" corrosion, so that only small values of ΔE (say, $\gtrsim 5$ mV) can be tolerated under just the conditions where neighbouring cathodic protection schemes are likely to exist. The bonding of all neighbouring structures into a single cathodic protection scheme may then be very desirable.

*Other cathodic factors, such as a high degree of aeration at parts of a structure, can of course lead to a very high corrosion rate at anodic parts, even though these are in bacterially inactive soil.

In practical operations, it would of course always be desirable to determine $dE_H/d \log i_a$ *in situ*, using a test plate fitted with means of measuring current density and potential. Since this will rarely be practicable, the "average" values for inactive and active soils, 60 and 40 mV respectively, together with the derived magnitudes underlined in Table 3, give a reasonable semi-quantitative guide as to tolerance of extra anodic current, used in conjunction with "true" values of ΔE and local knowledge of rates of "natural" corrosion.

Acknowledgements—Our thanks are due to the Joint Committee for the Co-ordination of the Cathodic Protection of Buried Structures for their continual interest in this research, and to the several public utilities represented on the Committee for their generous financial support of the work. We also thank Dr. D. I. Annear and Dr. W. Fry for help in the microbiological work, and Dr. J. M. West, Dr. G. H. Booth and Dr. F. Wormwell (Chairman of the Technical Panel of the Joint Committee) for valuable discussions.

REFERENCES

1. R. ALETTI, U. BERTOCCI, G. BIANCHI, C. GUERCI, R. POINTELLI, G. POLI and G. SERAVALLE, *Proc. 3rd Meeting CITCE, Berne* 1951, p. 30. Manfredi, Milan (1952).
2. BAARS, Dissertation, Delft (1930).
3. S. C. BRITTON, T. P. HOAR and U. R. EVANS, *J. Iron St. Inst.* **126,** 365 (1932).
4. T. P. HOAR and D. HAVENHAND, *J. Iron St. Inst.* **133,** 239 (1936).
5. W. M. LATIMER, *Oxidation States of the Elements and the Potentials Aqueous Solutions*, Prentice-Hall, New York (1938).
6. H. S. HARNED and B. B. OWEN, *The Physical Chemistry of Electrolytic Solutions*. Reinhold, New York (1943).
7. F. WORMWELL and G. H. BOOTH, private communication (1960).
8. T. P. HOAR, *Modern Aspects of Electrochemistry*, No. II, (ed. J. O'M. BOCKRIS), p. 273. Butterworths, London (1959).
9. K. F. BONHOEFFER and K. E. HEUSLER, *Z. phys. Chem. N.F.* **8,** 390 (1956).
10. T. P. HOAR and T. HURLEN, *Proc. 8th Meeting CITCE, Madrid 1956*, p. 445. Butterworths, London (1958).
11. T. P. HOAR and G. SEDZIMIR, unpublished work (1960).

APPENDIX I

PREPARATION OF SOLUTIONS FOR EXPERIMENTS USING SULPHATE-REDUCING BACTERIA

A culture of a particular strain of *Desulphovibrio desulphuricans* was prepared as follows. Silt samples were taken from the organic sediments developing under lacustrine conditions at Byron's Pool, Grantchester. 1 g portions of these samples were then inoculated into 10 ml portions of Baars' medium[2] and incubated in McIntosh-Filde anaerobic jars at 25°C, with a trace of ferrous ammonium sulphate in each tube as an indicator. The tubes were examined at frequent intervals, and as soon as growth of the bacteria was indicated by the precipitation of black ferrous sulphide, 1 ml of the culture was transferred to another tube containing 9 ml of Baars' medium with indicator. This process was repeated, each sub-culture being used as an inoculant for fresh medium immediately growth occurred. After the tenth sub-culture, a hanging drop of the medium was examined under the optical microscope. Since this indicated contamination by coccoid forms, the sub-cultures were continued, but with the addition of 0·5 ml of a 1 per cent solution of sodium sulphide to each 10 ml of Baars' medium used. The fifth sub-culture so prepared contained only vibrio forms. Further sub-cultures were then made with medium free from sulphide before using the cultures. In all, seven tubes each containing 10 ml of the purified culture were obtained in this manner. These were combined, mixed and re-divided before use to ensure uniformity throughout the cultures employed. Three portions of the purified culture were maintained under anaerobic conditions as stock cultures and were sub-cultured at 14-day intervals in order to preserve the stock.

Preparatory to the electrochemical experiments, the cell (Fig. 2) was sterilized in a steam autoclave (20 lb/in² for 20 min), 5 ml of the stock culture was inoculated into 100 ml of Baars' medium and incubated in a hydrogen-filled McIntosh-Filde jar at 25°C for the requisite time, generally 18

days. The medium was then admitted to the cell, and anodic etching carried out for 1 h prior to the run. At the beginning of each run, the gas space above the electrolyte surface was hydrogen-filled, and during the run further hydrogen was evolved at the cathode and collected in the space. Either autotrophic or heterotrophic growth of the organisms was thus possible during the run. However, electrochemical measurements were carried out while the bacterial population was as nearly constant as possible, approximate constancy having been reached after 18 days incubation at 25°C, and being maintained until the 20th day following inoculation; polarization curves were determined on the 19th day after inoculation. Possible contamination of the silver/silver chloride electrode by sulphide formed bacterially was prevented by the use of an inhibitor of sulphate-reduction, bis-p-chlorophenyl-diguanidinohexane diacetate, in the reference electrode compartment: at the concentration of 2 p.p.m. used it has no effect upon the reference electrode. Diffusion of bacteria and/or sulphide from the cell, or of the inhibitor into the cell, was in any case rendered very small by the Haber-Luggin capillary.

APPENDIX II

DETERMINATION OF BACTERIAL ACTIVITY— THE "ACTIVITY INDEX"

It was found convenient to assign an index number between 0 and 10 to indicate the activity of sulphate-reducing bacteria in soils, as assessed by a laboratory test,—the *Activity Index* (*A.I.*). The *A.I.* includes an assessment of the number of bacteria in a particular soil and also of the ability of these bacteria to develop in the soil.

Compact samples of the soil are examined with the minimum delay, since considerable changes in *A.I.* may occur after sampling. 1 g from the centre of a sample is inoculated into 10 ml the following sterile medium (chosen to give quick growth), previously saturated with cathodically evolved hydrogen:

Glucose	10·0 g
Peptone	5·0 g
Yeast extract	4·0 g
$MgSO_4 \cdot 7H_2O$	1·5 g
Na_2SO_4	1·5 g
$FeSO_4 \cdot 7H_2O$	0·05g
Tap water	1000 ml
pH	7·3

After thorough mixing, 1 ml of the mixture is mixed with a further 9 ml of medium. This is again diluted 1 in 10, and so on until five tubes of increasing dilution have been prepared. The whole test is carried out in triplicate, and the fifteen tubes are incubated at 25°C in McIntosh-Filde anaerobic jars under an atmosphere of 95% hydrogen, 5% carbon dioxide. The tubes are examined on the 3rd, 6th, 9th, 12th and 15th days following inoculation. The number of bacteria is indicated by the maximum dilution at which growth occurs after fifteen days. A soil in which growth occurs in all fifteen tubes after 15 days is assigned the maximum value of five for the first component of the *A.I.* (that referring to the number of organisms present). One in which growth only occurs in the first two sets of tubes, those of lowest dilution, is assigned a value of two.

The ability of the organisms to develop in the particular soil is indicated by the order in which growth occurs and the time taken for growth at various dilutions. If the soil is one that supports active growth of the bacteria, then those tubes of lowest dilution will produce the first growth. If the soil is acid or alkaline or contains some inhibitory material, then this material will be most concentrated at the lowest dilution and will tend to inhibit growth in these tubes, so that growth occurs preferentially in the tubes of higher dilution. If growth occurs first in the tubes of low dilution then a value of five is assigned to the soil for the second component of the *A.I.*, whereas if growth occurs first at high dilution the value is one. In the case of simultaneous growth at the various dilutions, or first growth at intermediate dilution, then first growth at 3 days is denoted by a value of five, at 15 days by a value of one.

The sum of the two components then gives the *Activity Index* assigned to the soil.

Corrosion Science, 1961, Vol. 1, pp. 62–64. Pergamon Press Ltd. Printed in Great Britain

ON THE RESISTIVITY OF VARIOUS MATERIALS TO ATTACK BY MOLTEN SALTS AND METALS*

A. LUNDEN
Department of Physics, Chalmers Institute of Technology,
Gothenburg, Sweden.

Abstract—In work with molten salts and metals, the container is often attacked by the melt. Practical experience with some 30 melts is summarized.
Résumé—Lors de travaux avec des sels et métaux fondus, les récipients sont souvent attaqués par la fonte. L'auteur relate, en résumé, les expériences recueillies avec 30 fontes différentes.
Zusammenfassung—Bei Versuchen mit geschmolzenen Salzen und Metallen werden oft die Behalter von der Schmelze angegriffen. Erfahrungen mit fast 30 Schmelzen sind hier zusammengestellt.

MACKENZIE has recently compiled a set of tables of container materials for melts.[1] As a further help in the choice of suitable materials for handling melts, this paper summarizes experience gained mainly in this laboratory in the course of studies of isotope effects occurring in electromigration in molten salts and metals. Since the duration of the experiments usually was from a couple of days up to several weeks, the apparatus has been kept at an elevated temperature for a longer time than is required for most other investigations on melts. (In a few cases reference is also given to experiences reported by other workers.)

It is a well-known fact that the reactivity of a melt often is increased by the presence of small amounts of impurities, such as water vapour, and this is one reason why the experience of different laboratories does not always coincide regarding the resistivity of individual container materials towards melts. Data on the solubility of water vapour is available for a few fused salts.[2] For some types of work special effort has been given to lower the reactivity by preparing very pure melts of the salts.[3] In our experiments, however, we have normally used commercially available salts, analytical grade if possible, without any further chemical purification. The salt was fused under a vacuum, poured out on a plate and then stored as lumps. LiI and PbI_2 decomposed to a certain extent during this vacuum treatment.[4] $ZnCl_2$ and $ZnBr_2$ were prepared either by distillation of commercial salt or by reaction between the elements.[5–8] The lumps of salt were filled into glass cells and melted under a vacuum and atmospheric pressure was restored before the electrolysis current was switched on. The principal part of the cell is the so-called separation column, a tube filled with powdered glass, quartz or alumina. After the run this powder was studied under a microscope to see to what extent it had been attacked by the melt. Glass from different parts of the cell walls was also examined for the same purpose. In several experiments with lithium salts we have measured the amount of Na, K and Ca ions that the melt had leached out from the glass.[4, 9] A common observation was that the attack was strongest at the interface between the melt and the surrounding atmosphere. The observed attack is often due to compounds formed at the cathode during electrolysis, and in

*Manuscript received 2nd January, 1961.

TABLE 1. FUSED SALTS

Liquid	Temperature (°C)	Duration (h)	Atmosphere	Material	Degree of attack	Reference
AgCl	650	50	Cl_2	Supremax	Not reported	11
	480	18	Cl_2	Pyrex	No attack	10
$CdBr_2$	580	126	air	Supremax	Not reported	12
$CdCl_2$–LiCl	700	50	Cl_2	Supremax	Strong attack; 5 mole per cent LiCl	13
				Quartz	Strong attack; 5 mole per cent LiCl	
CuCl	530	80	—	Pyrex	No attack	14
				Supremax	No attack	
				Quartz	No attack	
KCl–LiCl	530	80	Cl_2	Pyrex	No attack	14
				Supremax	No attack	
				Quartz	No attack	
	425	> 1500	A	Vycor	See ref.	15
				Hastelloy C	See ref.	
KNO_3	360	146	$NO_2 + O_2$	Supremax	No attack	16
				Quartz	No attack	
				Al	No attack, used as cathode	
KNO_3–$NaNO_3$	≃500	530	air	Pyrex	No attack	17
LiBr	560–620	7–165	Br_2	Supremax	Slight attack after a few hours; increased with time and temperature	9, 18
LiBr–LiCl	600	24	Cl_2	Supremax	Attack after a few hours	10
LiCl	≥620	≤1250	Cl_2; air	Alumina	Attack depending on grade of alumina; no attack at all on e.g. "Thermal 505"	12, 19
					Salt migrates through porous alumina grades	
	620	126	air	Pythagoras	Severe attack	12
	620	500	air	Quartz	Severe attack; might depend on grade of quartz	12
	≥620	≤1250	Cl_2; air	Supremax	Attack sometimes noticed after a few hours. Attack not as severe as in LiBr	12, 20
	620	500	air	Vycor	Salt seemed to diffuse through	12
LiCl–$PbCl_2$	650	<47		Supremax	Slight attack	21
LiI	500	12–31	I_2	Supremax	Severe attack, much more than in LiBr.	4, 9
$LiNO_3$	≥300	48–193	$NO_2 + O_2$	Supremax; Quartz	Hardly any attack noticeable at ≃300°, but severe attack at higher temperatures, ≃400°C	12, 22
	300	few	air	Pyrex	Serious attack	22
	300	400	$NO_2 + O_2$	Quartz	Attack after about 300 h.	23
$LiNO_3$–$RbNO_3$	≥360	≤193	$NO_2 + O_2$	Supremax; Quartz	Attack increasing with concentration of $LiNO_3$.	12, 24
Li_2SO_4	880	1	air	Vycor	No attack	12
$PbBr_2$	500	187	air	Pyrex	Very slight attack	25
	600	120	Br_2	Supremax	Slight attack	18
$PbCl_2$	530–640	≤235	Cl_2; air	Pyrex	Very slight attack	20, 26
				Supremax	Less attack than on Pyrex	
TlCl	530	190	air	Supremax	Not reported	27
	560–730	≤142	air	Alumina	Not reported; probably no attack	28
$ZnBr_2$	400–640	≤745	air	Supremax	Serious attack at high temperatures	29
$ZnCl_2$	≃650	198	Cl_2; air	Supremax	Attack increasing with temperature	7, 8

TABLE 2. MOLTEN METALS

Liquid	Temperature (°C)	Duration (h)	Material	Remarks	Reference
Cd	370–540	500	Pyrex		30
Ga	325–560	720	Pyrex		31
In	210–530	800	Pyrex		32
	820	360	Quartz		32
K	79–335	360	Pyrex	Attack increases with temperature	33
Li	300	160	Stainless steel		34
	630	1500	Stainless steel		35
Pb	520	190	Pyrex		25, 26
Rb	48–265	300	Pyrex	Attack increases with temperature	33, 36
Sn	285	400	Pyrex	Attack at ≃500°C	30
	590	650	Quartz		30
Zn	510	265	Pyrex		7, 8, 30

other cases the attack is located at a section where a compound with a high reactivity has been concentrated due to the relative mobility of its ions. (Lithium compounds are thus enriched towards the cathode.) However, there is some evidence that the presence of an electric field might have a tendency in itself to increase the reactivity.

Our experience with carbon electrodes in halides and with metal electrodes in nitrates has been summarized elsewhere.[10]

Molten metals have been used as electrodes in many experiments with molten salts,[10] and additional experience has been gained in the study of the isotope effect produced when a direct current passes through a molten metal.

REFERENCES

1. J. D. MACKENZIE, *Physicochemical Measurements at High Temperatures*, p. 334, ed. J. O'M. BOCKRIS, J. L. WHITE and J. D. MACKENZIE. Butterworths, London (1959).
2. W. J. BURKHARD and J. D. CORBETT, *J. Amer. Chem. Soc.* **79**, 6361 (1957). F. R. DUKE and A. S. DOAN, *Iowa St. Coll. J. Sci.* **32**, 451 (1958).
3. H. J. GARDNER, C. T. BROWN and G. J. JANZ, *J. Phys. Chem.* **60**, 1458 (1956). H. A. LAITINEN, W. S. FERGUSON, R. A. OSTERYOUNG, *J. Electrochem. Soc.* **104**, 516 (1957). D. L. MARICLE and D. N. HUME, *J. Electrochem. Soc.* **107**, 354 (1960).
4. A. LUNDEN, S. CHRISTOFFERSON and A. LODDING, *Trans. Chalmers Tek. Högsk. Handl.* No. 221 (1959).
5. A. KLEMM, H. HINTENBERGER and A. LUNDEN, *Z. Naturf.* **6a**, 489 (1951).
6. A. KLEMM, E. LINDHOLM and A. LUNDEN, *Z. Naturf.* **7a**, 560 (1952).
7. A. LUNDEN and W. HERZOG, *Z. Naturf.* **11a**, 520 (1956).
8. A. LUNDEN and A. LODDING, *Z. Naturf.* **15a**, 320 (1960).
9. A. LUNDEN, S. CHRISTOFFERSON and A. LODDING, *Z. Naturf.* **13a**, 1034 (1958).
10. A. LUNDEN, Thesis, Göteborg 1956.
11. S. FLOBERG, A. KLEMM and C. LANG, *Z. Naturf.* **8a**, 562 (1953).
12. A. LUNDEN, unpublished.
13. A. KLEMM, H. HINTENBERGER and W. SEELMANN-EGGEBERT, *Z. Naturf.* **3a**, 172 (1948).
14. A. LUNDEN and E. BERNE, *Z. Naturf.* **9a**, 684 (1954).
15. B. BLUMENTHAL and R. A. NOLAND, *Progr. Nuclear Energy*, Vol. 1 Series V, p. 62. Pergamon Press, London (1956).
16. A. LUNDEN, C. REUTERSWARD and N. G. SJOBERG, *Z. Naturf.* **10a**, 279 (1955).
17. A. LUNDEN and S. GUSTAFSSON, unpublished.
18. A. LUNDEN and G. BLOMQVIST, *Z. Naturf.* **15a**, 950 (1960).
19. *Thermal 505* from the Thermal Syndicate Ltd, Wallsend, Northumberland, England.
20. A. LUNDEN, G. HORLITZ and P. SIGNER, *Z. Naturf.* **11a**, 280 (1956).
21. A. KLEMM and E. U. MONSE, *Z. Naturf.* **12a**, 319 (1957).
22. A. LUNDEN, E. U. MONSE and N. G. SJOBERG, *Z. Naturf.* **11a**, 75 (1956).
23. J. I. HOOVER and C. E. HOLLOWAY, NRL-3897 (1951).
24. A. LUNDEN, *Ann. N. Y. Acad. Sci.* **79**, 988 (1960).
25. A. E. CAMERON, W. HERR, W. HERZOG and A. LUNDEN, *Z. Naturf.* **11a**, 203 (1956).
26. A. KLEMM and A. LUNDEN, *Z. Naturf.* **10a**, 282 (1955).
27. A. KLEMM, H. HINTENBERGER and W. SEELMAN-EGGEBERT, *Z. Naturf.* **3a**, 622 (1948).
28. W. HERZOG and A. KLEMM, *Z. Naturf.* **13a**, 7 (1958).
29. L.-E. WALLIN and A. LUNDEN, *Z. Naturf.* **14a**, 262 (1959).
30. A. LODDING, *Z. Naturf.* **12a**, 569 (1957).
31. M. GOLDMAN, G. NIEF and E. ROTH, *Compt. rend.* **243**, 1414 (1956).
32. A. LODDING, A. LUNDEN and H. v. UBISCH, *Z. Naturf.* **11a**, 139 (1956).
33. A. LODDING, *Z. Naturf.* **14a**, 934 (1959).
34. A. LUNDEN, A. LODDING and W. FISCHER, *Z. Naturf.* **12a**, 268 (1957).
35. D. B. TRAUGER, J. J. KEYES, G. A. KUIPERS and D. M. LANG, *Proc. Internat. Symp. Isotope Separation*, Edited by J. KISTEMAKER, J. BIGELEISEN and A. O. C. NIER, p. 350. Amsterdam (1958).
36. A. LODDING, *Z. Naturf.* **14a**, 7 (1959).

Corrosion Science, 1961, Vol. 1, pp. 65–75. Pergamon Press Ltd. Printed in Great Britain

SOME EFFECTS OF ELECTROLYTE MOTION DURING CORROSION *

T. K. Ross and B. P. L. Hitchen
Chemical Engineering Dept., Manchester College of Science and Technology
Manchester, England

Abstract—The effect of the rate of flow of water upon the electrochemical behaviour of tubular couples of iron and copper, carbon and copper, and copper tubes of different diameters is examined. The importance of water velocity in the depolarization of cathodic processes is shown, together with the probable results of changes of cross section. An explanation of the results in terms of the liquid boundary layer at the metal surface is suggested.

Résumé—Les auteurs ont étudié l'effet de la vitesse de passage de l'eau sur le comportement électrochimique de couples tubulaires en fer et cuivre, en carbone et cuivre, et de tuyaux en cuivre, de diamètres différents. Ils démontrent la signification de la vitesse de l'eau en ce qui concerne la dépolarisation des processus cathodiques, et les résultats probables d'un changement de la coupe transversale. Pour l'explication des résultats, on s'adresse à la couche liquide limite au niveau de la surface du métal.

Zusammenfassung—Die Auswirkung der Wasser-Durchflussmenge auf das elektrochemische Verhalten von röhrenförmigen Gebilden aus Eisen und Kupfer, Kohlenstoff und Kupfer und auf Kupferrohre verschiedenen Durchmessers wird untersucht. Es wird gezeigt, welche Bedeutung die Geschwindigkeit des Wassers für die Depolarisierung von Kathodenprozessen hat, daneben werden die voraussichtlichen Auswirkungen von Querschnitts-Veränderungen angedeutet. Zur erklärung der Ergebnisse wird die flüssige Grenzschicht an der Oberfläche der Metalle herangezogen.

1. INTRODUCTION

That relative motion between the environment and a metal surface results in a modification of the corrosion rate of the latter has long been recognized. The phenomenon is particularly associated with the difficulty of applying the results of static testing to the selection of materials for the construction of propellers, mixers, stirrers, or tubular heat exchangers. Heyn and Bauer[1] first called attention to the effect of relative motion upon the reaction between iron and oxygenated water, finding that a graph drawn between the corrosion rate and stirring speed exhibited a maximum; this result has been confirmed in one form or another by many workers. Roethelli and Brown[2] attributed the failure of rapid motion to maintain an increase in the corrosion rate to the formation of a protective scale. Speller's work[3–5] on the internal corrosion of iron pipes by oxygenated water led him to similar conclusions, and Whitman[6] outlined the theoretical problems associated with the phenomenon. That the normal distribution of dissolved oxygen at a corroding iron or steel surface was in fact disturbed by impressed motion in the electrolyte was later demonstrated conclusively by Hatch and Rice.[7, 8] More recent work on the long-term internal corrosion of pipe lines has led Eliassen and his associates[9–12] to explain their results in terms of classical fluid dynamic theory.[13] Wormwell,[14–16] on the other hand, investigated the effect of rotation upon the potential of a corroding iron specimen and observed that increasing the speed of rotation resulted in an ennobling of the metal surface. The potential reached a constant value at 600 revolutions/min, which maximum Wormwell attributed to the formation of a protective film.

Although the greater part of the literature on velocity effects is concerned with the

*Manuscript received 20 September 1960.

corrosion of iron and steel, the important industrial uses of copper and its alloys in tubular apparatus have also led to investigations of these materials. Bengough and Hudson's early work[17] illustrated that a copper surface experienced corrosion when exposed to the flow of oxygenated water. In an extensive investigation of this and related problems Bengough and May[18] found that corrosion increased with velocity up to a maximum of 25 ft/sec. They were also able to distinguish between the relatively minor importance of dissolved oxygen, and the much more serious effect of small air bubbles suspended in a turbulent liquid stream.

There is certain evidence that the action of corrosion inhibitors is substantially reduced by movement in the electrolyte. Chufarov[19] and Beck and Hessert[20] both recorded a reduction of inhibition at increased velocities and the latter attributed this in the case of colloidal inhibitors to more rapid dispersion of precipitating metallic ions. Some recent Russian work[21] has shown that increased flow rates may not only reduce the efficiency of inhibitors for the acid corrosion of iron, but may even cause them to act as stimulators.

2. EXPERIMENTAL

An investigation was conducted with the intention of establishing the effect of fluid velocity upon the electrochemical behaviour of cylindrical metal surfaces exposed to oxygenated water. This information was sought both as a basis for our own work into the effect of velocity upon inhibitor efficiency, and also in the hope that it might assist in predicting the corrosion resistance of tubes from static testing.

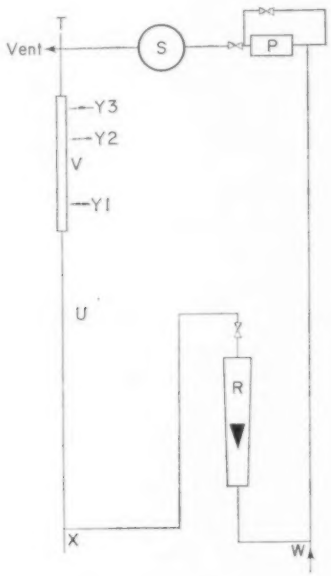

FIG. 1. Diagrammatic view of circulating system. P—pumps, R—Rotameters, S—Storage vessels, T—thermometer, U—test length, V—flow cell, W—oxygen addition, X—glass electrode, Y—calomel electrodes.

A glass circulating system was built, in which tubular or annular metallic specimens could be arranged in such a way that their polarization characteristics under flowing conditions could be observed. The circulation system (shown diagrammatically in Fig. 1) permitted the insertion of prepared metallic specimens so that a suitable length (in excess of one hundred pipe diameters) of straight tubing preceded the test section, thus ensuring that the flow conditions in the test section were properly established.

By means of the circuit shown in Fig. 2 the current flowing between parts of a couple was controlled at any desired value by use of the decade resistance. The steady potential was then observed on the potentiometer, and the current measured on the ammeter at zero resistance balance. A series of such readings were obtained at a given flow rate, from which a polarization diagram was constructed. The temperature and pH of the circulating system were also measured intermittently, the latter by means of the glass electrode of the electrical circuit.

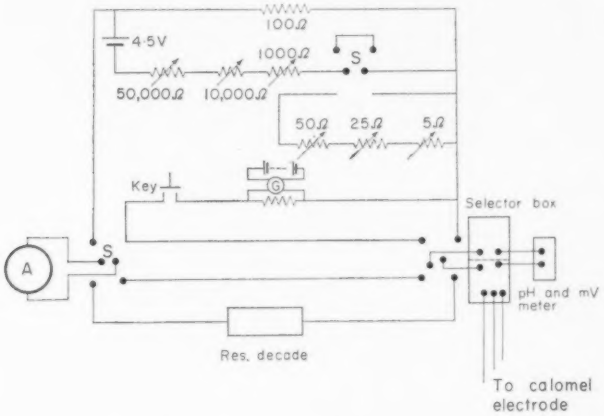

FIG. 2. Circuit for determining polarization data.

2.1. *Materials*

Three materials were used in the construction of the corrosion specimens; copper tubing to B.S. 659, mild steel rod (0·08% C, 0·39% Mn, 0·20% S), and high grade electrode carbon rod. When arranged singly or in pairs combination specimens in which the copper surface was placed in a cathodic or anodic role were possible. Three series of experiments were carried out, in which copper was paired with iron, carbon, or other copper surfaces respectively. The circulating fluid was in all cases distilled Manchester water of initial pH 6·8.

3. RESULTS

3.1. *The iron–copper couple*

The first experiments were conducted with a specimen constructed from a 6 ft length of copper tube 0·843 in. internal diameter, and 6·5 ft of mild steel rod of 0·250 in. external diameter. Three holes 0·188 in. diameter were drilled in the copper tube at points distant 6 in., 4 ft and 5 ft from one end, into which the tips of saturated calomel electrodes were fitted flush with the inside surface of the tube. These electrodes were secured in the flow system by flexible seals placed over glass T-pieces in the circulating system. After soldering electrical leads to both elements, the inner surface of the copper tube and the outer surface of the steel rod were cleaned prior to assembly with successive washes of dilute sulphuric acid, distilled water, and alcohol. The steel rod was then fixed centrally in the copper tube by means of two thin plastic supports, and the outer surface of the copper tube and both soldered joints coated with shellac.

The completed assembly was then connected to the glass circulating system, and the system filled with distilled water. The circulation was commenced at a low rate, and all entrapped air displaced by further filling. When the system was completely filled oxygenation was commenced and the desired circulation rate established. Potential and current measurements of the iron-copper couple were then recorded, and repeated at five-minute intervals until steady readings were obtained. Fig. 3

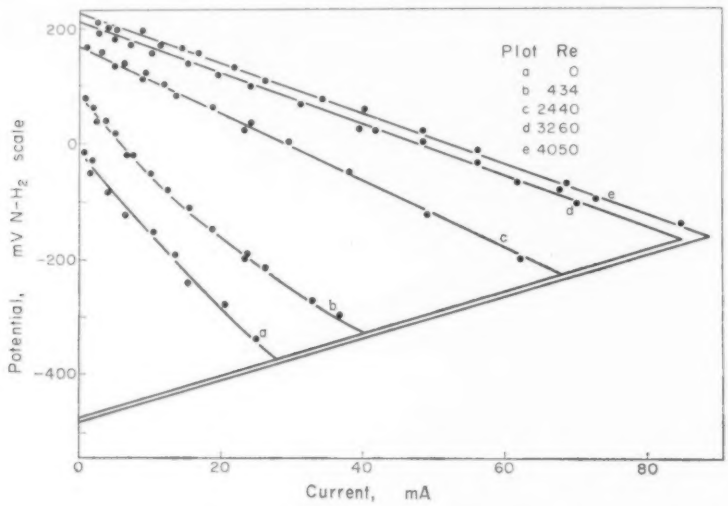

Fig. 3. Polarization curves of copper–steel couple at various flow rates of distilled water (pH 6·9, 20°C).

shows how the polarization properties of the couple varied with flow rate. The latter is conveniently expressed in the form of the dimensionless Reynolds Number,

$$Re = \frac{d\, v\, \rho}{\mu}$$

where d = the appropriate hydraulic diameter of the couple
v = the mean linear flow velocity in couple
ρ = the mean density of the fluid
μ = the mean viscosity of the fluid,
in any consistent units.

This value affords a criterion of the state of flow in the fluid, streamline flow being considered to exist at values of *Re* below 2000, and turbulent flow at values in excess of 3000.

It will be observed from Fig. 3 that the behaviour of the iron anode was little affected by flow rate, but that the copper cathode was rendered more noble and less polarized by increases in water velocity. Such data may also be plotted in the alternative form of Fig. 4, which shows how both the couple potential and current flow at short circuit are affected by flow rate. This effect is clearly more marked under streamline flow conditions.

The presence of metallic ions in the solution rendered accurate oxygen analysis

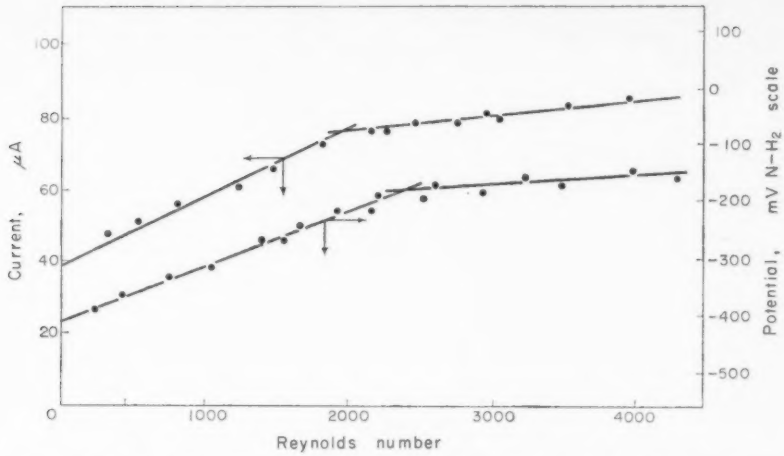

FIG. 4. Fully polarized potential and current flow at various flow rates of distilled water at pH 6·9, 20°C.

difficult, but that the oxygen content also had an important bearing on the behaviour of the couple is clear from Fig. 5. The results here shown were obtained by running at a constant value of $Re = 4000$, but without oxygenation, so that the oxygen content of the circulating water was gradually exhausted. Although the total corrosion current (and short circuit potential) fell with the oxygen content, the distinction between the role of copper cathode and iron anode persisted.

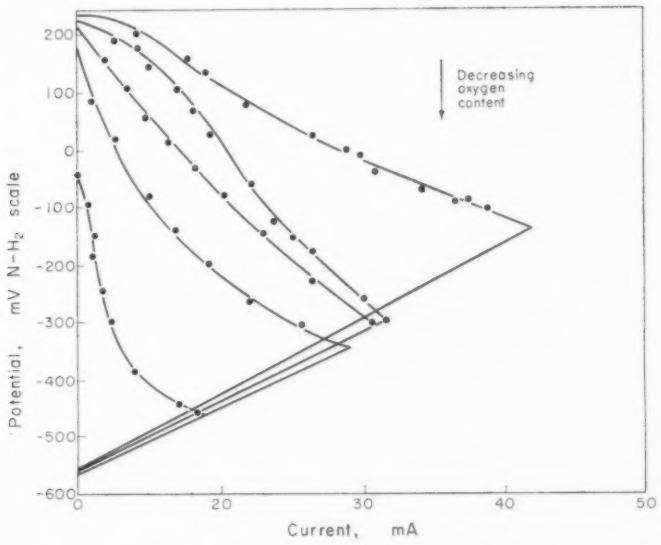

FIG. 5. Polarization curves of copper–steel couple at forced flow rate but decreasing oxygen content (pH, 6·9, 21°C).

3.2. *The carbon-copper couple*

Further experiments were conducted in which the copper tube was forced into a predominantly anodic role by replacing the mild steel rod with a carbon rod (external diameter 0·188 in.) which was secured inside a copper tube of internal diameter 0·750 in. The polarization curves of Fig. 6 show that under these circumstances the anodic processes on the copper surface are accelerated by increases in water flow, particularly

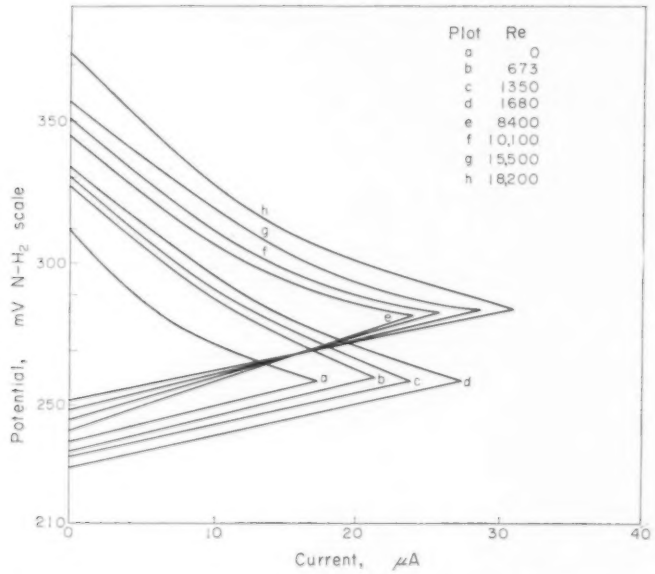

Fig. 6. Polarization curves of carbon–copper couple at various flow rates of distilled water (pH 6·8, 20°C).

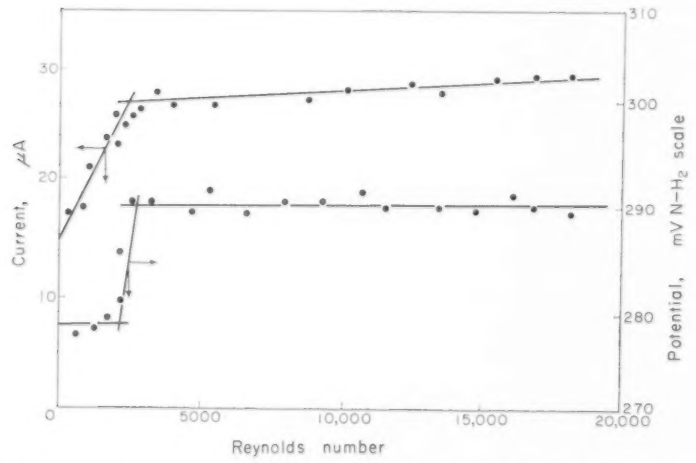

Fig. 7. Fully polarized potential and current flow at various flow rates (pH 6·9, 21°C).

in the region of streamline flow. The maximum current flow and fully polarized potential also experience (Fig. 7) sharp changes with velocity variation, although the total corrosion current available from the copper anode was, of course, less than that measured in the previous case. Under streamline flow the copper anode potential became less positive and less polarized, but on transition to turbulent conditions the anode became ennobled although depolarization continued.

The behaviour of the carbon cathodes is not of particular importance, but it is of interest that ennobling and depolarization of the carbon surface is also produced by increasing flow rate.

3.3. *Copper tubes of different diameter*

Earlier results suggested that the anodic and cathodic reactions on copper surfaces were effected by water velocity to different extents, and that differential potentials could develop when variously sized copper tubes were exposed to moving liquids. Some experiments were conducted in which these effects were demonstrated. Sections of copper tube of different internal diameter were placed in the circulating system in such a way that they were insulated from one another by a long plastic spacer whose internal diameter tapered from that of one tube to that of the other. The copper tubes were so sized that their internal surfaces were all equal to 3 in^2 and they were cleaned as previously described.

The results previously obtained indicated that at identical volumetric flow rates the smaller (or more turbulent) tube of a pair would become the anode with respect to its larger diameter partner. The results, in fact, confirmed this view, and the polarization curves revealed that anodic control was exerted whenever the flow regime was the same in both tubes. However, an anomalous situation was found to exist when the flow rate was such that streamline flow obtained in the larger tube,

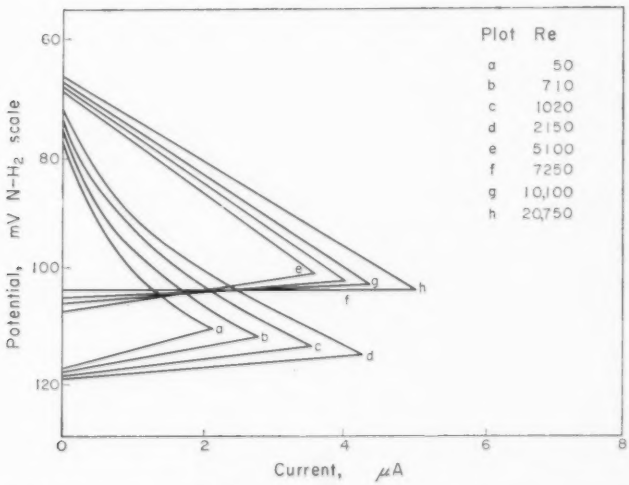

FIG. 8. Polarization curves obtained from copper surfaces at different flow rates (pH 6·8, 20°C).

but turbulence developed in the smaller, for in such cases the latter became the cathode of the pair. This was explained by an examination of the polarization of a single copper tube at different flow conditions. A copper tube of 0·843 in. inner diameter, and a total internal surface of 3 in² was mounted in the flow apparatus with a length of platinum wire at its axis. By connecting the copper tube and the platinum wire to a potentiostat the cathodic and anodic processes occurring on the surface at various flow rates were investigated. When such data are plotted in the usual form of a polarization diagram as in Fig. 8 it can be seen that pairs of surfaces in which both members were exposed to turbulent (points F, G) or streamline flow (points C, D) the fully polarized potential of local anodes and cathodes is such as to render the smaller member more negative, or anodic. On the other hand the potential of pairs of specimens exposed to different flow regimes (e.g. F and C, or G and D) are such as to force the smaller member to be cathodic. This is solely due to the change in the polarization characteristics of a copper anode upon transition from streamline to turbulent flow.

A further interesting phenomenon was observed, namely temporary reversals of polarity subsequent to a sudden change in the flow rate. Fig. 9 illustrates this effect and clearly shows how the two tubes are at almost the same potential at zero flow, but after suddenly establishing turbulent flow the smaller diameter tube develops cathodic properties which persist for some twenty minutes, when it reverts to its

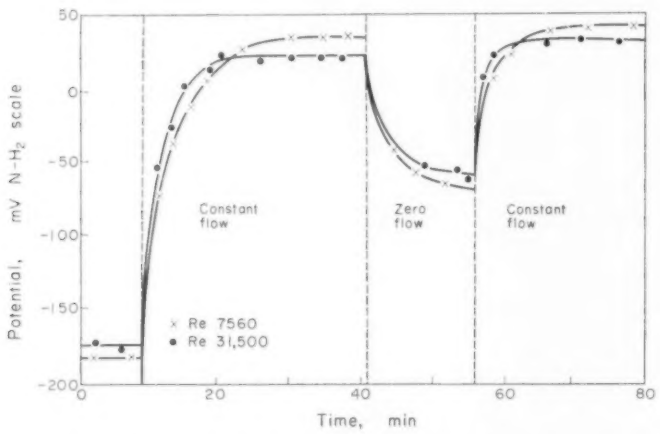

Fig. 9. Variation of open circuit potentials of two copper surfaces: intermittent turbulent flow (pH 6·9, 21°C).

normal anodic position. Repetition of this cycle is also seen to be possible; similar results were obtained by increasing the flow rate by the same amount (say from 100 to 190 gall/hr. When both tubes remained in streamline conditions throughout the flow rate change the potential of both tubes responded to the alteration (Fig. 10) but no reversal of polarity is observed.

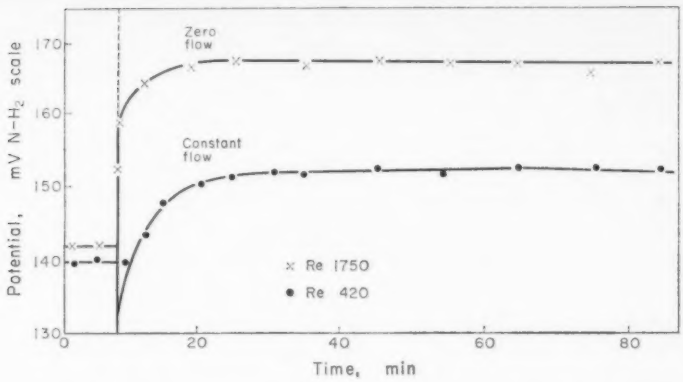

FIG. 10. Variations of open circuit potentials of two copper surfaces: intermittent streamline flow (pH 6·9, 20°C).

4. DISCUSSION

The results obtained with the iron-copper couple illustrates the importance of fluid velocity in its effect upon the cathodic processes. That this is due to the rate at which dissolved oxygen is made available at that surface is fairly clear. It is possible to express such a transfer by equations of the following form:
In streamline flow

$$N_S = \frac{D \,.\, \Delta C}{\delta_S}$$

where N_S = moles of oxygen transferred across a boundary layer of unit mean area in unit time.
δ_S = mean thickness of that boundary layer at the solid surface.
D = diffusivity of oxygen in water.
ΔC = mean difference of oxygen concentration between bulk solution and cathodic equilibrium.

Under turbulent flow the diffusional transfer is supplemented by eddy transfer (E) of bulk solution into the boundary layer, and if the diffusivity is written as ($D + E$) to represent this supplementation, the expression

$$N_T = \frac{(D + E)\Delta C}{\delta_T}$$

represents the transfer of dissolved oxygen to the cathode surface.

If it is assumed that the reaction by which oxygen is consumed at the cathode is rapid and irreversible the concentration difference ΔC approaches the bulk concentration unless the boundary layer is very thin. With this exception, the rate of cathodic depolarization is inversely proportional to the boundary layer thickness, which in turn depends on Reynolds Number. Under streamline conditions δ_S is comparatively large (ideally approaching the tube radius) and the cathodic depolarization is sensitive to flow rate. Under turbulent flow conditions δ_T is much less than δ_S under streamline conditions, so that the boundary layer is a less important barrier and the concentration difference ΔC may be less than the bulk concentration. Both δ_T and ΔC will decrease

as Reynolds Number increases, and as these quantities influence the rate of transport of oxygen in opposite senses the cathodic depolarization may be relatively insensitive to Reynolds Number. The difference in the degree of dependence of the corrosion current and polarized potential of the iron-copper couple (Fig. 4) on flow rate follows from these arguments.

Fig. 3 suggests that the iron anode is little effected by flow rate, being relatively constant in potential and polarization over a large range of Reynolds Numbers. This may be explained by an argument similar to that advanced by Colombier[22] for static conditions. This is that the rate of formation of ferrous ions at the iron surface always exceeds or equals the rate at which they are transported by diffusion and turbulence, and so no change in anode potential or polarization results.

When copper, which provides ions so much less readily in neutral aqueous solutions, is made the anode, this insensibility to the flow rate no longer obtains. In the carbon-copper couple, the polarization behaviour of the anode varies with the Reynolds Number. In general the open circuit potential falls with increase of flow in the streamline range; the slope of the anode line (Fig. 6) indicates that the dissipation of metal ions from the surface exceeds the rate of their formation. During further increases of flow into the turbulent range this slope continues to decrease, but the open circuit potential becomes progressively more positive. This ennobling of the surface is probably due to the passifying effect of the oxygen which is transferring to the anode at an increased rate under turbulent conditions.

These aspects of flow in the electrolyte serve to explain the results obtained with copper tubes of different diameter. The result of the combination of these two phenomena is that copper surfaces exposed to flow at higher Reynolds Numbers tend to become anodic with respect to similar surfaces exposed to lower flow rates. This is always true when both surfaces are exposed to flow of the same quality. However, when the total volumetric flow is such that a change of flow regime occurs with a change of cross-section, then the ennobling effect of turbulence results in a cathodic role of the surface exposed to the more rapidly moving stream.

That the boundary layer has important finite dimensions is shown by the interesting reversals of potential which occur after sudden changes of flow rate. The sense of these changes is that the surface exposed to rapid motion acquires its final potential very rapidly. The surface in the slower stream on the other hand is much slower in coming to equilibrium, so that although in accordance with previous arguments it is destined to be the cathode of the pair, it may spend some time at a lower potential. When exposed to slowly moving or stagnant water the initial distribution of local anodes and cathodes on each surface may be assumed to be roughly the same. The delay of the surface exposed to low velocities in attaining equilibrium may only be attributed to interference with diffusional processes at the surface. In fact, if the surface layers of liquid are assumed to be depleted of oxygen when stagnant, the sudden resumption of movement introduces a transitory effect during which the boundary layer is filled with dissolved oxygen by diffusion.

A general expression for the thickness δ_T of the boundary layer formed on a smooth surface under turbulent flow is

$$\frac{\delta_T}{d} = \frac{62}{(Re)^{0\cdot875}}$$

The total volume of boundary layer V_T formed over a cylindrical surface diameter d and length L is then

$$V_T = \pi dL \,.\, \delta_T = \frac{62\pi L}{(Re)^{0.875}}$$

Now in these experiments πdL was made constant, so that the effect of Reynolds Number upon the boundary layer volume was almost an inverse one, so that the transition period elapsing before a concentration gradient is established across the boundary layer varies in the same manner. Hence larger diameter tubes experience the larger delay in attaining their more positive, or cathodic, potential. Of course these results apply only to the very short-term electrochemical effects resultant upon flow, and take no account of the effects of accumulated scale or corrosion product. Nonetheless, in showing that flow rate may determine the electrochemical role of a surface from the outset the extent and distribution of such scale must be considered a result rather than a cause in the long term process.

5. CONCLUSIONS

The effect of fluid velocity on the short-term electrochemical behaviour of iron, copper and carbon arranged in annular couples exposed to distilled water has been shown to be such as would result in changes in corrosion rates. The effect of differences in flow rate caused by dimensional changes may be such as to produce areas of a selective electrochemical nature, which may experience reversals if the flow rate fluctuates.

Although measurements were made only with three materials exposed to moving distilled water, the results should be applicable to other situations. When the transport of ions to or from the metal surface is a controlling factor in corrosion, velocity effects may be expected to be important ones.

REFERENCES

1. E. Heyn and O. Bauer, *Mitt. Nat. Prut. Amt. (Berlin)* **28,** 100 (1910).
2. B. E. Roethelli and R. H. Brown, *Industr. Engng Chem.* **23,** 1010 (1931).
3. F. N. Speller and V. U. Kendall, *Industr. Engng Chem.* **15,** 134 (1923).
4. F. N. Speller, *Corrosion, Causes and Prevention.* McGraw-Hill (1935).
5. F. N. Speller, *J. New Enge. Wat. Wks Ass.* **52,** 231 (1938).
6. W. G. Whitman, *Chem. Rev.* **2,** 419 (1926).
7. G. B. Hatch and O. Rice, *Industr. Engng Chem.* **32,** 1572 (1940).
8. G. B. Hatch and O. Rice, *Industr. Engng Chem.* **37,** 753 (1945).
9. R. Elliassen, C. Pereda, A. J. Romeo and R. T. Skrinde, *J. Amer. Wat. Wks Ass.* **48,** 1005 (1956).
10. R. Eliassen and J. C. Lamb, *J. Amer. Wat. Wks Ass.* **45,** 1281 (1953).
11. R. Eliassen and J. C. Lamb, *J. Amer. Wat. Wks Ass.* **46,** 445 (1954).
12. R. Eliassen and J. C. Lamb, *J. Amer. Wat. Wks Ass.* **69,** 31 (1955).
13. A. J. Romeo, R. T. Skrinde and R. Eliassen, *Proc. Amer. Soc. Civ. Engrs.* Paper 1702 (1958).
14. F. J. Wormwell, *J. Appl Chem. Lond.* **3,** 164 (1953).
15. F. J. Wormwell, *J. Appl. Chem. Lond.* **3,** 276 (1953).
16. F. J. Wormwell and C. Ison, *Chem. and Ind. (Rev.)*, p. 549 (1950).
17. G. D. Bengough and O. F. Hudson, *J. Inst. Met.* **21,** 122 (1919).
18. G. C. Bengough and R. May, *J. Inst. Met.* **32,** 174 (1924).
19. G. Chuferov, *Uralsk. Metall.* **1,** 42 (1936).
20. Z. J. Beck and A. Hessert, *Z. Elektrochem.* **37,** 11 (1936).
21. I. N. Putilova, S. A. Balezin and V. P. Barronik, *Metallic Corrosion Inhibition*, p. 38. Pergamon Press, London (1960).
22. L. Colombier, Doctoral Thesis, Université de Nancy, 1936.

Corrosion Science, 1961, Vol. 1, p. 76. Pergamon Press Ltd. Printed in Great Britain

BOOK REVIEW

Technology of Non-Metallic Coating. A. YA. DRINBERG, E. S. GUREVICH and A. V. TIKHOMIROV, translated and edited by E. BISHOP. Pergamon Press, 1960. pp. XVI + 531, with 161 figures. 80s. net.

THIS Russian text-book is an attempt to bring within the compass of one volume the whole field of organic and non-metallic inorganic coatings on both metals and on non-metallic substrates. The major emphasis is on paint coatings and on metal substrates.

The book begins with four chapters (95 pp.) on corrosion theory and on the scientific principles of coating formation and of coating properties. Preparation of metal surfaces (17 pp.) and a general discussion of paint coatings on metals (70 pp.) then receive adequate treatment, but inorganic non-metallic coatings (16 pp.) and organic linings and greases (4 pp.) are very sketchily dealt with. The painting of wood, textiles, leather, plaster and concrete is given four chapters (89 pp.) and the book concludes with five chapters (197 pp.) on equipment and shop practice. There is an appendix containing miscellaneous tabulated information and an index of standard specifications. Small but adequate author and subject indexes are included—the author index being, of course, as overwhelmingly Russian as we have come to expect of Russian text-books.

The treatment throughout is usually sound, at a generally elementary level; paint chemistry is better handled than metal chemistry. A few errors of fact have been noted: for example the standard electrode potential of chromium is given (probably by a misprint, of which there are very few) as $-0{\cdot}41$ V (E_H); and the lowest layer of heat scale on steel is said to be ferrous oxide, which "readily changes to hydrated ferric oxide under the influence of water and oxygen"—its prior eutectoidal decomposition on cooling has evidently been overlooked. The brief electrochemical introduction to corrosion processes is rather unsound; thus the standard or normal potential of a metal electrode is defined as that for a "metal immersed in a solution of its own ions of concentration N", pH is "the logarithm of the hydrogen ion concentration", and the normal calomel electrode is depicted with two electrical leads to the mercury and no statement of the potassium chloride concentration. This kind of inexactitude is what one expects from a final-year student in the lower second class: it should not occur in the text-books he may have to use. On the other hand, technical processes are described clearly and simply, with good engineering calculations; only occasionally does simplicity lapse into naiveté, as in "The basic tools for the brush method of painting are brushes of various shapes and sizes".

The translation is throughout excellent, being remarkably free from the solecisms of language, jargon and taste so often found in less expert translation of technical matter. Perhaps a little more editing, for example the removal of some of the very short paragraphs (14 paragraphs on p. 125), would have made for better readability.

The book is produced by photolithography of typescript, and one must respect the publisher's apology for this on the grounds of speed and economy; books of this kind are of value only for a limited period after they are written and only if they can reach a wide audience through a reasonable price. At the same time, the general quality of the production *considered as typescript* is well below what could be achieved. Several typewriters have been used, the letter "w" often comes out irritatingly black, and some of the lay-out leaves something to be desired. If photolithographed typescript is to become widespread, can we at least have the typing done on modern electrical machines of the highest quality? The Americans have been doing it for years.

Despite the several points of criticism noted above, the book is of value to the practising corrosion technologist in that it will introduce him to many fields in which he may not be expert, and it should be read with advantage by the technological student to off-set some of the natural ties he may have formed to Western text-books and methods; after all, our own author indexes contain far too few Russian names.

T. P. HOAR

Corrosion Science, 1961, Vol. 1, pp. 77–87. Pergamon Press Ltd. Printed in Great Britain.

FACTORS OF CONTROL AND METAL PROTECTION AGAINST CORROSION*

N. D. TOMASHOV
Institute of Physical Chemistry, U.S.S.R. Academy of Sciences, Moscow, U.S.S.R.

Abstract—It is considered that a classification of the various methods of corrosion control according to the method of their application is not rational. A more scientific approach is to classify the methods of protection according to their effect on the mechanism of the corrosion, i.e. the effect on the thermodynamic instability of the corroding system, on the cathode and anode processes and on the ohmic resistance of the system.

It is suggested that the most efficient methods of protection are those which influence these processes. When several methods are used concurrently a higher efficiency of protection is obtained if all the methods used affect the same controlling factors; if they affect different controlling factors the overall efficiency may even be decreased.

Résumé—On constate qu'il est irrationnel de classifier les diverses méthodes de contrôle de la corrosion selon leur mode d'application. Une classification des méthodes de protection basée sur leur incidence sur le mécanisme de la corrosion—par exemple, leur effet sur l'instabilité thermodynamique du système en corrosion, sur les processus anodiques et cathodiques, et sur la résistance ohmique du système, est plus rationelle. On suggère que les méthodes de protection les plus efficaces sont celles qui influencent ces processus; lorsqu'on utilise en même temps plusieurs méthodes, on obtient la meilleure protection lorsque toutes les méthodes utilisées affectent le même facteur de contrôle des réactions. Si elles affectent des facteurs différents, leur efficacité globale peut en être diminuée.

Zusammenfassung—Es wird angenommen, dass die Klassifizierung der verschiedenen Methoden der Korrosions-Kontrolle ihren Anwendungen nach nicht rationell ist. Ein mehr wissenschaftlicher Angriff des Problems ist die Methoden nach ihrem Effekt auf den Vorgang des elektrochemischen Zellen-Mechanismus zu Klassifizieren, d.h. ihren Effekt auf die thermodynamische Unstabilität des korrodierenden Systems, auf die anodischen und katodischen Vorgänge, und auf den ohmischen Wiederstand des Systems.

Es wird vorgeschlagen, dass die besten Methoden diese sind, die einen Einfluss auf die oben gennanten Faktoren haben. Wenn verschiedene Methoden zusammen benützt werden, werden die besten Resultate erziehlt wenn alle diese Methoden auf denselben Mechanismus einen Einfluss haben. Wenn jede Methode auf einen anderen Mechanismus einen Einfluss hat, kann sogar eine Verringerung der Korrosions-Kontrolle entstehen.

IT IS of great interest to discuss the existing methods of corrosion protection[1–6] in terms of the manner in which each method affects the various electrochemical steps of the process. This approach, besides developing a rational scientific classification of the various methods of corrosion protection, provides an indication of the best manner in which the various methods can be used either singly or in combination.

METHOD

1. *Protective coatings*

Protective coatings may vary greatly in thickness from very thin protective layers, such as adsorbed passive films which are only a few Ångstrom thick, to linings which, at times, exceed 2-3 cm in thickness. There are various types of coatings such as organic coatings (paints, varnishes, high polymer coatings, greases, and oils); inorganic coatings (oxides, phosphates, chromates, etc.) and metal coatings of different types (metal spraying, hot dipping, thermochemical diffusion, cladding).

*Manuscript received 14 April 1961.

2. *Treatment of the corrosion medium*

This includes neutralization and de-aeration of a liquid medium, the employment of different types of inhibitors, including volatile inhibitors which are widely used in atmospheric conditions, and certain other methods of protection.

3. *Electrochemical protection*

The following varieties of electrochemical protection are used commercially:

(a) cathodic protection using inert or sacrificial anodes.
(b) anodic protection.
(c) protection from stray currents by electro-drainage.

4. *The development and production of new structural metals* of increased corrosion resistance.

5. *Rational design and exploitation* of metal structures and parts.

From the scientific point of view, it is more interesting to analyse and classify the various methods just enumerated from the point of view of the mechanism of the protective action than by considering the conditions under which they are used and the method of application. To do this, it is necessary to determine the particular step of the corrosion process which is mainly inhibited by the given method of protection, i.e. to determine the principal *controlling factor for each method of protection*. If this is done it is possible in every case to outline the mechanism of inhibition with sufficient certainty.

The dependence of the corrosion current, which is equivalent to the corrosion rate, on the main factors controlling electrochemical corrosion is given by:

$$I = \frac{E^\circ_C - E^\circ_A}{\eta_C + \eta_A + R}$$

where $E^\circ_C - E^\circ_A$ is the difference between the reversible potentials of the corrosion couple, i.e. of the equilibrium potentials of the cathodic process (E°_C), and of anodic metal dissolution (E°_A), for the corrosion reaction where η_C and η_A are the cathode and anode polarization and R is the ohmic resistance. This voltage is equivalent to the e.m.f. of the corrosion couple and is proportional therefore to the free energy decrease associated with the corrosion reaction. Thus, $E^\circ_C - E^\circ_A$ is *the degree of thermodynamic instability* of the given corrosion system. The denominator of this expression represents the overall inhibition of the system which is expressed by three parameters with the dimension of resistance.

It is logical to take these four factors as the basis for a scientific classification of the different methods for diminishing the corrosion rate.*

A number of methods for reducing corrosion are associated with inhibition of the cathodic process. Examples are inhibitors which increase the overvoltage of the cathodic reaction, treatments which decrease the concentration of the oxidizing substances in the solution such as the hydrogen ion concentration or the dissolved oxygen, and also methods which decrease the active cathodic inclusions in an alloy.

*Similar concepts are applicable not only to the analysis of the mechanism of inhibition of the electrochemical corrosion of metals but also to more general cases of determining the kinetics of chemical heterogenous reactions.

Cathodic protection, particularly with sacrificial anodes, is in this class. The association of cathodic protection with methods which increase the cathodic control of the corrosion cell, follows directly from the simplest determination of the nature of control. As has been indicated earlier from the known values of steady-state corrosion potentials (E_x) and the initial potentials of the cathodic (E_C°) and anodic (E_A°) processes[7-9] a quantitative evaluation of control is possible. In particular the degree (percentage) of cathodic control (C_C) will be determined by the expression:

$$C_C = \frac{E^\circ_C - E_x}{E^\circ_C - E^\circ_A} \cdot 100$$

From this it follows that when the values of E°_C and E°_A are stable, any decrease in the E_x value, i.e. a shift of the corrosion potential (E_x) to the negative side, will correspond to an increase in the degree of cathodic control. Thus, the cathodic protection associated with a shift of the corroding surface potential (E_x) in the negative direction may be interpreted as a reduction of corrosion because of an increase in the degree of the cathodic control of the corrosion cell.* In this way it can be seen that it is the cathodic process which is predominantly inhibited in the case of cathodic protection whether using impressed currents or sacrificial anodes. When a corroding surface is polarized cathodically by an external current, the microcathodes are so greatly overloaded by the external circuit that they cease working for the internal circuit, since the corroding surface is a less active anode than the attached galvanic protective anode.

Many methods of protection are based, however, on the inhibition of the anodic process. Examples include the addition of anodic inhibitors or passivators to the solution; the increase by alloying of the ability of the metal to passivate; the introduction of noble metal ions into the solution or the inclusion of noble metals into the metal. We may also class in this category the recently discovered method of combating corrosion—anodic protection—which can be used when the metal passivates easily.[10-18]

The possibilities of obtaining protection by increasing the ohmic inhibition are more limited. This is certainly due to the smaller part played by ohmic control in the processes of electrochemical corrosion, particularly when the corrosion process is determined by the operation of micro or sub-micro cells.[10] However, combating underground corrosion by macro-corrosion cells by drying out the ground around the structure can be classed in this group.

There are numerous methods of combating corrosion which depend on lowering the degree of the thermodynamic instability of the given corrosion system. The degree of the thermodynamic instability is determined not only by the nature of the metal but also by the surrounding corrosion medium and the general physical conditions of the system in question.

Examples of combating corrosion by reducing the thermodynamic instability of the system are the covering of a thermodynamically active metal by a continuous layer of a more thermodynamically stable metal (for instance the coating of copper or of a copper alloy with gold, the coating of steel with nickel). Another case is the alloying

*The increase of the cathodic control of corrosion due to the cathodic polarization of the electrode does not contradict with the increase in the total efficiency of the cathodic process which is observed in this case, because the extent of the cathodic control of the corrosion cell is not directly associated with the increase in the efficiency of the cathodic process brought about by the external cathodic polarization.

of nickel with a sufficiently high percentage of a more thermodynamically stable component, copper for instance (or chromium steel with nickel).

It is not always possible to decide with certainty in what group of protection a method should be classed. For instance the decrease of the concentration of cathodic and anodic depolarizers affects not only the cathodic and the anodic polarizability, but also the initial potentials (E°_{C}) and (E°_{A}) of the cathode and anode. A decrease in the oxygen content of a solution, for example, can be regarded as cathodic inhibition or as a lowering of the thermodynamic instability of the system. The quantitative solution of this question can be carried out on the basis of the determination of the nature of the change of the cathodic control value (C_C), with the changing conditions of corrosion. In this case it will probably be concluded that a small decrease in oxygen concentration in a solution should properly be regarded as cathodic inhibition. On the other hand the complete exclusion of oxygen from the system, just as the complete isolation of the metal surface from the active medium, should be fundamentally regarded as slowing down corrosion by decreasing the thermodynamic instability of the system.

This reasoning also classes the non-swelling insulating organic and inorganic coatings, glass-enamels and linings as methods which increase the thermodynamic stability of the system. If these coatings are not continuous but porous, then this statement would naturally apply only to that part of the metal surface which is isolated from the corrosive medium.

The swelling varnishes and paint coatings (permeable to ions) are however more rationally classed as methods which act by increasing both cathodic and anodic polarization and the ohmic resistance. A precise classification of coatings, according to the mechanism of their behaviour, is possible only after a quantitative study of the mechanism of their inhibitive action on the corrosion process and a qualitative determination of the controlling factor for every type of coating has been made.

In the cases in which we have no quantitative data of the mechanism of the protective action of a coating, we shall conditionally class their action with the isolation of the metal from the corrosive medium, i.e. we will assume that they increase the thermodynamic stability of the system.

Table 1 presents a classification of the various protective methods according to the mechanism of the electrochemical corrosion. The classification is based on the nature of the influence of a given type of protection upon the motive factor of corrosion (the change in the degree of the thermodynamic instability) or on the principal controlling factors of corrosion. In keeping with the conclusions of the electrochemical theory of corrosion, all the known and possible methods of corrosion protection fall into four main groups, differentiated by the nature of the influence of protection upon the corrosion process.

1: Methods which lower the degree of the thermodynamic instability of the corrosive system.
2: Methods which retard the corrosion rate by inhibiting the cathodic process (increase in cathodic control).
3: Methods which inhibit mainly the anodic process (increase in anodic control).
4: Methods which inhibit the corrosive process due to the ohmic factor (increase in ohmic control).

TABLE 1. RATIONAL CLASSIFICATION OF POSSIBLE METHODS OF METAL CORROSION CONTROL BASED ON THE ELECTROCHEMICAL THEORY

Change in the accelerating or inhibiting factors of the corrosion process	General characteristics of the protective measures	Concrete methods of corrosion protection	Practical examples of a given method of protection
1.	2.	3.	4.
Decrease in the degree of the thermodynamic instability of the system.	Change in the metal.	1. Alloying, increasing the thermodynamic stability of an alloy. 2. Additions to the metal which facilitate greater continuity of the corrosion products.	1. Alloying of copper with gold. Alloying of nickel with copper. Alloying of chromium steel with nickel. 2. Introduction of copper to low alloy steels for exposure to atmospheric corrosion (increase in the continuity of rust on copper-steels).
	Changes in surface factors.	1. Coating of the object by a solid layer of a more noble metal. 2. Insulating coatings. 3. Greases and oils. 4. Non-metal linings and facings. 5. Oxide, phosphate, and other films. 6. Enamelling. 7. Plating with metals which give denser layers of corrosion products.	1. Plating of iron by copper or nickel. 2–6. Numerous practical formulation for appropriate protective coatings. 7. Plating of iron with zinc in atmospheric or sea water exposure (formation of more protective corrosion products on Zn).
	Change in external factors (external conditions or corrosive medium).	1. Change in external medium, facilitating the formation of more protective layers on the surface of the object. 2. Change in the corrosion conditions, facilitating the formation of more protective layers on the surface. 3. Change in the corrosion conditions so that the access of the corrosive agent to the metal surface is eliminated or radically decreased.	1. Removal of free carbonic acid from water and displacement of the reaction equilibrium: $CaCO_3 + CO_2 + H_2O \rightleftarrows Ca(HCO_3)_2$ towards predominating formation of $CaCO_3$ (to the left). Employment of inhibitors with covering action (phosphate etc.). 2. Secondary action of cathodic protection in marine conditions (formation of carbonate protective films). 3. Elimination from the solution of complex-formers or increase in the concentration of metal ions in the solution (during the corrosion of Zn and Cu). Elimination of cathodic depolarizers (H^+, O_2) and other oxidizers from the solution.

TABLE 1—*continued*

Change in the accelerating or inhibiting factors of the corrosion process	General characteristics of the protective measures	Concrete methods of corrosion protection	Practical examples of a given method of protection
1.	2.	3.	4.
			Preservation of objects in special containers in inert and strongly dehydrated atmospheres (the employment of silica gel, alumogel and other hygroscopic materials). Employment of protective atmosphere (N_2, Ar, etc.), to eliminate gaseous high temperature corrosion.
Increase in cathodic control.	Change in the metal.	Decrease in the area of cathodic sections in the metal.	1. Increase in the stability of zinc, aluminium, magnesium, iron and some other metals in solutions of HCl, H_2SO_4 (also in NaCl for Mg) by increasing metal purity. Transformation of cathodic inclusions in the alloy to a solid solution, for instance by heat treatment of carbon steels or duraluminium.
		2. Introduction of additions to the alloy increasing the cathodic overvoltage (usually the hydrogen overvoltage).	2. Amalgamation of commercial zinc. Alloying of impure zinc with cadmium. Alloying of commercial magnesium with manganese. Alloying of steel with As, Sb, Bi (when dissolving in acids).
	Change in the surface factors.	1. Metal coatings with a high cathodic reaction overvoltage. 2. Non-metallic coatings which increase the cathodic reaction overvoltage or the diffusion overvoltage or which retard the cathodic process.	1. Coating steel with zinc or cadmium for exposure to acidified solutions. 2. A similar mechanism of action is proposed for some oxide or hydroxide films on the surface of iron.
	Change in the external factors (external conditions or corrosive medium).	1. Introduction of cathodic inhibitors to the solution.	1. Employment of As, Sb, Bi during pickling. of iron in acids.

TABLE 1—*continued*

Change in the accelerating or inhibiting factors of the corrosion process	General characteristics of the protective measures	Concrete methods of corrosion protection	Practical examples of a given method of protection
1.	2.	3.	4.
		2. Diminishing of the concentration of cathodic depolarizers at the cathodes. 3. Cathodic electrochemical protection (inhibition of cathodic processes by the removal of cathodic depolarizers by an external polarization current).	2. Increase of pH of the medium, decrease in the O_2 concentration in the solution. 3. Cathodic polarization by impressed current (protection of iron and steel structures in neutral aerated corrosive media).
Increase in anodic control.	Change in the metal.	1. Alloying, increasing the anodic passivation ability of the metal. 2. Introduction of active cathodes to the alloy (under the conditions of possible passivation).	1. Alloying of iron or nickel with chromium. Alloying of stainless steels. 2. Alloying of stainless steels and also of titanium and other easily passivating metals with Cu, Ag, Pd, or Pt and other noble metals. Introduction of Cu to low alloy steels (increase in the passivation of copper steels in atmospheric conditions).
	Change in surface factors.	1. Surface treatment of metal facilitating passivating. 2. Coating of an object by a continuous layer of a more easily passivating metal. 3. Employment of varnish and paint coatings or greases and oils with a passivating pigment.	1. Polishing of the surface of stainless steels. 2. Coating of iron with chromium. 3. Introduction of zinc-chromate pigment to varnish and paint films or greases and oils (protection from atmospheric corrosion).
	Change in external factors (external conditions or corrosive medium).	1. Introduction of anodic inhibitors or, in general, the creation of a more passivating external medium. 2. Anodic electrochemical protection (inhibition of anodic processes due to passivity).	1. Introduction of passivating anions (chromates, nitrates, nitrites, and others). 2. Anodic polarization by external current. Contact with a more positive metal (for instance, non-continuous cathodic metal coating).
Increase in ohmic control.	Change in the metal.	It is impossible to give an example of an increase in the corrosion stability achieved through the increase in the ohmic resistance of the metal proper, with the possible exception of metal transistor systems.	

TABLE 1—*continued*

Change in the accelerating or inhibiting factors of the corrosion process	General characteristics of the protective measures	Concrete methods of corrosion protection	Practical examples of a given method of protection
1.	2.	3.	4.
	Change in surface factors.	It is possible that some insulating protective coatings increase the corrosion stability due to ohmic inhibition. It is very difficult to give an example of an increase of the corrosion stability achieved through the increase in the ohmic resistance of the metal proper. For metal semiconductor systems however such inhibition of the corrosion current can take place.	
	Change in the external factors (external conditions or corrosive medium).	Change in the external medium which facilitates an increase in the ohmic resistance.	1. Drainage of the soil to diminish underground corrosion under the influence of macro-corrosive cells. Removal of moisture from liquid fuel in order to reduce its corrosive activity.

Within each of the above groups we can differentiate another three subgroups which do not depend on fundamental considerations of mechanism. This sub-classification is made according to whether the action of a given method of protection depends on a change in the metal (for instance, by changing the metal composition or structure); whether the method influences the surface of the metal (for instance, a metal surface treatment or the application of a coating); or whether it changes the corrosive medium, i.e., depends in the main upon the external factors of corrosion.

All the known and possible methods of protection should find their place within this system of classification which is based on the action of every type of protection. It is felt that the classification will enable us to make a fuller and more correct use of the known methods of protection and moreover will enable us to foresee the most rational avenues of research into new protective systems. Let us consider some examples.

If the basic controlling factor of a given method of protection is known, then it is possible to indicate the instances when its employment will be most efficient, and the factors that will augment or weaken its action.

For instance, corrosion control by increasing metal purity and thus the content of cathodic inclusions is successful provided the basic controlling factor of corrosion is the overvoltage of the cathodic process. This is why this method of corrosion control is effective when metals are dissolved in acid media (corrosion with hydrogen depolarization). High purity zinc, aluminium, magnesium and a number of other metals, which do not contain cathodic inclusions with a lower value of hydrogen overvoltage than the base metal, corrode more slowly in dilute acids than the impure metals (in the case of aluminium and magnesium this is also so in neutral chlorides).

The position is different however, in the case of corrosion with oxygen depolarization. In this case the main controlling factor is, as a rule, oxygen diffusion, so that an increase in the metal purity will not yield a positive effect. In cases of corrosion with anodic control, an increase in the metal purity will generally also be useless and may even be harmful. This has been shown in recent work[10, 19–22] in which it was found that when there is a possibility of passivity (i.e. corrosive conditions characteristic of the presence of a high anodic control[10, 13, 20]), the alloys which contain cathodic inclusions passivate more easily.

A decrease in the concentration of oxygen or oxidizing agents in the solution, which is a good method of protection under the conditions of cathodic control (the corrosion of copper and of iron in a solution of chlorides or in sea water), is useless or even harmful if the corrosion process is determined to a great extent by anodic control. The rate of corrosion of stainless steel may in fact increase if the solution is de-aerated.

Another example is the alloying of steel with a high percentage of chromium, a perfect method of protection under conditions which ensure stable passivity (anodic control), but useless in non-oxidizing acids (HCl, H_2SO_4) where we depend on cathodic control.

The following general rule may be deduced for the choice of the suitable method of protection. The most likely and the most practical method of protection will normally be a method which inhibits that factor controlling the corrosion process, in other words, when the controlling factor of protection coincides with the controlling factor

of corrosion. This does not mean that methods of protection with dissimilar controlling factors cannot be employed in principle. Even when we deal with passivating systems which are mainly under anodic control, it is also possible to achieve protection from corrosion by complete inhibition of the cathodic process, by, for instance, intensive cathodic polarization even though low cathodic currents may cause a certain increase in the corrosion rate. As a general rule however, if the method of protection can offer only a partial inhibition of some stage of corrosion, it is easier to achieve effective inhibition of corrosion when the method of protection used influences the main factor controlling the corrosion reaction.

When several methods of protection are employed concurrently, then as a rule, greater effectiveness of protection can be achieved if all the methods applied influence the basic controlling factor of corrosion. For instance, when metal corrosion in acids is diminished by increasing the purity of the metals, other factors inhibiting the cathodic process, such as the addition of cathodic inhibitors, the increase of pH, etc., augment the protection.

When we restrain corrosion by promoting a passive state, for instance by introducing a passivator, the effect can be increased by the introduction of cathodic additions to the metal which facilitate anodic polarization, i.e. by a series of methods which all have an inhibiting effect on the anodic process. On the other hand methods with dissimilar controlling factors, as a rule, will be less effective and may, at times, even be harmful because the methods of protection with different controlling factors might interfere with one another.

For instance, if corrosion has been restrained by inhibiting the anodic process (the alloying of a metal with chromium, addition of oxidizing agents or other inhibitors to a solution) then it would be unreasonable to attempt to employ simultaneously methods which inhibit the cathodic process (the elimination of cathodic inclusions in the alloy, the diminishing of the aeration of the solution or the addition of cathodic inhibitors to the solution).

The employment of protective methods decreasing the degree of the system's thermodynamic instability will always facilitate a decrease in the corrosion rate, regardless of the basic control in the corroding system or of the controlling factor of another method of protection used simultaneously. However, with a large general overall inhibition (i.e. when $\eta_K + \eta_A + R$ is very great) the system will be so inert that little can be achieved by a change in the degree of the thermodynamic instability. For instance, if the system is stable owing to a very strong anodic inhibition, as is the case for stainless steels, then the additional isolation of the metal from the corrosion medium would not materially alter the overall corrosion stability of the system.

The classification of different methods of protection which is given in the table is a first attempt at compiling a system of protective measures in keeping with the nature of their influence upon the inhibition of the main stages of the electrochemical corrosion process, or on the degree of thermodynamic instability. Undoubtedly, in the future when more data become available regarding the quantitative characteristics of the influence offered by every type of protection upon the electrochemical process of corrosion, this classification will be developed and elaborated to a much greater extent. However, even in its present form the classification might be useful for a correct assessment of the advantages and peculiarities of each method of protection

and for a more rational employment of one or other of the methods of protection for a given condition.

CONCLUSIONS

1. From the scientific point of view it is rational to classify different methods of corrosion control on the basis of the electrochemical cell mechanism, i.e. from the nature of the main controlling factors or the thermodynamic instability of the system. This is considered to be a more rational classification than methods based on the technology of implementations or conditions of employment of the method of corrosion control.

2. Various methods of protection have been classified by their influence upon:
   (a) the decrease in the degree of the thermodynamic instability of the system,
   (b) the inhibition of the cathodic process,
   (c) the inhibition of the anodic process, or
   (d) the increase in the ohmic resistance of the system.

3. It is considered that, in general, the most efficient methods are those which influence the main controlling process of corrosion.

4. When several methods of protection with the same controlling factors of protection are employed concurrently, their overall efficiency increases; when different controlling factors of protection are involved the overall efficiency may be, at times, even reduced. The methods of protection which diminish the degree of the thermodynamic instability will always facilitate the retarding of corrosion but their influence will not be efficient when the overall inhibition in the system is very great.

REFERENCES

1. U. Evans, *The Corrosion and Oxidation of Metals*, Edward Arnold, London (1960).
2. O. Bauer, O. Kröhnke und G. Masing, *Die Korrosion Metallischer Verstoffe*, Hirzel, Leipzig (1940).
3. H. Uhlig, *The Corrosion Handbook*, J. Wiley, New York (1948).
4. F. Speller, *Corrosion: Causes and Prevention*, McGraw Hill, New York (1935).
5. F. Tödt, *Korrosion und Korrosionsschutz*. de Gruyter, Berlin (1955).
6. G. V. Akimov, *Methods and Theory of Metal Corrosion Research*, Academy of Science, U.S.S.R., Moscow (1945).
7. N. D. Tomashov, *Zh. Obshch. Khim. Mosk.* **12**, 585 (1942).
8. N. D. Tomashov, *Corrosion of Metals with Oxygen Depolarization*, Academy of Science, U.S.S.R., Moscow (1947).
9. N. D. Tomashov, *Theory of Metal Corrosion*, Metallurgizdat, Moscow (1952).
10. N. D. Tomashov, *Theory of Corrosion and Protection of Metals*, Academy of Science, Moscow (1959).
11. N. D. Tomashov and G. P. Chernova, *Dokl. Akad. Nauk*. U.S.S.R. **104**, 104 (1955).
12. N. D. Tomashov, R. M. Altovsky and A. G. Arakelov, *Dokl. Akad. Nauk*. U.S.S.R., **121**, 885 (1958).
13. N. D. Tomashov, *Usp. Khim. Mosk*. **24**, 458 (1955).
14. N. D. Tomashov, and G. Chernova, *Khim. Mashinostroyeniye* **2** (1960).
15. C. Edeleanu, *Nature, Lond.* **23**, 739 (1954).
16. J. D. Sudbury, O. L. Riggs and D. A. Shock, *Corrosion* **2** (1960).
17. D. A. Shock, O. L. Riggs and J. D. Sudbury, *Corrosion* **2** (1960).
18. O. L. Riggs, M. Hatchison and N. L. Conger, *Corrosion* **2** (1960).
19. N. D. Tomashov and G. P. Chernova, *Dokl. Akad. Nauk*. U.S.S.R. **89**, 121 (1953).
20. N. D. Tomashov, *Z. Elektrochem.* **62**, 717 (1958).
21. N. D. Tomashov, *Corrosion* **14**, 229t (1958).
22. M. Stern and H. Wissenberg, *Trans. Electrochem. Soc.* **106**, 759 (1959).

Corrosion Science, 1961, Vol. 1, pp. 88–107. Pergamon Press Ltd. Printed in Great Britain.

SOME EFFECTS OF ALLOY COMPOSITION ON THE STRESS-CORROSION BEHAVIOUR OF AUSTENITIC Cr–Ni STEELS*

J. G. HINES and E. R. W. JONES

Imperial Chemical Industries Limited,
Billingham Division, Billingham, Co. Durham, England

Abstract—Stress-corrosion data obtained at Cambridge University and at Billingham on fully-softened specimens of austenitic and duplex Cr–Ni steels have been subjected to regression analysis using a computer. The results give the dependence of time to fracture on composition of the steel and applied stress.

The most important compositional variables are carbon and molybdenum. With increase in amount of both elements the time to fracture passes through a minimum, and the positions of the minima are influenced by the amount of the second element and, in the case of molybdenum, by applied stress. These minima are in the ranges 0·065 per cent–0·085 per cent C and 1·5 per cent–2·1 per cent Mo. Titanium modifies the effect of carbon to some extent, but the effect is not large, while nickel has only a slight beneficial effect in the range of interest. Copper also has a minor effect, but this is not of practical importance.

The results indicate that many common British alloys are close to the worst possible compositions for stress-corrosion resistance. Furthermore, changes in composition of the materials during the last 20 years have tended to reduce the resistance. However, considerable improvement can be obtained in favourable circumstances by limiting the carbon content and controlling the molybdenum content.

Possible lines on which resistant alloys might be developed are discussed briefly.

Résumé—Les données concernant la corrosion de charge, obtenues à l'Université de Cambridge et à Billingham, avec des échantillons complètement adoucis d'aciers austénitiques et duplex chromés-nickelés, ont été soumises à l'analyse de régression, moyennant un compteur électronique. Les résultats font entrevoir que le temps de fracture dépend de la composition de l'acier et de la charge mise en oeuvre.

Le carbone et le molybdène sont les facteurs de la composition qui sont le plus sujets à des variations. Lorsque la concentration de ces deux éléments augmente, le temps de fracture passe par un minimum, et les positions des minimas sont influencées par le taux du second élément; s'il s'agit de molybdène, la charge appliquée joue encore un rôle. Ces minimas sont de l'ordre de 0,065 pour cent à 0,085 pour cent de carbone et de 1,5 à 2,1 pour cent de molybdène. Le titane modifie quelque peu les effets du carbone, cependant l'effet n'est pas trop grand; le nickel n'a, dans le domaine d'intérêt, qu'un effet favorable insignifiant. Le cuivre a aussi un effet moindre, mais ceci n'a pas d'importance pratique.

Ces résultats permettent de conclure que bon nombre des alliages britanniques communs sont tout près des compositions les plus mauvaises en ce qui concerne la résistance à la corrosion de charge. De plus, les modifications qui ont eu lieu dans la composition des matériaux au cours de ces dernières 20 années, ont eu la tendance à réduire davantage cette résistance. Toutefois, dans des conditions favorables, on peut obtenir une amélioration nette, ceci en limitant la teneur en carbone et en contrôlant le taux de molybdène.

Pour terminer, l'orientation à choisir dans le but de créer des alliages résistants est brièvement indiquée.

Zusammenfassung—Belastungs-Korrosions-Daten, die an der Universität Cambridge und in Billingham an vollständig enthärteten Proben von austenitischem und Duplex-Chromnickel-Stählen erarbeitet worden waren, wurden unter Benutzung eines Elektronengehirns Regressions-Analysen unterzogen. Die Ergebnisse geben Aufschluss über die Abhängigkeit der Bruchzeit von der Zusammensetzung des Stahls und der Belastung.

Kohlenstoff und Molybdän stellen in der Zusammensetzung die wichtigsten Variablen dar. Bei steigendem Gehalt an diesen beiden Elementen verläuft die Bruchzeit durch ein Minimum. Die Lagen der Minimalwerte werden durch den Gehalt an dem 2. Element beeinflusst, und soweit es sich

*Manuscript received 5 October 1960.

dabei um Molybdän handelt, auch durch die Belastung. Diese Minimalwerte liegen bei 0,065 bis 0,085 Prozent Kohlenstoff und 1,5 bis 2,1 Prozent Molybdän. Titan verändert den Kohlenstoff-Effekt in einem gewissen Ausmass, aber nicht sehr stark. Nickel hat in dem interessierenden Bereich nur eine geringfügige günstige Auswirkung. Auch Kupfer hat eine geringe Wirkung, die aber praktisch ohne Bedeutung bleibt.

Diese Ergebnisse lassen erkennen, dass viele der üblichen britischen Legierungen nicht weit von der bezüglich des Belastung Korrosions-Widerstandes schlechtesten Zusammensetzung entfernt sind. Die Veränderungen, die sich in der Material-Zusammensetzung in den letzten 20 Jahren ergeben haben, haben die Tendenz sur Herabsetzung dieses Widerstandes erkennen lassen. Unter günstigen Umständen können allerdings merkliche Verbesserungen erzielt werden, indem man den Kohlenstoffgehalt begrenzt und den Molybdän-Gehalt reguliert.

Es werden kurz die Arbeitsrichtungen angedeutet, in welchen man sich zur Entwicklung widerstandsfähiger Legierungen bewegen muss.

INTRODUCTION

A NUMBER of investigations[1–7] have covered some aspects of the effect of composition of Cr–Ni steels on their stress-corrosion behaviour. A variety of test methods has been used and in many cases the applied stress and/or the metallurgical condition of the specimens used was uncertain; comparison of the results obtained is therefore difficult and unreliable. Moreover, the effects of variations of composition within the usual ranges based on the 18–8 Cr–Ni steels are not very marked compared with the experimental scatter, so that the only compositional effects that have been established were observed in work including alloys outside the usual composition ranges.

For a number of years one of us has been concerned with investigations at Cambridge University and Billingham into the stress-corrosion cracking of these alloys in chloride solution. These have been concerned mainly with the mechanism of the process and with the effects of various treatments on the behaviour of representative steels; no attempt has hitherto been made to separate the effects of composition. However, data have been obtained on a number of steels in a variety of metallurgical conditions, and as the test conditions have been closely similar throughout (except for variations in specimen size) it seemed possible to the other of us that the data could be combined and the effects of composition determined by statistical analysis. It was thought that an analysis of this type might reveal effects of composition within the usual ranges of composition of the 18–8 type steels.

The stress-corrosion behaviour of austenitic Cr–Ni steels is modified by cold working[4,5,6,8,9], heat treatment,[10] and the condition of the surface film;[9,11] structural factors, particularly the amount and distribution of δ–ferrite or martensite, are also important in some cases.[1,12] Any attempt to include these factors in the analysis would have led to considerable complication, particularly as they are all dependent on composition to some extent. The analysis was, therefore, confined to results obtained on specimens pickled after being fully softened. This condition was selected as:

(i) more data were available on specimens in this condition than in any other;
(ii) it is more easily reproduced than other possibilities;
(iii) of all practical cases it is the most easily simulated.

Consistent behaviour was obtained from fully austenitic steels, duplex molybdenum-bearing steels and "molybdenum-free" steels containing less than *circa* 3 per cent δ–ferrite. The effects of composition in this group of steels appeared relatively simple, and no effect of δ–ferrite in those amounts could be detected. This last finding agrees with results reported by Edeleanu, who states that the presence of δ–ferrite

had no detectable effect in molybdenum-bearing steels but that in quantities of 5 per cent or more it tended to delay fracture in molybdenum-free steels.[1]

This paper deals with the effect of composition on the stress-corrosion behaviour of steels of the classes outlined above in boiling magnesium chloride solutions containing 42 per cent w/v $MgCl_2$; work is in progress on the behaviour of the steels in more dilute solutions.

EXPERIMENTAL DETAILS

The apparatus used at Cambridge has been described in detail previously;[11] the apparatus used at Billingham is essentially similar.

Data were available on pickled, fully softened specimens of five steels tested at Cambridge and fourteen steels tested at Billingham. The specimens used at Cambridge were 0·051 cm and those tested at Billingham were 0·320 or 0·400 cm dia. The compositions and specimen sizes of the nineteen steels included in the analysis are listed in Table 1. Seven of the steels contain molybdenum (two of these also contain deliberate additions of copper), five are 18–8–Ti steels, four unstabilized 18–8 steels and three higher alloy unstabilized molybdenum-free steels.

RESULTS AND INTERPRETATION

Preliminary analysis

The multiple regression technique consists essentially of fitting a polynomial equation to the data points by the method of least squares.* Before the main analysis could be undertaken it was necessary to carry out a preliminary analysis to determine the form of the equation to be fitted. It was thus essential to find a means of expressing the data in a compact form. It is known that linear relations between log t_f (time to fracture) and S (applied stress) exist over considerable ranges of applied stress and it seemed likely that linear regression analysis of log t_f on S would be a profitable approach. This analysis reduces the data to two regression coefficients for each regression line.

It was found that:

(i) where data for a steel are available over a range of stresses above the 0·1 per cent proof stress as well as below it, the data can best be represented by two straight lines intersecting at a stress close to the 0·1 per cent proof stress. In no case is there significant curvature of either line.

In most cases the approximate position of the intersection is clearly defined on a plot of log t_f against S; it is always close to the 0·1 per cent proof stress measured at room temperature. In a few cases, however, several pairs of lines appear to fit the data equally well. In such cases, the residual variances about each pair of lines were compared. In no case is the difference significant, but with one exception the residual variance is smaller when the nearest intersection to the 0·1 per cent proof stress is taken.

Other results on cold-worked specimens[8, 10] are also best represented by two straight lines intersecting near the 0·1 per cent proof stress. If these results are combined with those on fully softened specimens, the mean value of the ratio S_c/P (where S_c is the applied stress at which the lines intersect and P the 0·1 per cent proof stress

*A convenient account of the statistical concepts used in this paper is given by Davies[13].

TABLE 1. ANALYSES OF THE EXPERIMENTAL STEELS

Steel	Composition (wt %)											
	Mn	Si	C	N	Cr	Ni	Mo	Ti	Nb + Ta	Cu	S	P
A	0·79	0·40	0·050	0·020	16·8	5·69	1·23	0·26	<0.05	2·25	0·003	0·021
B	0·34	0·42	0·021	<0·005	16·7	10·2	1·60	<0·05	<0·05	0·07	ND	ND
C	0·43	0·47	0·021	0·030	16·4	12·02	1·59	<0·05	<0·05	0·08	ND	ND
D	0·44	0·60	0·028	0·010	18·2	11·82	2·61	<0·05	<0·05	0·07	ND	ND
E*	0·36	0·32	0·070	0·060	18·7	8·00	3·00	<0·05	<0·05	0·30	ND	ND
F	1·48	0·47	0·045	0·030	17·6	10·07	2·65	0·30	<0·05	<0·05	0·005	0·031
G	0·81	0·62	0·040	0·025	18·7	9·25	0·23	0·325	<0·05	0·09	0·009	0·012
H	0·72	0·79	0·070	0·020	18·1	8·87	0·32	0·535	<0·05	0·40	0·019	0·023
I*	0·38	0·50	0·11	0·005	19·5	7·80	0·23	0·70	<0·05	<0·05	ND	ND
J	0·81	0·79	0·10	0·030	18·2	8·87	0·33	0·56	<0·05	0·22	0·025	0·020
K*	0·65	0·43	0·07	0·030	19·0	8·10	0·23	0·16	<0·05	0·40	ND	ND
L	0·40	0·48	0·023	0·010	19·1	10·00	<0·05	<0·05	<0·05	0·06	ND	ND
M	0·46	0·60	0·025	<0·005	17·7	10·10	<0·05	<0·05	<0·05	0·05	ND	ND
N*	0·84	0·45	0·07	0·040	19·2	9·8	<0·05	<0·05	<0·05	0·20	ND	ND
O*	0·78	1·00	0·09	0·065	17·1	9·2	0·18	<0·05	<0·05	0·10	ND	ND
P	1·56	0·74	0·10	0·030	24·6	12·7	<0·05	<0·05	<0·05	0·07	ND	ND
Q	1·48	0·82	0·05	0·04	26·6	18·1	<0·05	<0·05	<0·05	<0·05	ND	ND
R	1·30	0·86	0·09	0·025	26·1	19·8	<0·05	<0·05	<0·05	<0·05	ND	ND
S	ND	ND	0·10	0·04	20·25	39·96	3·05	<0·05	<0·05	1·98	ND	ND

< = not detected at this sensitivity. ND = not determined. *Steels tested at Cambridge.

measured at room temperature) is 1·003, which is certainly not significantly different from unity.

In some cases few or no points are available at stresses above the 0·1 per cent proof stress, so that the regression line at high stresses cannot be defined. The results at lower stresses can be represented by a straight line and the residual variance is lower if such data as are available at stresses above the 0·1 per cent proof stresses are not included in the line.

(ii) the time to fracture of the various steels at the 0·1 per cent proof stress shows relatively little scatter and appears to vary with composition in a simple way. Moreover, the effect of specimen size on the time to fracture at the 0·1 per cent proof stress can be adequately allowed for by the addition to log t_f of a constant characteristic of the specimen size. The time to fracture at the 0·1 per cent proof stress is thus a characteristic of the steel. The time to fracture at zero stress, on the other hand, varies considerably and in a complex way with both composition and specimen size. This variation is largely produced by corresponding variations in the proof stress; in particular it may be noted that the proof stress determined on 0·051 cm dia. specimens tends to be higher than that obtained on larger specimens of similar composition.

(iii) the slopes of the regression lines at stresses above the 0·1 per cent proof stress for different steels are almost identical, and appear independent of specimen size.

(iv) the slopes of the regression lines at lower stresses vary considerably with composition, but also appear to be independent of specimen size. The scatter of these slopes is smaller and the apparent effects of composition and specimen size simpler when stress is used as the independent variable than when the ratio S/P is used. (The latter might be preferred as it makes allowance for the mechanical properties of the steels.)

The theoretical implications of these observations are considered elsewhere [8, 14] they are quite consistent with a mechanism of stress-corrosion cracking based on that proposed by Hoar and Hines.[11]

The behaviour of fully softened specimens of an individual steel is, therefore, best represented by two straight lines intersecting at the 0·1 per cent proof stress measured at room temperature. The equations of these lines are:

$$\log t_f = A' + B_1 (P\text{-}S) \tag{1}$$

$$\log t_f = A' - B_2 (S\text{-}P) \tag{2}$$

where A' is the logarithm of the time to fracture at the 0·1 per cent proof stress (P) and B_1 and B_2 are respectively the slopes of the regression lines below and above the proof stress. Equation (1) holds at stresses below the 0·1 per cent proof stress and equation (2) at higher stresses. The values of A' depends on composition and specimen size, that of B_1 on composition, but B_2 appears to be invariant.

The regression equation required for the main analysis is, therefore, of the form

$$\begin{aligned} \log t_f = {} & \alpha_1 + \ldots + \alpha_i \\ & + \beta_1 X_1 + \ldots + \beta_j X_j \\ & + \gamma_0 (P\text{-}S) + \gamma_1 (P\text{-}S) X_1 + \ldots \gamma_k (P\text{-}S) X_k \\ & + \delta (S\text{-}P), \end{aligned} \tag{3}$$

in which $X_1 - X_k$ and $X_1 - X_j$ are composition terms; negative values of $(P\text{-}S)$ or $(S\text{-}P)$ are to be taken as zero; and the variables corresponding to the coefficients $\alpha_1 - \alpha_i$ take the values 1 or 0 depending on whether or not the specimens are of the

TABLE 2. STRESS-CORROSION DATA USED IN THE REGRESSION ANALYSIS

Steel	Size (cm dia.)	0·1% Proof (ton/in²)	log t_f (t_f min) at stress (ton/in²) indicated: Note (1) Each box contains Applied Stress log t_f of replicates (2) *Represents unbroken specimen (see text)
A	0·320	17·5	15·9 2·190 2·218 2·538 / 12·3 3·468 2·301 / 8·6 2·810 2·878 3·895 / 5·0 3·441 4·003* 3·535 / 3·1 3·857 3·444 4·003*
B	0·400	12·6	14·4 1·929 2·204 1·929 2·240 2·586 / 10·8 2·590 2·568 2·295 2·310 2·695
C	0·400	15·3	13·5 2·654 2·796 2·917 / 9·9 2·744 2·782 2·834 / 6·4 3·391 3·220 / 3·6 4·340* 4·199 / 2·2 4·158
D	0·320	16·5	13·5 2·869 2·748 / 9·9 3·039 3·472 / 6·4 3·491 3·614 / 3·1 3·783 3·842
E	0·051	21·0	21·4 1·323 1·415 1·446 1·477 1·645 / 17·9 1·415 1·523 1·569 1·615 1·646 / 14·3 1·477 1·646 1·692 1·815 1·923 / 10·7 2·585 2·600 2·708 2·200 2·340
F	0·320	18·3	25·3 1·929 1·903 / 21·3 2·079 2·230 / 19·6 2·079 1·929 2·204 / 17·7 2·283 2·041 / 15·9 2·352 2·736 2·342 2·248 2·279 / 14·1 2.596 2.845 2.642
			12·3 2·568 2·484 2·684 2·537 2·613 / 10·5 2·845 2·775 3·255 3·061 2·833 3·301 / 8·6 3·210 3·023 3·407 / 5·0 3·316 3·412 3·956* / 4·3 3·947* 3·946*
G	0·320	14·2	28·8 1·903 1·903 / 28·0 1·925 1·896 / 24·3 1·929 2·079 / 23·3 1·875 2·000 / 22·4 1·845 2·538 / 21·3 1·903 1·813 / 19·6 2·245 2·265
			17·7 2·255 2·255 / 15·9 2·204 2·243 2·301 / 14·1 2·431 2·439 2·447 / 12·3 2·668 2·743 2·816 / 10·5 3·415 3·415 3·049 / 8·6 3·241 4·003* 4·003*
H	0·320	14·6	25·2 1·954 1·602 / 21·5 2·255 2·204 / 19·6 2·021 2·190 / 15·9 2·061 2·322 2·431 / 12·3 2·854 2·470 2·618 / 8·6 3·172 3·079 2·836 / 6·5 3·565 3·565 / 5·0 4·003* 4·003* 4·003*
I	0·051	19·6	21·4 1·662 1·738 1·815 1·892 / 17·9 1·723 1·877 1·954 2·092 2·169 / 16·1 2·169 2·262 2·462 1·878 1·908 / 14·3 2·492 2·646 2·723 2·877 / 12·5 2·923 3·046 3·230 3·276 3·354
J	0·320	15·9	23·3 1·929 1·954 / 21·5 1·978 1·854 / 17·7 1·978 1·929 / 15·9 2·130 2·204 / 13·1 2·470 2·218 / 12·3 2·500 3·025 / 10·5 2·957 3·299 / 8·6 3·900 3·998*
K	0·051	18·75	21·4 1·554 1·585 1·630 1·692 1·800 / 17·9 1·554 1·769 1·785 1·908 / 14·3 1·877 1·923 2·031 2·062 2·692 / 10·7 2·908 2·956 3·092 3·215 3·446
L	0·400	13·9	13·5 2·823 2·927 2·863 / 11·3 3·334 3·535 3·425 / 9·9 3·629 3·977 3·376
M	0·400	13·0	14·4 2·940 2·880 2·995 3·090 3·405 / 10·8 3·009 2·703 3·430 2·765 3·455
N	0·051	19·6	21·4 1·523 1·615 1·692 1·831 / 17·9 1·769 1·862 1·908 1·969 2·077 / 14·3 2·523 2·585 2·662 2·800 2·877 / 10·7 3·062 3·169 3·308 3·385 3·492
O	0·051	19·1	25·0 1·309 1·415 1·492 1·569 1·708 / 21·4 1·603 1·692 1·769 1·886 / 19·6 1·646 1·763 1·806 1·972 / 17·9 2·015 1·677 1·862 1·708 1·908
			16·1 2·000 2·046 2·200 2·246 2·353 / 14·3 2·492 2·631 2·662 2·862 / 12·5 3·046 3·062 3·123 3·169 3·277
P	0·400	21·0	18·9 3·167 3·422 / 15·5 3·635 3·616 / 13·1 4·410 4·374 / 9·7 4·410 4·425
Q	0·320	15·9	19·6 2·839 3·083 / 15·9 3·217 3·009 / 12·3 3·655 3·524 / 8·6 4·220 4·500
R	0·400	15·3	16·7 3·366 3·366 / 15·5 3·090 3·125 / 13·1 3·400 3·450 / 12·0 3·394 3·672 / 9·7 4·325* 4·335*
S	0·320	17·6	16·6 4·332 4·460 / 13·9 4·405 4·201 / 10·6 4·732 4·864

size corresponding to the coefficient in question. The use of an equation of this type allows all the data to be taken into account at the same time; for specimens of a given size equation (3) reduces to

$$\log t_f = \alpha_i + \beta_1 X_1 + \ldots + \beta_j X_j + \gamma_0(P\text{-}S) + \ldots + \gamma_k(P\text{-}S)X_k \qquad (3a)$$

at stresses below P, and to

$$\log t_f = \alpha_i + \beta_1 X_1 + \ldots + \beta_j X_j + \delta(S\text{-}P) \qquad (3b)$$

at stresses above P. Equations (3a) and (3b) are equivalent to equations (1) and (2), where $A = \alpha_i + \beta_1 X_1 + \ldots \beta_j X_j$, $B_1 = \gamma_0 + \ldots + \gamma_k X_k$ and $B_2 = \delta$.

Main analysis

The results of 310 individual stress-corrosion tests on fully softened specimens of the nineteen steels of the compositions listed in Table 1 are shown in Table 2. A few tests in which the specimens did not break are included; this was done only when the life was known to exceed the expected value. Equations of the form of equation (3) were fitted to these data using an Elliott 402 Computer. The initial equation included twenty-six terms which were selected following preliminary examination of the composition dependence of the constants A' and B_2 in equation (1); terms expected to be significant and those which might prove significant were included, while those possibilities that were clearly not significant were rejected. The twenty-six terms comprise three specimen sizes, two first order stress terms and twenty-one composition terms (including composition/stress interactions and other higher order terms). Terms that proved to be non-significant, in the sense that they could well have been due to experimental error, were then eliminated successively, the equation being refitted at each stage until an equation consisting only of significant terms was obtained. At this stage the expected values corresponding to the data points were computed and examination of the residuals (observed value—expected value) disclosed an effect of titanium that could not be detected earlier. Suitable terms were added to the equation, which was re-computed. The final equation was of the form

$$\begin{aligned}\log t_f = {} & \alpha_1 + \alpha_2 + \alpha_3 + \beta_1 \mathrm{Ni} + \beta_2 \mathrm{Mo} + \beta_3 \mathrm{C} + \beta_4 \mathrm{Ti} + \beta_5 \mathrm{Cu} \\ & + \beta_6 \mathrm{C}^2 + \beta_7 \mathrm{Mo}^2 + \beta_8 \mathrm{MoC} + \beta_9 \mathrm{TiC} + \gamma_0 (P\text{-}S) \\ & + \gamma_1 (P\text{-}S)\mathrm{Mo} + \gamma_2 (P\text{-}S)\mathrm{Cu} + \gamma_3 (P\text{-}S) + \delta(S\text{-}P) \end{aligned} \qquad (4)$$

The coefficients of this equation are listed in Table 3 together with their standard deviations and t values. Some of the stages in the derivation of the final equation are shown in the Appendix.

The coefficients α_2 and α_3 (the constants for 0·320 cm dia. and 0·400 cm dia. specimens) were almost identical and certainly not significantly different, and the data for these specimen sizes were combined to obtain a more accurate value. It is in fact, not surprising that no significant difference exists between these coefficients.[8] The coefficient β_4 (titanium) is not significant according to the t test. The coefficient must be retained because those of two higher order terms containing titanium are significant, and the reduction in sum of squares due to the three titanium terms is significant (Appendix). (These three coefficients are not independent and if the first order term were eliminated an arbitrary restraint would be placed on the coefficients.)

Interpretation of the regression equation

The regression equation represents the second order polynomial which gives the

TABLE 3. COEFFICIENTS OF THE REGRESSION EQUATION

Coefficient	Variable	Value	Standard Deviation	t
α_1	0·051 cm dia.	2·4416	0·1463	16·7
α_{2+3}	0·320 or 0·400 cm dia.	3·0371	0·1297	23·4
β_1	Ni	0·05652	0·004608	12·3
β_2	Mo	0·9274	0·07980	11·6
β_3	C	− 34·646	4·772	7·26
β_4	Ti	0·6271	0·3785	1·66
β_5	Cu	0·2896	0·06744	4·30
β_6	C^2	254·92	39·84	6·40
β_7	Mo^2	0·3150	0·04492	7·01
β_8	MoC	− 2·312	1·093	2·12
β_9	TiC	− 9·404	4·150	2·27
γ_0	(*P-S*)	0·1752	0·007701	22·8
γ_1	(*P-S*) Mo	− 0·02843	0·003442	8·26
γ_2	(*P-S*) Cu	− 0·01555	0·005921	2·63
γ_3	(*P-S*) Ti	0·04308	0·01875	2·30
σ	(*S-P*)	− 0·03605	0·006520	5·53

Note: For 294 degrees of Freedom

t =	1·96	2·58	3·29
P =	0·05	0·01	0·001
	probably significant	significant	highly significant

best fit of the data. However, while the fit is adequate, there is no *a priori* reason to suppose that the true behaviour of the steels is of this form; it thus follows that the individual terms are included for their curve-fitting properties and not because they have any theoretical significance. For example, the two purely compositional interactions, TiC and MoC, do not imply that the amount of titanium or molybdenum carbide in the steel is important, but merely that the effect of these metals depends on carbon content. Moreover, when an element is included in several terms the sign of the first order coefficient may be misleading; thus, the coefficients β_4(Ti) and γ_3Ti(*P-S*) are both positive, so that titanium apparently increases log t_f, but there is little doubt that the element is deleterious.

At a given specimen size the equation includes six independent variables and one dependent variable; applied stress, carbon, molybdenum, titanium, nickel and copper contents; and log t_f. Seven-dimensional space would be necessary to represent the equation fully and it is not easy to comprehend the details of the compositional effects. The main complications are in the effects of carbon, molybdenum and titanium, and it is convenient to consider these elements first.

If either carbon or molybdenum is considered singly, log t_f passes through a minimum as the concentration increases. The position and "depth" of each minimum varies with the concentration of the other element, and those of the "molybdenum minimum" vary with applied stress. The joint effect of carbon and molybdenum on

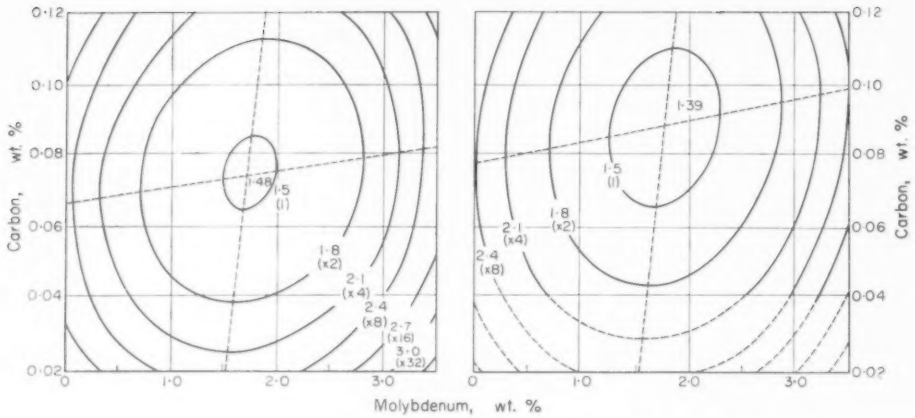

FIG. 1. "Contour map" showing the effects of carbon and molybdenum contents on log t_f for steels containing 10·0% Ni and 0·00% Cu at their 0·1 per cent proof stresses.
(a) Unstabilized steels (Ti = 0·00%)
(b) Stabilized steels (Ti = 6 × C)

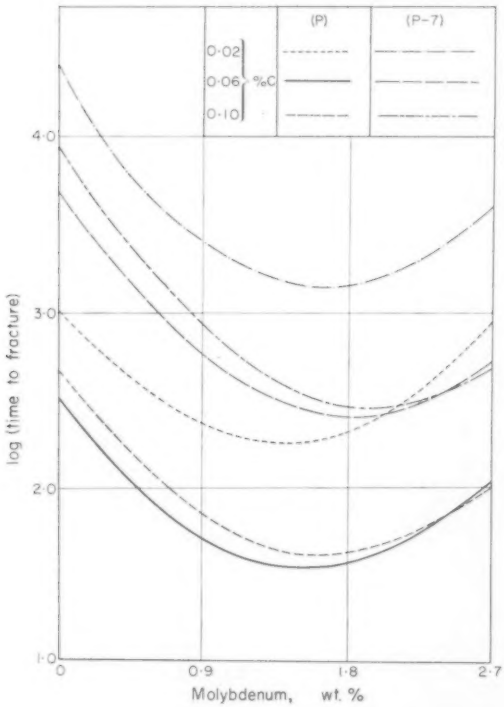

FIG. 2. Effect of variations in molybdenum content and of applied stress on log t_f for steels of constant carbon content; 10·0% Ni, 0·00% Cu.

log t_f in unstabilized steels is represented as a "contour map" of the response surface in Fig. 1(a); this represents the behaviour of steels containing 10·00% Ni, 0·00% Ti, 0·00% Cu tested at their 0·1 per cent proof stress. The contour interval of 0·3 represents a factor two on life. The loci of the carbon and molybdenum minima (the carbon or molybdenum content corresponding to the worst steel at a given molybdenum or carbon content) are indicated as interrupted lines. The surface takes the form of a skewed elliptical bowl, the "grand minimum" occurring at the intersection of the loci of the simple minima.

At a given molybdenum content the presence of titanium reduces the curvature of the carbon parabola, shifts the carbon minimum in the direction of higher carbon contents and reduces the value of log t_f at the minimum. At low carbon contents the behaviours of stabilized and unstabilized steels are indistinguishable, at intermediate carbon contents stabilized steels are slightly superior, while at higher carbon contents unstabilized steels are appreciably better. These effects are shown in Figs. 3 and 4 and the carbon/molybdenum response surface for stabilized steels (Ti = 6 × C) is shown in Fig. 1(b).

The effects of the remaining variables are best considered in relation to Figs. 1(a) and (b). An increase in applied stress above the 0·1 per cent proof stress simply reduces log t_f and thus depresses the surfaces without changing their form. The

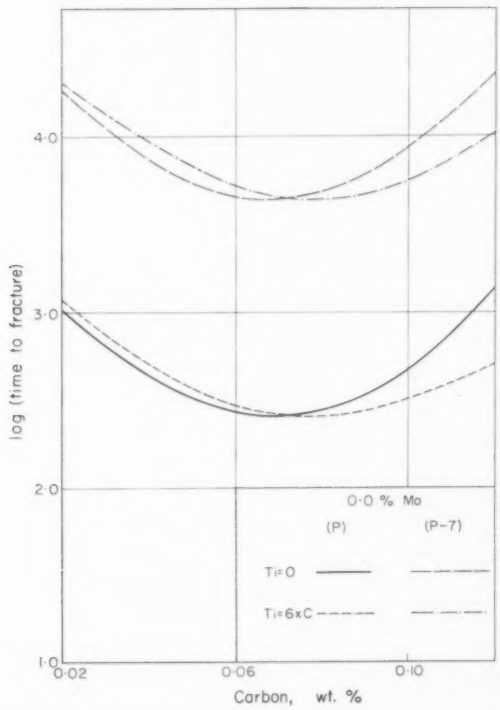

FIG. 3. Effect of variations in carbon content and of applied stress on log t_f for molybdenum-free stabilized and unstabilized steels; 10·0% Ni, 0·00% Cu.

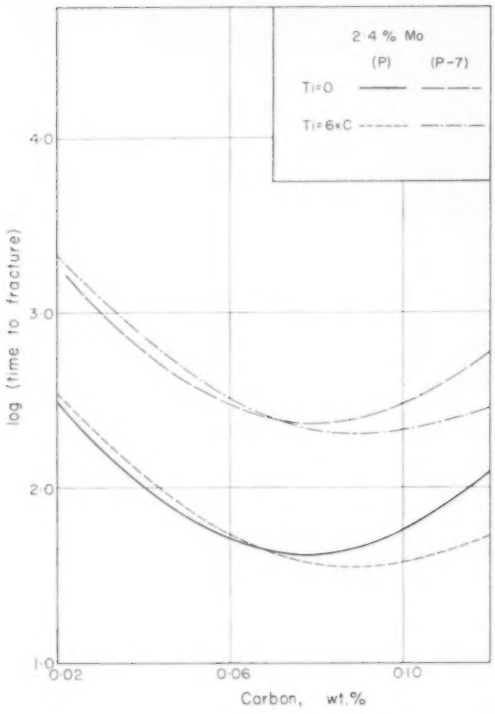

FIG. 4. Effect of variations in carbon content and of applied stress on log t_f for stabilized and unstabilized steels containing 2·4% Mo, 10·0% Ni, 0·00% Cu.

effect of stress is small and surfaces at equal stress intervals are relatively close. A reduction in applied stress below the proof stress increases log t_f and shifts the position of the "grand minimum" in the direction of higher molybdenum contents. In stabilized steels the "grand minimum" is also shifted in the direction of lower carbon contents, whereas in unstabilized steels it is shifted to higher carbon contents. Stress has a much greater effect in this range and surfaces at equal stress intervals would be wider apart than at higher stresses; they will, however, be more closely packed at high than at low molybdenum contents. These effects are shown in Figs. 2–4 and are also apparent in the data listed in Table 4.

An increase in nickel content produces a simple increase in log t_f, which can be represented by raising the response by an amount which is independent of stress. Copper has a similar but more complicated effect; increase in copper content increases log t_f at all stress levels but the effect becomes progressively smaller as the stress is reduced below P.

From a practical point of view only two elements, carbon and molybdenum, are of major importance. The effect of titanium is small except at carbon contents of 0·10 or more, while nickel has only a small effect in the range 6–12 per cent and is of little interest as regards the 18–8 type steels. Nickel has a more pronounced effect on life

TABLE 4. THE EFFECTS OF CARBON, MOLYBDENUM, TITANIUM AND APPLIED STRESS ON THE COMPOSITION GIVING THE MINIMUM VALUE OF LOG t_f.

	P-S	Composition giving minimum log t_f.	
		Unstabilized steels	Stabilized steels*
Grand Minimum	0	0·0758% C 1·75% Mo	0·0883% C 1·80% Mo
	7	0·0774% C 2·07% Mo	0·0852% C 2·10% Mo
AT Mo = 0%	0	0·0680% C	0·0778% C
	7	0·0680% C	0·0730% C
AT Mo = 2·4%	0	0·0788% C	0·0918% C
	7	0·0788% C	0·0870% C
AT C = 0·02	0	1·55% Mo	1·55% Mo
	7	1·86% Mo	1·86% Mo
AT C = 0·10	0	1·69% Mo	1·69% Mo
	7	2·01% Mo	2·01% Mo
	0	1·84% Mo	1·84% Mo
	7	2·16% Mo	2·16% Mo

*Titanium Content = 6 × Carbon content.

in more highly alloyed steels, when it is of considerable practical importance. Variations of copper contents are of little or no practical importance.

Elements eliminated from the equation

A number of other elements were eliminated from the analysis because no significant effect could be detected, or for other reasons. It is of interest to consider the implications of these results.

Manganese and Silicon. No significant effects were detected. The experimental steels contain a considerable range of manganese and silicon contents (approximately 0·3–1·5 per cent in each case) and any important effect of either element should have been detected.

Nitrogen. The range of nitrogen contents was small, so that the fact that no significant effect could be detected is not evidence that the element is not important. There is, in fact, evidence that nitrogen does influence stress-corrosion behaviour;[7] it might be expected that its effect would be rather similar to that of carbon as the two elements are similar in their effects on other properties.

Chromium. The chromium and nickel contents of the steels are closely correlated and it proved impossible to include both elements in the analysis. The correlation could only be eliminated by selecting steels in which the chromium and nickel contents varied independently and, if structural complications are to be avoided, this could only be achieved by working with steels containing considerably more than 10 per cent of nickel.

Part of the effect ascribed to nickel may be caused by chromium. However, other investigations have shown that nickel is an important variable and that chromium has little effect; moreover, in the range of nickel contents of interest values calculated from the equation agree well with data obtained by Edeleanu on steels with essentially constant chromium content.[1] It seems clear, therefore, that little error is introduced into the coefficient as a result of this correlation.

Niobium. Very few data on niobium-stabilized steels were available and no attempt was made to include these in the analysis. None of the steels tested contained appreciable quantities of niobium. The element was therefore not included.

Accuracy of equation (4)

The equation is strictly applicable only to compositions and stresses within the ranges covered by the experiments—approximately 3–30 ton/in², 6–40% Ni, 0·02–0·13% C, 0·0–3·0% Mo, 0·0–2·0% Cu, and either 0·0% Ti or Ti = 4 × C to 8 × C.

As the majority of experiments were carried out on 18–8 type steels at stresses a little below their proof stresses, estimates of log t_f made from the equation are most accurate under these conditions. Estimates for other conditions within the experimental ranges are less accurate; extrapolation of a complex equation of this type may be very inaccurate.

The standard deviation (σ_{Est}) of an estimate of log t_f (log $t_{f\,Est}$) is a convenient measure of the accuracy of the estimate, as the value of σ_{Est} for a given composition at a given stress may be calculated from data given in the Appendix. A number of representative cases have been calculated and the results show that σ_{Est} is in the range 0·06–0·12 for steels within the normal composition ranges of the 18–8 type at stresses between (P — 8) and (P + 5) ton/in². These values are rather less than the standard deviation of replicates, as would be expected. Thus, the 95 per cent confidence limits are between log $t_f \pm 0{\cdot}12$ and log $t_{f\,Est} \pm 0{\cdot}24$. The contour interval in Figs. 1(a) and 1(b) is 0·3, which is of the same order as the width of the 95 per cent confidence band.

The values of σ_{Est} discussed above apply to the accuracy of individual estimates–i.e. to the scatter expected in the time to fracture of individual specimens or the time to the appearance of the first crack in an item of equipment. For some purposes the accuracy of the mean value of log t_f is of greater interest. The standard deviation of the estimate of the mean value of log t_f is

$$\frac{\sigma_{Est}}{\sqrt{\text{No. of data points}}} = \frac{\sigma_{Est}}{18}.$$

The width of the 95 per cent confidence band for mean values is thus in the range 0·014 to 0·03.

The goodness of fit of the equation may be measured by a χ^2 test (Appendix); the value of χ^2 obtained is approximately on the 10 per cent level of significance, indicating that the fit is not quite as good as would be obtained if all sources of variation other than that between replicates had been accounted for. No account was taken of experimental errors in chemical analysis or of minor changes in the test conditions during the investigations, so that this value of χ^2 is reasonable. It is not significantly different from the ideal (50 per cent value) which indicates that no important variable was omitted from the analysis.

DISCUSSION

Comparison with previous work

The analysis has provided the first clear demonstration of compositional effects within the normal ranges of the 18–8 type steel, and also represents the first examination of the interactions between stress and composition. As most of the experiments on which the analysis was based were done on conventional steels, predictions of

stress-corrosion behaviour of steels with compositions outside these ranges may not be very accurate. However, as the only composition effects previously established were demonstrated in experiments on steels outside the normal ranges of composition, it is of interest to consider how far predictions made from the analysis agree with the evidence obtained elsewhere.

Nickel. Edeleanu[1] and Copson[3] have reported results of tests in which austenitic Cr–Ni steel specimens containing 6–20% Ni and 8–60% Ni respectively were stressed axially and exposed to boiling 42% $MgCl_2$ solution—conditions essentially similar to those used in the present work. Over the range 6–12% Ni the effect of nickel was found to be small and the present results agree well with those of the earlier investigations. The agreement between the present results and Copson's data for steels containing 35–45% Ni is also reasonable. Copson reports that an increase in nickel content from 8 per cent to 40–45 per cent increased t_f by a factor of approximately 500, which may be compared with factors of 66 (40% Ni) and 125 (45% Ni) predicted by equation (4). Because of the extrapolation, the equation is not very accurate in this region, and Copson's data are within the 95 per cent confidence limits for individual estimates.

The agreement between the present work and the earlier investigations is less satisfactory in the range 15–30% Ni, the times to fracture reported by Copson and Edeleanu being considerably greater than those used in the analysis. No explanation of this discrepancy is known, but it may be noted that the chemical analyses reported by Copson and Edeleanu are much less complete than those used in our regression analysis.

Copson's steels had a wider range of nitrogen content and covered the range 20–45% Ni more completely than do those on which equation (4) was based. An attempt was therefore made to incorporate his results in the regression analysis. The equation obtained was not unlike equation (4) but the fit was much worse; it is clear that the two sets of data are not fully compatible. The reason for this is not known, but possibilities are:

(i) The experimental techniques are not sufficiently alike. For example, Copson used electropolished specimens, whereas the analysis is based on work on pickled specimens.

(ii) Some of the apparent discrepancy might be accounted for if more complete analyses were available.

(iii) A real difference may exist between alloys of English and American origin in the concentration of an element that has not been considered and that has an important influence on stress-corrosion behaviour. Some support for this suggestion is provided by the fact that Edeleanu's results (on English steels) are in closer agreement with the present results in the range 6–12% Ni than are Copson's, and by indications that high purity alloys behave differently from commercial alloys.

Carbon. Uhlig, Lincoln and White[7] found that the time to fracture of 18–8 type steels containing less than 0·005 per cent carbon was much greater (at least 100 times) than that of otherwise similar steels containing 0·05–0·09% C. The present results are in general agreement with these observations, although the predicted improvement on reducing the carbon content from 0·068 per cent to 0·005 per cent (about fifteen times) is less than that found experimentally. However, an equation which fits the data for steels containing 0·02–0·12% C is not necessarily appropriate outside this range, and

the difference between the predicted and observed behaviour is thus not surprising. Moreover, if molybdenum-free unstabilized steels are considered separately, the predicted improvement would be greater than that given by the equation; Uhlig was working with steels of this type. His steels also had unusually low nitrogen contents, and this element was not included in the analysis.

Practical considerations

The frequency of stress-corrosion failures of austenitic Cr–Ni steels has increased markedly since the first case was reported in 1940, and the trend appears to be continuing. Several factors have undoubtedly contributed to this apparent increase in susceptibility, but it is interesting that, in Britain, refinements in steelmaking techniques and changes in specifications designed to avoid other troubles encountered with the materials have both resulted in a reduction of carbon contents, and of molybdenum contents in molybdenum-bearing steels. There is also some evidence that the amount of residual molybdenum in nominally molybdenum-free steels has increased. These trends would all reduce the resistance of steels to stress-corrosion cracking.

The conclusions reached from the present results are strictly applicable only to 42% $MgCl_2$ solution, and most environments encountered in practice are nominally less severe than the test solution. However, many service failures are caused by hot, concentrated solutions formed by local boiling, or when the conditions pass through the dew point, and the test conditions are not unrepresentative of such cases. Nevertheless, the behaviour of more dilute solutions must be investigated before the full value of the work can be obtained. Preliminary experiments have shown that the relative behaviour of representative steels in more dilute solutions is very similar to that observed in 42% $MgCl_2$ solutions, except that the detailed effect of molybdenum may be rather different in that molybdenum-bearing steels are superior to, or at least as good as, molybdenum-free steels at stresses below the 0·1 per cent proof stress. Other evidence, including some service experience, also indicates that molybdenum-bearing steels are relatively more resistant under some, but not all, conditions. On the other hand, the presence of small amounts of molybdenum appears to be detrimental in more dilute solutions. Further work is necessary to clarify the position. At the present time, the best interpretation is that the molybdenum minimum is shifted in the direction of lower molybdenum contents in some dilute solutions; this picture is consistent with other known effects of molybdenum on corrosion behaviour and with the mechanism of stress-corrosion cracking.

There is, on the other hand, no reason to expect that relatively minor alterations in the environment would markedly influence the other compositional effects demonstrated; this is particularly true of the beneficial effect of reduction in carbon content below 0·03 per cent, which leads to the most important practical conclusion. Three groups of existing alloys are markedly superior to the remainder; the ELC (0·03% C max) molybdenum-bearing and molybdenum-free steels, and unstabilized molybdenum-free steels containing more than 0·11% C. This last class may be ruled out as a constructional material for chemical or steam-raising plant because of the various troubles associated with unstabilized high carbon steels. On the other hand, the ELC steels are widely used in North America and in parts of Europe, and their fabrication

presents no special difficulty; moreover, their corrosion-resisting properties are at least as good as those of the corresponding steels of more conventional carbon contents. The molybdenum content should be as low as possible in the molybdenum-free steels and as high as practicable in molybdenum-bearing grades, and, as nickel is beneficial, the nickel content should be at the upper end of its range; this is probably necessary in any case to compensate for the loss of austenitic stability caused by the reduction in carbon content. It is also clear that reduction in local peak stresses by effective stress-relieving treatments can lead to considerable improvement.

The results also indicate several ways by which alloys of even greater resistance might be obtained. The most promising of these are the limitation of carbon (and nitrogen[7]) contents to levels below those reached in ELC steels, and an increase in nickel content. Copson's results[3] indicate that nickel contents of the order of 50 per cent are needed for complete resistance, and alloys of this type are expensive. Commercial production of alloys of the very high purity obtained by special laboratory techniques would also be difficult and expensive, and it may well be that the most attractive solution is to combine the two approaches – i.e. to develop alloys with moderately high nickel contents (20–30 per cent) and carbon or nitrogen contents around 0·01 per cent. High molybdenum contents might be less troublesome in alloys of this type in more conventional steels; they would be beneficial for stress-corrosion resistance.

Theoretical considerations

No completely satisfactory explanation of the compositional effects disclosed by the analysis is possible as there is little or no information on the corresponding effects on other properties which may be relevant. One of us has considered some possibilities elsewhere;[14] here we consider the effect of titanium.

If titanium had no effect on stress-corrosion behaviour it might be expected that stabilized steels would behave as if their carbon contents were reduced to a constant low level corresponding to the solubility of titanium carbide at 1050°C. The observed behaviour of stabilized steels does not agree with this hypothesis, although at carbon contents below about 0·08 per cent, titanium does produce some improvement in resistance. It appears that titanium (or possibly titanium carbide) has a deleterious effect, even though the reduction in effective carbon content it brings about is beneficial. Niobium carbide is believed to be less soluble than titanium carbide, so that if the above hypothesis were correct niobium-stabilized steels should be superior to titanium-stabilized steels; they should, in fact, be comparable with the high purity steels used by Uhlig. There is, however, no evidence that niobium stabilized steels are appreciably superior to unstabilized steels, which suggests that niobium has a similar effect to titanium.

CONCLUSIONS

The following conclusions are strictly applicable only to environments similar to the boiling 42% $MgCl_2$ solution used in the experimental work. Preliminary experiments in less severe environments indicate that the nature of the environment has little effect except that the details of the molybdenum effect may be altered slightly.

(i) The stress-corrosion behaviour of an individual austenitic Cr–Ni steel may be

represented by two straight lines of log (time to fracture) against applied stress. The lines intersect at a stress very close to the 0·1 per cent proof stress measured at room temperature. The slope of the line at stresses above the proof stress shows no significant variation with composition, whereas that at lower stresses is sensitive to composition. The time to fracture at the proof stress varies with composition and increases with increasing specimen size, although the increase is small for specimens larger than 0·3 cm dia.

(ii) The most important compositional variables are carbon and molybdenum. Log t_f passes through a minimum as the amount of either element is increased, the position of the minimum being influenced by the concentration of the second element. The slope of the log t_f/S curve at stresses below the 0·1 per cent proof stress is smaller the larger the molybdenum content of the alloy. Titanium modifies the effect of carbon to some extent, and also increases the slope of the log t_f/S curve at low stresses. Nickel and copper both increase log t_f to some extent, the effect of copper being less pronounced at low stresses. Neither of these elements nor titanium is of great practical importance in the ranges in which they are present in 18–8 type steels, but nickel is important in more highly alloyed steels.

(iii) The austenitic Cr–Ni steels most widely used in this country are close to the worst possible compositions for these classes of material. A considerable improvement over existing practice could be obtained by using the corresponding ELC grades (carbon 0·03% max.).

(iv) A considerable improvement in life can be obtained by suitable stress relieving heat treatments, particularly with nominally molybdenum-free steels; such treatments should be used whenever possible. The incidence of failures should be reduced considerably by the use of stress-relieved ELC steel equipment.

Acknowledgements—We are pleased to acknowledge the assistance of Dr. F. C. Roesler, Dr. C. M. Reeves and Mr. J. P. Baty, who carried out the parts of the analysis in which the computer was used. We also thank Mr. W. Spendley for advice on some esoteric statistical points.

REFERENCES

1. C. EDELEANU, *Stress-Corrosion Cracking and Embrittlement*, p. 126. Wiley, New York, and Chapman and Hall, London (1956).
2. C. EDELEANU, *J. Iron St. Inst.* **173,** 140 (1953).
3. H. R. COPSON, *Physical Metallurgy of Stress-Corrosion Fracture*, p. 247. Interscience, New York (1959).
4. M. A. SCHIEL, *Stress-Corrosion Cracking of Metals*. p. 435. A.I.M.M.E./A.S.T.M., Philadelphia, 1945.
5. H. J. ROCHA, *Stahl u. Eisen, Düsseldorf* **62,** 1091 (1942).
6. W. TOFAUTE and H. J. ROCHA, *Techn. Met.* **12,** 427 (1950).
7. H. H. UHLIG, M. LINCOLN and A. WHITE, *Acta Met.* **5,** 473 (1957).
8. J. G. HINES, *J. Corros. Sci.* **1,** 2 (1961).
9. J. G. HINES and T. P. HOAR, *J. Iron St. Inst.* **184,** 166 (1956).
10. J. G. HINES, Unpublished Work (1956–9).
11. T. P. HOAR and J. G. HINES, *J. Iron St. Inst.* **182,** 124 (1956).
12. J. G. HINES and R. W. HUGILL, *Physical Metallurgy of Stress-Corrosion Fracture*, p. 193. Interscience, New York (1959).
13. O. L. DAVIES, *Statistical Methods in Research and Production*, Oliver and Boyd, London (1949).
14. J. G. HINES, *J. Corros. Sci.* **1,** 21 (1961).

APPENDIX

This appendix contains details of several calculations and statistical tests which are mentioned in the text; these details are not essential to the comprehension of the text. The appendix also includes data which could be used as the basis of further calculations which might be required in the application or extension of the work.

(1) *Derivation of the regression equation*

The raw data are listed in Tables 1 and 2. The items were coded and, where appropriate, the origins shifted, and a matrix of sums of products built up using a programme written for the purpose by Dr. C. M. Reeves. This matrix was solved to give values of the coefficients of the regression equation, and its leading minor was inverted (this gives the covariance matrix).

Some of these stages are shown in Table 5. The coding factors and origin shifts are indicated at the top of the table. Below these is the matrix of sums of products, with its inverse below it to the left; as both matrices are symmetrical only half the matrix is shown in each case. The three lines below the inverse matrix show the values of the regression coefficients as computed, together with their standard deviations and Student's t values. The sum of squares of residuals, number of degrees of freedom and the residual variance are in the bottom right-hand corner.

The values shown in Table 5 have been rounded to five decimal places except when, as in some entries in the inverse matrix, the limit of arithmetical significance is less than this.

The coefficients and their deviations in Table 5 are coded. The coding factors were therefore removed and the origins restored to give the values listed in Table 3.

The data in Table 5 may be used for other purposes. For example, the standard deviations of an estimate of an individual or mean value of log t_f may be calculated from the residual variance, the inverse matrix and the relevant values of the independent variables. Alternatively, other data could be included by building up a matrix of sums of products from the new results and adding this matrix to that in Table 5; this process would involve much less computation than would be required if the new matrix had to be derived completely from the raw data.

(2) *Analysis of variance; significance of titanium terms*

Examination of the residuals of the original equation (which did not include any terms containing titanium) indicated that:

(i) titanium increased the slope of the log t_f curves below P;

(ii) titanium reduced the curvature of the carbon parabola, shifted the carbon minimum towards higher carbon contents and altered the minimum value of log t_f.

Four terms are necessary to cover these effects:

Ti(P-S), Ti, TiC and TiC^2

However, as the range of titanium contents at a given carbon content is limited it was possible that a satisfactory fit would be obtained if the TiC^2 term were omitted. The following analysis was therefore carried out:

	Sum of squares of residuals:		
(1)	When no Ti term is included	0·16418824	297 D.F.
(2)	Including Ti(P-S), Ti, TiC	0·15814517	294
(3)	Including Ti(P-S), Ti, TiC and (TiC)^2	0·15754870	293
	Hence the reduction of squares due to:		
(4)	Ti(P-S), Ti, TiC	0·00604307	3
(5)	Ti(P-S), Ti, TiC, (TiC)^2	0·00663954	4
	Hence variances:		
(2a)	Including Ti(P-S), Ti, TiC	0·000537909	–
(3a)	Including Ti(P-S), Ti, TiC, (TiC)^2	0·000537709	–
(4a)	Ti(P-S), Ti, TiC	0·0020143566	–
(5a)	Ti(P-S), Ti, TiC, (TiC)^2	0·0016598850	–

Variance ratios (F)

4a:2a (3:294) = 3·77 5a:3a (4:293) = 3·09

With 3:294 DF, F = 2·6 at 5 per cent level = 3·8 at 1 per cent level

4:293 DF, F = 2·4 at 5 per cent level = 3·3 at 1 per cent level

Thus the reduction in sum of squares due to Ti(P-S), Ti and TiC is significant, but no increase in significance is obtained by including (TiC)^2. Moreover, in the latter case only Ti(P-S) is significant according to the t test, whereas if (TiC)^2 is omitted TiC also is significant. It may also be shown that the difference between the two equations is very small unless the titanium/carbon ratio is much greater than in a real steel, and unless the carbon content exceeds 0·12 per cent, which is the upper limit of the experimental points. Hence, while the use of four titanium terms would be legitimate, the increase in precision which would be obtained compared to the use of three coefficients is insufficient to justify the greater complication.

TABLE 5.

0	1	2	3	4	5	6	7	8	9	10	11	12	13	14	15	
0·051 cm	0·320 + $\frac{0\cdot400}{10^{-1}}$	(Ni − 10)	(Mo − 1·0)	(C − 0·05)	Ti	Cu	(C − 0·05)²	(Mo − 1)²	(Mo − 1) (C − 0·05)	Ti(C − 0·05)	(*P-S*)	(*P-S*) (Mo − 1)	(*P-S*) Cu	(*P-S*) Ti	(*S-P*)	log*f*
10^{-1}		10^{-3}	10^{-1}	10		10^{-1}	10^{3}	10^{-1}		10	10^{-2}	10^{-2}	10^{-3}	10^{-1}	10^{-3}	10^{-1}
1·12995	0·00000	−0·15612	−0·37107	3·81996	2·09146	0·21171	1·57196	1·44477	−0·19756	1·07827	0·40248	−0·05161	0·08206	0·74839	0·07049	2·45859
	1·96992	0·28201	0·07951	0·53197	4·61744	0·62533	1·37339	2·25167	−0·12116	0·50266	0·78676	0·33410	0·38369	1·73297	0·27678	5·83968
14·173		0·76182	0·26372	0·61675	−0·77548	0·18566	0·37693	0·68019	0·15137	−0·26409	0·02949	0·10165	0·00461	−0·32789	−0·01974	0·91640
13·728	18·713		3·72852	−3·18798	−1·73992	0·22347	−1·36950	2·83866	0·45602	−1·27196	0·28286	1·65779	0·15932	0·06193	−0·19054	−0·73552
1·8073	−0·82489	3·9477		29·45432	15·81090	1·34880	11·06366	4·65131	−1·36979	9·09386	1·48475	−1·30570	0·48744	5·44932	0·29927	10·74435
4·7895	5·2744	0·11201	2·9002		30·05358	1·79564	9·09363	6·11075	−1·27152	10·03521	2·48151	0·06055	1·03250	10·65528	1·07253	17·28381
1·4638	2·3889	−0·34697	0·73011	0·47200		1·05280	0·59649	0·97039	0·08635	0·24360	0·46575	0·15873	0·75032	1·03253	0·05281	2·51665
−1·0242	−2·1988	0·45436	−0·29582	−0·24152	0·68412		6·31319	2·73144	−0·71015	4·79144	1·02577	−0·36098	0·21297	3·07663	0·22481	7·94041
−6·6866	−7·4612	−0·86160	−2·6991	−1·09255	0·18075	8·4512		8·42324	0·16281	0·79544	1·65510	1·81968	0·40577	2·64139	0·25931	9·87999
−3·7009	−5·0622	−0·66826	−0·9976	−0·68230	0·80228	1·5363	2·9500		0·27582	−0·64682	−0·13052	0·16492	0·03637	−0·47122	−0·02715	−0·77745
−6·2630	−6·8393	−0·22656	−2·8166	−0·95397	0·33625	3·3748	1·3157	3·7513		5·61033	0·54506	−0·47184	0·08125	3·45538	0·12129	3·85292
10·193	13·371	−2·5439	4·4970	2·17241	−0·78055	−8·0360	−1·7039	−6·6954	22·216		0·92159	0·38676	0·4420	1·89421	0·00000	3·79755
2·2614	4·1103	0·06116	0·45713	0·35290	−1·1788	−0·48665	−2·4040	0·50875	0·9372	3·2024		1·32625	0·13773	0·40176	0·00000	0·77705
−1·9070	−2·0572	−0·21407	0·22513	0·02808	0·45587	0·59013	0·14076	−0·30278	1·8243	−0·15201	6·6555		0·78080	1·03631	0·00000	1·59331
0·66349	0·79452	−0·00710	−0·61189	0·13679	−0·07658	−0·12922	−0·12302	−0·37877	0·47510	0·02156	−1·0839	2·20311		7·51456	0·00000	7·82965
1·7774	1·2922	1·1980	0·37666	0·11627	0·21382	−5·0925	−0·23449	0·27839	0·80723	−0·05538	−1·9356	0·05885	6·5175		0·24936	0·68524
0·28770	0·37120	−0·03792	−0·05718	−0·00935	−0·28228	0·21118	−0·00716	0·05735	−0·19442	0·10231	−1·21442	0·13328	−0·25775	0·65374		24·20004
−1·5175	−1·3844	−0·02116	0·07995	−0·15922	−0·73551	1·2529	−0·15147	0·60703	−1·5740	1·1431	1·3188	−0·79900	−0·91918	0·51645	7·9025	
Coefficients 1·183887	1·779318	0·565220	−0·412929	−0·114666	0·015687	0·289600	0·254916	0·315023	−0·231240	−0·094044	1·46814	−0·284273	−0·155522	0·043082	−0·360481	0·158145[1]
Standard Deviations 0·08616	0·10029	0·04608	0·03950	0·01594	0·01899	0·06744	0·03984	0·04492	0·10933	0·04156	0·05983	0·03442	0·05920	0·01873	0·06520	0·537909 $\times 10^{-3}$ [2]
"*t*" *Values* 13·7	17·8	12·3	10·7	7·20	0·83	4·29	6·39	7·02	2·12	2·27	24·4	8·25	2·63	2·30	5·57	294[3]

(1) Residual sum of squares. (2) Residual Variance. (3) Degrees of Freedom.

(3) *Tests for goodness of fit*

The initial sum of squares was 24·20004 and the sum of squares of residuals 0·15814517; hence the regression analysis has accounted for 99·34 per cent of the original variation in log t_f. Some of this variation is due to the scatter between replicates, and this can be estimated independently by computing the sum of sums of squares of replicates about their means. This process was not carried out in full, but a sample of 103 data points ($\frac{1}{3}$ of the total) was selected to include the appropriate proportions of specimens of different sizes, of high, intermediate and low stresses and of types of steel. An estimate of the variance between replicates (σ^2ext) of 0·000477885 (66 *DF*) was made from this sample; this corresponds to a sum of squares of 0·14050 at 294 *DF*. Hence the maximum reduction in sum of squares which could be obtained is 24·05954; and that obtained by the regression analysis was 24·04187, or 99·927 per cent of the maximum. It is clear that very little variation remains other than that between replicates.

A more precise test makes use of the fact that

$$\frac{\Sigma \text{res}^2}{\sigma^2 \text{ext}} = \chi^2$$

Taking the above values, $\chi^2 = \dfrac{0{\cdot}15814517}{0{\cdot}000477885} = 330{\cdot}93$

The value of χ^2 at 294 *DF* and various significance levels may be calculated using Fisher's approximation;* this gives $\chi^2 = 295{\cdot}5$, and its standard deviation = 24·27. Then the following values may be obtained:

Significance level	χ^2
50%	$(\chi^2) = 295{\cdot}5$
10%	$(\chi^2 + 1{\cdot}28\sigma) = 326{\cdot}6$
7%	$(\chi^2 + 1{\cdot}47\sigma) = 331{\cdot}2$
5%	$(\chi^2 + 1{\cdot}64\sigma) = 345{\cdot}9$

The experimental value of χ^2 is thus approximately at the 7 per cent level of significance. This is a reasonable value, as no account was taken of errors in chemical analysis.

*R. A. Fisher, *Statistical Methods for Research Workers*. Table 3, p. 112. 12th Ed. Oliver and Boyd, Edinburgh, (1954).

Corrosion Science, 1961, Vol. 1, pp. 108–119. Pergamon Press Ltd. Printed in Great Britain.

THE ELECTROCHEMICAL BEHAVIOUR OF SPRAYED ALUMINIUM COATINGS ON MILD STEEL—I. IMMERSED FOILS AND PANELS*

T. K. Ross and E. L. Smith
Department of Chemical Engineering, Manchester College of Science and Technology, Manchester 1 England

Abstract—Foils and panels prepared by spraying aluminium of commercial (99·5%) and super purity (99·9%) on plastic or mild steel were exposed to N/1000 NaCl solutions of various pH. Both metals are more reactive in the sprayed state than in the massive form, but potential behaviour and distribution of attack depend on purity and pH. Internal stresses within the sprayed coat are only partly responsible for the reactivity of the coating. Coatings of thickness greater than 6 mil give physical protection to basis steel, electrochemical and pore plugging reactions becoming important as thickness decreases.

Résumé—Des feuilles et panneaux en plastique ou en acier doux recouverts par projection d'aluminium commercial à 99,5% et d'aluminium de haute pureté (99,9%) ont été exposés à des solutions 1/1000e normales de NaCl de différents pH. Les deux qualités d'aluminium sont plus réactives sous forme de revêtement par projection qu'à l'état massif, mais l'évolution du potentiel et la distribution des zônes d'attaque dépendant de la pureté de l'aluminium et du pH. Les tensions internes dans la couche obtenue par projection ne sont que partiellement responsables de la réactivité de celle-ci. Au-delà de 6 mils. d'épaisseur, de tels revêtements donnent à l'acier une protection de nature physique, l'influence des réactions électrochimiques et le colmatage des pores devenant de plus en plus importants à mesure que l'épaisseur décroit.

Zusammenfassung—Folien und Platten, hergestellt durch Aufspritzen von technisch reinem (99,5%) und hochreinem (99,9%) Aluminium auf Kunststoff oder weichen Stahl wurden in N/1000 NaCl-Lösungen mit verschiedenem pH der Korrosion ausgesetzt. In beiden Fällen ist das aufgespritzte Metall reaktiver als das Massivemetall; Potentialverhalten und Verteilung des Angriffs hängen sowohl vom pH als auch von der Reinheit ab. Innere Spannungen im aufgespritzten Metall können nur teilweise für die erhöhte Reaktivität verantwortlich sein. Ueberzüge von mehr als 6 mil Dicke ergeben physikalischen Schutz für den Basisstahl.

INTRODUCTION

Metal spraying has been established commercially for many years,[1] but further investigation appeared necessary into the mechanism of the protection of mild steel by sprayed aluminium.[2] Sprayed coatings are built up from tiny particles of metal, produced by atomizing molten metal in a stream of compressed air. The particles acquire a thin protective oxide film during flight, and upon impact flatten into plate-like sections, the oxide film being partly torn away. The oxide is trapped between the metal leaflets, giving the structure a stratified appearance. The particles in the coating probably bind together not only by a "mutual grappling action" but by the merging of individual plastic droplets.[3, 4] As might be expected, the nature of the spraying process results in a change of properties of the metal compared with those of the massive metal.[1] The surface of the deposit, as sprayed, is rough and matt in appearance, and the actual surface greatly exceeds the superficial area. Porosity is an important feature of sprayed coatings and in the normal thicknesses used, pores leading to the basis metal are to be expected. A feature which has received little attention in the literature is the residual stresses present in deposits after spraying.

*Manuscript received 20 January 1961.

Metal sprayers for many years[5] have been aware of these stresses, which may lead to stripping of the coatings or to deformation of the basis metal. Stanton[6] and Tour[7] have made comparative measurements of these stresses, which are quite marked in the case of sprayed aluminium.

Extensive field tests[8, 9, 10] have indicated that coatings of sprayed aluminium give excellent protection to mild steel under both atmospheric and immersed conditions, but little fundamental laboratory work has been undertaken. Tolley[11] found that sprayed aluminium is initially anodic to steel in a number of electrolytes, and Mayne and Van Rooyen[12] have shown that this polarity relationship depends largely on the nature of the electrolyte. In a hard tap-water, sprayed aluminium tends to be cathodic to steel, but in sodium chloride solutions sprayed aluminium is strongly anodic to mild steel. Their work also indicated that sprayed aluminium was more reactive than massive aluminium.

The present paper concerns the potential behaviour of sprayed aluminium in dilute sodium chloride solutions of various pH values, the effect of metal purity and the factors responsible for the reactivity of aluminium in the sprayed form. A second paper deals with the behaviour of sprayed aluminium in contact with mild steel, with particular reference to steel exposed at pores.

EXPERIMENTAL

Materials and preparation of specimens

Aluminium wires of two purities were used in preparing the sprayed deposits: they are referred to subsequently as super-pure (99·99%) aluminium (2 mm diameter) and commercial purity (99·5%) aluminium ($\frac{1}{8}$ in. diameter). The analyses (wt. per cent) are:—

99·5% Commercial Purity

Cu, 0·01; Sn, nil; Pb, nil; Fe, 0·25; Ni, 0·01; Ti, 0·01; Zn, 0·01; Mn, 0·01; Si, 0·09; Mg, 0·01.

99·99% Super-Pure

Cu, 0·0020; Si, 0·0030; Fe, 0·0045.

Mild steel panels were purchased as bright rolled strip (20 SWG) to B.S. 970, En. 2, the composition limits of which are:–C, 0·20% max.; S, 0·06% max.; Pb, 0·05% max.

All mild steel panels were shot-blasted before spraying with a Mark 16 pistol (manufactured by Messrs. Metallisation Ltd) using acetylene and oxygen at 25 lb/in^2 as the fuel gases and air at 55 lb/in^2 as propellant. The nozzle distance used was 6 in. For many of the experiments, aluminium was sprayed direct on to the shot-blasted perspex; such specimens are referred to as "foils". Sprayed and unsprayed mild steel panels were always waxed at the back and edges, but neither these nor the foils were subjected to any other treatment. As soon as the specimens had been prepared, they were stored in a desiccator for at least a fortnight before use.

Chemicals and solutions

All solutions were made up in freshly distilled water with A.R. grade chemicals. N/1000 sodium chloride solutions, adjusted initially to pH's of about 3·5, 6·0 and 10·5 with dilute hydrochloric acid or sodium hydroxide, were used throughout.

Experimental Method

Initial work indicated that potential measurements and visual observations gave a good guide to the nature and extent of corrosion of a sprayed aluminium surface; these techniques were used throughout. Potential and pH measurements were made with a direct reading valve millivoltmeter. A small saturated potassium chloride-calomel standard electrode was immersed directly in the test solutions about 1½ in away from the surface of the specimens whenever readings were taken. All specimens were partially immersed vertically in the test solutions, a 4 in × 2 in area of metal being exposed to 700 ml of solution. Beakers containing the solutions were placed in a constant temperature bath at 25°C and the solutions, which were unstirred, were left exposed to the laboratory atmosphere. A constant levelling device was used to maintain the level of the solutions in the beakers. Measurements were usually continued for about a fortnight. All the experiments, except where stated, were repeated at least twice with different batches of specimens. Although the replicate potential/time curves often showed differences of ± 100 mV during the first few days after immersion, the general trends were followed closely.

RESULTS

Shot-blasted mild steel, and sprayed aluminium foils

Typical potential and pH measurements obtained with shot-blasted mild steel panels and sprayed aluminium foils are plotted in Figs. 1, 2 and 3.

In acid solution (Fig. 2) hydrogen evolution was observed soon after immersion of the aluminium specimens, the maximum rate of bubble formation corresponding closely to the minimum potential recorded. The potential of the mild steel specimens fell to −700 mV; that of the aluminium fluctuated but finally attained more negative values. The solution was rapidly depleted of hydrogen ions during this period, the pH quickly rising to a value (pH 4) at which alumina films are stable. Hydrogen evolution then slowly decreased and the potential increased. On super-pure aluminium, hydrogen evolution was more prolonged but corrosion generally was not as severe as on the 99·5% aluminium foils.

In alkaline solutions, a sharp initial fall in potential probably indicated that aluminium was entering solution as the aluminate ion since some hydrogen evolution

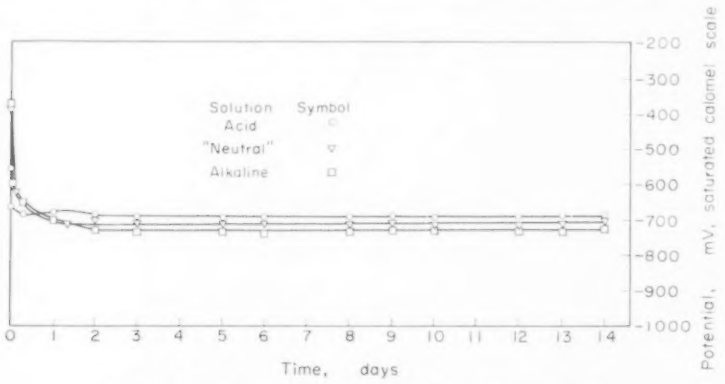

Fig. 1. Potential/time observations with mild steel panels.

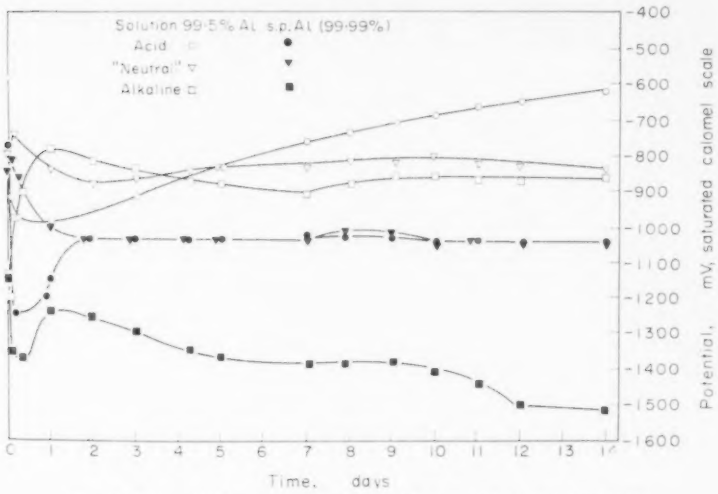

FIG. 2. Potential/time observations with sprayed aluminium foils.

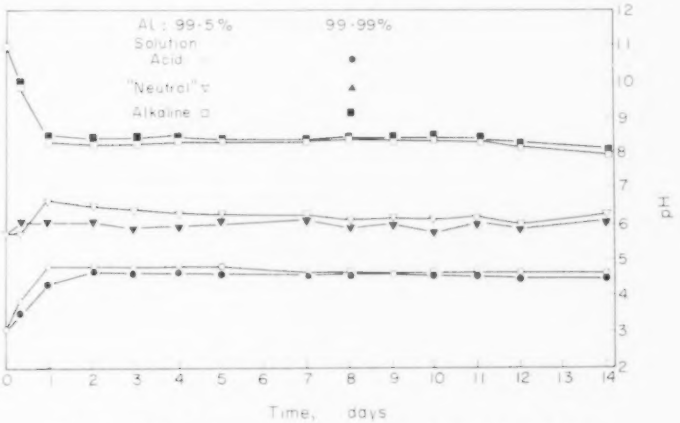

FIG. 3. pH/time observations with sprayed aluminium foils.

was observed. Soon after immersion the potential of the foils began to increase and the foils became covered with a brownish coloured stain. During this period, the pH had usually fallen to about 8·5, at which value the alumina film is more stable. After several days' immersion, the potentials of the foils, particularly super-pure aluminium, began to fall, but this did not indicate general film breakdown; corrosion was very localized.

In neutral solutions (initial pH of about 6) little reaction was observed for several hours after immersion. After 24 hr, however, vigorous hydrogen evolution was observed and a fall in potential recorded. Several days later, hydrogen evolution had decreased considerably and two distinct types of area formed on the 99·5% aluminium foils. About 50–80 per cent of the metal surface became covered with a brownish coloured stain, apparently identical to that observed in alkaline solution. Hydrogen

was evolved from the remainder of the surface, which was bright and clean. After about fourteen days a considerable volume of white corrosion product developed at the boundaries between the bright and stained areas. Qualitative work with indicators suggested that the stained areas were cathodes, and the bright areas anodes with a local pH of 3–4. On super-pure aluminium foils in "neutral" solution corrosion was usually very localized, no staining was observed, and hydrogen evolution often continued slowly for at least a fortnight.

Aluminium-sprayed mild steel panels

Mild steel panels were coated to nominal thicknesses of 0·5, 2, 4 and 8 mil with aluminium of both purities. The potential/time curves are shown in Figs. 4, 5 and 6. The experiments were not duplicated. There was some evidence of pore plugging and intense activity in pores with the specimens coated to thicknesses of 0·5 mil and 2 mil respectively. The potentials of 0·5 mil specimens rapidly approached the values for uncoated steel, indicating that the coatings were rapidly dissolved in protecting the basis metal; this was confirmed by visual observations. In neutral solution these panels were badly coated with rust within a few days; only traces of aluminium were visible after a fortnight. In alkaline solution, about 50 per cent of the metal surfaces of 0·5 mil specimens were streaked with rust, the remainder being coated with aluminium corrosion products. In acid solution, 0·5 mil super-pure specimens were only slightly rusted after a fortnight, whereas the corresponding panel coated with 99·5% aluminium was badly rusted. No rusting was visible on specimens coated to a thickness of 2 mil and over.

Massive aluminium

It appeared from the experiments described above that aluminium in the sprayed form was probably more reactive than massive aluminium. To confirm this, potential

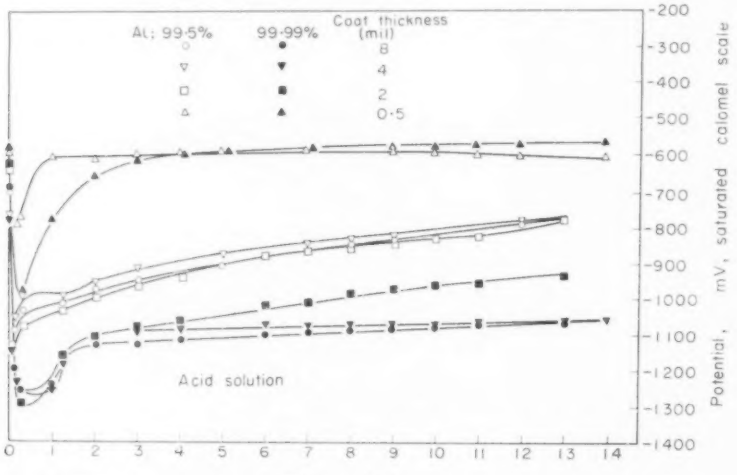

Fig. 4. Potential/time observations with aluminium-sprayed mild steel panels in acid solution.

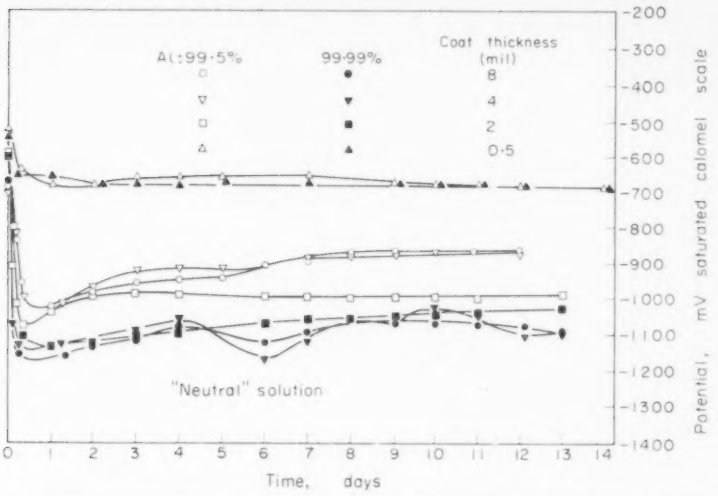

FIG. 5. Potential/time observations with aluminium-sprayed mild steel panels in neutral solution.

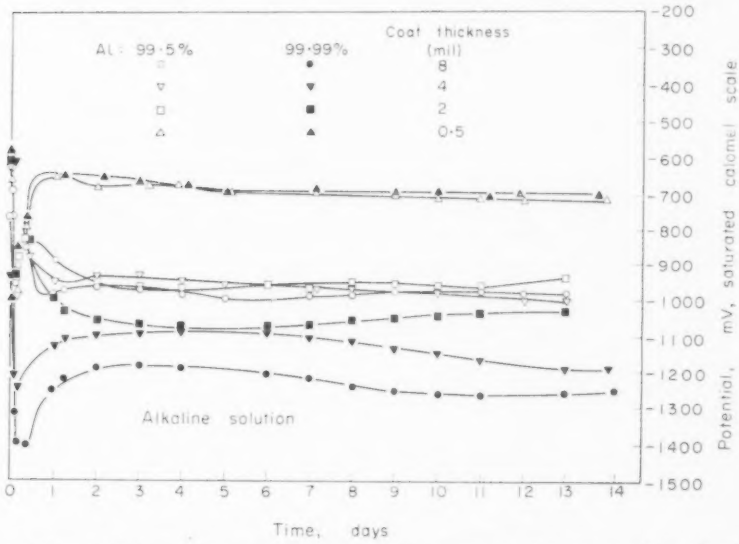

FIG. 6. Potential/time observations with aluminium-sprayed mild steel panels in alkaline solution.

measurements were made with the aluminium wires used for spraying the deposits, the superficial surface area to solution volume ratio being maintained. The specimens were polished with emery down to 00 grade, given a final finish with alumina and degreased. The results of this experiment, are plotted in Figs. 7 and 8.

Little gas evolution was observed from the wires and corrosion took the form of shallow etching or extensive pitting. The pits were usually associated with pustules of white precipitate, which often formed around bubbles of gas.

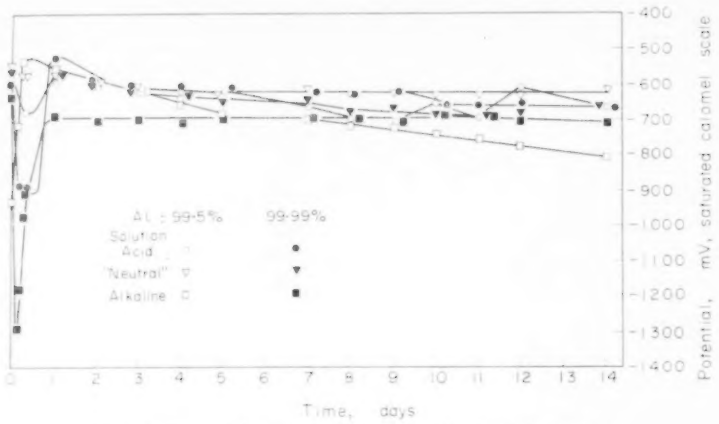

Fig. 7. Potential/time observations with aluminium wires.

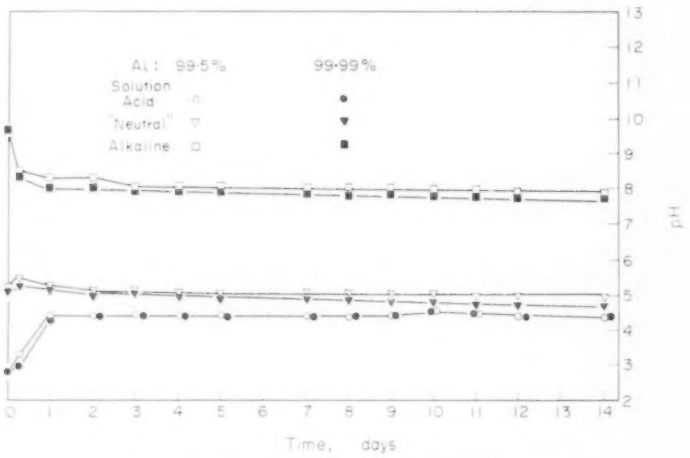

Fig. 8. pH/time observations with aluminium wires.

Effect of oxide on the behaviour of sprayed aluminium

Some oxide film becomes trapped in sprayed metal deposits and it was thought that this might influence the nature and distribution of corrosion during the initial stages of immersion. Foils were sprayed using a high frequency induction coil for melting the wire and argon as the propellant, the whole apparatus being contained in an air-tight chamber filled with argon gas under pressure. The specimens were immersed in the usual N/1000 sodium chloride solutions. The potential and pH measurements recorded during this experiment, which was not repeated, were not significantly different from those obtained with foils sprayed with a standard pistol.

Numerous very heavily oxidized particles are formed in the outer spray beam from a wire pistol and are often included in the sprayed deposit.[13] Such particles are clearly visible in the outermost layers of the deposit and it was decided to determine whether they had any marked influence on the behaviour. The marginal spray beam was masked

off so that the deposits were free from heavily oxidized particles. Potential and pH measurements, and visual observations made under standard immersion conditions indicated that there was no difference between specimens formed from the restricted beam and those prepared with the full beam.

Effect of heat treating sprayed aluminium

This experiment was carried out in an attempt to evaluate the effect on the electrochemical behaviour of the foils of the internal stresses set up during the formation of a sprayed deposit. The specimens were prepared by spraying aluminium on to smooth glass plates to a thickness of about 6 mil. These deposits could be easily detached from the glass as a continuous foil. The "smooth" side of the foil was then carefully sprayed. The foils were heat treated in an argon atmosphere for 20 min at temperatures of 150, 300 and 450°C. The potential measurements obtained with these specimens in N/1000 sodium chloride solutions are shown in Figs. 9, 10 and 11. Measurements of pH were also recorded, but since they closely followed the curves plotted in Fig. 3, they have not been included. In acid solution the 99·5% aluminium foils heat treated at 300°C and 450°C showed less reactivity than the other two foils; this is indicated by the more positive potentials (Fig. 9). In "neutral" solution, similar foils showed an "induction period" of several days before the usual vigorous hydrogen evolution occurred. Although the super-pure foils immersed in "neutral" solution did not show such differences, they corroded very readily and unusually negative potentials were measured. In alkaline solution, the potential measurements did not reveal any marked difference in the behaviour of either the super-pure or 99·5% aluminium foils, but visual observations indicated that attack on specimens annealed at 300°C and 450°C was initially less vigorous and more localized.

Polished sprayed aluminium

Microscopic examination during immersion revealed that hydrogen evolution took place predominantly within pores of the foil; even in neutral solutions gas

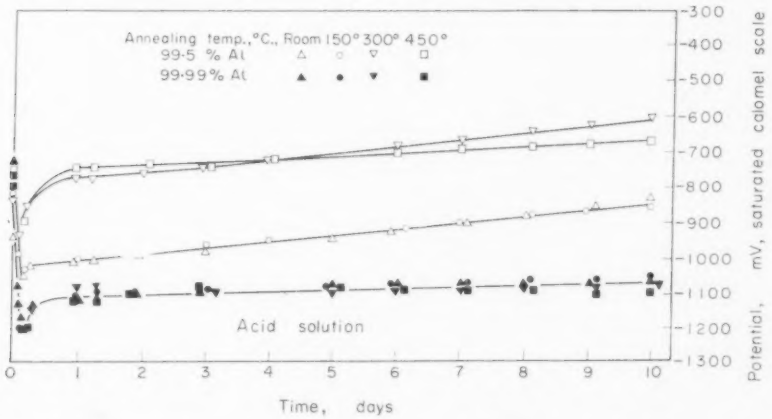

FIG. 9. Potential/time observations with annealed sprayed aluminium foils in acid solution.

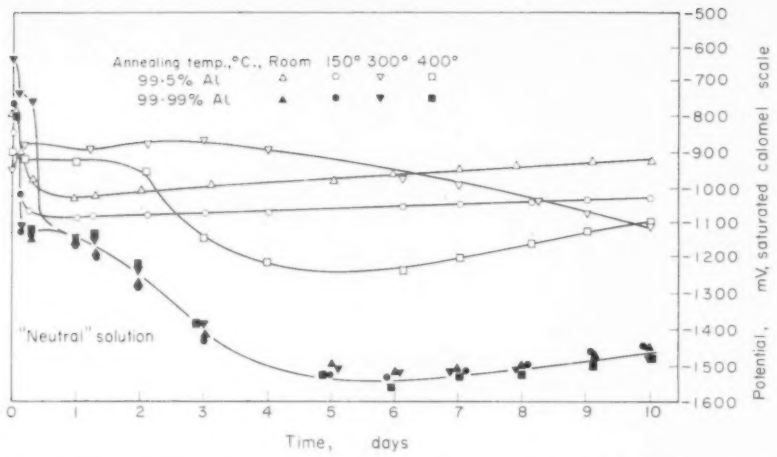

Fig. 10. Potential/time observations with annealed sprayed aluminium foils in neutral solution.

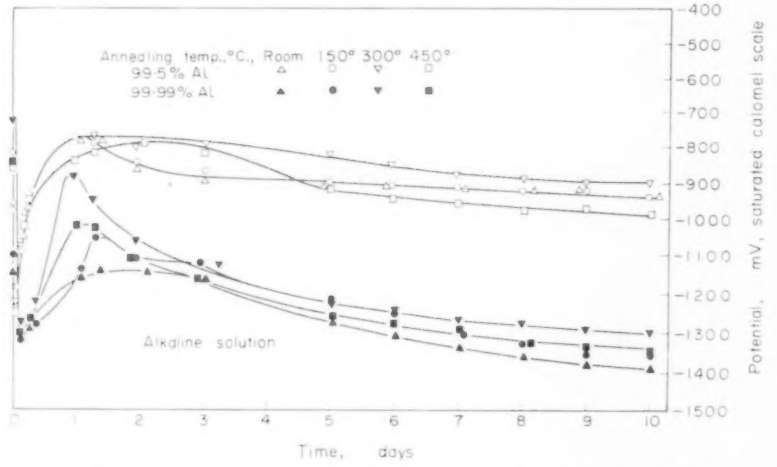

Fig. 11. Potential/time observations with annealed sprayed aluminium foils in alkaline solution.

bubbles were often observed being ejected at the rate of a bubble each second. These observations suggested that the porosity of sprayed aluminium foils was an important factor in their reactivity. In an attempt to confirm this hypothesis, aluminium of both purities was sprayed on to Perspex to a thickness of 6 mil, and the deposits polished down with corundum papers to 0 grade. After the polishing operation, scratch marks and pores were clearly visible within the deposits, although the surface area was generally much reduced. Before immersion in the usual N/1000 sodium chloride solutions, the specimens were cleaned and degreased in an acetone-alcohol mixture. The experiments were repeated several times with 99·5% aluminium and good agreement was found. There was little difference between the behaviour of these polished foils

and that of "as sprayed" foils, except that the potential/time curve for the super-pure aluminium foil in neutral solution reaches very negative values. These results obtained were disappointing but, as mentioned above, polishing did not greatly reduce the porosity, this porosity appears to account for much of the reactivity of aluminium in the sprayed form.

DISCUSSION

The experimental work confirms that sprayed aluminium is more reactive than the massive metal, and also shows that the purity of the aluminium and solution pH have an important effect on the corrosion potential of the metal. Super-pure aluminium in the sprayed form has a more negative potential than sprayed commercial purity aluminium. Sprayed coatings of super-pure aluminium might thus be expected to give better protection to mild steel than sprayed deposits of 99·5% aluminium. Some early experiments[14] showed that a greater protective current is in fact obtained. The potential/time measurements plotted in Fig. 2 also illustrate that in neutral solutions the oxide film on aluminium takes several days to break down; consequently the sprayed coating does not achieve maximum reactivity for some time after immersion.

The reason for the large difference in the potentials of sprayed 99·5% and super-pure aluminium has not been fully investigated. However, it must be emphasised that the very negative potentials recorded with super-pure aluminium foils, particularly in alkaline solution, are not necessarily indicative of oxide film break-down and rapid corrosion. Indeed in alkaline solution, attack was usually very slow, and became localized after several days' immersion. An important observation made during the experiments was that attack on the 99·5% aluminium foils tended to be stifled more rapidly than on the super-pure foils, where corrosion usually continued slowly at isolated areas. Certain evidence[15] suggests that impurities in aluminium sometimes promote the formation of protective alumina films, and might thus be responsible for the rapid stifling. It is also known that impurities in aluminium such as Al_3Fe are strongly cathodic to aluminium,[16] and such impurities in the sprayed 99·5% aluminium deposits may be responsible for the more positive potentials observed.

The staining of aluminium is frequently referred to in the literature[17, 18, 19] and appears to form when an aluminium surface has been fairly uniformly etched and then covered with a protective film of alumina; impurities in the oxide film may also be partly responsible for the coloration. In the present work, staining was always associated with oxide film formation under alkaline conditions and appeared to be merely an optical effect.

Although some explanation of the potential behaviour of sprayed aluminium has already been attempted, differences between the metal in the sprayed and massive forms merit further discussion. Of the various factors examined, the presence of oxide film and heavily oxidized particles in the sprayed deposit is of little importance. Insufficient work on heat treatment of sprayed aluminium has so far been done to justify any definite conclusions, but it does appear that internal stress is not of supreme importance. Roughness and porosity are distinctive features of metal in the sprayed form, and activity within the pores of sprayed aluminium foils is very marked. During those periods when hydrogen is evolved in some quantity from the metal, bubbles are continually formed within the pores. This behaviour bears striking resemblance to the

pitting type attack encountered with massive aluminium, in which anodic acidity plays an important role. Anodic acidity, the accumulation of which has been studied by Edeleanu and Evans[20], favours continuation of attack at the same place in preference to a fresh start being made elsewhere, provided that acidity is not swamped by alkali from the cathodes and provided that alkaline attack on the aluminium does not lead to general corrosion. Evans[21] has also discussed the importance of anodic acidity in wider terms. Sometimes anodic acidity is sufficient to lead to the local evolution of hydrogen.[20, 22, 23, 24, 25] For example, Porter and Hadden[22] have observed gas evolution from nodular pits in the corrosion of massive aluminium by supply waters. They also found that the pH within the dome of corrosion products covering the pit was 3·5–4·0 and that the local concentration of chloride and sulphate ions was higher than in the bulk of the solution. Now many "ready-made" pits are present in sprayed aluminium deposits and observations clearly show that, in neutral N/1000 sodium chloride solutions, pores in the deposits are the sites for hydrogen evolution. It seems probable, therefore, that reactions leading to the accumulation of anodic acidity within the pores may to some extent be responsible for the reactivity of sprayed aluminium. Cathodically formed alkali possibly swamps the anodic acidity more readily in the case of 99·5% aluminium, since hydrogen evolution decreases more rapidly.

Although reactions leading to anodic acidity may explain why attack continues at the same point, the reasons for the initiation of attack at that point must be explained on other grounds. It is well known that surface defects such as scratches, indentations, small cavities and cracks may affect the continuity of the air-formed oxide film on metals and are frequently the predetermining points of attack. Thus the roughness of sprayed metal may be expected to result in very general attack during the initial stages of corrosion. Differential aeration of the metal and differences in the internal stress of the deposit may also affect the distribution of attack and of acidity in the setting up of anodic and cathodic zones.

A considerable potential difference exists between mild steel and sprayed 99·5% and 99·99% aluminium foils (Figs. 1 and 2), except in the case of 99·5% aluminium in acid solution. Other measurements, not here reported, have indicated that this relationship between mild steel and sprayed aluminium holds for at least two months. Good cathodic protection should thus be afforded to mild steel as a result. The measurements made with the aluminium sprayed mild steel panels yield useful information. The potential/time curves indicate that coatings of aluminium above about 6 mil in thickness give merely physical protection to any basis steel. Only a few pores penetrate down to the basis steel and so the coatings may be expected to behave in a similar way to the sprayed foils. Below 4 mil, reactions within pores of the coating become increasingly important as coat thickness decreases and more basis steel is exposed to the electrolyte. The potential measurements do not illustrate this point very well except in the case of super-pure aluminium sprayed panels in alkaline solution. Blockage and activity within the pores of coatings 4 mil thick and below was observed, however. Coatings 0·5 mil in thickness offered quite good protection although rusting was observed within a few days of immersion and noble potentials were recorded. Rather surprisingly, the super-pure coatings did not appear to give any better protection than the 99·5% aluminium coatings, except in acid solution.

CONCLUSIONS

Sprayed aluminium foils behave very reactively in N/1000 sodium chloride solutions in the pH range 3–11. The potential behaviour and distribution of attack is dependent both on pH and metal purity.

99·5% and super-pure aluminium are more reactive in the sprayed than in the massive state, and potential measurements suggest that sprayed aluminium will give cathodic protection to steel in N/1000 sodium chloride whereas massive aluminium will not.

The reactivity of sprayed aluminium is due partly to internal stresses within the deposit and also to porosity and surface roughness. It is suggested that "ready-made" pores in the deposits are ideal sites for the development of anodic acidity. The presence of impurities in aluminium probably account for differences in the potentials of the 99·5% and super-pure aluminium foils under the same conditions of immersion.

Sprayed aluminium coatings above a thickness of 6 mil give mainly physical protection to any underlying steel. Pore-plugging reactions become important as thickness decreases and coatings 0·5 mil thick, only afford complete protection to steel for some days.

REFERENCES

1. W. E. Ballard, *Metal Spraying and Sprayed Metal*, Griffin, London, (1949).
2. *Chem. and Ind.* 1956, pp. 195, 382, 464, 528.
3. L. V. Krashnichenko and M. N. Schhirzhetsky, 3 *hur. Tekhn. Fiziki*, **25**, 791 (1955).
4. A. Matting and K. Becker, *Electroplating*, **8**, 101 (1955); **9**, 84 (1956).
5. W. E. Stanton, Private Communication, July 15th, 1958.
6. W. E. Stanton, *Electroplating*, **12**, 65 (1959).
7. S. Tour, *Weld. J. Easton Pa.* **31**, 199 (1952).
8. J. C. Hudson and T. A. Banfield, *J. Iron St. Inst.* **154**, 229 (1946); **158**, 99 (1948).
   J. C. Hudson and J. F. Stanners, *J. Iron St. Inst.* **175**, 381 (1953).
9. American Welding Soc., *Weld. J. Easton Pa.* **38**, 215 (1959).
10. R. E. Mansford, *Corros. Tech.* **3**, 314 (1956).
11. G. Tolley, *J. Iron St. Inst.* **162**, 377 (1949).
12. J. E. O. Mayne and D. Van Rooyan, *Chem. and Ind. (Rev.)* 718 (1957).
13. J. E. Clive, R. T. Thurston and J. Wulff, *Weld. J. Easton Pa.* **29**, 205 S (1950).
14. T. K. Ross, E. L. Smith and R. E. Mansford, *Werkst. u. Korrosion, Mannheim* **9**, 755 (1958).
15. J. M. Bryan, *Food Investigation Board, Special Report* No. 50. London: H.M.S.O. (1948).
16. R. B. Mears and R. H. Brown, *Industr. Engng. Chem. (Industr.)* **33**, 1001 (1941).
17. J. Fischer and W. Geller, *Z. Metallk.* **30**, 192 (1938).
18. J. M. Bryan, *J. Soc. Chem. Industr.* **69**, 169 (1950).
19. D. Altenpohl, *Aluminium (Berl.)* **29**, 361 (1953); **33**, 78 (1957).
20. C. Edeleanu and U. R. Evans (*Trans. Farad. Soc.* **47**, 1121 (1951).
21. U. R. Evans, *J. Electrochem. Soc.* **103**, 73 (1956).
22. F. C. Porter and S. E. Hadden, *J. App. Chem.* **3**, 385 (1953).
23. P. T. Gilbert and S. E. Hadden, *J. Inst. Met.* **77**, 237 (1950).
24. T. Hagyard and J. R. Santhiapillai, *J. App. Chem.* **9**, 323 (1959).
25. D. E. Davies, *J. App. Chem.* **9**, 651 (1959).

Corrosion Science, 1961, Vol. 1, pp. 120–131. Pergamon Press Ltd. Printed in Great Britain.

THE ELECTROCHEMICAL BEHAVIOUR OF SPRAYED ALUMINIUM COATINGS ON MILD STEEL—II. IMMERSED COUPLES AND ARTIFICIAL PORES*

T. K. Ross and P. H. N. Webster

Department of Chemical Engineering, Manchester College of Science and Technology, Manchester 1 England

Abstract—Specimens were constructed in which sprayed aluminium coatings were separated from mild steel panels by a thin insulating layer of plastic. The electrochemical interaction of the two surfaces when immersed in dilute NaCl solutions was studied. The result of varying surface area ratios in pores or damage areas is shown, as well as the role of ageing of the coating in determining its initial reactivity. Both phenomena are important to the suggested mechanism of protection. The formation of cathodic alkali is shown to maintain activity at a pore until the precipitation of corrosion products or hardness salts lead to stifling of the pore.

Résumé—On a préparé des échantillons composés de panneaux d'acier doux recouverts d'aluminium par projection, l'acier étant séparé de l'aluminium par une couche isolante en matière plastique. On a étudié l'interaction électrochimique des deux surfaces en immersion dans des solutions diluées de chlorure de sodium. L'influence de la modification des rapports de surfaces dans les pores ou aux zônes endommagées et explicitée ainsi que l'influence du vieillissement de la couche protectrice sur sa réactivité initiale. Les deux phénomènes interviennent de facon importante dans le mécanisme de protection proposé. On montre que la réaction cathodique conduisant à la formation d'alcali maintient les pores en activité jusqu'à ce que la précipitation de produits de corrosion ou de sels alcole notereux conduise au bouchage des pores.

Zusammenfassung—Es wurden Proben hergestellt, bestehend aus einer aufgespritzten Aluminiumschicht, die durch einen dünnen isolierenden Kunststofffilm von einer weichen Stahlplatte getrennt wird. Man untersuchte das elektrochemische Verhalten der beiden Oberflächen bei Eintauchen in verdünnte NaCl-Lösung. Die Ergebnisse der Variation der Oberflächenverhältnisse in Poren oder Verletzungen werden dargestellt, wir auch durch Bestimmung der anfänglichen Reaktivität der Einfluss des Alterns der Schicht. Beide Vorgänge sind für den vorgeschlagenen Schutzmechanismus von Wichtigkeit. Es wird gezeigt, dass die kathodische Bildung von Alkali die Aktivität einer Pore erhält, bis die Ausfällung von Korrosionsprodukten oder Härtungssalzen zur Verstopfung der Pore führt.

INTRODUCTION

Part I was concerned chiefly with the potential/time characteristics of sprayed panels and of isolated sprayed coatings in the form of a mounted foil. The measurement of single electrode potentials has certain limitations as a means of studying metallic corrosion and the work was extended so that current measurements could be made under the conditions arising in the actual aluminium/mild steel couple. A major problem in such a study is the preparation of a representative model in which the two couple elements, the coating and the steel backing, are completely isolated electrically. It is clearly desirable to obtain as nearly as possible an accurate model of the real couple, where a porous aluminium layer is in contact with a grit-blasted mild steel surface. The type of specimen aimed at, therefore, was one in which the sprayed coating was separated from the steel by the thinnest possible insulating layer. A number of designs were tried with varying degrees of success, but in the following account only two model designs are used.

*Manuscript received 2 March 1961.

EXPERIMENTAL

Conventional method

For all work involving the measurement of conventional polarization curves, the couple consisted of a grit-blasted mild steel and a deposit of the sprayed metal separated by a $\frac{1}{16}$ in. Perspex sheet. The deposit was sprayed directly onto the Perspex sheet previously roughened by grit blasting; the sheet was then cut on a band saw to the desired dimensions and glued with polystyrene cement to the grit-blasted and degreased steel panels (6 in $\times$ 2 in). By cutting the appropriate strips of coated perspex away before joining to the steel backing, any desired area of mild steel could be exposed. The back and edges of the panel were coated with wax and also the front surface down to $\frac{1}{4}$ in. below the waterline. The total exposed surface of coating and mild steel was 2 in $\times$ 2 in. The couples were mounted vertically in Perspex clamps, the upper edge of the unwaxed portion being $\frac{1}{4}$ in. below the waterline. Electrical connections to the couples were made by means of crocodile clips. Normally four specimens, each in a separate beaker, were mounted in a bath maintained at 25°C. A saturated calomel electrode was used for reference, being mounted in a central beaker and connected to each individual system by a filter paper strip. The level of the solution in the beakers was maintained by a constant head arrangement.

Polarization curves were obtained by regulating the current of the cell by means of a variable resistance; in no case was current applied to the system from an external source. The complete circuit for the measurement of the polarization characteristics incorporated a bridge system for the measurement of current flow at "zero resistance", and potential measurements were made by means of a high impedance electronic millivoltmeter. A small chart recorder was attached to the output of the electrometer to assist in the estimation of equilibrium at each stepwise introduction of resistance. The use of a recorder proved vastly superior to methods involving so-called "immediate" readings or time methods, as a standard "degree of equilibrium" can be easily assessed from the slope of the trace on the chart; in this way greater accuracy is obtained.

The calomel electrode was situated at a distance from the couple so that changes in position did not affect the reading. Composite electrode potentials were therefore measured against a bulk reference potential and any local ohmic effects near the surfaces were included as total polarization.

Polarization decay technique

A new technique was developed to give a closer approximation to the conditions existing in a pore. The dimensions of the couple were necessarily reduced and the normal methods of measuring polarization characteristics became too insensitive; a new method was therefore developed, which has been termed the "polarization decay method".

One of the chief disadvantages in the use of conventional technique for plotting polarization curves is the time elapsed during the actual measurement. This was particularly important in this investigation because the insertion of resistance for the purposes of measurement results in disturbances which may affect subsequent readings. While the full protective current is restricted by a high resistance in the external circuit, irreversible reactions may occur which result in permanent changes at the exposed

surfaces. In the polarization decay method the couple is disturbed from the naturally corroding condition for periods of only 20 sec while the readings are made, and a large number of such measurements can be taken over a long exposure to examine the changes in polarization characteristics as corrosion proceeds.

The method is not to be confused with the measurement of potential decay curves as used in double layer investigations, but it is similar to a technique used by Hines and Hoar[1] in a study of copper and austenitic steel couples in hot chloride solutions, and by Greene and Fontana[2] in the study of the growth of artificial pits in stainless steel. In the first case the high temperature allows "equilibrium" to be reached quickly so that the closed circuit potential was almost unaffected when a reading was taken. At lower temperatures "equilibrium" is reached more slowly; Greene and Fontana attempted to make instantaneous reading of potential after the couple is disturbed from the closed circuit condition, but due to the very rapid drift in the first few seconds it was found that such a method was extremely inaccurate. We have found, however, that if the output of the millivoltmeter is fed into a high-speed electronic recorder an accurate value could be read from the chart at any desired time during the decay of polarization.

The shape of the trace obtained as the potentials of the two components of the couple decay from the short circuited condition was found to be very characteristic of the couple. The conditions of polarization were accurately reflected in the shape of the decay curve during the first few seconds at open circuit, and a current measurement was only required in order to make the observation quantitative with respect to absolute corrosion rate. The method thus gives a representation of the polarization existing in the system on a time instead of a current basis. Used with very small couples where current measurements are impracticable, the technique has proved of great value. It has been used purely as a comparative tool and no special electrochemical significance was read into the shape of the curves, but it is hoped to conduct a detailed investigation of the method with simple electrodes.

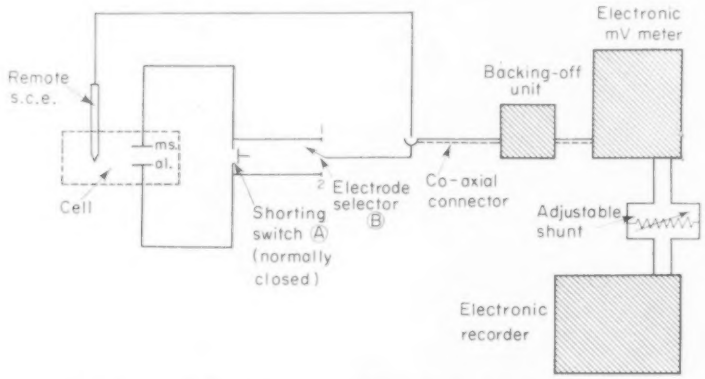

Fig. 1. Circuit diagram for recording polarization decay curves.

The circuit used in the measurement of polarization decay curves is very simple (Fig. 1), and the procedure adopted was as follows. The switch B is set to position 1, the chart motor started and as the pen reaches a certain point on the chart, the switch A is opened. After the required time has elapsed (i.e. 20 sec or 2 in of chart at 6 in/min) the switch is closed and the chart allowed to run until

the reading returns to the original potential of the combined couple. The chart is then rewound to the original start position and the process repeated with the switch B in position 2. In this way the decay curves for the two components of the couple are superimposed and a complete polarization decay curve obtained. The 20 sec time base was adopted as an optimum standard and in all cases it was found that after being at open circuit for this length of time the couple was not permanently affected and would return exactly to the original equilibrium position within the subsequent 20 seconds. The backing-off unit and adjustable shunt are used to obtain the desired zero suppression and sensitivity, and a wide range of potentials and trace magnifications are available with this arrangement.

The curves included are of data extracted from the recorder chart and are effectively a polarization time plot over the period of the run. The values used to plot the three curves are the combined couple potential (marked C) and the potentials to which the mild steel component (marked M.S.) and the aluminium component (marked Al.) have decayed in 20 sec at open circuit. The results are shown as potential (vs. saturated calomel reference) against the time of exposure in hours.

The couple used with the polarization decay technique was designed to represent a pore in the coating. Grit-blasted panels were first coated with a layer of filter paper impregnated with an epoxy-resin cement, which after curing and light grit-blasting received a deposit of sprayed metal. The paper-resin system proved a very effective separator and no case of peeling of the coating or separator was experienced. Specimens were cut to the required size on a band-saw and the edges and back of the specimen waxed, the coated side being waxed to leave exposed the desired area. The steel surface was exposed by piercing the sprayed metal and separator with a fine drill, pores down to thirteen thousandths of an inch diameter being produced in this fashion. With this procedure a freshly machined surface was obtained at the base of the pore and this further improved the reproducibility of the specimens. The prepared specimens were mounted in Perspex clamps and exposed to the corrosive solutions in a vessel with optically flat glass faces. Close observation of the pore and the surrounding sprayed coating could thus be made during the course of the run with the aid of a traversing microscope.

EXPERIMENTAL RESULTS

In Part I it is shown that in the initial stages following immersion in N/1000 NaCl solution sprayed aluminium is more reactive than the massive metal, and is sufficiently electronegative to give protection to mild steel.

Some workers have doubted that cathodic protection plays any part, but the results described here have shown that in the environments used sacrificial dissolution of the sprayed metal is the main mechanism of the protection of the mild steel. This was tested in exploratory work by comparing the extent and amount of corrosion on the steel components in coupled and uncoupled model cells. The existence of very low resistance contact between the sprayed metal coating and the basis metal is very easily demonstrated with the aid of a simple resistance measuring instrument and no exceptions have been found.

When an area of steel is exposed to a corrosive environment either through the pores in the coating or by damage of the coating it has been found that the factors determining whether or not protection will occur may be grouped under three main headings: geometrical factors; coating reactivity; and the nature of the attacking environment.

Geometrical factors

The most important factors are the relative areas of exposed mild steel and available sprayed metal, and the size and shape of the individual exposed areas. This latter factor is only significant when considering the protection given to steel exposed at pores; the size and shape of the individual pore is of great importance.

Figs. 2 and 3 show the effect of changing the relative areas of sprayed aluminium and exposed mild steel in the standard model couple of a total exposed area of 4 in². The areas quoted are all superficial areas, as it has been found that a reliable roughness factor for the electrochemical behaviour of sprayed metals is not available. The complete polarization curves are shown in Fig. 2 for a selection of area ratios; it will be seen that control moved from the anodic type at the 1: 1 ratio through a mixed condition to a strong cathodic control in the case of couples with a smaller relative area of exposed mild steel. The currents should strictly be compared on a current density basis, and the cathodic portions of the curves are therefore plotted in Fig. 3 as potential against current density on the cathodic steel. As one would expect, the current density increased as the aluminium-mild steel ratio increased. Comparison of the curves for the 7: 1 and 15: 1 couples shows that the closed circuit potential falls considerably for a small increase in current density. This indicates that the critical current density at which complete cathodic protection is attained has been reached with the smallest area of mild steel. This view is confirmed by the observation that after three weeks exposure both the 1: 1 and 3: 1 couples were heavily rusted but the 15: 1 couple remained completely unattacked. The 7: 1 couple was in the main fully protected, but small patches of dark corrosion product were visible near the waterline. The curve for this couple has a maximum at 20 μA/in² and it has been found that this shape of curve is characteristic of the critical condition existing when

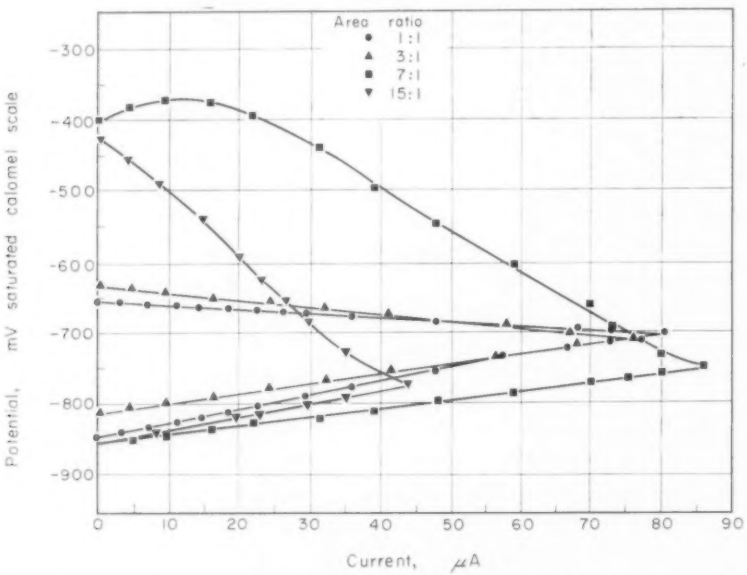

Fig. 2. Polarization curves of aluminium/mild steel couples of various area ratios.

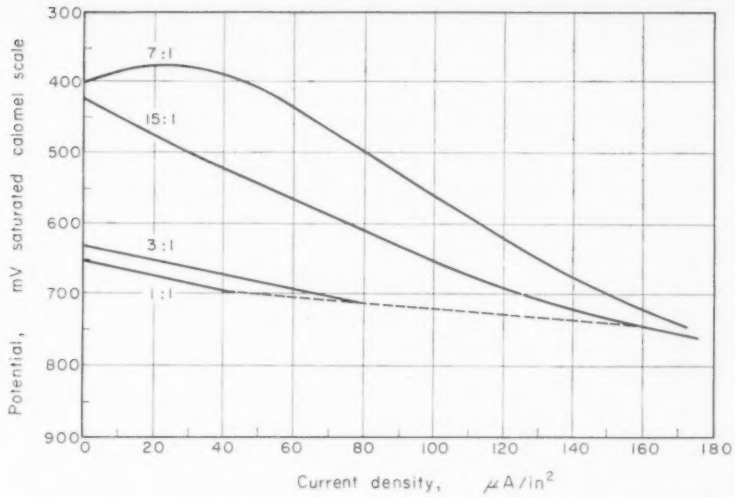

FIG. 3. Protective current densities of aluminium/mild steel couples of various area ratios.

barely sufficient current is being furnished by the coating to give complete protection to the steel.

The effect relative area of coating to exposed steel was also studied using the artificial pore model and similar results obtained. The size of the pore through which the basis metal is exposed was here found to be of great significance, as pore blocking reactions become increasingly important as the size is reduced. This is discussed later in the light of the results obtained by varying the environment.

The reactivity of the sprayed coating

The ability of a given area of sprayed aluminium to protect a fixed area of exposed steel depends upon the rate at which the coating can pass into solution to furnish protective current. This depends in turn on both the aggressive nature of the environment and the reactivity of the coating.

Little attention has been given to the possibility that the reactivity of a coating might change with time. However, this was the only explanation of the wide divergence in results of replicate experiments in our earlier work.

The ageing effect was not observed in the work using potential measurement described in Part I of this paper, because the curves were plotted over a period of two weeks and differences in the potential behaviour of replicate specimens during the first few hours were attributed to experimental error. It has since been found that when the storage atmosphere is fairly dry, no long-term ageing effect is observed with uncoupled foils, the only significant difference being in the time taken to reach maximum reactivity. However, if the coatings are aged in damp conditions the effect of "ageing" is very noticeable. This is illustrated in Fig. 4, which is based on potential/time curves over the first few hours immersion obtained on specimens previously aged for 3 weeks in a variety of atmospheres. The chief influence in the ageing process is the presence of water vapour; dry oxygen alone has little influence on the coating.

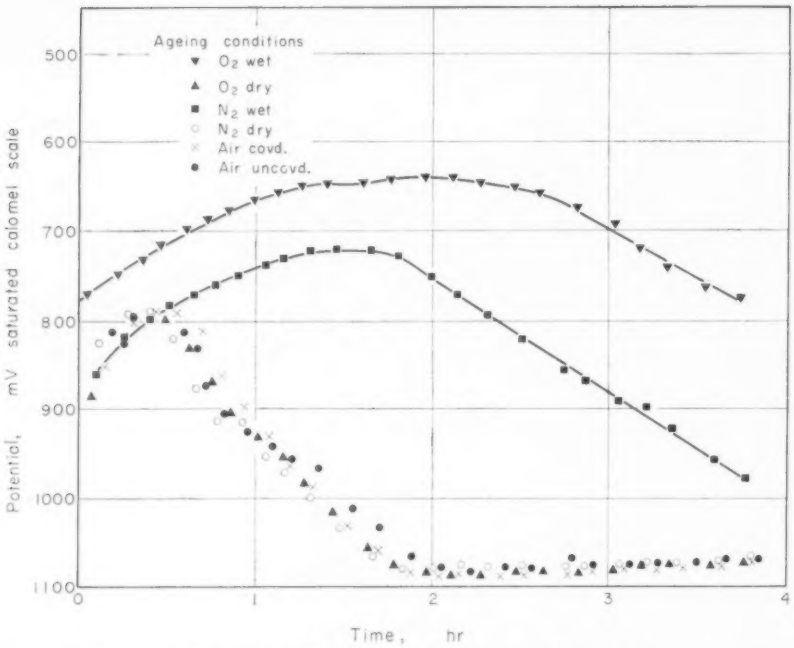

Fig. 4. Potential of aluminium foil aged under various conditions before exposure.

When a relatively large area of steel is coupled to the coating, however, the effect of ageing is very marked even when the specimens were stored in dry conditions. Fig. 5 shows the plarization curves after 24 hours' immersion of three 7: 1 couples after various periods of ageing in the dry laboratory atmosphere. The curves for the anodic aluminium has become more positive at the rate of about 5 mV/day and the

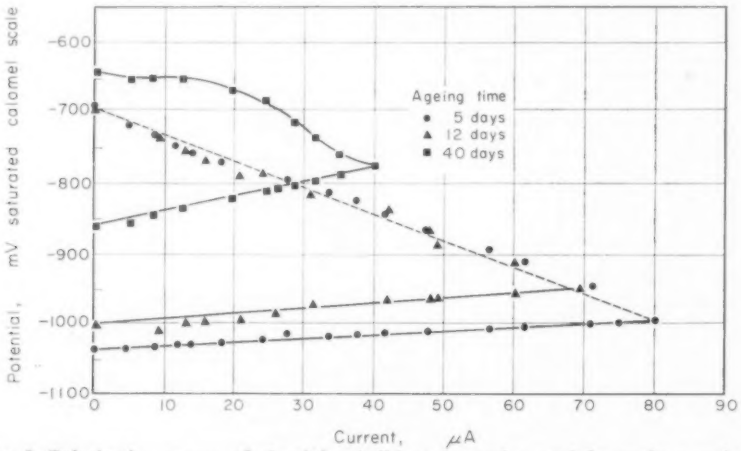

Fig 5. Polarization curves of aluminium/mild steel couples aged for various periods before immersion.

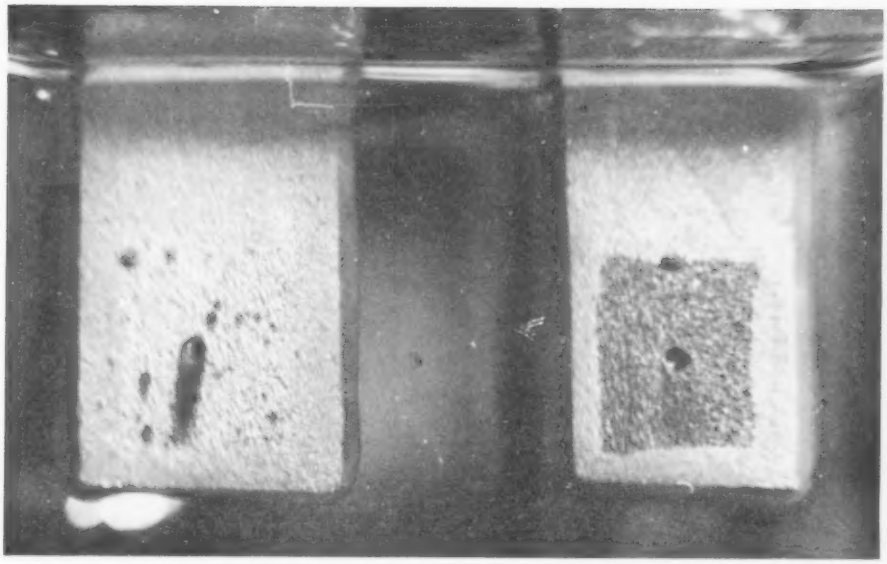

FIG. 6. Appearance of artificial pore on super-pure aluminium mounted on mild steel/and immersed in distilled water.

FIG. 7. Appearance of artificial pore in 99·5% purity aluminium mounted on mild steel/and immersed in distilled water.

total current flow is progressively reduced. The specimen aged for 40 days was in the critical condition and a slight rusting of the mild steel was observed. It was noticed throughout the work that the maximum current flow coincided with maximum rate of hydrogen evolution from the coating. As the period of ageing was increased, the rate of hydrogen evolution and the intensity of staining decreased, both phenomena being symptomatic of a reduction in reactivity (see Part I).

With uncoupled sprayed deposits, a significant effect of ageing was manifested in the induction period of the specimen, although the steady potentials reached after a few hours showed little difference. The potential/time curves for sprayed aluminium all show a rapid fall to potentials below −1000 mV (vs. saturated calomel electrode) after which a slow rise to the equilibrium potential occurred. The minimum of the curve corresponded to the most reactive condition and a good correlation existed between the time taken to reach this state of maximum reactivity and the extent of previous ageing of the foils. This explains why the phenomena was first observed with the couple specimens, as here the sprayed deposit is required to furnish protective current to an area of mild steel which would normally rust rapidly. Clearly, if the aluminium reaches a sufficiently reactive condition before the steel has been significantly attacked, little rusting will occur and the sprayed metal will remain at a low potential. If, on the other hand, the specimen is heavily aged and the induction period large, a considerable amount of rusting will have taken place on the steel before protection can be given, and a modified cell exists in which a large part of the cathode is obstructed. In this way, the ageing effect is exaggerated by contact with mild steel. It is likely that the rust staining which has been a source of trouble with sprayed metals (the decorative appearance of the coatings being impaired) depends on the age of the coating before service and that the rust develops during the induction period of the coating.

In work using the artificial pore technique better protection has usually been given to the exposed steel by the super-pure (99·99% Al) grade of metal than by the normal (99·5%) purity material. The super-pure coating gave excellent protection to the basis steel even in distilled water, while the steel was slightly rusted in the case of the 99·5% Al specimen. This result is surprising, as on theoretical grounds the higher purities might be expected to be insufficiently reactive to give protection in the milder environments.

It has been found that the mechanism of attack on the two purities is different, the dissolution of the high purity aluminium being much more dependent on the stimulation by the mild steel. Microscopic examination of the specimen during the course of the test revealed that the super-pure coating is noticeably attacked and cut back at the bottom edge of the artificial pore. The bright active area at the edge tails off into a dark stained area which is visible to the naked eye (Fig. 6). Under certain conditions similar, but less marked, local stimulation is also observed with normal purity aluminium; staining is usually more general however (Fig. 7). It appears that the aluminium is stimulated by the cathodic alkali flowing from the pit, and that a very large portion of the total dissolution is occurring within a very small area at the pit edge. This would account for the strong protection given by super-pure aluminium even in the very weak environments in which it would not normally be expected to dissolve due to the stability of the oxide film. This autocatalytic action in the pores

is considered to be an important feature of the mechanism and will be discussed in a later section.

The influence of the attacking environment

The investigations here described are based on the electrochemical behaviour of the sprayed coatings in dilute aqueous solutions. Most of the work was carried out in static N/1000 NaCl solution as a standard environment but a number of variations on this basic media were used to indicate the effect of some of the more important variables. The main effects of changes in salinity, the presence of hardness salts and the availability of oxygen were investigated.

Figure 8 shows the effects of varying the availability of oxygen for model 7: 1 couples. Oxygen and nitrogen were introduced through sintered glass aeraters as a fine stream of bubbles passing over the surface of the specimen. The agitation was by a motor-driven glass stirrer. Neither the stirring rate nor the rate of gas introduction was measured, but the rates were constant for replicates.

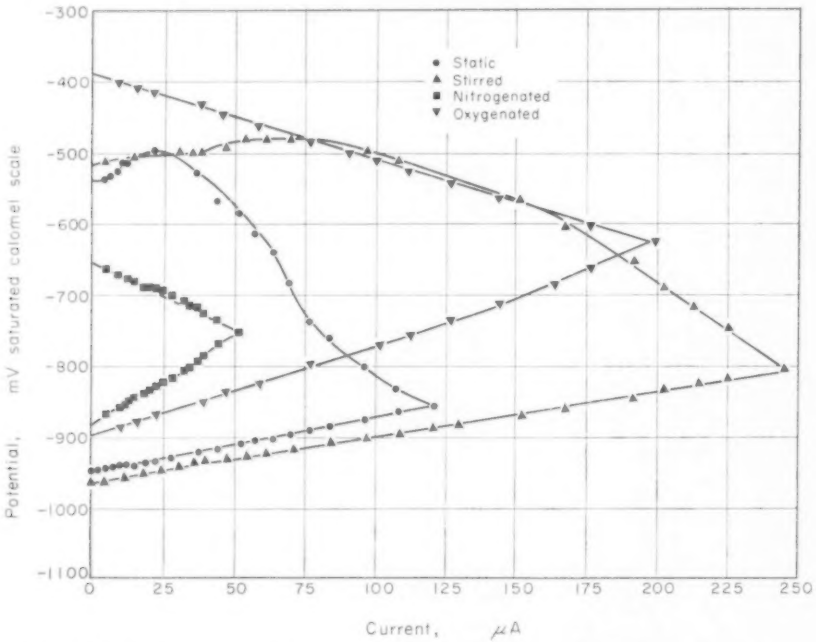

Fig. 8. Polarization curves of couples immersed in N/1000 NaCl solution under various states of oxygenation.

General agitation resulted in a stimulation of the reactions on both the sprayed metal and the steel to a similar extent; the corrosion rate was doubled, but the shape of the polarization curve was not greatly changed. The critical maximum was still present and the severity of attack on the mild steel was similar to the specimen in static solution. Oxygenation resulted in stimulation of the cathodic reaction on the mild steel and control shifted towards the anode; rapid rusting of the steel occurred.

The removal of oxygen by a continuous nitrogen purge produced a rather unexpected suppression of both the reactions on the mild steel and also at the anodic aluminium. The steepening of the anodic line is not easily explained, but it is thought that the absence of cathodic alkali is restricting film breakdown and that this, together with the greatly reduced demand for current by the suppressed cathodic steel, is causing the ennoblement.

TABLE 1

Artificial Hard Water	
$CaCO_3$	0·234 g/l
$MgCO_3$	0·027 ,,
$CaSO_4$	0·085 ,,
$MgCl_2$	0·056 ,,
NaCl	0·123 ,,

Artificial Sea Water	
NaCl	27·26 g/l
KCl	0·69 ,,
$MgCl_2$	3·51 ,,
KBr	0·09 ,,
$MgSO_4$	1·84 ,,
$CaSO_4$	1·29 ,,
$NaNCO_3$	0·10 ,,

A number of experiments were carried out using the artificial pore type specimen to study changes in dissolved salts and of these the curves in hard water and sea-water are of particular interest. Artificial waters were made up according to the figures listed in Table 1. Oxygen is much less important in sea-water than in distilled water or dilute brine. This indicates that the important cathodic reaction is hydrogen evolution in the more aggressive environment.

In artificial hard water a potential crossover occurred (Fig. 9), the steel becoming

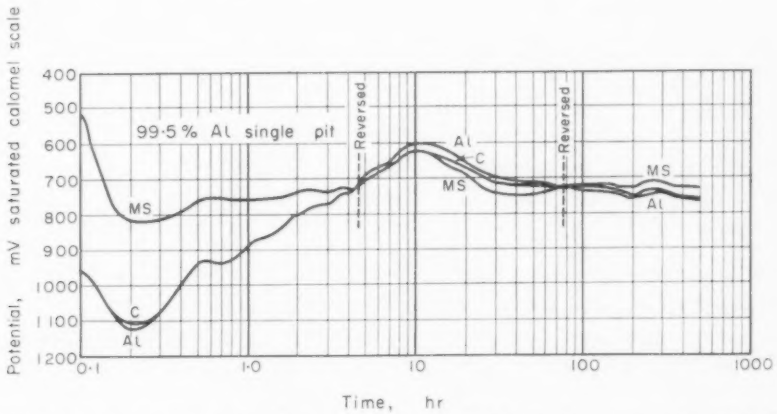

FIG. 9. Polarization/time plot of components of artificial pore in oxygenated artificial hard water.

between 20 and 40 mV more negative than the coating for approximately 80 hr. Microscopic observation of the pore during this period revealed no evidence of rusting, but the pore was filled with a transparent gelatinous material which slowly coagulated into globular shapes and finally aged to a white precipitate. As the layer began to coagulate, the aluminium became anodic once more in order to protect the steel now exposed. This ability of aluminium to re-assume the protective role when required was very apparent throughout the investigation. Work on specimens with larger numbers of artificial pores has shown that the crossover is not caused by the inability of the aluminium to maintain a sufficiently negative potential. Blockage of the pores relieves the coating of its sacrificial duties and allows it to move to an equilibrium or rest potential which may be more positive than that of the obstructed steel.

DISCUSSION AND CONCLUSIONS

The protective action of sprayed aluminium deposits on mild steel in dilute aqueous solution can conveniently be considered in three distinct stages.

Stage 1

Dissolution of aluminium is initiated at random points of activity caused by weaknesses in the oxide film. Such active sites occur more frequently in the sprayed than in the massive state as the numerous individual particles are under considerable stress and the film break-down repair cycle is more frequent. The distribution of these active sites is quite random in any given batch of specimens, but the probability of a sufficiently reactive site being present in a given area at any particular time is dependent on two factors:—the age of the deposit before it is immersed; and the purity of the coating metal.

The ageing of the deposit is mainly a film thickening process and is particularly sensitive to the presence of moisture. Little evidence has been found to support the view that ageing may also be connected with the relief of internal stresses. The presence of impurities in the deposit influences the distribution of the active sites in a radical fashion. With 99·5% purity aluminium, these sites are numerous and evenly distributed over the surface whereas with the super-pure material, such sites are isolated and intensely active. This difference is presumably due to discontinuities in the alumina film being caused by impurities at the surface of the particles.

The rate of dissolution rises rapidly to a maximum, shown by the coating reaching its most negative potential and a maximum rate of gas evolution. At this stage the maximum current is available for protection of any exposed steel. The time taken to reach maximum reactivity is very sensitive to previous ageing of the foil, the induction period being lengthened by increased ageing. During the induction period the available current for the protection of any exposed mild steel may be inadequate, and if it is protracted, rusting of the steel will occur. It is considered that the rust-staining which sometimes appears on sprayed aluminium coatings is caused during this induction period and is not detrimental except from the point of view of the appearance of the coated article.

Stage 2

Once maximum reactivity is reached and the exposed steel is under cathodic

protection, a new set of variables begin to control the process. These are chiefly geometrical factors such as the overall relative areas of exposed mild steel and sprayed aluminium and the size and shape of the individual exposed areas of steel.

The area ratio is very important, as would be expected, but its effects are complicated by ageing, and the two effects must be considered together if an estimate of the degree of protection is to be made. When mild steel is exposed only at small pores in the coating (as is normally the case with an undamaged deposit) the detailed geometry of the pore is of importance. The cathodic alkali produced at the protected steel surface is of a sufficiently high pH to dissolve alumina and the cathodic protection process becomes self-stimulating. If the individual area exposed is small, the catholyte flowing over the edge of the pore will maintain an area of aluminium in a sufficiently reactive condition to support the total demands of the exposed steel for protective current. Once this localized autocatalytic process is established, more remote sites of initial activity may be stifled without affecting the protection. The system now tends to a state of equilibrium in which the major portion of the coating is inactive but any exposed steel is under cathodic protection from small areas of aluminium in its immediate vicinity. This process explains why continuous protection was given to an artificial pore by sprayed super-pure aluminium in distilled water, a medium which would not normally be expected to support the protective reaction.

Stage 3

Finally, precipitation of corrosion products and hardness salts, etc. may lead to blanketing of the exposed steel and in most cases many of the pores will be sealed within a few weeks. This may be the most important source of long-term protection; however the results of this investigation suggest that even when stifling has occurred, the deposit is always capable of taking up the sacrificial role should this be required by sudden exposure of fresh steel.

The mechanism discussed above refers to neutral solutions. In solutions outside the pH limits of alumina, stability of the process is simplified. The general effects of pH are discussed in more detail in Part I of this paper.

REFERENCES

1. J. G. Hines and T. P. Hoar, *J. Appl. Chem.* **8**, 764 (1958).
2. M. Greene and M. C. Fontana, *Corrosion*, **15**, 1 (1959).

Corrosion Science, 1961, Vol. 1, pp. 132–160. Pergamon Press Ltd. Printed in Great Britain.

LES PROBLEMES DE CORROSION AQUEUSE DANS LE DOMAINE DE L'ENERGIE NUCLEAIRE*

H. CORIOU

Chef de Section d'Etude de la Corrosion Aqueuse et d'Electrochimie, Département de Métallurgie, au Commissariat à l'Energie Atomique (Centre d'Etudes Nucléaires de Saclay)

Résumé—Après une étude sommaire des principales formes de la corrosion aqueuse, on étudie l'influence du rayonnement ainsi que les méthodes d'essais généralement utilisées. On examine le comportement de divers matériaux nucléaires (uranium, aluminium, zirconium, Zircaloy, aciers inoxydables, alliages de nickel) dans les réacteurs refroidis par l'eau et les réacteurs homogènes.

Abstract—After studying briefly the main forms of aqueous corrosion, the influence of nuclear radiations is investigated as well as the commonly used testing methods.

The behaviour of different nuclear materials such as uranium, aluminium, zirconium, Zircaloy, stainless steels and nickel alloys is further investigated for their use in water-cooled reactor vessels and in homogeneous reactors.

Zusammenfassung—Nach einer kurzen Studie der Hauptformen der Korrosion durch Wasser werden speziell die Einflüsse nuklearer Strahlung sowie die gebräuchlichen Testverfahren einer Untersuchung unterzogen. Das Verhalten verschiedener Reaktormaterialien wir Uran, Aluminium, Zircaloy, rostfreier Stähle und Nickellegierungen wurde auf ihre Verwendbarkeit in wassergekühlten und homogenen Reaktoren geprüft.

Dès que les recherches théoriques en Physique Nucléaire eurent permis de passer aux réalisations pratiques, se posèrent des problèmes de corrosion souvent délicats. Dans le domaine de l'Energie Nucléaire, les matériaux travaillent fréquemment dans des conditions dures et leur choix se trouve limité par des impératifs de section de capture neutronique. On doit également faire intervenir l'action du rayonnement, celle-ci étant en particulier susceptible d'entraîner la libération de produits accélérant la corrosion, de faire varier certaines cinétiques de réactions ou bien même de provoquer des modifications dans la structure des matériaux.

Les problèmes de corrosion aqueuse dans l'Energie Nucléaire se rencontrent, au cours des opérations suivantes:

Traitement chimique des minerais d'uranium.

Elaboration de l'uranium.

Fonctionnement des réacteurs.

Traitement des combustibles irradiés.

Le traitement chimique des minerais nécessite de nombreuses manipulations pour conduire à des "concentrés". A partir de ces concentrés solides ou liquides, on prépare le tétrafluorure d'uranium. Celui-ci réduit par le calcium permet l'obtention de l'uranium métal. L'ensemble de ces opérations posent, sur le plan de la corrosion, des problèmes classiques déjà rencontrés dans un grand nombre d'usines chimiques.

Les réacteurs peuvent se diviser en trois grands groupes:

1. Les réacteurs modérés au graphite et refroidis par l'air atmosphérique ou le gaz carbonique.

*Conférence présentée à Bruxelles, le 30 août 1960, sous les auspices du Centre Belge d'Etude de la Corrosion (CEBELCOR).

2. Les réacteurs modérés et refroidis par l'eau.
3. Les réacteurs homogènes utilisant un mélange "homogène" du modérateur et des sels de matières fissiles.

La première classe de réacteurs pose essentiellement des problèmes de corrosion par les gaz caloporteurs, cette étude ne sera pas abordée ici. Toutefois, les éléments combustibles de ces réacteurs étant gainés par du magnésium ou des alliages de magnésium, le stockage des éléments après irradiation soulève des problèmes de corrosion aqueuse.

Après un certain temps de fonctionnement, il est nécessaire de traiter les combustibles irradiés afin d'en extraire en particulier le plutonium. Une fois mises en marche les usines prévues à cet effet, il s'avère très difficile d'accéder aux appareils pour une éventuelle réparation, en raison de leur activité extrêmement élevée. On conçoit aisément l'importance des problèmes de corrosion dans ces usines très particulières où les aciers inoxydables sont utilisés dans divers milieux souvent assez agressifs.

Nous décrirons, en les illustrant éventuellement par quelques exemples, les différentes formes de corrosion que l'on est susceptible de rencontrer dans le domaine nucléaire.

I. LES DIFFERENTES FORMES DE CORROSION

1. *Corrosion intergranulaire*

La corrosion intergranulaire consiste en une attaque localisée aux contours des cristaux du métal ou alliage. Cette attaque est susceptible de conduire à une véritable décohésion du métal sous l'action d'un effort mécanique même très faible.

Voici une trentaine d'années, cette forme de corrosion faillit arrêter net l'essor des aciers inoxydables; fort heureusement, l'évolution de la technique a permis de limiter considérablement le danger.

Nous signalerons trois cas de corrosion intergranulaire caractéristiques:

L'attaque des aciers inoxydables.

Le "season cracking" des laitons.

L'attaque de l'aluminium raffiné.

Ces exemples mettent en évidence l'influence de trois facteurs très différents. Le premier cas résulte, en effet, de l'apparition d'une seconde phase aux contours des grains à la suite de certains traitements thermiques. Le second cas est dû à l'existence de tensions internes dans l'alliage. Enfin, l'attaque intergranulaire de l'aluminium raffiné provient de la nature structurale propre des contours de grains.

Nous nous limiterons au premier cas, en l'étudiant sommairement. Considérons un acier inoxydable 18/10, non stabilisé. Cet acier, outre 18 pour cent de chrome et 10 pour cent de nickel renferme certaines impuretés, dont le carbone.

Lors de l'hypertrempe, c'est-à-dire maintien prolongé de l'acier à 1050–1150°C suivi d'un refroidissement rapide, le carbone entre en solution solide dans la solution solide ternaire austénitique Fe–Cr–Ni, mais si l'acier est soumis à un revenu dans une zone de températures comprise entre 500 et 800°C (zone de sensibilisation) le carbure de chrome de formule $Cr_{23}C_6$, très riche en chrome, précipite aux contours des grains. Quand cette précipitation se produit, on observe le long des contours de grains une

zone étroite de solution solide appauvrie en chrome, élément protecteur, cette zone devenant attaquable par certains milieux corrosifs.

D'un point de vue pratique, ce phénomène est très important. Dans le cas d'une soudure, certaines régions de l'alliage sont en effet maintenues dans la zone de sensibilisation durant un intervalle de temps plus ou moins grand, suivant l'épaisseur du métal à souder et le mode de refroidissement, d'où précipitation du carbure de chrome aux joints de grains.

Le mécanisme même de l'attaque permet de trouver différents remèdes à la corrosion intergranulaire des aciers inoxydables.

On peut en effet par exemple:

(1) Abaisser la teneur en carbone de l'acier jusqu'à des valeurs très faibles inférieures à 0,03 pour cent. On obtient des aciers dits "très bas carbone".

(2) Introduire dans l'acier un élément appelé stabilisant qui possède pour le carbone une affinité supérieure à celle du chrome. On utilise comme stabilisant le *titane* ou le *niobium*.

La micrographie (Fig. 1) donnée à titre d'exemple est relative à la corrosion intergranulaire d'un acier inoxydable austénitique, non stabilisé, "très bas carbone", mais contaminé accidentellement en surface par du carbone (cas rencontré au cours d'essais concernant un réacteur homogène).

Il paraît évident que la corrosion intergranulaire ne peut être en général décelée que par un examen micrographique car, seule une portion extrêmement faible du métal subit l'attaque.

Corrosion en "lame de couteau" (*Knife edge attack*). On doit également faire état d'un phénomène de corrosion intergranulaire susceptible de se manifester sur deux lignes parallèles *adjacentes* aux soudures d'aciers inoxydables stabilisés. Cette corrosion que nous avons eu l'occasion d'observer récemment se caractérise de la façon suivante:

(1) Elle ne se produit que pour les aciers du type 18/10 *stabilisés* au titane ou au niobium, *a l'exclusion des nuances non stabilisées*. Toutefois, seules sont atteintes les nuances relativement carburées (C>0,06 pour cent).

(2) Elle affecte les zones portées à des températures voisines de 1300°C pendant l'opération de soudage. Elle se distingue ainsi de la corrosion intergranulaire qui affecte de part et d'autre d'une soudure la région maintenue dans la zone de sensibilisation (500–800°C), cette zone étant distante de *quelques millimètres* du cordon de soudure.

(3) Des aciers parfaitement insensibles à la corrosion intergranulaire par chauffage dans la zone de sensibilisation peuvent néanmoins subir une très forte corrosion en "lame de couteau".

L'explication de l'attaque en "lame de couteau" n'est pas encore complètement satisfaisante. L'hypothèse suivante a été avancée par divers auteurs: l'acier étant chauffé à très haute température (~ 1300–1400°C) au voisinage immédiat du cordon, la solubilité du carbure de titane ou de niobium devient importante, la quasi totalité du carbone passe en solution solide et lors du refroidissement dans la zone de sensibilisation le carbure de chrome $Cr_{23}C_6$ précipite aux joints de grains appauvrissant en chrome la zone intergranulaire.

La Fig. 2 illustre d'une façon particulièrement démonstrative l'attaque en "lame de couteau". Il s'agit d'une soudure entre un acier 18/10 très bas carbone et un acier

18/10 au molybdène stabilisé au titane (C = 0,08 pour cent). L'échantillon a été exposé durant environ 400 h à l'action des vapeurs se dégageant de l'acide nitrique 11 N à l'ébullition.

2. *Corrosion par piqûres*

Une attaque intense et locale est très fréquemment liée à la combinaison large cathode et petite anode.

Les aciers inoxydables ne sont pas exempts de ce type de corrosion. Si, par exemple, un point de l'acier devient anodique par suite d'un appauvrissement local de la solution corrosive (en oxygène) le rétablissement de la passivité ne peut s'effectuer en ce point. En raison de l'importante zone à l'état passif entourant la zone anodique dépassivée et de très faible surface, nous nous trouvons dans la cas de la combinaison large cathode–petite anode, d'où formation d'une piqûre. Les solutions renfermant des chlorures peuvent, dans certaines circonstances particulières, conduire à de véritables catastrophes. A titre d'exemple, au cours d'un essai d'étanchéité une cuve de stockage en acier inoxydable (18/10 très bas carbone) remplie durant seulement 45 jours par de l'eau renfermant 225 mg/l. d'ions Cl^- s'est trouvée perforée en de nombreux endroits.

Il paraît enfin nécessaire d'attirer l'attention sur la tendance marquée des salissures à produire une corrosion par piqûres. Les salissures ne constituent pas uniquement une pollution des surfaces, elles peuvent provoquer de sérieuses piqûres même sur les aciers inoxydables.

3. *Corrosion générale*

Cette forme de corrosion est relative à une attaque uniforme de la surface du métal produisant un amincissement régulier. Il paraît évident que si le métal a été convenablement choisi pour le milieu d'utilisation, cette corrosion ne peut être dangereuse. Il ne semble pas nécessaire de s'y attarder.

Le trois formes de corrosion que nous venons de passer en revue ne sont pas les seules, nous allons en examiner d'autres, d'ailleurs plus ou moins liées aux précédentes:

(a) *Corrosion par "poches gazeuses" (blistering attack)*

Cette forme de corrosion nous intéresse particulièrement puisqu'elle intervient fréquemment sur les alliages légers dans l'eau à haute température donc, dans les conditions de fonctionnement de réacteurs de puissance refroidis par l'eau.

Dans ce type d'attaque, une partie des atomes d'hydrogène produits au cours de la réaction de corrosion diffuse à l'intérieur du métal, principalement aux défauts de structure. La formation d'hydrogène moléculaire dans les petites "cavités" du métal provoque des poches de pression de gaz amenant des "gonflements" locaux (blisters).

La rupture des poches permet à l'eau de s'introduire à l'intérieur, il se produit à nouveau de l'hydrogène, le processus de corrosion s'entretenant ainsi de lui-même (cas de nombreux alliages d'aluminium dans l'eau à température élevée). La micrographie (Fig. 3) donnée à titre d'exemple représente la cavité formée dans un alliage d'aluminium après éclatement d'une poche gazeuse.

(b) *Corrosion au contact entre métaux différents*

Deux métaux différents couplés dans un milieu aqueux peuvent constituer une véritable cellule électrolytique, l'attaque tombant en général sur le plus anodique. Toutefois, dans le cas où l'hydrogène produit dans la partie cathodique de la réaction de corrosion est le principal agent corrosif, le fait de polariser cathodiquement un métal peut, au lieu de lui assurer une protection, conduire au contraire à des dégats sévères, une polarisation anodique étant par contre très favorable.

Pour illustrer cette assertion, il nous suffit d'exposer à l'action de l'eau à haute température un échantillon d'aluminium commercial d'une part non couplé, d'autre part couplé à un acier inoxydable 18/10 par exemple. L'échantillon d'aluminium polarisé anodiquement du fait de son couplage avec l'acier inoxydable se trouve considérablement protégé (Fig. 4).

(c) *Corrosion aux recoins*

Si l'on n'a jamais été surpris par la corrosion due à l'effet de couplage on a été jadis désorienté par la corrosion intense observée en certains points où un corps même non conducteur repose sur un métal. L'explication du phénomène est aujourd'hui connue. Entre un corps étranger et le métal se forment des recoins dans lesquels le réapprovisionnement de certaines substances (en particulier l'oxygène) ne peut se faire que lentement, permettant ainsi la formation de "piles de concentration".

Pile due à la distribution non uniforme de l'oxygène. Une différence de distribution de l'oxygène peut engendrer des courants de corrosion fréquemment appelés "courants d'aération différentielle". Les régions "oxygénées" deviennent cathodiques tandis que

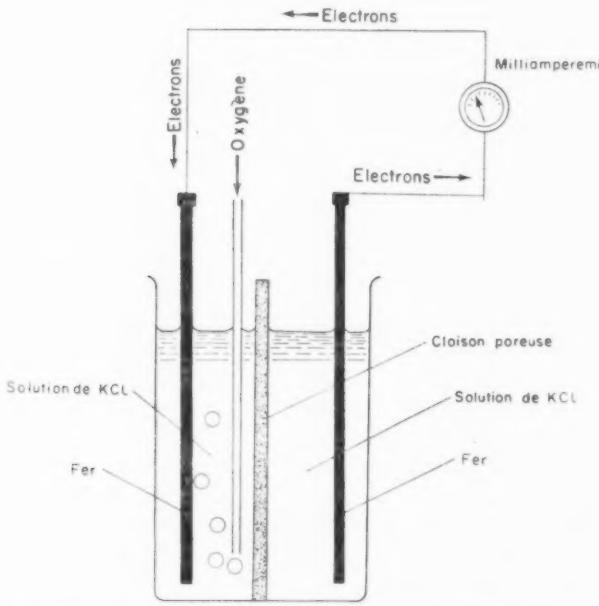

FIG. 5. Production d'un courant d'oxygénation différentielle entre électrodes de fer immergées dans une solution de KCl.

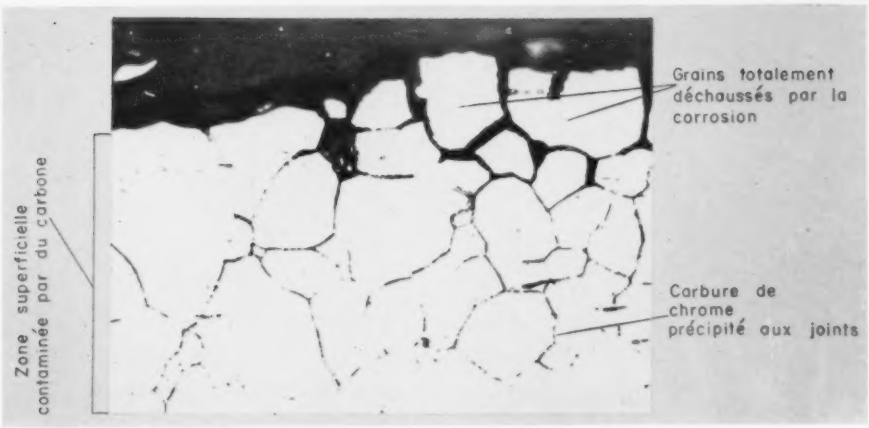

FIG. 1. Corrosion intergranulaire d'un acier inoxydable austénitique "très bas carbone" mais contaminé en surface par du carbone. Zone sensibilisée voisine d'une soudure (milieu corrosif, SO_2H_2, 0,5 N; température 70°C). (× 480)

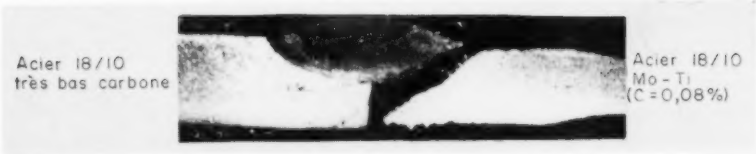

FIG. 2. (d'après Hochman, C.A.F.L.). (× 6)

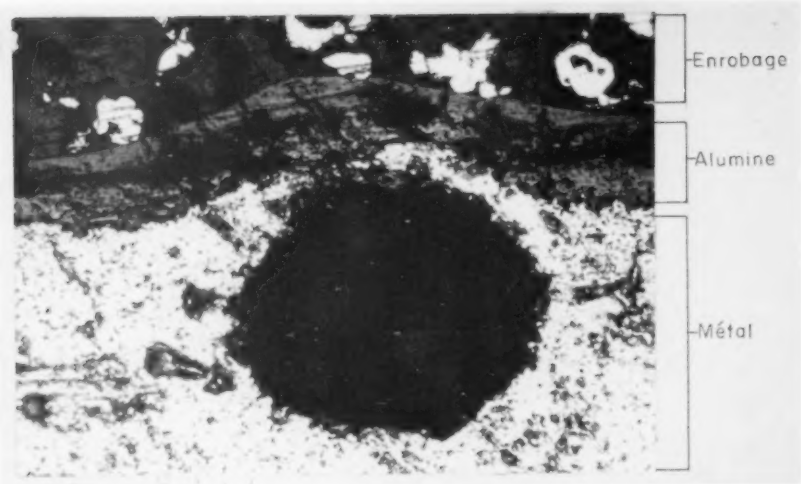

FIG. 3. Exemple d'attaque par "poches gazeuses". (× 250)

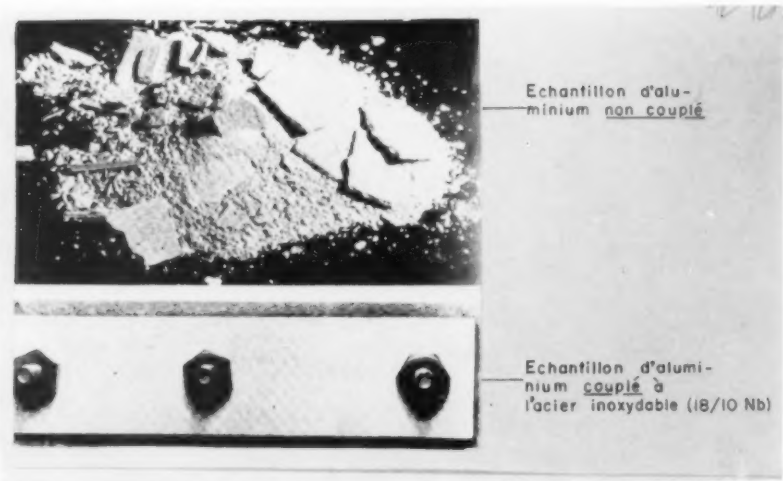

FIG. 4. Echantillons d'aluminium 1100 exposés 4 h à l'action de l'eau à 315° (d'après Draley). (× 1)

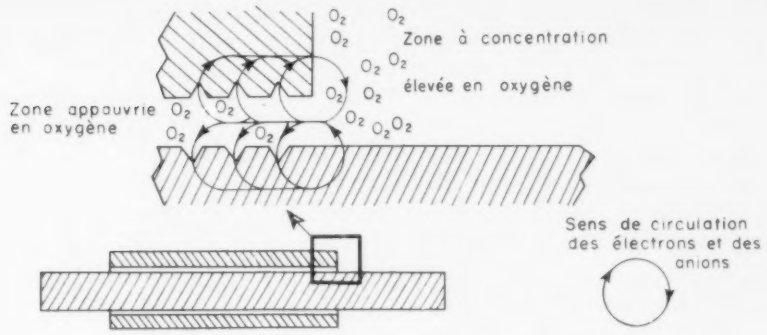

FIG. 6.

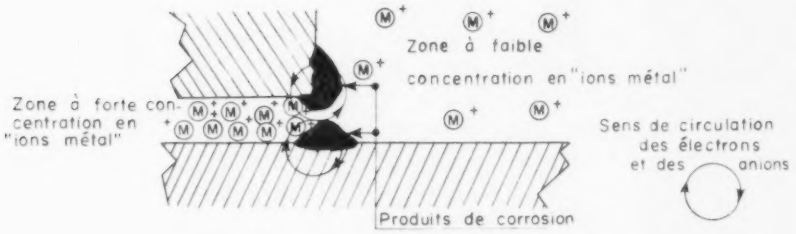

FIG. 7.

les régions "non oxygénées" deviennent anodiques, donc généralement attaquables. Il semble à ce sujet intéressant de rappeler quelques expériences caractéristiques de Evans:

Deux électrodes de fer connectées à un milliampèremètre sont plongées dans deux compartiments d'une pile cloisonnée. Si nous introduisons des bulles d'oxygène dans un compartiment, nous enregistrons un courant provoqué par l'oxygénation différentielle, l'électrode oxygénée étant cathode (Fig. 5).

Dans les réacteurs la corrosion aux recoins peut provoquer des contraintes importantes et des grippages de pièces dus à l'augmentation de volume en passant du métal aux produits de corrosion. Il convient de signaler, en particulier, la complexité de certaines pièces où les zones de mauvais renouvellement sont particulièrement nombreuses.

Des informations récentes sur les réacteurs de puissance refroidis par eau signalent que la corrosion par effet de concentration ne serait pas un problème, à condition: soit de maintenir la teneur en oxygène de l'eau à des valeurs de l'ordre de 0,1 ml/l. soit d'opérer dans l'eau à pH élevé (10–11) ou additionnée d'hydrogène (25–50 ml/l.), l'un et l'autre de ces deux facteurs pouvant contrecarrer le rôle néfaste joué par une concentration trop importante en oxygène.

Dans l'eau à haute température, les dangers apparaissent surtout à l'intérieur des espacements inférieurs à 50μ, ils dépendent évidemment de la nature des matériaux en présence, des couplages éventuels; ils sont enfin d'autant plus importants quel a

température est plus élevée. La Fig. 6 schématise l'attaque par oxygénation différentielle dans le recoin formé par deux cylindres coaxiaux.

Pile due à la distribution non uniforme des "ions métal". Cette forme de corrosion est provoquée par des courants circulant entre des régions entre lesquelles existent des différences de concentration en "ions métal". La Fig. 7 illustre le mécanisme d'attaque.

On remarque dans ce cas, contrairement à une pile par oxygénation différentielle, une accumulation de produits de corrosion aux lèvres du recoin.

Nous avons eu récemment l'occasion d'observer sur un tube en acier inoxydable (18/10 très bas carbone) une corrosion par effet de recoin extrêmement importante. Le tube maintenu par un collier en acier de même nuance se trouvait au fond d'un vaste réservoir de 150 m^3 rempli d'eau à température ambiante renfermant 225 mg/l. d'ions Cl^-. La Fig. 8 représente l'état du tube après 45 jours.

(d) *Corrosion sous contrainte* (*stress corrosion*)

La corrosion sous contrainte se caractérise par une fissuration susceptible d'apparaître sous l'action combinée d'une tension et d'un milieu corrosif. Les fissures peuvent être intergranulaires, intragranulaires ou une combinaison des deux formes, leur aspect est très spectaculaire et même les tubes les plus épais sont susceptibles d'être traversés de part en part.

Les tensions peuvent résulter de l'action de forces extérieures ou de contraintes internes. Actuellement, on établit une distinction entre la corrosion accélérée par la tension et la fissuration par corrosion sous contrainte. En effet, si un métal est déjà sensible à la corrosion intergranulaire, les tensions externes peuvent élargir les rainures entre les grains et faciliter ainsi la pénétration il s'agit d'une corrosion intergranulaire accélérée par la tension, le terme "fissuration par corrosion sous contrainte" doit être limité aux cas pour lesquels aucune pénétration significative n'apparaît en absence de tensions.

Les ions chlorures jouent un rôle important dans l'apparition de cette forme de corrosion, aussi dans une installation convient-il d'éviter de leur laisser la possibilité de se concentrer localement. Le couple chlorure–oxygène est tout particulièrement dangereux, nous y reviendrons plus en détails dans l'étude de la corrosion des aciers.

La corrosion sous contrainte peut, en particulier, affecter les aciers inoxydables austénitiques; or, dans les réacteurs à eau, on se trouve fréquemment dans l'obligation d'utiliser de tels aciers pours les échangeurs.

La micrographie (Fig. 9) donnée à titre d'exemple montre un cheminement intragranulaire survenu dans un acier inoxydable 18/10 travaillant sous contrainte. Il s'agissait d'un tube d'échangeur parcouru intérieurement par un fluide à 300°C et refroidi extérieurement par de l'eau de ville à 40°C.

(e) *Corrosion due à l'inégalité des conditions mécaniques*

L'assemblage de deux métaux différents dans un milieu aqueux n'est pas nécessaire pour constituer une cellule électrolytique, les électrodes peuvent être tout simplement deux zones d'un même métal, si pour une raison quelconque leurs potentiels de dissolution sont différents. Cette dissymétrie provient éventuellement d'une inégalité dans la répartition des conditions mécaniques (zones plus ou moins écrouies). Nous

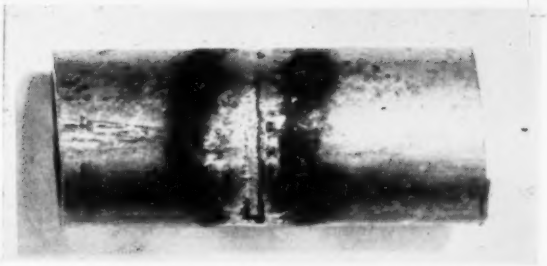

FIG. 8. Effet de recoin sur un tube en acier inoxydable (18/10 très bas carbone). Remarquer la corrosion très profonde sous le collier. (× 1)

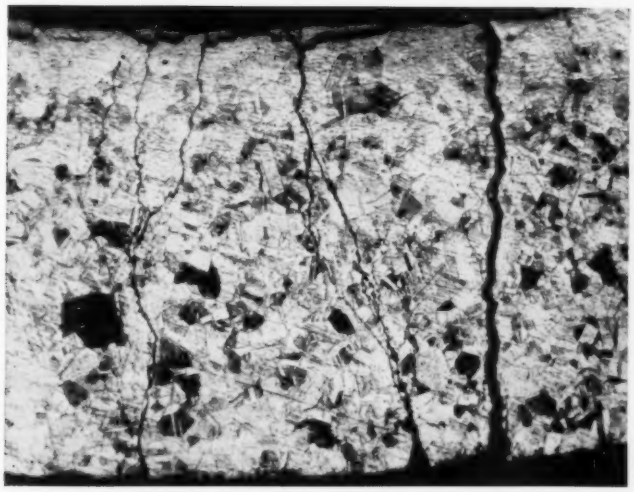

FIG. 9. Fissuration intragranulaire dans un acier inoxydable 18/10. (× 80)

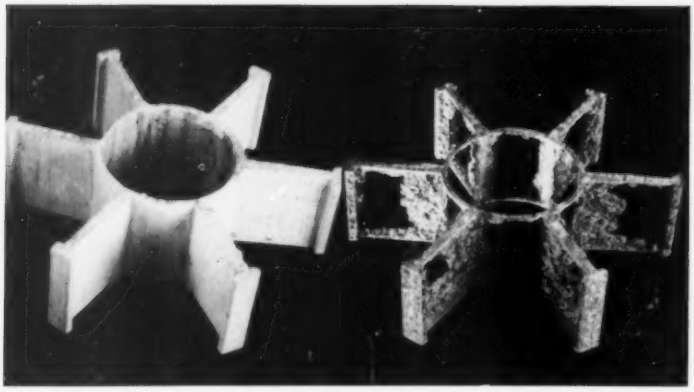

FIG. 10. Influence de l'écroissage sur la corrosion du magnésium par une solution de chlorures. ($Cl^- = 10^{-3}$ ion g/l; $t = 20°$; durée d'immersion, 48 h).

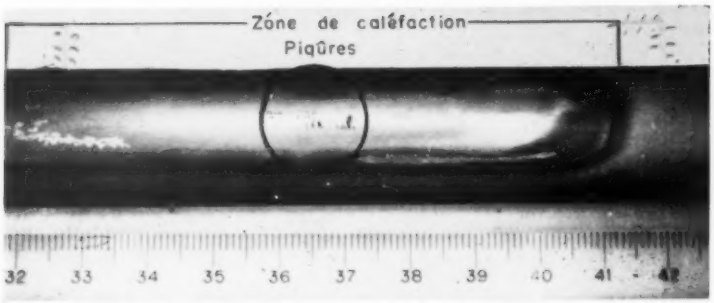

FIG. 11. Phénomène de cavitation à la surface d'une gaine en aluminium (remarquer les piqûres provoquées par la cavitation) Echelle 1.

avons vu apparaître cette forme de corrosion au cours d'essais de laboratoire destinés à des stockages de gaines en magnésium dans de l'eau.

La Fig. 10 nous paraît très démonstrative. L'échantillon représenté sur les photographies a été prélevé par sciage dans une gaine en magnésium, la photographie de droite montre l'aspect de l'échantillon après immersion de 48 hr dans une solution de cholures à 10^{-3} ion g/l., seules subsistent encore les zones très écrouies en particulier celles écrouies lors du sciage.

(f) *Corrosion par cavitation*

La cavitation est un phénomène surtout d'ordre mécanique accéléré simplement, dans certains cas, par le milieu corrosif. Cette corrosion se manifeste par la formation de piqûres et de cavités plus ou moins profondes sous l'effet dynamique d'un liquide. Lorsque l'eau circule par exemple dans un tube rétréci localement, il se forme des zones de très faible pression, d'où l'apparition de poches de vapeur appelées improprement "bulles de vide".

L'énergie mise en jeu dans la résorption de ces bulles est très grande et, si le métal est frappé toujours au même endroit, les dégâts sont sévères. Le milieu corrosif peut accélérer l'attaque mais n'est pas nécessaire.

On a pu provoquer des attaques par cavitation sur des substances telles que le verre, frappées par l'eau distillée. La cavitation est accélérée par élévation de la température.

En résumé, le mécanisme de la cavitation peut être ainsi présenté:

(1) Formation de zones à très faible pression sous l'effet de modifications dans l'écoulement d'un liquide.
(2) Formation de poches de vapeur dans ces zones de faible pression.
(3) A la suite d'un changement momentané dans les conditions de pression provoqué par l'irrégularité du mouvement du liquide, résorption brutale des bulles à la paroi, d'où effet de choc intense.

Au cours d'essais reproduisant des flux thermiques très élevés ($\sim$ 200 W/cm²) à travers des gaines en aluminium refroidies par un courant rapide d'eau déminéralisée ($V \sim 5$ m/s, $t \sim 50°$) nous avons observé des phénomènes de cavitation particulièrement démonstratifs.[1] Dans le cas d'un décentrement suffisant de la gaine, un matelas de vapeur bien localisé occupait l'espace compris entre la gaine et le manchon. En quelques minutes, la zone de caléfaction était marquée par des auréoles très visibles sur la Fig. 14.

Des piqûres apparaissaient dans la zone de caléfaction en raison des fluctuations locales de pression. Le phénomène accompagné de claquements très secs provoquait une attaque rapide de la paroi. Les cratères de cavitation se formaient sur la gaine (Fig. 11) et sur le manchon en silice fondue transparente quand celui-ci se trouvait assez proche de la gaine.

II. INFLUENCE DU RAYONNEMENT

Des précisions sur l'incidence du rayonnement seront apportées pour chaque métal étudié. Nous nous bornerons à donner ici quelques indications d'ordre général.

L'irradiation peut influencer la corrosion en modifiant la composition du milieu et/ou en altérant les propriétés des métaux.

D'après les idées généralement admises, les effets primaires du rayonnement sur l'eau sont l'excitation des molécules et une ionisation:

$$H_2O \rightarrow H_2O^+ + e^-$$
$$H_2O + e^- \rightarrow H_2O^-$$
$$H_2O^+ \rightarrow H^+ + OH$$
$$H_2O^- \rightarrow OH^- + H$$

Le résultat global de cette suite de réactions peut se résumer ainsi:

$$H_2O \rightarrow H + OH$$

Les particules α, les protons, les fragments de fission produisent le long de leur course une ionisation très importante. Une proportion considérable de radicaux se combinent suivant les réactions:

$$H + H \rightarrow H_2$$
$$OH + OH \rightarrow H_2O_2$$
$$H + OH \rightarrow H_2O$$

Dans ce cas, le processus global se traduit par la réaction:

$$2\,H_2O \rightarrow H_2 + H_2O_2$$

La densité des radicaux dus au rayonnement γ et aux particules β de grande énergie est par contre beaucoup plus faible que celle provoquée par les particules que nous venons de considérer. On observe également dans ce cas la formation d'hydrogène et d'eau oxygénée, mais de nombreux radicaux deviennent disponibles pour réagir éventuellement avec diverses substances présentes dans la solution.

Si nous considérons une solution de sulfate d'uranyle dans un réacteur homogène, on peut distinguer toutes les formes de rayonnement, toutefois la radiolyse provient essentiellement des particules lourdes. La durée de vie de l'eau oxygénée est très courte à la température du réacteur (>250°C). Les produits de radiolyse sont donc l'hydrogène et l'oxygène, mais ceux-ci se forment par des radicaux intermédiaires dont l'activité chimique est très élevée. Il peut en résulter des réactions sur les parois du récipient qui renferme la solution (par exemple, oxydation ou hydruration) et la corrosion se trouve modifiée.

Dans les premiers réacteurs à eau lourde, la corrosion observée a été fréquemment due à la formation d'acide nitrique et d'oxydes d'azote sous l'action du rayonnement par suite de la présence d'air et d'humidité.

Il convient également de tenir compte de l'effet des radiations d'un réacteur sur un certain nombre de corps organiques. Par exemple, les radiations provoquent la formation de radicaux libres dans les liquides organiques tels que certaines huiles utilisée pour la lubrification. Le zinc, l'aluminium, l'étain sont susceptibles de réagir avec ces radicaux pour former des composés organo-métalliques.

On doit, en outre, du point de vue de la corrosion, faire intervenir l'action du rayonnement sur les films protecteurs formés à la surface des métaux, cette action est certes très complexe. Voici plus d'un siècle que Faraday a attribuée la passivation du fer dans l'acide nitrique un film superficiel renfermant de l'oxygène, aujourd'hui, nous ne sommes pas encore certains de la structure même de ce film, nous manquons également de renseignements sur le mécanisme qui joue dans le transport des corps

FIG. 12a

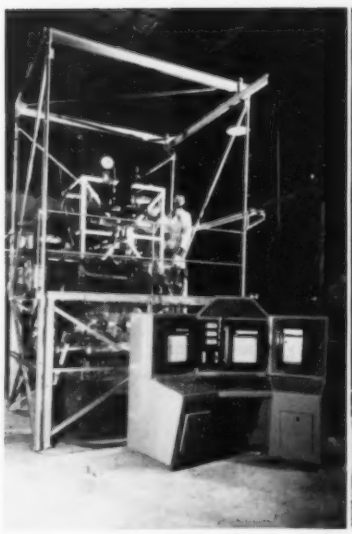

FIG. 12b

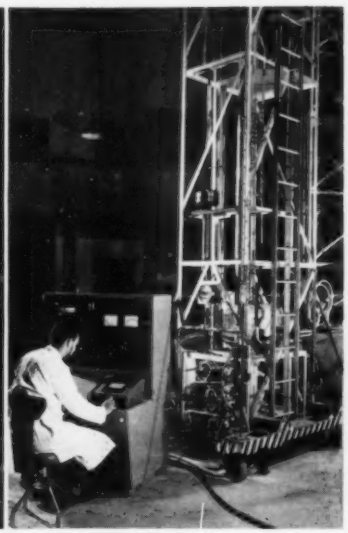

FIG. 12c

FIG. 12(a). Salle d'essais statiques en autoclaves.
FIG. 12(b). Thermosiphon pour essais dynamiques de corrosion par l'eau à haute température (eau 350°C; pression 180 kg/cm²).
FIG. 12(c). Cellule pour l'étude de la corrosion de gaines traversées par des flux thermiques élevés (eau, 350°C; pression, 180 kg/cm²; flux, 100–150 W/cm²).

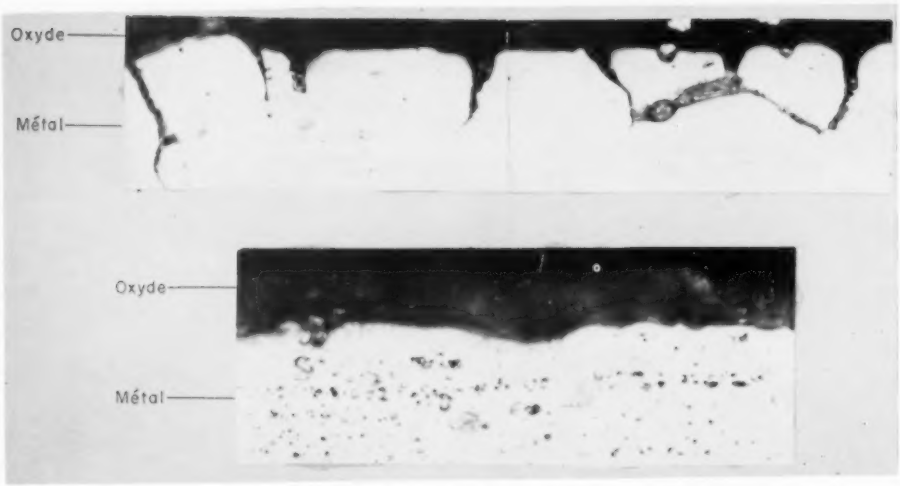

FIG. 16. Echantillons d'aluminium A_5 et A_9 recuits préafablement et corrodés par l'eau déminéralisée (60 jours à 90°C). Les deux coupes micrographiques sont au grossissement 700, celle du haut est relative à l'aluminium A_9, celle du bas à l'aluminium A_5.

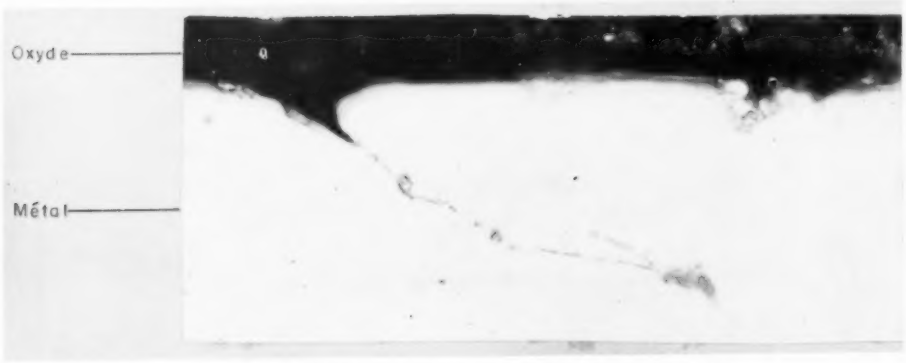

FIG. 17. Corrosion intergranulaire d'aluminium A_9. (× 970)

réagissant à travers les films protecteurs, on conçoit aisément les difficultés d'interprétation en présence du rayonnement. Lorsqu'un film protecteur est soumis au rayonnement d'un réacteur, les effets peuvent être variés. Les fragments de fission conduisent à des chocs élastiques avec les atomes du film et à une ionisation. Des neutrons de fission provoquent également des chocs élastiques susceptibles d'entraîner des modifications de réseaux. Ainsi, l'altération du réseau et les modifications dans les propriétés électriques associées aux défauts de structure dans le film peuvent modifier la cinétique de corrosion.

III. METHODES D'ESSAIS POUR L'ETUDE DES PROBLEMES DE CORROSION DANS LES REACTEURS

Les essais doivent être définis de façon très précise et l'extrapolation modérée de beaucoup de prudence, surtout dans le domaine de l'énergie nucléaire. Les expériences de laboratoire ont en général une durée relativement faible par rapport à la durée exigée en pratique, on pourrait en conséquence être tenté d'appliquer des tests très sévères, la sévérité du milieu corrosif devant suppléer au court laps de temps imparti pour les expériences de laboratoire. Afin d'abréger la durée des essais il convient d'agir essentiellement sur la précision de la méthode de mesure, les conditions de milieu restant les mêmes que celles utilisées pratiquement.

Quel critérium peut-on utiliser pour définir quantitativement la résistance des matériaux à la corrosion?

Les variations de poids des échantillons ne peuvent être employées que si l'attaque des éprouvettes est uniforme, mais seules elles n'ont qu'une signification relative lorsqu'une attaque intergranulaire ou par piqûres prend naissance. La micrographie est en général la méthode de choix qui permet également d'élucider dans de nombreux cas le mécanisme intime de la corrosion.

Les premiers essais de corrosion par l'eau à haute température sont effectués dans des conditions statiques ou "semi-statiques" avec renouvellement d'eau. Ces tests sont destinés à une présélection des matériaux. Les autoclaves utilisés sont en acier inoxydable. La Fig. 12 a représente notre salle d'essais statiques en autoclaves.

Certains matériaux pour confection de gaines doivent être soumis à l'action de l'eau à haute température et à grandes vitesses (5–10 m/s). Dans ces conditions, l'étude de la corrosion dynamique des gaines par l'eau déminéralisée nécessite la construction de circuits spéciaux reproduisant les conditions de travail des gaines dans un réacteur.

On réalise en conséquence des circuits traduisant le plus fidèlement possible les phénomènes de corrosion, en fonction des caractéristiques thermiques, chimiques, hydrauliques. Des appareils du type "thermosiphons" permettent d'opérer avec de l'eau jusqu'à 350°C et à des vitesses de 8 à 10 m/s à l'intérieur de tubes de "Venturi" où se trouvent placés les échantillons. D'autres cellules plus complexes reproduisent également à travers des gaines des flux thermiques élevés de l'ordre de 100 à 150 W/cm^2. Pour l'étude de l'action du rayonnement certains circuits expérimentaux peuvent être montés à l'intérieur d'un réacteur.

Dans les essais de corrosion dynamique, des échangeurs d'ions permettent de maintenir l'eau à une résistivité élevée de l'ordre de 1 à 2 MΩ $\times$ cm. Nos principaux appareillages pour essais de corrosion par l'eau à température élevée sont représentés sur les Fig. 12(a), 12(b) et 12(c).

ETUDE DE LA CORROSION DE DIVERS MATERIAUX NUCLEAIRES

1. *Uranium et alliages d'uranium*

L'uranium est un métal très réactif, sensible aux réactions anodiques (formation de UO_2) et aux réactions cathodiques (formation de UH_3).

Dans l'eau distillée saturée d'air et pour des températures inférieures à 70°C, on observe une période initiale durant laquelle la corrosion est faible, suivie d'une période caractérisée par une vitesse de corrosion beaucoup plus importante. Au moment où le film protecteur d'oxyde se rompt, la vitesse s'accélère, il apparaît des surfaces sur lesquelles les produits de corrosion sont poreux. Ces zones s'élargissent ensuite pour couvrir l'ensemble de l'échantillon. La cinétique de corrosion est alors sensiblement la même que celle observée dans l'eau saturée d'hydrogène. Par élévation de la température, la période de protection initiale diminue de plus en plus, et à partir de 80°C elle n'existe pratiquement plus (Fig. 13).

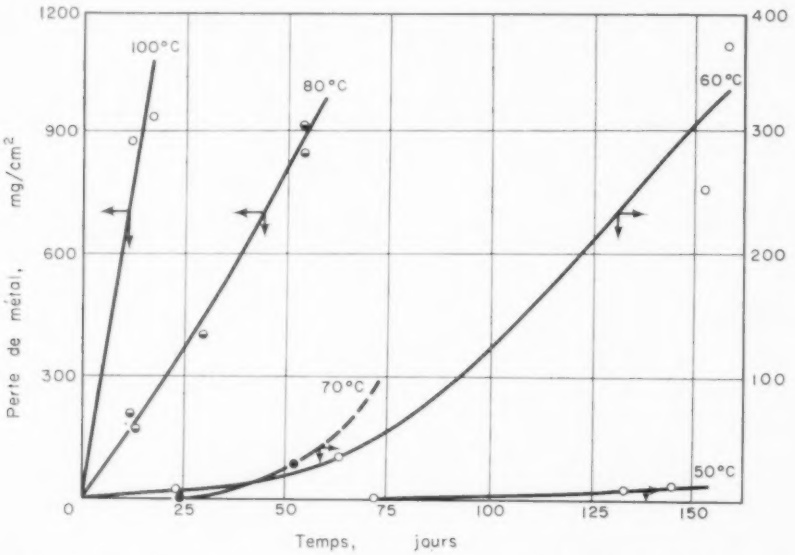

FIG. 13. Corrosion de l'uranium dans l'eau déminéralisée et aérée (McWhirter et Draley).

On pense que les résultats précédents sont dûs à la migration d'ions hydrogène à travers le film d'oxyde, ces ions forment de l'hydrure à l'interface métal–oxyde provoquant la décohésion du film d'oxyde.

Dans l'eau saturée d'hydrogène ou dégazée, l'intensité de l'attaque est une fonction *linéaire* du temps. La Fig. 14 représente les vitesses d'attaque en fonction de la température. On observe une relation exponentielle entre la vitesse de corrosion et l'inverse de la température absolue.

Les alliages d'uranium

En raison de sa mauvaise résistance à la corrosion, il est nécessaire de gainer l'uranium par un métal dont le comportement soit satisfaisant dans les conditions

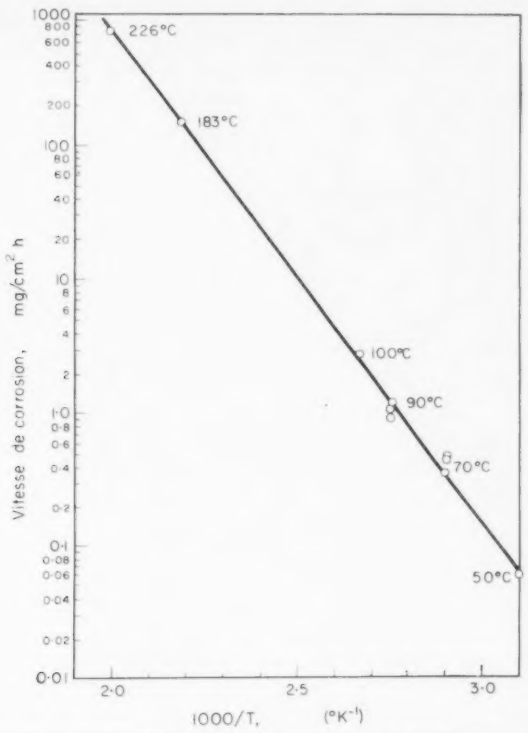

FIG. 14. Vitesse de corrosion de l'uranium dans l'eau saturée d'hydrogène (McWhirter et Draley)

d'utilisation. On doit cependant toujours redouter une rupture de gaine, et dans ce cas l'uranium se trouverait attaqué très rapidement, en particulier dans l'eau à haute température (voir Fig. 14), il en résulterait une contamination importante du circuit et l'arrêt du réacteur. On a donc essayé de mettre au point des alliages d'uranium permettant de stabiliser le film protecteur d'oxyde même dans l'eau désoxygénée et à 350°C. La Fig. 15 montre, en fonction de la température, les vitesses de corrosion par l'eau distillée d'un certain nombre d'alliages d'uranium parmi les plus intéressants.

Il paraît utile de donner quelques précisions sur le mécanisme de corrosion de l'uranium par l'eau et d'essayer de montrer le rôle de certains éléments d'alliage. Nous venons de voir que l'uranium exposé à l'action de l'eau saturée d'oxygène forme initialement un film protecteur (températures inférieures à 70°C). Après un certain temps d'exposition, le film se rompt localement et aux points de rupture le produit de corrosion est un UO_2 à grains très fins. Ces points de rupture représentent les endroits où l'hydrogène produit dans la réaction de corrosion a réagi au-dessous du film protecteur pour former de l'hydrure. L'hydrure empêche évidemment la liaison entre le film d'oxyde et le métal.

Similairement à la corrosion de l'aluminium et de ses alliages par l'eau à haute température, il convient de limiter l'accès de l'hydrogène au métal. Comment prévenir l'accès de l'hydrogène à la surface du métal? On peut agir dans deux directions:

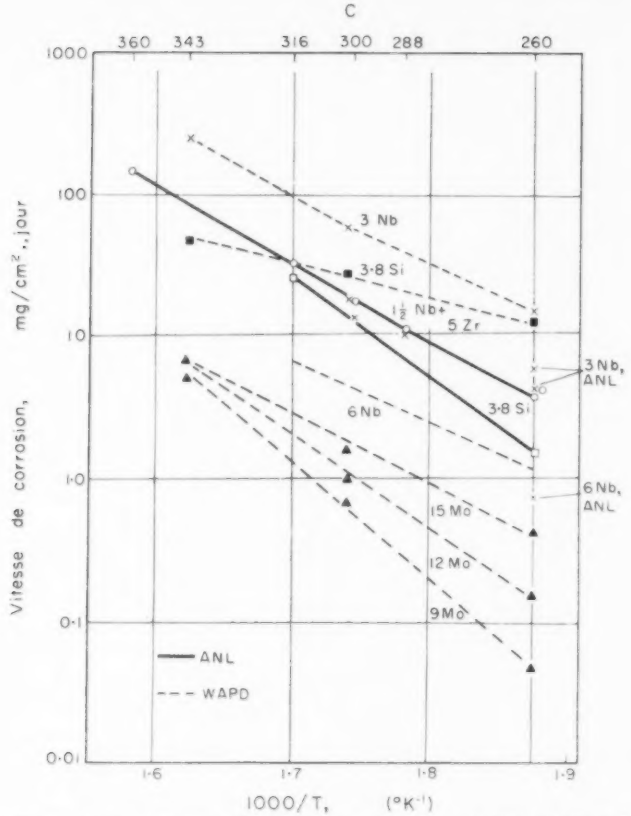

FIG. 15. Corrosion des alliages à base d'uranium par l'eau distillée (d'après Foote).

en formant des surfaces "getter" d'hydrogène,

en formant des microcathodes à faible surtension d'hydrogène.

Le zirconium et le niobium agiraient comme "getter", tandis que le nickel sous forme d'élément d'alliage ou par dépôt sur le métal à partir de la solution (addition de Ni^{+2} à l'eau) permettrait la formation de micro-cathodes. L'incorporation de zirconium peut également rendre plus difficile la migration d'hydrogène à travers le film, cette assertion semble également logique puisqu'on a montré que la présence de zirconium dans l'oxyde formé sur ces alliages réduit les dimensions du réseau de UO_2.

Dans le cas où l'on dispose d'uranium très enrichi en isotope 235, certains alliages peuvent se révéler particulièrement intéressants. Ainsi, pour les combustibles des piles piscines à basse température on utilise fréquemment des alliages *aluminium–uranium* à teneur en uranium de l'ordre de 20 à 50 pour cent. Ces alliages se présentent généralement comme une dispersion du composé UAl_4 dans une matrice d'aluminium. Les essais de corrosion que nous avons effectués sur certains de ces alliages à 80°C dans l'eau déminéralisée ont montré que l'attaque était relativement lente. En cas de rupture de gaine, le phénomène n'aurait donc pas la brutalité habituelle observée avec l'uranium métal. Pour les réacteurs de puissance refroidis par l'eau, on peut employer

avec satisfaction des alliages *zirconium–uranium* de 3 à 8 pour cent d'uranium.

Influence de l'irradiation. Pour de nombreux alliages d'uranium dont la résistance à la corrosion est satisfaisante, l'irradiation conduit malheureusement à des résultats catastrophiques. Le Tableau 1 donné, à titre d'exemple, les vitesses de corrosion "avant" et "après" irradiation relevées sur deux alliages d'uranium dans l'eau à haute température.

TABLEAU 1

Composition de l'alliage	Burn up Atomes (%)	Résistance à la corrosion
U–3% Nb	0	Aucun dégat sérieux après 2000 h à 260°C. Perte de poids: 4,3 mg/cm² jour
(trempé à partir de la phase gamma)	0,1	Désagrégation après 1 h à 260°C
U–5% Zr–1,5% Nb	0	Aucun dégat sérieux après 360 jours à 265°C. Perte de poids: 2,7 mg/cm² jour
(trempé à partir de la phase gamma)	0,04	Dégats très sérieux après 63 jours à 260°C. Perte de poids: 23 mg/cm² jour

2. *Aluminium et alliages d'aluminium*

Dans les réacteurs à l'eau lourde fonctionnant à basse température l'aluminium est le métal de base. L'aluminium présente en effet un certain nombre d'avantages: faible section de capture neutronique, abondance du métal, méthodes de fabrication et d'usinage bien connues et largement développées. Nous avons personnellement utilisé l'aluminium commercial A_5 (Al = 99,5 pour cent) comme métal de contact avec l'eau lourde dans les réacteurs EL_1–EL_2–EL_3, son comportement s'est révélé satisfaisant.[2] Toutefois, l'emploi de l'aluminium pour le gainage ne peut être qu'assez limité, en effet l'aluminium s'allie à l'uranium au-dessus de 175°C.

Nous donnerons en premier lieu quelques détails sur la corrosion de l'aluminium en milieu aqueux *au-dessous de 100°C*. La bonne tenue de l'aluminium dépend de la formation et du maintien à sa surface d'un film d'alumine. La protection peut disparaître pour deux raisons:

solubilité du film dans le milieu utilisé donnant lieu à une corrosion générale,
ruptures locales du film conduisant à une corrosion par piqûres.

La solubilité du film est liée à une question de pH, l'alumine se présente en effet comme un corps amphotère soluble à la fois dans les acides et dans les bases. Pour un comportement satisfaisant de l'aluminium il est en conséquence nécessaire de maintenir le pH entre 5 et 7.

Les ruptures locales du film peuvent provenir d'une polarisation anodique de l'aluminium due part exemple:

à la jonction avec un conducteur noble vis à vis de l'aluminium, tel que: cuivre, argent, laiton, mercure, graphite, acier,
à des métaux redésposés électrochimiquement à partir de la solution (cuivre, argent, mercure),
à une réaction d'oxydoréduction liée aux espèces moléculaires ou ioniques présentes dans l'eau, par exemple réduction de l'oxygène.

Les chlorures et les fluorures réduisent le potentiel "critique" de rupture du film protecteur, ils peuvent donc également conduire à une corrosion par piqûres. La teneur en ions Cl^- doit dans l'eau d'un réacteur être maintenue au-dessous d'une partie par million.

Dans certaines circonstances, la juxtaposition d'échantillons d'aluminium est susceptible de provoquer une corrosion par effet de "recoin" même dans l'eau de haute pureté, mais cette forme d'attaque peut devenir très grave si l'aluminium se trouve couplé à un métal cathodique tel que l'acier inoxydable.

Lorsque l'isolement électrique entre l'aluminium et l'acier inoxydable s'avère impossible, on peut réaliser la jonction par des joints en alliage d'aluminium à 1 pour cent de zinc, cet alliage effectuant une protection cathodique de l'aluminium. Cette forme de protection ne peut être, toutefois, employée que dans les zones facilement *accessibles*, on se trouve en effet dans l'obligation de procéder périodiquement au remplacement des joints. Certains modèles de brides permettent actuellement d'éviter en pratique l'effet de recoin.

Nous signalerons l'influence extrêmement néfaste des ions cuivre en solution. Des quantités de cuivre aussi faibles qu'un dixième de partie par million peuvent déjà provoquer des piqûres. On proscrira donc, sur le circuit d'eau tous les matériaux cuivreux.

Contrairement à ce qu'on pourrait penser, l'aluminium très pur A_9 (Al = 99,99 pour cent) présente déjà dans certaines conditions des signes de faiblesse dans l'eau à 90°C. En effet, l'examen d'échantillons A_5 et A_9 recuits préalablement à 350°C durant 1 hr et traités 60 jours dans l'eau déminéralisée non désaérée montre une différenciation complète des deux métaux (Fig. 16).

L'aluminium A_5 est exempt de *pénétration intergranulaire* et présente un bon comportement général; l'aluminium A_9, par contre, donne lieu à une pénétration intense et capable de cheminer en profondeur. Remarquez la zone pointillée formée de vésicules séparées par des tronçons inaltérés et la poche importante de produits de corrosion terminant la pénétration (Fig. 17).

Si l'on continue à augmenter la température, la différenciation des deux métaux précédents ne fait que s'accentuer[3] ainsi, par immersion dans l'eau déminéralisée portée à 210°C, on obtient au bout de 15 hr les résultats représentés par la Fig. 18.

L'aluminium A_5 est encore relativement satisfaisant, par contre l'échantillon A_9 très fortement corrodé présente par rapport à l'échantillon initial *une augmentation de surface de plus de 70 pour cent*. L'examen micrographique de la tranche montre dans le cas d'aluminium A_9 une corrosion de type intergranulaire extrêmement sévère.

Dans l'eau au-dessus de 200°C, après une période de corrosion apparemment "normale", on observe sur l'aluminium commercial l'apparition de "pustules". Au cours du temps ces pustules deviennent plus larges et on constate un type d'attaque susceptible de conduire à une véritable désagrégation du métal. Plus la température est élevée, plus ce type d'attaque apparaît rapidement. Draley a le premier donné l'explication suivante à ce phénomène: une partie des atomes d'hydrogène produits dans la réaction de corrosion diffuse dans le métal.

La formation d'hydrogène moléculaire dans les "cavités" du métal provoque des poches de pression. Des pustules prennent naissance à partir de ces poches de pression, leur éclatement permet à l'eau de pénétrer à l'intérieur, il en résulte à nouveau la

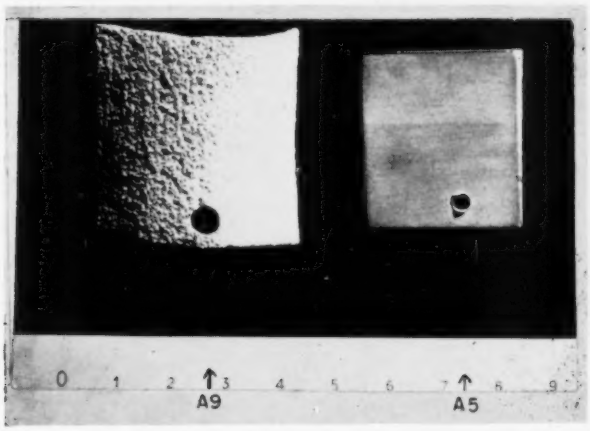

FIG. 18. Tenue respective d'échantillons d'aluminium A_9 et A_5, recuits à 350°C et traités 15 h à 210°C dans l'eau déminéralisée (pH initial 5,5). Les deux échantillons avaient initialement les mêmes dimensions: (30 × 30 × 1 mm). (Remarquer l'expansion importante de l'échantillon A_9.)

FIG. 19. Influence du degré de division et de dispersion du composé intermétallique Al_9NiFe sur la tenue à la corrosion d'un alliage aluminium–nickel–fer dans l'eau à haute température (350°C, 15 h).

FIG. 20. Aspect du phénomène de "breakaway". (× 3)

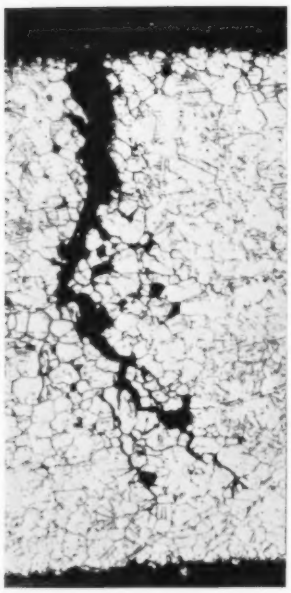

FIG 26. Fissuration sous contrainte d'un alliage Inconel.

formation d'hydrogène et le phénomène de corrosion s'entretient de lui-même.

Pour éviter le type d'attaque par "pustules" précédemment décrit on peut:

(a) rendre le métal imperméable à l'hydrogène,

(b) polariser anodiquement le métal,

(c) former à la surface du métal des microcathodes à faible surtension d'hydrogène.

La première méthode est évidemment pratiquement inapplicable. La protection anodique est efficace, on se rapportera aux résultats donnés dans les généralités sur le couplage aluminium–acier inoxydable dans l'eau à haute température. Une expérience est également très démonstrative: en faisant passer un courant de 1 à 2 mA/cm² entre deux échantillons d'aluminium commercial 2S immergés partiellement dans l'eau à 250°C on observe une corrosion importante en phase vapeur dans laquelle il ne passe que peu on pas de courant par contre, en phase liquide *l'anode* est efficacement protégée. Pour créer des microcathodes, on peut ajouter à la solution des cations réductibles (Ni^{2-} par exemple) qui se déposent sur les zones cathodiques de l'échantillon en formant des dendrites et favorisent ainsi le dégagement de l'hydrogène. Pour une utilisation pratique il est naturellement préférable de former des alliages renfermant des composés intermétalliques à faible surtension d'hydrogène, d'où l'intérêt des alliages: aluminium–fer, aluminium–nickel, aluminium–fer–nickel.

Nos premières recherches nous ont aussi orientés rapidement vers le domaine des alliages contenant soit du fer, soit du nickel, soit ces deux éléments simultanément, cette dernière classe d'alliages paraissant d'ailleurs la plus intéressante. Nous avons dégagé en particulier comme facteurs importants:

la présence du composé intermétallique Al_9 NiFe,

son degré de division et de dispersion.

A ce sujet la Fig. 19 est particulièrement démonstrative, elle représent après corrosion par l'eau à 350°C deux échantillons d'alliages aluminium–nickel–fer ayant la même composition centésimale. L'échantillon très fortement attaqué correspond précisément à une répartition "grossière" du composé Al_9NiFe.

Sur la corrosion des alliages d'aluminium par l'eau à haute température, on pourra consulter notamment les articles définis par les références 3–13.

Effet de l'irradiation

Hittman et Kuhl[22] ont exposé aux radiations gamma (dose 300,000 r/hr–42 jours) des échantillons d'aluminium dans l'eau de ville et dans l'eau distillée à température ambiante. Les échantillons irradiés présentaient des gains de poids plus faibles que ceux des échantillons non irradiés. Les piqûres sur les échantillons irradiés étaient d'autre part moins profondes que celles apparues sur les échantillons témoins. Les auteurs pensent que la différence de comportement provient du caractère plus oxydant de la solution irradiée par suite de la formation d'eau oxygénée et de radicaux libres oxydants. Nous avons, nous-mêmes, soumis des échantillons d'aluminium A_5 à l'action d'un flux de neutrons rapides afin d'observer les modifications éventuelles produites sur les caractéristiques de corrosion. Les échantillons se trouvaient immergés dans de l'eau déminéralisée ($t = 50°$), les flux intégrés étaient de l'ordre de 10^{19} n.v.t. La différenciation se révélait très faible entre les échantillons irradiés et les échantillons témoins non soumis au rayonnement, toutefois, on pouvait noter une tendance à la corrosion plus faible sur les échantillons irradiés.

3. *Zirconium et alliages de zirconium*

Le zirconium et les alliages à forte teneur en zirconium trouvent en particulier leur application dans les réacteurs de puissance refroidis par l'eau à haute température. L'attaque du zirconium non allié par l'eau à haute température peut se diviser en deux phases. La première phase est caractérisée par la formation d'un film adhérent d'oxyde de couleur noire ou laissant apparaître des teintes d'interférences. La cinétique de corrosion obéit à la formule empirique

$$\Delta m = kt^n$$

Δm représente l'augmentation de poids par unité de surface,
t le temps,
k et n des constantes à température donnée.

Durant cette première période n est voisin de 1/3 montrant une action protectrice efficace des produits de corrosion. Le facteur n croît faiblement avec la température:

à 287° $n = 0{,}27$
à 316° $n = 0{,}30$
à 360° $n = 0{,}33$

Après un temps, très variable d'ailleurs suivant divers facteurs, une forme de corrosion nouvelle et beaucoup plus rapide prend naissance. Les produits de corrosion deviennent blanchâtres et ne sont plus adhérents, on dit qu'on a atteint le "breakaway" dont l'équivalent francais le plus fidèle semble être le terme "desquamation".

La Fig. 20 représente l'aspect d'un échantillon de zirconium ayant subi le breakaway.

Le breakaway intervient quand le film d'oxyde correspond à une augmentation de poids $\Delta m \sim 40$ mg/dm². Il marque la fin de l'utilisation pratique du métal.

La relation $\Delta m = kt^n$ est fréquemment utilisée sous la forme logarithmique: $\log \Delta m = \log k + n \log t$, la Fig. 21 traduit sous cette forme la corrosion du zirconium non allié dans l'eau à haute température.

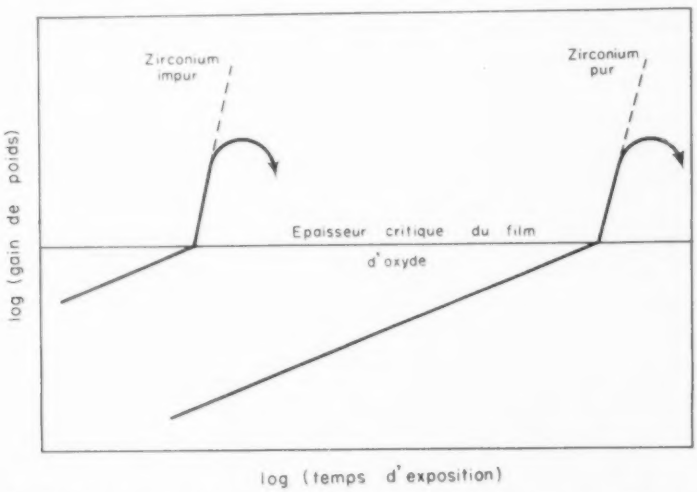

FIG. 21. Représentation schématique de la corrosion du zirconium non allié dans l'eau à température élevée.

Influence de la température

Pour un métal donné, la température influe considérablement sur l'apparition du breakaway. Par exemple, pour le zirconium très pur immergé dans l'eau à 287°C, le breakaway n'est pas encore atteint au bout de 200 jours, tandis qu'à 360°C il apparaît déjà sur certains échantillons au bout d'une semaine.

L'effet de la température sur la corrosion du zirconium a été étudié particulièrement dans des essais statiques (eau déminéralisée et dégazée–vapeur), à des températures comprises entre 260°C et 400°C. Les résultats obtenus par Lustman sont représentés sur la Fig. 22.

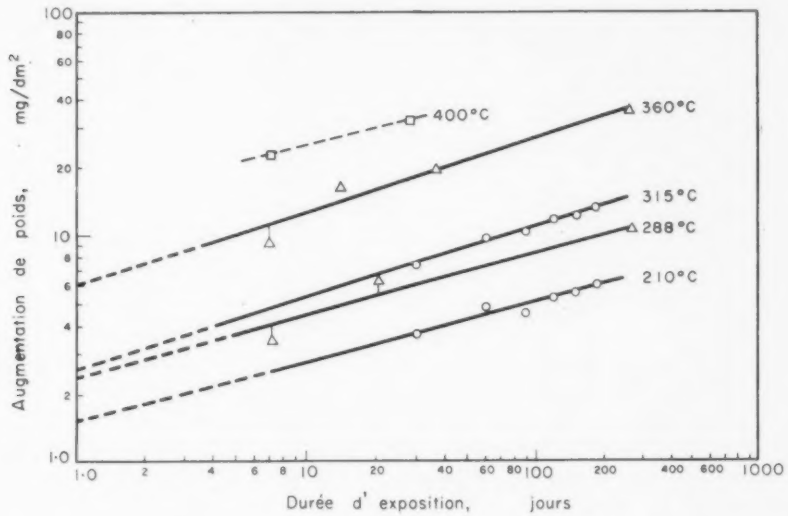

FIG. 22. Influence de la température sur la corrosion du zirconium par l'eau et la vapeur (Lustman et Kerze).

Influence des impuretés

Certaines impuretés dans le métal agissent fortement sur l'apparition du breakaway, l'effet le plus marquant est celui de *l'azote* dont l'action commence à se faire sentir pour des teneurs très faibles de l'ordre de 0,004 pour cent. Parmi les autres impuretés les plus dangereuses, on peut citer *le titane*, *l'aluminium*, *le plomb*, *le carbone*, pour lesquelles les concentrations limites sont fixées respectivement à 0,008%; 0,01%; 0,01%; 0,02%. Le calcium, le magnésium, le chlore, sont également néfastes, leurs limites de tolérance étant cependant plus grandes que pour les impuretés précitées.

Au sujet de l'influence du silicium, la communication soviétique[14] à la deuxième Conférence de Genève signale un désaccord avec les résultats américains, les auteurs affirment en effet que le zirconium avec de faibles additions de silicium possède une bonne résistance à la corrosion par l'eau jusqu'à 370°C, même si le métal est insuffisamment pauvre en azote. Les additions de silicium les plus favorables se situeraient entre 0,10 et 0,15 pour cent en poids.

La corrosion du zirconium est généralement beaucoup moins affectée par les impuretés de l'eau que par celle du métal.

Autres effets

L'état de surface joue un très grand rôle dans la résistance du zirconium à la corrosion: un usinage normal produit une couche de métal perturbé sur une épaisseur de 40 à 50μ, il est donc indispensable d'éliminer cette couche par une attaque chimique avant les essais de corrosion. On utilise à cet effet des bains fluonitriques.

Les traitements thermiques ne semblent pas affecter la résistance à la corrosion du zirconium à condition, toutefois, que ce dernier soit de pureté suffisante.

Le zirconium ne serait pas sensible à la corrosion par couplage ou par effet de crevasse.

D'après la littérature américaine, la présence d'hydrogène ou d'oxygène dissous jusqu'à quelques 100 ml par kilogramme d'eau n'affecte pas sensiblement la tenue à la corrosion.

Influence de l'irradiation

Des échantillons de zirconium ont été soumis à des essais à l'intérieur d'un circuit de pile dans les conditions suivantes:

Eau à 280°C, vitesse de circulation maximum 3 m/s, flux intégré de neutrons thermiques: 10^{18} n.v.t. Selon les auteurs américains, l'irradiation ne semblerait pas avoir affecté la résistance du métal à la corrosion.

Les Zircaloys

Des alliages de zirconium ont été mis au point dans le but d'éliminer ou au moins de reculer le breakaway, tout en utilisant d'un point de vue pratique le zirconium Kroll au lieu du zirconium très pur van Arkel. L'addition d'étain au zirconium s'est révélée très intéressante, elle neutralise l'effet néfaste de l'azote et même, dans une certaine mesure, celui du carbone. Actuellement le plus utilisé parmi ces alliages est le Zircaloy-2 (1,5% Sn; 0,12% Fe; 0,10% Cr; 0,05% Ni) avec moins de 60 p.p.m. d'azote, cet alliage est très employé comme matériau de gaine.

Propriétés de résistance à la corrosion du Zircaloy-2

Contrairement au zirconium non allié,

(1) Le film d'oxyde reste encore adhérent un temps relativement long après l'apparition de la 2ème période.

Le point de changement de cinétique sera pour ces alliages désigné par "temps de transition".

(2) Le "temps de transition" est reproductible.

(3) L'effet d'un grand nombre d'impuretés néfastes pour le zirconium se trouve considérablement atténué.

Les autres propriétés de comportement à la corrosion du zirconium se conservent.

Nous avons représenté sur la Fig. 23 les différentes courbes de cinétique relevées sur des tôles en Zircaloy-2 dans l'eau et la vapeur à différentes températures. Dans la vapeur à 400°C (105 kg/cm^2), nous obtenons 3 périodes de corrosion.[23]

Influence du traitement thermique

D'après Thomas et Forscher[15] le Zircaloy-2 recuit à 900°C ou 1000°C conduit dans l'eau à 360°C ou la vapeur à 400°C à une cinétique de corrosion légèrement plus

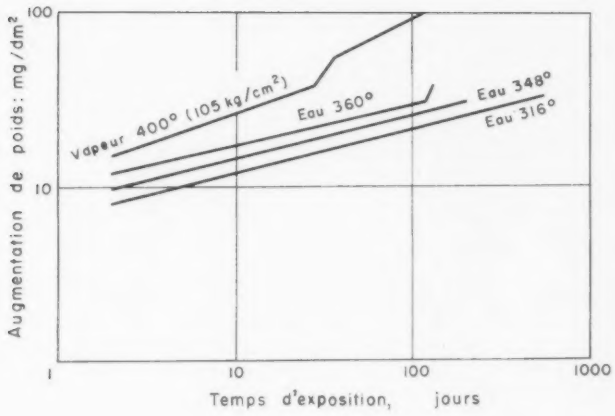

FIG 23.

élevée que celle obtenue sur le même alliage recuit à plus basse température. Les propriétés de résistance à la corrosion du Zircaloy ne sembleraient pas modifiées par la vitesse de refroidissement.

Toutefois, Goodwin[24], après avoir également étudié l'effet des traitements thermiques, montre que le mode de refroidissement a une influence significative mais faible sur la résistance à la corrosion du Zircaloy-2 (vapeur à 400°C, 105 kg/cm²), le refroidissement lent dans le four produisant des vitesses de corrosion légèrement plus grandes que celles relevées sur des échantillons ayant subi un refroidissement à l'air.

Des résultats très intéressants sur la corrosion du Zircaloy-2 par la vapeur surchauffée ont été décrits à la 2ème Conférence de Genève dans la communication canadienne (15/P/194). Dans la vapeur surchauffée au-dessus de 450°C (pression 100 atm) Krenz *et al.*[16] ont trouvé un comportement très différent du Zircaloy-2 suivant les traitements thermiques préalablement subis par cet alliage. Pour un alliage à l'état brut de transformation ou recuit en *phase* α une attaque accélérée intervient

au-dessus de 450°C, il en résulte une destruction rapide de l'échantillon: ce phénomène porte le nom "d'hydriding attack", il est en effet toujours caractérisé par la formation d'une quantité importante d'hydrure. Le Zircaloy traité thermiquement en *phase* β et placé dans les mêmes conditions se comporte au contraire de façon relativement satisfaisante.

Les quelques ruptures de gaines apparues à Chalk River au cours d'essais dynamiques (combustible, UO_2; gaine, Zircaloy-2; eau de refroidissement, $t = 260$°C; vitesse, 6 m/s; flux thermique, 100–200 W/cm²) se caractérisaient par une corrosion importante à l'interface combustible–gaine, la gaine se révélant fortement hydrurée au voisinage du défaut. On observait les concentrations d'hydrure à la surface externe de la gaine, la fragilité du métal hydruré conduisant fréquemment à l'apparition de nombreuses fissures. Aucune réaction avec l'UO_2 n'a été mise en évidence. Le type d'attaque précédemment décrit est dû vraisemblablement à l'interruption du flux thermique à travers la gaine d'où élévation de la température, "l'hydriding attack" devenant possible.

Influence de l'irradiation

Les travaux de Galonian[25] effectués sur le Zircaloy-2 dans les conditions suivantes: (eau 316°C; pH neutre ou 8–9,5; flux intégré de neutrons thermiques 10^{21}) montrent que l'irradiation n'a pas produit de modifications sensibles sur la corrosion du Zircaloy-2. L'étude portait uniquement sur la période de "prétransition".

Une attaque localisée et destructive a été signalée sur le Zircaloy-2 par Alcock et Cox[26] en phase vapeur à 300°C sous irradiation dans BEPO. Malgré la similitude apparente avec "l'hydriding attack" du Zircaloy-2, phénomène observé à Chalk River et dont nous avons parlé précédemment, les examens micrographiques n'ont pas permis de mettre en évidence une accumulation anormale d'hydrure dans le métal.

Autres effets

Similairement au zirconium *l'état de surface* du Zircaloy-2 joue un très grand rôle dans la résistance à la corrosion. Après les opérations de transformation il est nécessaire également d'éliminer, par décapage chimique dans des bains fluonitriques, une couche de métal perturbé de l'ordre de 40 à 50μ. Le rinçage doit être particulièrement soigné, les moindres traces d'ions fluor provoquant des corrosions graves.

Nous avons récemment montré que *sur le plan de l'oxydation du métal*, le Zircaloy-2 pouvait être utilisé très longtemps après la "transition" dans l'eau à 350°C, ceci même en présence de vitesses de circulation d'eau élevées (~ 8 m/s). Il convient, cependant de signaler que *l'absorption* par le métal d'une quantité importante de l'hydrogène provenant de la réaction de corrosion peut amener, en fragilisant l'alliage, une limitation dans l'emploi du Zircaloy-2. Le nickel que contient l'alliage se révélant responsable dans une large mesure de cette absorption, on tend actuellement à modifier la formule du Zircaloy-2en supprimant le nickel et en augmentant éventuellement le fer et le chrome (Zircaloy-4).

Nous avons également étudié sur des gaines en Zircaloy-2 l'influence du *passage d'un flux thermique* sur la cinétique et la structure de corrosion. Les conditions expérimentales étaient les suivantes:

température de l'eau à l'entrée sur la gaine 340°C

température de l'eau à la sortie	350°C
résistivité de l'eau	1 à 2 MΩ × cm
vitesse de l'eau sur la gaine	5,5 m/s
flux à travers la gaine	100 W/cm²

Les essais ont duré 1100 h. Le métal s'est révélé bien protégé et ne subit qu'une attaque régulière, à l'exclusion de toute pénétration en profondeur. Les couches d'oxyde sont très adhérentes, elles sont d'autant plus épaisses que le flux est plus important.

Autres alliages de zirconium

A la 2ème Conférence de Genève, le travail d'ensemble soviétique[14] fait état de nouveaux alliages désignés sous le nom d' "ozhennite" et susceptibles d'une bonne résistance à la corrosion dans l'eau et la vapeur de 300° à 400°C. Les "ozhennite" comprennent un groupe d'alliages de zirconium avec étain, nickel, fer, niobium, la teneur totale des additions restant comprise entre 0,5 et 1,5 pour cent.

Les vitesses de corrosion du Zircaloy-3 A (0,25 pour cent Sn; 0,25 pour cent Fe) sont comparables à celles du Zircaloy-2. Toutefois, le Zircaloy-3 A n'a guère été utilisé en raison des taches d'oxyde blanchâtre qui apparaîtraient durant son expositions dans l'eau à haute température.

Le Zircaloy-2 dans les réacteurs homogènes

Les réacteurs homogènes emploient un mélange "homogène" du modérateur et des sels de matières fissiles. La plus utilisée parmi les solutions est une solution de UO_2SO_4 en milieu acide, la température d'utilisation étant de l'ordre de 250°–300°C. Le mécanisme de corrosion des alliages de zirconium exposés à des solutions aqueuses acides et oxydantes serait une réaction extrêmement rapide du métal avec l'eau ou l'agent oxydant pour former un revêtement protecteur d'oxyde. Ce film particulièrement adhérent n'est pas affecté même pour des vitesses de circulation très grandes du fluide (15–20 m/s), seuls les ions fluorures font perdre au métal sa résistance à la corrosion.

(1) *Essais "hors pile"*. Les expériences ont montré que dans les solutions de matières fissiles on n'observe pas de différence essentielle entre le comportement du Zircaloy-2 et celui du zirconium très pur van Arkel. Toutefois, le Zircaloy-2 a toujours été utilisé dans les réacteurs homogènes en raison de ses meilleures qualités mécaniques.

Le Zircaloy-2 est pratiquement inattaquable par les solutions de sulfate d'uranyle. Apres 100 ou 200 h d'exposition un film de couleur noire se forme, l'augmentation de poids de l'échantillon devenant ensuite négligeable.

On n'observe pour le Zircaloy ou le zirconium pur, ni attaque localisée ni corrosion par effet de crevasse, ni action galvanique par couplage, ni corrosion sous contrainte (en présence d'ions Cl^-). Les fluorures à l'état d'impuretés conduisent par contre à une corrosion par piqûres et tout particulèrement à une attaque par effet de crevasse.

(2) *Essais sous rayonnement*. Le zirconium et le Zircaloy-2 exposés en milieu de sulfate d'uranyle à l'action des produits de fission subissent une attaque corrosive importante. La vitesse de corrosion croît avec la puissance spécifique et la température, elle décroît avec la concentration en uranium, l'acidité et l'addition de sulfate de lithium.

Les vitesses de corrosion obtenues dans des essais statiques et dynamiques peuvent être reliées à la puissance spécifique par une équation de la forme:

$$v = AP\,[1 - \exp(-B/v^{1,5})] \qquad \text{(équation de Jenks)}^{17}$$

v représentant la vitesse de corrosion,
P la puissance spécifique,
A et B des constantes dépendant des conditions expérimentales.

Diverses questions relatives à l'accroissement de la corrosion du zirconium ou du Zircaloy sous l'action des fragments de fission ont été développées au cours de la 2ème Conférence de Genève. Dans l'une de ces communications,[18] travail de synthèse sur les progrès récents dans la métallurgie du zirconium et du titane, les auteurs précisent que des alliages de zirconium avec le niobium, le palladium ou le platine, placés dans des solutions de sulfate d'uranyle présentent sous l'action des fragments de fission une cinétique de corrosion plus faible que celle obtenue pour le zirconium et le Zircaloy exposés aux mêmes conditions. L'alliage zirconium–niobium a 15 pour cent de niobium serait particulièrement intéressant. Pour des raisons d'ordre métallurgique on réalise dans cet alliage une addition de 2 pour cent de molybdène ou 2 pour cent de palladium.

Le titane et le niobium se rélèvent beaucoup moins sensibles que le zirconium ou le Zircaloy à l'effet des fragments de fission, on a en conséquence préconisé en particulier[19]:

(a) le revêtement du coeur en Zircaloy par du titane, mais en raison de la forte absorption du titane on ne peut tolérer que des épaisseurs très faibles (0,25 mm environ). On a même envisagé de séparer l'isotope Ti^{50} (abondance 5 pour cent dans le titane naturel, coefficient d'absorption 40 fois plus faible que le titane naturel), il serait alors possible de construire le coeur entier en titane.

(b) l'emploi du niobium qui a une plus faible section de capture que le titane. On pourrait, en conséquence, l'utiliser pour le revêtement interne du coeur en Zircaloy à des épaisseurs de l'ordre de 1,5 mm, sa résistance à la corrosion sous irradiation serait bien meilleure que celle du Zircaloy. Malheureusement, le film d'oxyde de niobium jouit de propriétés d'adsorption relativement grandes vis-à-vis de l'uranium, d'où instabilité de la solution et accroissement du nombre et de l'énergie des fragments de fission à l'interface métal–oxyde.

Enfin, on doit également signaler que le bombardement du métal par des électrons accélérés dans un Van de Graaf n'a pas d'effet significatif sur la vitesse de corrosion du Zircaloy-2, par contre le bombardement à l'aide de particules lourdes (neutrons rapides, tritons et particules α) produit un effet comparable à celui des fragments de fission, la vitesse de corrosion (milieu UO_2SO_4 t = 250–300°C) se trouvant ainsi accélérée.[20]

4. *Aciers inoxydables*

Les aciers inoxydables austénitiques constituent en général une partie très importante d'un réacteur refroidi par l'eau ou d'un réacteur homogène. Les aciers austénitiques sont les plus résistants à la corrosion par l'eau à haute température, leurs propriétés sont satisfaisantes jusqu'à 370°C. Le Tableau 2 fournit, à titre indicatif, les vitesses de corrosion de divers aciers inoxydables austénitiques.

En raison de leur section de capture neutronique élevée, les aciers inoxydables ne

TABLEAU 2*

Nuances	Composition					Milieu: eau					
	C (%)	Cr (%)	Ni (%)	Mn (%)	%	Température (degrès C)	Oxygène (ml/l.)	Hydrogène (ml/l.)	pH†	Vitesse maximum de circulation de l'eau (m/s)	Vitesse de corrosion (mg/dm². mois)
304	0,08	18–20	8–12	2,0		260	1–5		7	9	5
						315		200	7	9	5–15
						315		200	11	9	5
304 L	0,03	18–20	8–12	2,0		260			10	3	5
						260		25–50	7	9	5
316	0,10	16–18	10–14	2,0	2–3 Mo	260	0–5		7	9	5
347	0,08	17–19	9–13	2,0	0,8 Nb	260			7	9	10
						315		100	7	9	5–15
						315		200	7	9	5
						315		200	11	9	5

*Tableau extrait de *Corrosion and Wear Handbook for Water-Cooled Reactors* édité par D. J. De Paul (TID—7006—Mars 1957).
†Les pH alcalins sont obtenus par additions de LiOH.

peuvent être utilisés comme matériaux de gainage que sous des épaisseurs très faibles de l'ordre du dixième de millimètre. Il est, d'autre part, impossible de les employer pour gainer des alliages d'uranium par suite de la formation d'eutectiques à bas point de fusion. En général, on réalise un gainage à l'acier inoxydable sur une dispersion d'oxyde d'uranium dans une matrice en acier inoxydable.

L'acier inoxydable le plus utilisé pour la construction des réacteurs américains fut sans aucun doute l'acier 347. Cet acier stabilisé au niobium est pratiquement immunisé contre la corrosion intergranulaire. Dans l'eau très pure à haute température, la précipitation du carbure de chrome aux joints de grains causée par soudure ou traitement thermique n'affecte pas toutefois la résistance à la corrosion des aciers austénitiques. Certains chercheurs américains signalent d'ailleurs que, lors de la construction de PWR, c'est en raison du manque d'informations sur le comportement des aciers non stabilisés dans l'eau à des températures de l'ordre de 300°C qu'ils ont choisi un acier stabilisé. Toujours d'après les mêmes sources, un acier "type 304", donc non stabilisé, aurait très bien pu remplacer le 347.

Au sujet de la corrosion sous contrainte des aciers austénitiques, il semble que cette forme de corrosion dans un réacteur refroidi par l'eau ne présente pas de problème dans le circuit primaire, si ce n'est pour certaines pièces telles que les ressorts trempés; toutefois les questions de corrosion sous contrainte ont été encore insuffisamment explorées. Dans le circuit secondaire le problème est très différent en raison des chlorures que peut contenir le circuit. Les chlorures, nous l'avons vu dans les généralités, peuvent influer considérablement sur la corrosion sous tension.

Nous avons eu récemment l'exemple de fissurations transgranulaires de tubes d'échangeurs de température en acier inoxydable austénitique (18/10 très bas carbone et 18/10 Mo–Ti). Ces tubes fonctionnaient sur des machines pour essais dynamiques de corrosion; ils étaient parcourus intérieurement par de l'eau déminéralisée (résistivité, 1 à 2 MΩ $\times$ cm; température, 350°C; pression, 180 kg/cm^2) et refroidis extérieurement par de l'eau de ville (température maximum, 60°C; teneur en Cl^-, $\sim$ 40–50 mg/l.). Les contraintes pouvaient atteindre les 3/4 de la limite élastique des aciers. Toutes les fissures partaient de la zone externe des tubes.

Une méthode pour éliminer le problème de la corrosion sous contrainte dans le circuit secondaire serait de construire ce dernier en acier ferritique. On sait en effet que les aciers ferritiques sont pratiquement immunisés contre la corrosion sous contrainte. Cependant, si l'acier inoxydable est employé pour le circuit primaire, une transition entre l'acier austénitique du circuit primaire et l'acier ferritique du circuit secondaire introduit des problèmes de fabrication relativement délicats. Les endroits les plus dangereux en phase vapeur sont ceux qui se trouvent alternativement "mouillés" et "séchés", néanmoins, des zones hautement dangereuses peuvent aussi exister au-dessous du niveau d'eau. Les zones les plus vulnérables sont celles des crevasses formées par les joints de tubes et celles sous les dépôts de corrosion où des points chauds peuvent se développer et permettre la vaporisation de l'eau. Il est certes souhaitable de maintenir les chlorures à une concentration très faible, mais on doit toujours craindre des concentrations locales. Il semblerait démontré qu'il est nécessaire d'avoir à la fois chlorures et oxygène pour observer une corrosion sous contrainte des aciers austénitiques dans l'eau ou la vapeur.

Aussi, la meilleure façon d'éviter cette forme de corrosion est de maintenir dans le

circuit secondaire un taux d'oxygène inférieur à 1 p.p.m. (0,5 p.p.m. dans les zones dangereuses), ces concentrations étant valuables pour les teneurs en chlorures habituellement rencontrées dans un équipement pour génération de vapeur.

Les aciers inoxydables dans les réacteurs homogènes

Puisque nous parlons d'aciers inoxydables, il convient d'indiquer leur application dans les réacteurs homogènes.

Les solutions de sulfate d'uranyle doivent être acidifiées pour éviter l'hydrolyse, leur température d'utilisation, nous l'avons vu, est de l'ordre de 250°–300°C. Elles doivent également renfermer un oxydant tel que l'oxygène dissous afin d'éviter la réduction de l'ion "uranyle" et la précipitation de UO_2 qui conduit à la formation d'acide sulfurique et à une sévère corrosion aux températures élevées.[21] On doit aussi tenir compte de ce dernier phénomène dans le cas des recoins où un appauvrissement en oxygène peut se produire, on maintient en conséquence au moins 500 p.p.m. d'oxygène dans la solution de sulfate d'uranyle en circulation. Pour éviter la corrosion sous contrainte la teneur en ions chlorures ne doit pas dépasser 5 p.p.m., pour certains auteurs la limite descend même à 2 p.p.m.

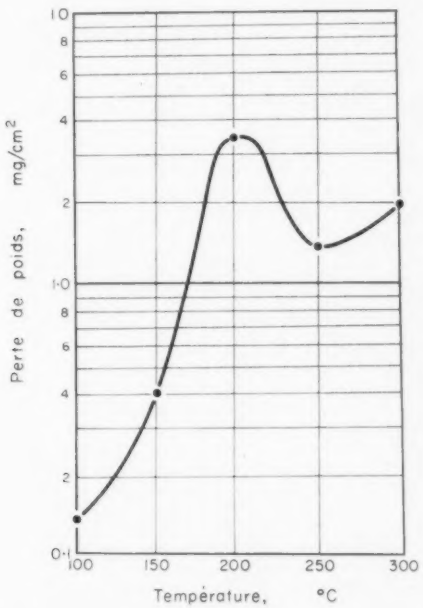

FIG 24.

La Fig. 24 donnée à titre d'exemple montre l'effet de la température sur la corrosion de l'acier 347 dans une solution de sulfate d'uranyle 0,02 M, renfermant de l'acide sulfurique (0,005 M). La forme de la courbe de corrosion avec vitesse maximum de corrosion à 200°C est caractéristique d'un grand nombre d'alliages placés dans les conditions précédemment définies.

La Fig. 25 met en évidence le facteur vitesse de circulation. Au-dessus d'une

certaine "vitesse critique" du fluide le film protecteur n'est plus stable et la vitesse d'attaque s'accélère brutalement.

Essais sous rayonnement

En raison de la complexité des phénomènes, les renseignements à ce sujet sont encore fragmentaires.

Le rayonnement d'un réacteur tendrait à abaisser la "vitesse critique", il apparaîtrait d'autre part que la fission dans la solution au voisinage immédiat des échantillons de corrosion est requise pour une augmentation de la corrosion. Aucune attaque localisée n'a été observée sur l'acier 347.

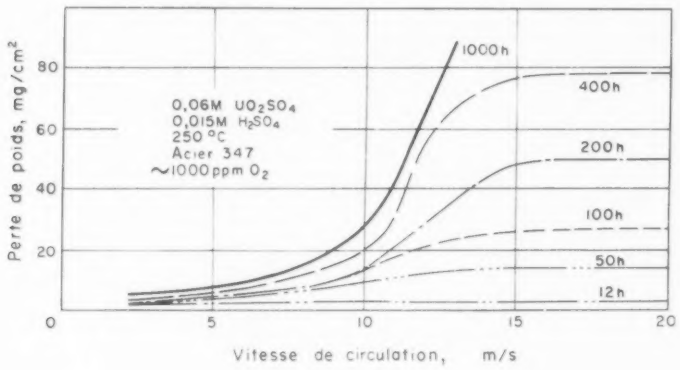

FIG 25.

5. *Les Alliages à teneur élevée en nickel*

Certains alliages, tels que les "Inconel", ont été préconisés pour la fabrication de pièces de réacteurs (échangeurs en particulier) fonctionnant sous contrainte dans l'eau à température élevée. Nous avons toutefois observé des fissurations par corrosion sous contrainte sur différents échantillons d'alliages Inconel dans l'eau à 350°C et en absence d'ions chlorures.[27] Les fissurations se révélaient essentiellement de type *intergranulaire* (Fig. 26).

6. *Béryllium, Magnésium, Titane*

(a) *Béryllium*

Les essais de corrosion effectués sur le béryllium sont fréquemment peu reproductibles. Ce phénomène peut provenir d'une hétérogénéité dans la répartition des impuretés du métal, il est en effet particulièrement difficile d'obtenir un métal de pureté satisfaisante. Des essais effectués aux U.S.A. sur du béryllium fritté ont montré un comportement très différent selon les échantillons, certains se montrent par exemple très résistants à la corrosion par l'eau à 350°C, d'autres exposés aux mêmes conditions se désagrègent complètement. Couplé à l'acier 347 ou à l'aluminium commerciel, le béryllium subit une attaque galvanique. Il est très sensible aux impuretés du milieu, les plus néfastes étant les ions: chlorures, cuivre, fer, sulfate. Des inhibiteurs tels que $NaNO_3$ (3–4 p.p.m.) ou Na_3CrO_4 (5 p.p.m.) réduisent la corrosion.

Il semble qu'il soit nécessaire d'obtenir des échantillons de métal suffisamment purs avant de pouvoir déterminer la véritable résistance du béryllium à la corrosion.

(b) *Magnésium*

La vitesse de corrosion du magnésium de pureté commerciale dans l'eau distillée portée à l'ébullition est environ 18 mg/cm² mois, elle croît très rapidement avec la température. On peut accroître considérablement la résistance du magnésium à la corrosion en opérant à pH compris entre 9 et 11.

Après plusieurs distillations on a pu obtenir du magnésium de grande pureté au moins égale à 99,998 pour cent. Des essais de corrosion effectués sur cette qualité de métal (eau distillée à 50°C et 100°C) montrent que la résistance à la corrosion du magnésium très pur est inférieure à celle du magnésium de pureté commerciale.

Il est évident que le magnésium et les alliages de magnésium sont très sensibles à l'attaque galvanique.

(c) *Titane*

Le titane pur présente une bonne résistance à l'attaque par l'eau jusqu'à 360°C les plus faibles vitesses de corrosion étant observées dans l'eau dégazée. Le titane n'est en outre pas sensible à l'effet de couplage; exposé à l'action de l'eau à haute température, il forme un film d'oxyde de haute résistance électrique réduisant très fortement l'action des couples.

Dans les réacteurs homogènes, en milieu UO_2SO_4 à haute température, la corrosion du titane est accélérée sous l'action des fragments de fission mais nettement moins que celle du Zircaloy-2. On a donc songé, nous l'avons vu précédemment, à effectuer en titane le revêtement du coeur en Zircaloy, toutefois, pour des raisons d'absorption, l'épaisseur devrait se limiter à 0,25 mm. D'autre part, on a découvert récemment une autoignition du titane au contact de vapeurs renfermant une quantité suffisante d'oxygène. Le zirconium donnerait lieu au même phénomène, mais les pressions critiques d'oxygène seraient beaucoup plus élevées que pour le titane.

Nous avons donc repris en particulier dans ces pages les principaux problèmes de corrosion relatifs aux réacteurs refroidis par l'eau et aux réacteurs homogènes. Il aurait été certes intéressant de nous attarder davantage sur certains points uniquement signalés, mais nous serions sortis du cadre fixé. Nous pensons néanmoins avoir montré dans cet exposé obligatoirement fragmentaire la diversité et la complexité des phénomènes de corrosion dans le domaine de l'energie nucléaire.

BIBLIOGRAPHIE

1. M. Berthod, H. Coriou, L. Grall et J. Hure, *2ème conférence de Genève sur l'utilisation pacifique de l'energie atomique. Genève* 1958. Communication 15/P/1169. Volume 7 (France).
2. H. Coriou, la pile EL3. pp. 187–207. Le Commissariat à l'Energie Atomique (Centre d'Etudes Nucléaires de Saclay 1958).
3. H. Coriou, L. Grall, J. Hure, P. Lelong et J. Herenguel, *Rev. Métall.* **53**, 776 (1956).
4. J. E. Draley et W. E. Ruther, *2ème conférence de Genève sur l'utilisation pacifique de l'energie atomique Genève* 1958. Communication 8/P/535. Volume 17 (U.S.A.).
5. J. E. Draley et W. E. Ruther, *Corrosion resistant aluminium alloys above 200°C* (A.N.L. 5430. July 1955).
6. J. E. Draley et W. E. Ruther, *J. Electrochem. Soc.* **20** (1956).

7. H. CORIOU, L. GRALL, A. HAUPTMAN et J. HURE, *Symposium de la métallurgie physique de matériaux nucléaires, Stockholm* 4-5 *Octobre* 1956.
8. H. CORIOU, L. GRALL, J. HURE et A. ROUX, *Rev. Métall.* **55**, 953 (1958). Communication aux Journées d'Automne 1957 de la Société Francaise de Métallurgie.
9. F. M. KRENZ, *Corrosion U.S.A.* **9**, 43 (1957).
10. R. L. DILLON et V. R. TROUTNER, General Electric W.H. 51849, September (1957).
11. H. CORIOU, R. FOURNIER, L. GRALL, J. HERENGUEL, J. HURE et P. LELONG, *2ème conférence de Genève sur l'utilisation pacifique de l'energie atomique. Genève* 1958. Communication 15/P/1271. Volume 5 (France).
12. F. H. KRENZ, G. J. BIEFFER et N. A. GRAHAM, *2ème conférence de Genève sur l'utilisation pacifique de l'energie atomique. Genève* 1958. Communication 15/P/194 2ème partie. Volume 5 (Canada).
13. J. E. DRALEY, C. R. BREDEN, W. E. RUTHER et N. R. GRANT, *2ème Conférence de Genève sur l'utilisation pacifique de l'energie atomique. Genève* 1958. Communication 15/P/714. Volume 5 (U.S.A.).
14. R. S. AMBARTSUMYAN *et al.*, *2ème conférence de Genève sur l'utilisation pacifique de l'energie atomique. Genève* 1958. Communication 15/P/2044. Volume 5 (U.R.S.S.).
15. D. THOMAS et F. FORSCHER, *Conférence de Cleveland* 1955, W.A.P.D.T. 268.
16. F. H. KRENZ, G. F. BIEFFER et N. A. GRAHAM, *2ème conférence de Genève sur l'utilisation pacifique de l'energie atomique. Genève* 1958. Communication 15/P/194. Volume 5 (Canada).
17. G. H. JENKS, ORNL Chemistry Division, Seminar on October 24, 1956.
18. G. M. ADAMSON, J. O. BETTERTON, J. H. FRYE et M. L. PICKLESIMER, *2ème conférence de Genève sur l'utilisation pacifique de l'energie atomique. Genève* 1958. Communication 15/P/1993. Volume 5 (U.S.A.).
19. J. K. DAWSON *et al.*, *2ème conférence de Genève sur l'utilisation pacifique de l'energie atomique. Genève* 1958. Communication 15/P/46. Volume 7 (Royaume Uni).
20. Ensemble des membres du "Projet Réacteur Homogène" au Laboratoire National d'Oak Ridge, *2ème conférence de Genève sur l'utilisation pacifique de l'energie atomique. Genève* 1958. Communication 15/P/2391. Volume 7 (U.S.A.).
21. Ensemble des membres du "Projet Réacteur Homogène" au Laboratoire National d'Oak Ridge, *2ème conférence de Genève sur l'utilisation pacifique de l'energie atomique. Genève* 1958. Communication 15/P/2391. Volume 7 (U.S.A.).
22. F. HITTMANN et O. A. KUHL, BNL-2257 (1955). U.S. Atomic Energy Commission.
23. H. CORIOU, J. GAUDUCHEAU, L. GRALL, M. PELRAS, *Mém. Sci. Rev. Métall.* **57**, 511 (1960).
24. J. G. GOODWIN, *Bettis Tech. Rev.* WAPD; BT; 1958. p. 203–111.
25. G. E. GALONIAN, *15ème conférence annuelle N.A.C.E. Chicago, Illinois, Mars* 1959. (Edit. NACE 1959.)
26. K. ALCOCK et B. COX, AERE C/R/2826 (1959).
27. H. CORIOU, L. GRALL, Y. LE GALL et S. VETTIER, *3ème Colloque de Métallurgie sur la corrosion, sèche et la corrosion aqueuse, Juin* 1959. (Centre d'Etudes Nucléaires de Saclay); *Colloque de Stockholm sur les matériaux de réacteurs* 5 *Octobre* 1959.

Corrosion Science, 1961, Vol. 1, pp. 161–169. Pergamon Press Ltd. Printed in Great Britain.

A RADIOTRACER STUDY OF THE PASSIVATION OF ZINC IN CHROMATE SOLUTIONS—I*

K. G. McLaren,†‡ J. H. Green§ and A. H. Kingsbury‡

Abstract—When zinc is immersed in dilute Cr^{51}-labelled chromate solution, chromium deposition on the metal continues for at least three weeks. The pH of the solution has a marked influence on the reaction rate, but dissolved oxygen has little effect. It is concluded that chromate ions are reduced at the zinc surface producing an invisible zinc-oxide–chromic-oxide film. On abraded specimens the chromium was evenly distributed over the surface, but on polished zinc discrete spots of high chromium concentration gradually developed, suggesting that defects in the film are healed by reaction of the inhibitor. The addition of chloride ions to the chromate solution resulted in the gradual development of localized concentrations of chromium both on abraded and on polished specimens. Using Cl^{36} as tracer, it was found that chlorine was taken up irreversibly at discrete sites on abraded zinc in chromate–chloride solutions. The results are in line with the conclusion of Hoar and Evans for steel, that film breakdown by chloride will involve subsequent repair by chromate.

Résumé—Lorsqu'on immerge du zinc en solution diluée de chromate contenant du Cr^{51}, le chrome continue à se déposer sur le métal au moins pendant trois semaines. Le pH de la solution a une influence marquée sur la vitesse de la réaction mais l'oxygène dissous n'a que peu d'effet. On en conclut que les ions chromate sont réduits à la surface du zinc avec formation d'un film invisible d'oxyde de zinc et d'oxyde chromique. Sur les échantillons soumis à l'abrasion le chrome était distribué également sur la surface, mais sur le zinc poli il y avait développement progressif de plages séparées de haute concentration en chrome, ce qui laisse supposer que les défauts du film sont réparés par action de l'inhibiteur. L'addition d'ions chlore à la solution de chromate aboutissait à l'accroissement graduel de concentrations locales en chrome, aussi bien sur les surfaces abrasées que sur les surface polies. En utilisant du Cl^{36} comme traceur en solutions de chlorure-chromate, on touva que, sur du zinc préalablement soumis à l'abrasion, le chlore était fixé de façon irréversible en des endroits distincts. Les résultats s'alignent sur les concisions de Hoar et Evans pour l'acier, à savoir que la destruction du film par les chlorures est suivie d'une réparation par le chromate.

Zusammenfassung—Bei Eintauchen von Zink in mit Cr^{51} markierte Chromatlösungen findet während mindestens drei Wochen Chromatabscheidung statt. Die Reaktionsgeschwindigkeit wird stark durch den pH der Lösung beeinflusst, während gelöster Sauerstoff praktisch keinen Effekt zeigt. Man schliesst daraus, dass an der Zinkoberfläche Chromationen reduziert werden und sich ein unsichtbarer Film bildet von Zinkoxyd-Chromoxyd. Auf geschliffenen Oberflächen war die Chromverteilung regelmässig, während sich auf poliertem Zink zunehmend einzelne Flecken hoher Chromkonzentration bildeten, was einer Inhibitorwirkung auf die Filmbildung zugeschrieben werden muss.

Die Zugabe von Chlorionen zu den Chromatlösungen hatte zur Folge, dass sowohl auf geschliffenen wie auf polierten Overflächen sich graduell lokale Chromkonzentrationen finden liessen.

Durch Verwendung von Cl^{36} konnte festgestellt werden, dass Chlor irreversibel an diskreten Stellen an geschliffenen Zinkoberflächen aus Chromat-Chlorid-Lösungen aufgenommen wird.

Diese Ergebnisse sind in Uebereinstimmung mit den Resultaten von Hoar und Evans für Stahl, dass sich an einen Filmdurchbruch hervorgerufen durch Chlorid eine Reperatur des Defektes durch Chromat anschliesst.

Theories of the mechanism by which chromates act as corrosion inhibitors for metals in aqueous solutions fall into two main groups. One considers that oxidation of the metal by chromate ions produces a protective mixed-oxide film which separates the metal from its environment,[1,2,3] the other favours stifling of the surface reactions by adsorption of unreduced chromate ions alone or in conjunction with adsorbed oxygen.[4,5]

Most of the work on the mechanism of corrosion inhibition by chromates has been

*Manuscript received 16 November 1960.

†Present address: Research Laboratory for the Physics and Chemistry of Solids, University of Cambridge.

‡Australian Defence Scientific Service, Defence Standards Laboratories, N.S.W. Branch, Sydney.

§ Department of Nuclear and Radiation Chemistry, University of N.S.W., Sydney, Australia.

carried out with ferrous materials. Useful information should be obtained by studying other metals of different reactivities, and zinc was chosen for this work.

Under passivating conditions the amounts of material involved in metal surface reactions are below the limits for conventional analytical techniques. Radiotracer methods with Cr^{51}-labelled solutions have been used in studying the reactions between chromates and ferrous metals.[6, 7, 8] Eisler *et al.*[9] studied the occlusion of sulphates in the thick chromate coatings formed on zinc-plated material in acid chromate baths, using Cr^{51} and S^{35} tracers. Apart from brief references,[10, 11] no other radiotracer study of the passivation of zinc has come to our attention.

As chromates are "dangerous" inhibitors[12] which may stimulate corrosion at concentrations too low to inhibit it, they are usually used industrially and studied experimentally at concentrations no lower than 100 p.p.m., well above the threshold (ca. 5 p.p.m.) for inhibition of corrosion of zinc under stagnant conditions. In this investigation we chose a concentration of 10^{-4}M (11·6 p.p.m.), only slightly above the threshold, so that the effects of other factors influencing the surface reactions might more readily be observed.

EXPERIMENTAL

Specimen preparation

The zinc was electrolytic grade rolled sheet, the main impurities being Fe (0·01 per cent) and Pb (<0·01 per cent). Specimens 11 mm square were mounted in acrylic resin, then abraded successively on 220, 400 and 600 grade silicon carbide papers under running water. Preliminary polishing was carried out on cloth charged with 8 μ diamond paste, and the specimens were finished on a 1 μ diamond pad. After degreasing with alcohol and then benzene, specimens were stored in a desiccator over silica gel and potassium hydroxide pellets for a predetermined time.

When specimens were to be studied in the abraded condition, the final abrasion was carried out under benzene; degreasing and air-exposure were performed as described above.

Preparation of $Na_2Cr^*O_4$ *solution*

Sodium chromate labelled with Cr^{51}, designated $Na_2Cr^*O_4$, was purchased as a pure aqueous solution from the Radiochemical Centre, Amersham. The concentration was checked by absorptiometric analysis using the diphenyl carbazide complex. For use, it was diluted with pure sodium chromate, giving an initial specific activity of 700 mc Cr^{51}/g Cr. The concentration was finally adjusted to 10^{-4}M. pH adjustments were made by addition of sodium hydroxide or passage through acid Zeo-KARB 225 resin as required.

Reaction of zinc and sodium chromate

Specimens were placed in 5 ml of chromate solution in 1-in. Pyrex test tubes fitted with vented stoppers and suspended in a waterbath at 22 ± 1°C. Apart from an initial shake to ensure wetting of the metal surface, there was no agitation. After the appropriate reaction time, the specimens were withdrawn, washed and rubbed well with cotton wool under running water, dipped in methanol and dried in an air-blast.

Tests were run in triplicate and mean results have been reported. In general, individual determinations varied from the mean by not more than 10 per cent, except when localized concentrations of chromium developed.

Measurement of chromium uptake

Chromate solution was found to penetrate the specimen mounts, apparently through shrinkage cracks. In order to eliminate spurious counts the specimens were taken out of their mounts and abraded on the back and edges. By means of a thick lead mask, counting was confined to an area of 0·774 cm² in the centre of the specimen. An end-window Mullard MX123 Geiger tube coupled to a quenching amplifier with a 300 μ sec "dead-time" was used, and paralysis losses were negligible, as count rates did not exceed 400 c/min.

Corrections were made for the 27·8 day half-life of the Cr^{51}, and for background. Standards were prepared by drying out measured volumes (0·010–0·100 ml) of chromate solutions spread over a 0·774 cm² area of clean zinc. These standards were counted periodically as a check on the stability of the electronic equipment. Their decay rate observed over about three half-lives corresponded to that of Cr^{51}.

The "probable" statistical error was of the order of 1·5 per cent for the higher count rates rising to 3·5 per cent when the chromium uptake was less than 4×10^{-8} g/cm². A surface roughness factor of unity was assumed in all calculations.

Cl^{36} *tracer experiments*

A solution of 10^{-4}M Na_2CrO_4 plus 10^{-3}M NaCl was prepared with a specific activity of 120 μ curie Cl^{36}/g Cl. Zinc disks, 2·54 cm in diameter, were mounted in cells (Fig. 3) holding 5 ml of solution. After a given reaction time the specimens were taken out, washed thoroughly and rubbed with cotton wool under running water, dried in an air-blast, then counted.

Progressive measurements of chlorine uptake were obtained by repeating the

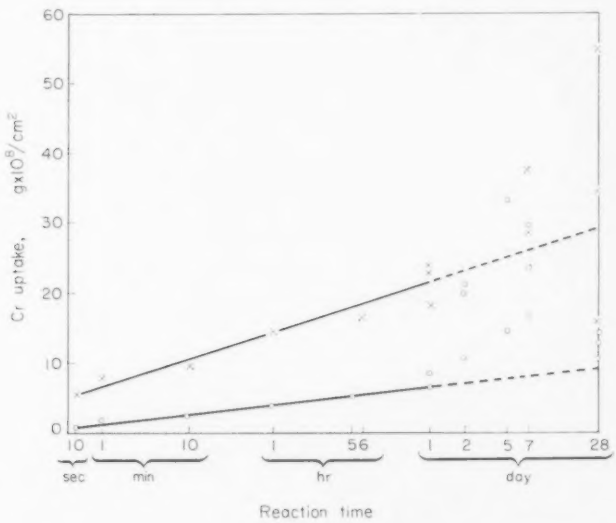

FIG. 1. Chromium uptake on polished zinc in 10^{-4}M Na_2CrO_4, 22°C.
Zinc, 1 μ polish, 1 day air-exposure.
○ . . . pH 8·4
× . . . pH 3·96

cycle. The Geiger equipment was used and by means of a lead mask, counting was confined to the central area of the specimen thus avoiding counts from localized concentrations of chlorine which were found to develop along the line of contact of the zinc and the polythene gasket (Fig. 4). Count rates were low, and the "probable" statistical error of the counts was approximately 15 per cent for chlorine uptake up to 5×10^{-8} g/cm², falling to less than 5 per cent for higher chlorine concentrations.

Standards were prepared by spreading measured volumes of the solution over the appropriate area of zinc disks.

Autoradiography of specimens

Specimens were clamped against Ilford-G X-ray film and kept in a desiccator during exposure, to avoid corrosion artefacts. Exposure times varied from a few days for Cr^{51} experiments to three weeks for Cl^{36} tests. Non-active zinc did not affect the film.

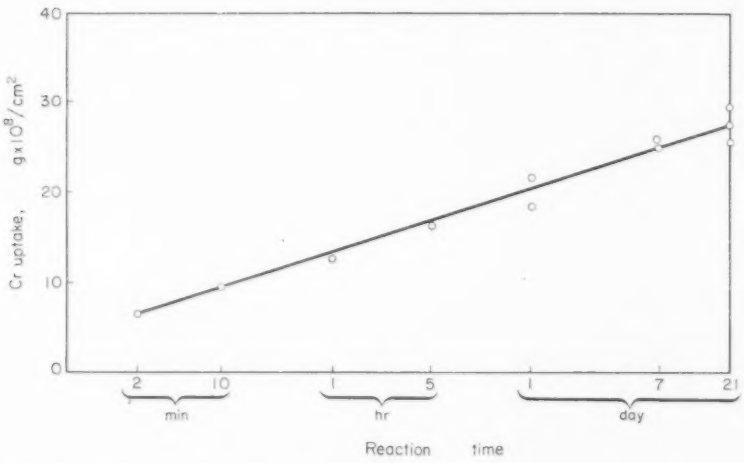

FIG. 2. Chromium uptake on abraded zinc in 10^{-4}M Na_2CrO_4, 22°C, pH 7·2. Zinc abraded on 400 grade silicon carbide, ½ hr air-exposure.

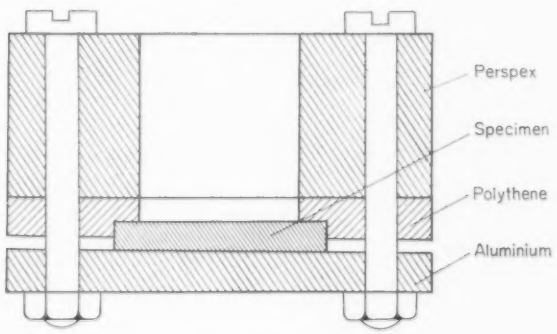

FIG. 3. Reaction cell.

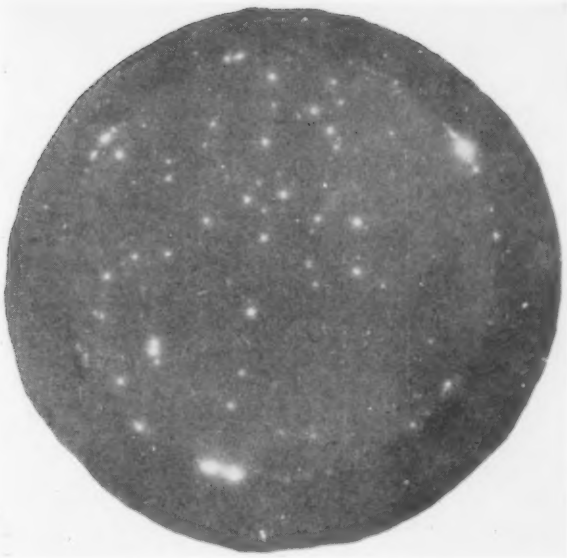

FIG. 4. Autoradiograph showing local concentrations (white spots) of Cl^{36} on abraded zinc surface after 60 h intermittent treatment with 10^{-4}M Na_2CrO_4 + 10^{-3}M NaCl, pH 7·1. × 3.

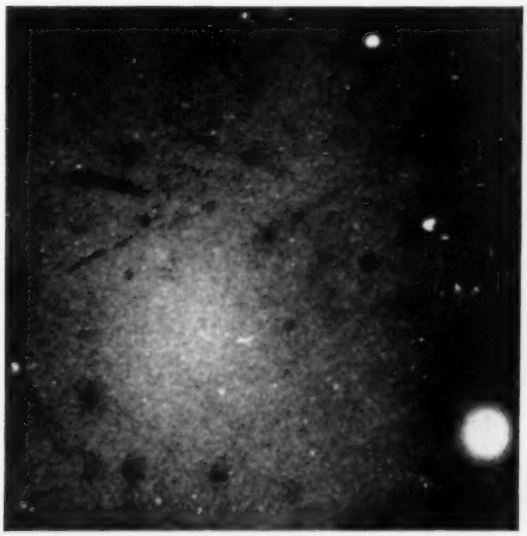

FIG. 5. Autoradiograph showing local concentrations of Cr (white spots) on polished zinc after 5 days immersion in 10^{-4}M Na_2CrO_4, pH 8·4. × 7.

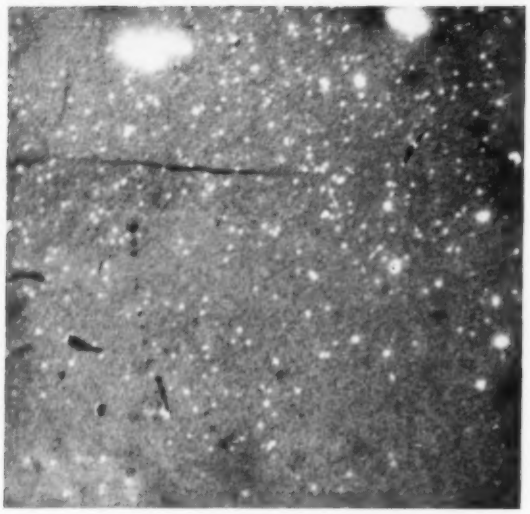

FIG. 6. As for Fig. 5, but after 7 days in 10^{-4}M Na_2CrO_4, pH 3·96. × 7.

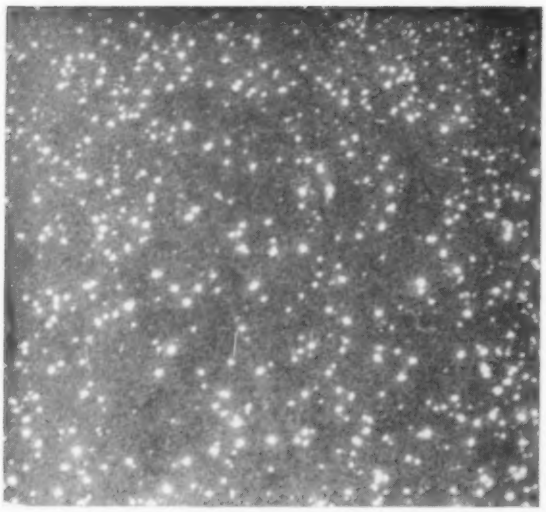

FIG. 7. Autoradiograph showing local concentrations of Cr (white spots) on polished zinc after 1 day in 10^{-4}M Na_2CrO_4 + 10^{-4}M NaCl, pH 8·4. × 7.

FIG. 8. Autoradiograph showing beginning of chromium repair at defect areas (white spots) on abraded zinc after 1 day immersion in 10^{-4}M Na_2CrO_4 + 10^{-4}M NaCl, pH 7·2. × 7.

FIG. 9. As for Fig. 8; but after 7 days immersion. × 7.

RESULTS

Chromium uptake as a function of reaction time

The sensitivity of the method enabled measurements to be made after only a few seconds reaction time. The results with polished and abraded specimens are shown in Fig. 1 and Fig. 2 respectively with reaction time (t sec) plotted on a convenient logarithmic scale (following the practice of Brasher and Kingsbury[8] who found a linear relationship between chromium uptake and log ($t + 1$) for iron and steel in chromate solutions).

The considerable scatter of results with polished specimens after more than 1 day of immersion was shown by autoradiographs (Figs. 5, 6) to be associated with the development of localized deposits of chromium. With abraded specimens on the other hand reproducible results were obtained up to 21 days. Autoradiographs (not printed here) of abraded specimens after 7 days immersion showed even distribution of chromium over the surface.

In all cases the zinc specimens appeared unchanged after immersion in chromate solutions.

Effect of temperature on chromium uptake

In limited experiments with reaction times up to 1 hr, no significant difference was found between the chromium uptake at 45°C and that at 22°C on polished specimens in 10^{-4}M $Na_2Cr^*O_4$ at pH 8·4.

Effect of pH *on chromium uptake*

The marked difference between uptake rates at pH 3·96 and pH 8·4 is shown in Fig. 1. Experiments were also conducted with solution of pH 11·0, but no chromium uptake was detected after 1 hr immersion and only $1{\cdot}4 \times 10^{-8}$ g Cr/cm² after 5 hr immersion. The specimens began to corrode after more than 5 hr immersion at pH 11·0.

Effect of de-aeration of sodium chromate solution

$Na_2Cr^*O_4$ solution (10^{-4}M, pH 8·4) was de-aerated by bubbling oxygen-free nitrogen (purified by vanadous sulphate solution as recommended by Meites and Meites[13]) through it. Polished specimens pre-exposed to air for 1 day, were immersed in the de-aerated solution under a nitrogen atmosphere at 22°C. The chomium uptake on the zinc in reaction times up to 1 hr was the same (within experimental limits) as that in chromate solution in equilibrium with air. Other specimens were abraded on 400-grade silicon carbide and exposed to air for $3\frac{1}{2}$ hr before chromate treatment. De-aeration of the chromate solution had no significant effect on the chromium uptake during a 65-hr immersion period.

These results contrast with those of similar tests made with mild steel abraded on 400-grade silicon carbide paper and exposed to air for 42 hr before immersion in the chromate solution. Chromium uptake in $5\frac{1}{4}$ hr was $22{\cdot}4 \times 10^{-8}$ g/cm² in the solution exposed to air and $31{\cdot}5 \times 10^{-8}$ g/cm² in the de-aerated solution. This 40 per cent increase in chromium pick-up on steel is of a similar order to that reported by Brasher and Kingsbury.[8]

The effect of chloride ions on chromium uptake

The initial effect of adding sodium chloride (10^{-4}M) to chromate solution

(10^{-4}M, pH 8·4) was to depress the chromium uptake by about one third, but with polished zinc this effect was quickly masked by the development of numerous local concentrations of chromium (cf. autoradiograph Fig. 7) and after about one day the uptake was higher than that from the chloride free solution. With ten times the chloride concentration (10^{-3}M) the polished specimens showed visible corrosion in 1 day and the depression of chromium uptake was not observed even with immersion time as short as 1 min.

Abraded specimens in a solution of pH 7·2 showed more resistance to chloride than the polished specimens in a solution at pH 8·4, but eventually developed local concentrations of chromium in the same way (cf. autoradiographs Fig. 8, 9). After 1 day the chromium uptakes with both 10^{-4}M and 10^{-3}M chloride were still less than in chloride-free solutions; but after 7 days the uptake values were as high as the chloride-free values, and with 10^{-3}M chloride pinhole corrosion was observed on some specimens.

Uptake of radioactive chlorine on zinc

Polished zinc in a solution of 10^{-4}M Na_2CrO_4, 10^{-3}M NaCl, pH 7·1 became tarnished with white patches, but in a triplicate test no chlorine pick-up was detected in 39 hr. The detection limit was about 10^{-8} g Cl/cm².

Abraded specimens showed a slight visible tarnish only along the gasket line, the central area being unchanged in appearance except for a slight darkening; chlorine pick-up was detected, however, to the extent of 5×10^{-8} g/cm² after 15 min on each of three specimens. On one of these the chlorine value remained at $6{\cdot}4 \times 10^{-8}$ g/cm² in successive immersions from 1 hr up to a total of 60 hr. A second specimen rose to $8{\cdot}5 \times 10^{-8}$ g Cl/cm² and the third to $12{\cdot}8 \times 10^{-8}$ g Cl/cm² in 60 hr. The autoradiograph of one of these specimens (Fig. 4) shows local concentrations of chlorine. We could not correlate the location of these concentrations with any visible macro-defects such as scratches.

Pre-treatment of zinc with chromate solution for half an hour before immersion in chromate–chloride solution did not alter the amount of chlorine taken up on the metal.

Irreversibility of chromium uptake

The reversibility of the chromium adsorption/deposition was examined by immersing $Na_2Cr^*O_4$-treated specimens in various solutions. There was no loss of activity into the solution after 72 hr in 10^{-4}M Na_2CrO_4, or 70 min in a solution of chromate-chloride (10^{-4}M each), or 6 hr in 10^{-3}M E.D.T.A. solution, or 19 hr in distilled water, even when tarnishing occurred. Both polished and abraded specimens which had been treated with chromate solution at pH 3·96, pH 8·4 or pH 11·0 for times varying from 1 min to 5 hr, were used in these tests.

DISCUSSION

As discussed in the succeeding paper[14] much evidence has accumulated to indicate that chromate ions have pronounced surface active properties and many workers believe that this propensity is responsible for their inhibiting powers, the subsequent formation of oxide layers being merely incidental. Opposing theorists regard the oxide layer as being the essential inhibiting agent. We believe that the balance of evidence

is in favour of the latter view, but that adsorption can contribute to the effective building up of an impervious oxide layer. With such a reactive metal as zinc it is unlikely that a monolayer of adsorbed ions alone could provide any real protection. In any case, it is certain that in experiments similar to ours bare zinc metal is never presented to the chromate solution except possibly for minute areas exposed by rupture of the preformed oxide film. Reaction at these spots is likely to be so intense that protection by adsorption is inconceivable and our experimental observation is consistent with the assumption that the healing of these breaks is achieved by piling up of reaction product rather than by a mechanism of adsorptive covering followed by smooth growth of oxide film. Thus if adsorption comes into the picture at all it is adsorption on oxide, hydroxide or other intermediate layer, rather than on bare metal. It is conceivable, however, and to us it seems a highly plausible hypothesis, that adsorption on the oxide does promote the continued growth of a dense, closely packed oxide film of low ionic permeability instead of a less protective film containing hydroxyl ions, or other ions conferring comparatively high ionic mobility. (This hypothesis is favoured by Anderson and Hocking[15] when discussing anodic films on aluminium.) Possibly the benefit of having a layer of adsorbed chromate ions on the surface of the film lies solely in that zinc atoms diffusing through the film make first contact with a reactant that produces unhydrated oxide, but the codeposition of chromium oxide (Cr_2O_3) could well be an additional factor of importance in producing a less permeable film, perhaps by virtue of a more favourable stacking habit compared with plain zinc oxide, or because of an inherently lower ionic conductivity (cf. Hauffe's valency rule discussed by Evans[16]).

The changes in chromium uptake accompanying changes in pH may be taken to support a hypothesis of competitive adsorption between hydroxyl and chromate ions such as that postulated by Powers and Hackerman[7] in the case of steel in chromate solutions. The significant consequence of this competition, however, would not be, in our view, the partial substitution of a non-protective adsorbant for a supposedly protective adsorbant, but rather that the film growing under the hydroxyl ions would be less protective than that growing under the chromate ions. The failure of inhibition at high pH's has previously been observed [17] and this work shows that it is associated with low uptake of chromium.

The effect of surface preparation on the reactivity of metal surfaces has been emphasized in recent work.[6,18] The polishing techniques[19] used in this study were chosen to eliminate, as far as possible, side effects due to surface deformation. Other work in these laboratories [20] indicated that a zinc surface abraded on 600 grade silicon carbide paper has a "roughness factor" about twice that of a polished surface. In the absence of absolute values for surface area, film thickness calculations are more realistic for the polished specimens.

If the chromium is assumed to be bound as close-packed chemisorbed chromate ions with a cross-sectional area[21] of 24·6(Å)^2, our uptake values on polished specimens after 1 day would be equivalent to 2·1 and 6·2 monolayers at pH 8·4 and pH 3·96 respectively. It is unlikely that so many ion layers would be irreversibly bound to the surface by purely adsorptive forces. It is evident that the chromium is strongly bound to the metal because it was not removed by the washing process after immersion nor by the leaching tests with various electrolytes.

The continuing reaction between zinc and chromate with growth of an oxide film probably occurs by a mechanism somewhat analogous to that operating with air oxidation as suggested by Hoar and Evans.[22] The over-all reaction may be that expressed by:

$$3Zn + 2(CrO_4)^{2-} + 2H^+ = 3ZnO + Cr_2O_3 + 2(OH)^- \qquad (1)$$

or slight variants of this if $(HCrO_4)^-$ or $(Cr_2O_7)^{2-}$ are taken to be the reacting ions. On this basis 1 g of chromium gives rise to 1·46 g of Cr_2O_3 and 2·35 g of ZnO. If these are deposited with a density of say 5·4 g/cm³ (intermediate between the densities of the individual oxides) the thickness of film would be 70 Å per μ g of Cr deposited on 1 cm² of surface. The calculated thicknesses of film formed in chromate solution of pH 8·4 are 5 Å after 1 day and 7–11 Å after 28 days. In a solution of pH 3·96 the thicknesses are about three times these. The actual thickness of film is almost certainly greater than that calculated on the basis of equation (1) because, apart from the pre-existing film, oxidation by dissolved oxygen could go on to some extent as well. Nevertheless, the rate of chromium uptake is probably a good relative indicator of the rate of film growth and it is evident that the chromium-containing films are much less permeable than air-formed oxide films (the latter at 20–40 Å thickness[23] provide little protection to zinc immersed in water). The rate obeys a logarithmic law similar to that observed by Vernon *et al.*[24] for zinc oxidizing in air at elevated temperatures and, at least for the first four days, at 25°C. The rates of air oxidation at 25°C found by them are, however, of the order of ten times those of chromate oxidation observed by us. Like them we found the results with abraded surfaces more consistent than with polished.

The increase in the rate of chromium uptake as the hydrogen-ion concentration is increased might be accounted for in a general way on the basis of equation (1), but many possible explanations are conceivable as to precisely how pH affects the rate, according to what is assumed to be the rate controlling step. We have already referred to the hydroxyl-chromate, competitive adsorption hypothesis which is an alternative approach.

Great emphasis has been placed on the role of dissolved oxygen in corrosion inhibition with ions of the $(XO_4)^n$ type,[5, 25, 26] and Evans and Davies[27] have shown the marked effect of oxygen on the behaviour of zinc in distilled water; but the present work suggests that zinc is oxidized more readily by chromate ions than by dissolved oxygen, since the chromium uptake rate was found to be independent of oxygen supply.

The development of localized concentrations of chromium on apparently unchanged polished specimens immersed in chromate solution for a few days (Figs. 5, 6) suggests that defects arise in the thickening film and are then healed by a process involving considerable deposition of chromium. The details of this process are still somewhat obscure. Defects could arise from stray abrasive particles embedded in "flowed" metal as suggested by Takahashi[28] or from residual strain in deformed areas. Stress relief in the recrystallization process which occurs in the outer layer of abraded zinc surfaces[19] may explain the difference in behaviour of abraded compared with polished specimens in this respect.

The effect of chloride ions on chromate inhibition processes has generally been inferred from indirect evidence. Theories mainly favour either a competitive reversible

adsorption process at the metal surface[29] or penetration of the oxide film by the small chloride ions, with subsequent repair by the inhibitor.[1] In the present work some evidence was found for both hypotheses, since we observed both suppression of chromium uptake by chloride in the early stages of immersion and also a considerable incidence of local deposition of both chromium and, with abraded specimens, chlorine. (The failure of polished specimens to give indication of bound chlorine requires further clarification.) It seems that once chloride-induced defects are present in the film, the healing action of chromate ions continues for some time, even though chloride deposition may not continue. Anderson and Hocking[15] suggest that the incorporation of chloride ions in an oxide film lattice would be comparatively easy and would lead to high ionic mobility in the film.

Acknowledgements—This paper is published by permission of the Chief Scientist, Australian Defence Scientific Service, Department of Supply, Melbourne. The work was carried out at the Australian Defence Scientific Service, Defence Standards Laboratories, N.S.W. Branch, Sydney, Australia.

REFERENCES

1. T. P. Hoar and U. R. Evans, *J. Chem. Soc.* 2476, (1932).
2. U. R. Evans, *Z. Elektrochem.* **62**, 619 (1958).
3. M. Cohen and A. F. Beck, *Z. Elektrochem.* **62**, 696 (1958).
4. H. H. Uhlig and A. Geary, *J. Electrochem. Soc.* **101**, 215 (1954).
5. H. H. Uhlig and P. F. King, *J. Electrochem. Soc.* **106**, 1 (1959).
6. M. T. Simnad, *Properties of Metallic Surfaces.* Monograph and Report Series No. 13, p. 23. Institute of Metals, London (1953).
7. R. A. Powers and N. Hackerman, *J. Electrochem. Soc.* **100**, 314 (1953).
8. D. M. Brasher and A. H. Kingsbury, *Trans. Faraday Soc.*, **54**, 214 (1958).
9. S. L. Eisler, J. Doss and M. A. Henderson, *Plating* **41**, 147 (1954).
10. K. Kimura, *Proc. Int. Conf. Peaceful Uses Atomic Energy, Geneva*, United Nations Publication IX.1, Vol 15, p. 220 (1956).
11. *Chemistry Research*, H.M.S.O., London (1959).
12. U. R. Evans, *Metallic Corrosion Passivity and Protection* (2nd Ed.) Chap. 10. Edward Arnold. London (1946)
13. L. Meites and T. Meites, *Analyt. Chem.* **20**, 984 (1948).
14. K. G. McLaren, J. H. Green and A. H. Kingsbury, *Corrosion Sci.* **1**, 170 (1961).
15. P. J. Anderson and M. E. Hocking, *J. Appl. Chem.* **8**, 352 (1958).
16. U. R. Evans, *The Corrosion and Oxidation of Metals*, p. 61. Edward Arnold, London (1960),
17. U. R. Evans, *Metallic Corrosion Passivity and Protection* (2nd Ed.) p. 559. Edward Arnold. London (1946).
18. U. R. Evans, *Properties of Metallic Surfaces.* Monograph and Report Series No. 13, p. 253. Institute of Metals, London (1953).
19. L. E. Samuels and G. R. Wallwork, *J. Inst. Metals* **86**, 43 (1957).
20. K. G. McLaren. M.Sc. Thesis, University of New South Wales (1959).
21. J. J. Miller, *Z. Kristallogr.* **94**, 131 (1936).
22. T. P. Hoar and U. R. Evans, *J. Electrochem. Soc.* **99**, 212 (1952).
23. H. Raether, *J. Phys. Radium* **11**, 11 (1950).
24. W. H. J. Vernon, E. I. Akeroyd and E. G. Stroud, *J. Inst. Metals* **65**, 301 (1939).
25. M. J. Pryor and M. Cohen, *J. Electrochem. Soc.* **100**, 203 (1953).
26. G. H. Cartledge, *J. Phys. Chem.* **60**, 28 (1956).
27. U. R. Evans and D. E. Davies, *J. Chem. Soc.* 2607 (1951).
28. N. Takahashi, *Metaux et Corros.* **26**, 189 (1951).
29. R. F. Sympson and G. H. Cartledge, *J. Phys. Chem.* **60**, 1037 (1956).

Corrosion Science, 1961, Vol. 1, pp. 170–176. Pergamon Press Ltd. Printed in Great Britain.

A RADIOTRACER STUDY OF THE PASSIVATION OF ZINC IN CHROMATE SOLUTIONS—II*

K. G. McLaren,†‡ J. H. Green‡ and A. H. Kingsbury§

Abstract—Zinc, surface-labelled by exchange with $Zn^{65}Cl_2$ solution, was used in a study of corrosion inhibition mechanisms. Corrosion of these Zn^{65}-labelled specimens in water and dilute salt solutions was accompanied by a slow, continuing loss of activity from the metal surface. By contrast, while the metal remained untarnished in 10^{-4}M chromate solutions, a rapid loss of activity was observed. Treatment with 10^{-4}M molybdate solution also produced a rapid initial loss of activity, but corrosion inhibition was only temporary. Other oxidizing and non-oxidizing solutions under similar conditions did not protect the metal or produce rapid loss of zinc from the surface.

When specimens labelled by electrodeposited or evaporated Zn^{65} were placed in passivating chromate solution, loss of zinc occurred slowly and continued for a considerable time, showing that the barrier film formed by reaction of zinc with chromate ions is not sufficiently impermeable to prevent zinc ions leaving the metal and passing into the solution.

Résumé—Pour l'étude de l'inhibition du processus de corrosion on a utilisé du zinc marqué en surface par échange avec une solution de chlorure de zinc.^{65} La corrosion dans l'eau et dans des solutions salines diluées de ces échantillons marqués au Zn^{65}, était accompagnée d'une diminution lente et continue d'activité de la surface métallique. Par contre, alors que le métal ne se ternissait pas dans des solutions 10^{-4}M de chromate, une chute rapide d'activité était observée. Un traitement avec des solutions de molybdate 10^{-4}M produisait aussi une chute rapide de l'activité initiale, mais l'inhibition de la corrosion n'était que temporaire. D'autres solutions oxydantes et non oxydantes dans des conditions analogues, ne protégeaient pas le métal et n'entraînaient pas une dissolution rapide de métal en surface. Lorsque des échantillons marqués au moyen de zinc^{65} électrodéposé ou évaporé étaient placés en solutions passivantes de chromate la dissolution du zinc se produisait lentement et se prolongeait pendant un temps considérable, montrant que le film formé par réaction du zinc sur les ions chromate n'est pas suffisament imperméable pour empêcher que les ions zinc ne quittent le métal pour passer en solution.

Zusammenfassung—Zum Studium des Korrosions-Inhibitions-mechanismus verwendete man oberflächlich mit Zn^{65} (durch Austausch in $Zn^{65}Cl_2$-Lösung hergestelltes) markiertes Zink. Die Korrosion dieser Proben in Wasser und verdünnten Salzlösungen war von einem langsamen aber kontinuierlichen Aktivitätsverlust begleitet. Im Gegensatz dazu blieb das Metall in 10^{-4}M Chromatlösung unangegriffen, jedoch trat ein rascher Aktivitätsabfall ein. Die Behandlung mit 10^{-4}M Molybdatlösung rief ebenfalls diesen raschen Aktivitätsabfall hervor, jedoch war die Korrosionsinhibition nur vorübergehend. Andere Lösungen, oxydierende und nicht oxydierende, hatten weder einen Aktivitätsabfall noch eine schützende Wirkung auf das Metall zue Folge.

Im Kontakt mit passivierender Chromatlösung erlitten sowohl durch Aufdampfen als auch durch elektrolytische Abscheidung mit Zn^{65} markierte Proben einen langsamen aber über längere Zeit andauernden Verlust an Zink, was zeigt, dass der durch die Reaktion des Zinks mit dem Chromat gebildete Schutzfilm nicht dicht genug ist, um das Inlösunggehen von Zink vollständig zu unterbinden.

This paper reports an attempt to test the theory that chromates inhibit the corrosion of zinc by preventing the escape of cations from the metal surface into the aqueous environment. The work of Haissinsky[1] and his collaborators indicated that isotopic exchange between zinc and its ions in solution might prove a suitable technique for labelling the metal, since only the surface layers take part in the reactions in passivating solutions. In view of the apparently anomalous results we observed on immersion

*Manuscript received 16 November 1960.

†Present address: Research Laboratory for the Physics and Chemistry of Solids, University of Cambridge.

‡Australian Defence Scientific Service, Defence Standards Laboratories, N.S.W. Branch, Sydney.

§Department of Nuclear and Radiation Chemistry, University of N.S.W., Sydney, Australia.

of labelled zinc in chromate solutions, the work was extended to cover a number of other electrolytes, and alternative surface labelling techniques.

EXPERIMENTAL

Labelling of zinc surfaces by exchange

The zinc used was electrolytic grade rolled sheet, the main impurities being Fe (0·01 per cent) and Pb (<0·01 per cent). Surfaces were prepared by polishing or abrasion as described in our previous paper.[2] Zn^{65} obtained from the Radiochemical Centre, Amersham, as a solution of zinc chloride, was used to prepare a $4{\cdot}5 \times 10^{-4}$M solution with a specific activity of 70 mc Zn^{65}/g Zn, adjusted to pH 3·9 with HCl to prevent hydrolysis. Zinc disks were mounted in plastic cells and one face of the metal was allowed to react with 1 ml of the solution of labelled zinc chloride, designated Zn^*Cl_2. They were then withdrawn, washed thoroughly and dried.

In early experiments Geiger counting equipment was used. Later a scintillation probe was obtained and the specimens to be counted were placed on the thin aluminium sheath around the sodium iodide crystal. Heavy lead shielding maintained a stable low background of about 20 c/min. Standards were prepared by spreading measured volumes of the zinc chloride solution over the appropriate area of clean zinc disks which were then dried. The probable statistical error of all counts was less than 2 per cent.

Labelling by electro-deposited zinc

An electrolyte (approximately 2×10^{-5}M with respect to zinc) was prepared by adding 2 μ curie of Zn^*Cl_2 to a solution containing 1 g of sodium acetate and five drops of glacial acetic acid per 100 ml of distilled water. Zinc disks were mounted in plastic cells holding 4 ml of electrolyte. With a platinum wire as anode, electrolysis was carried out at 7V with a current density of about 25 mA/cm². After 10 min the specimens acquired an activity comparable with that obtained in five minutes exchange in Zn^*Cl_2 solution.

Labelling by evaporated zinc

High specific activity zinc as used in the previous work was electrodeposited on a molybdenum foil for use as a resistance heated vapour source. This was placed in a small crucible on top of which the specimen was mounted with a single face exposed to the zinc vapour. The assembly was enclosed in a glass container inside a metal evaporation unit which was operated at a vacuum of about 10^{-4} mm Hg. The amount of zinc deposited on the specimens was of the order of 10^{-7} g/cm².

The effect of immersion of labelled zinc in corrosive and inhibitor solutions

Zn^{65}-labelled disks were placed in beakers containing 10 ml of solution. After a measured time, they were withdrawn, washed and re-counted. A progressive record was obtained by repeating this cycle. Qualitative checks were also made on the radioactive content of the solution.

RESULTS

Labelling of zinc surfaces by exchange with Zn^*Cl_2 *solution*

Freshly polished zinc rapidly acquired radioactivity when treated with Zn^*Cl_2

solution. For short reaction times (5–10 min) there was no visible change in the surface; after 1 hr, specimens were unevenly tarnished. The effect of surface pretreatment on the exchange process may be seen from Table 1. The exchanged zinc was not evenly distributed over the surface (Fig. 4) and the surface coverage indicated in Table 1 is included as a guide only.

Table 1. Exchange of Zinc with Zn^*Cl_2 Solution ($4{\cdot}5 \times 10^{-4}$M; pH 3·9)

Specimen treatment before labelling	Activity acquired in 5 min (c/min)	Zinc uptake ($g \times 10^7/cm^2$)	Equivalent number of atom layers
Polished, then air-exposed for 15 min	1115	6·3	3·7
Polished, then oxidized for 1 hr at 210°C	1252	7·2	4·2
Polished, then dipped in N/10 HCl for 15 sec	708	4·1	2·4
Polished, then immersed in 10^{-4}M Na_2CrO_4 for 34 days	899	5·1	3·0
Polished, then air-exposed for 1 hr	Activity acquired in 1hr—2367 (specimen tarnished)	13·5	7·9

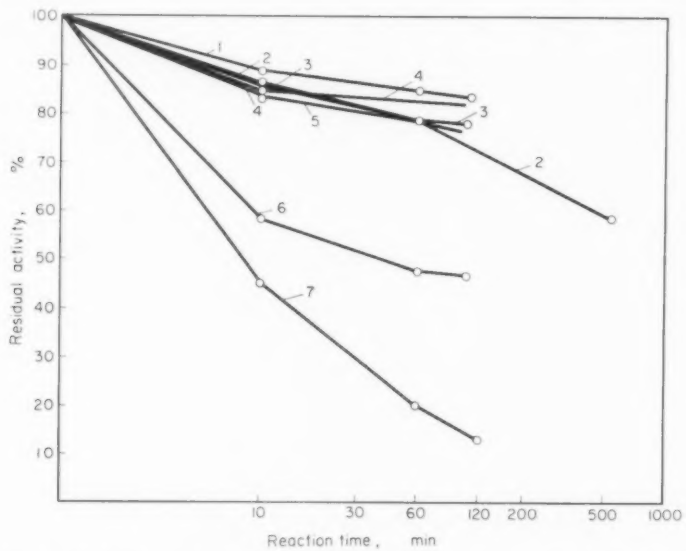

Fig. 1. The behaviour of polished zinc (labelled by exchange with $Zn^{65}Cl_2$ solution) on immersion in electrolytes.
1, 10^{-4}M Na_2SO_4, pH 6·9; 2, H_2O;
3, 10^{-4}M NaCl; 4, 10^{-4}M Na_2SO_4;
5, 10^{-4}M $KMnO_4$, pH 3·9;
6, 10^{-4}M $(NH_4)_6Mo_7O_{24}$, pH 4·3;
7, 10^{-4}M K_2CrO_4, pH 7·2.

The retarding effect of chromate ions on the exchange process was demonstrated by placing polished specimens, pretreated with 10^{-4}M Na_2CrO_4 for 15 min, in a solution 10^{-4}M with respect to both Na_2CrO_4 and Zn^*Cl_2. Exchange was slow, the zinc uptake being about $0{\cdot}2 \times 10^{-7}$ g/cm² after 5 min and $1{\cdot}7 \times 10^{-7}$ g/cm² after 17 hr.

The effect of electrolytes on surface-labelled zinc

1. *Polished zinc, labelled by exchange.* Representative results are set out in Fig. 1 and 2. When polished zinc, labelled after short air exposure, was placed in distilled water, 10^{-4}M NaCl or 10^{-4}M Na_2SO_4, there was a slow, continuing loss of activity from the surface and the specimens corroded. The onset of corrosion was noticeably delayed and the brief labelling treatment (with dilute $ZnCl_2$ solution) appeared to have a temporary protective effect on the zinc.

In 10^{-4}M Na_2CrO_4 (pH 7·2) the specimen activity first fell rapidly, then decreased slowly, approaching equilibrium after about 100 min. There was no visible change in the surface. Specimens labelled after the various other treatments described in Table 1 all exhibited a similar accelerated loss of activity on being placed in chromate solution. When the zinc was tarnished by prolonged exchange with $ZnCl_2$, or when a thick air-formed oxide film was present on the metal surface, the displacement of zinc was more gradual than when the surfaces were bright, with a minimal oxide film.

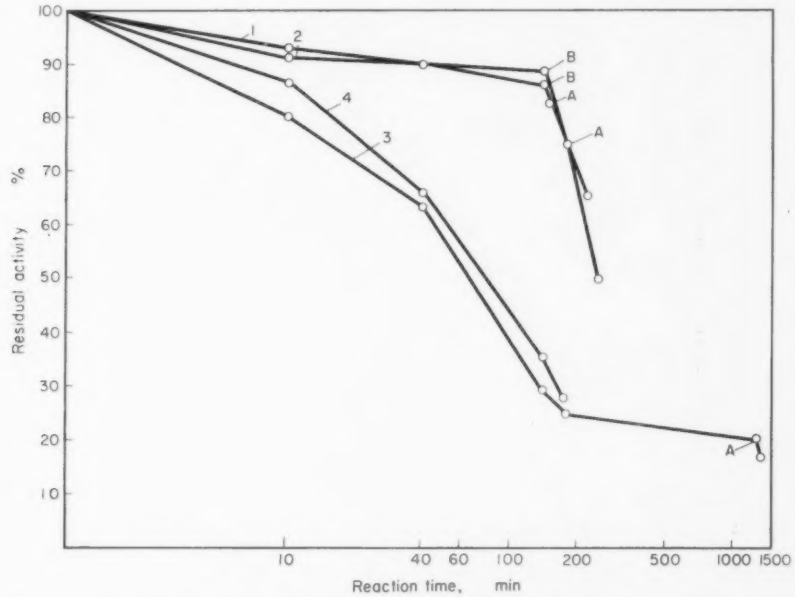

FIG. 2. The behaviour of polished zinc (labelled by exchange with $Zn^{65}Cl_2$ solution) on immersion in electrolytes.
1–3, polished, then oxidized 1 hr at 210°C; 5 min exchange.
4, polished; tarnished after exchange for 1 hr.
1, H_2O; 2, 10^{-4}M NaCl; 3–4, 10^{-4}M K_2CrO_4, pH 7·2.
A, Transferred to fresh chromate solution.
B, Transferred to chromate solution.

When zinc specimens were placed in 10^{-4}M potassium permanganate (pH 3·9) the solution slowly decolourized and a brown precipitate formed. The loss of activity from the zinc in permanganate solution was similar to that in distilled water, and the specimens corroded. In 10^{-4}M sodium tungstate solution (pH 6·9) the zinc slowly lost activity and corroded. Immersion in 10^{-4}M ammonium molybdate (pH 4·3) caused a rapid loss of activity similar to that in chromate solution, and the zinc corroded slowly.

By means of autoradiographs it was found that some of the zinc displaced from the central, labelled area of the specimens by the action of the electrolytes was redeposited on previously inactive regions mainly concentrated at the edges of the disks (Fig. 5). If specimens which had almost come to equilibrium with the original solution were placed in fresh chromate or molybdate solution, there was a sharp drop in activity (Fig. 2).

2. *Abraded zinc, labelled by exchange.* The behaviour of labelled, abraded zinc in 10^{-4}M chromate, molybdate, tungstate, phosphate, nitrate and benzoate solutions is shown in Fig. 3. The loss of zinc from the metal surface in chromate solutions was slower than with polished specimens. Increasing the chromate concentration did not have a great over-all effect, and 10^{-4}M chromate solution saturated with zinc oxide

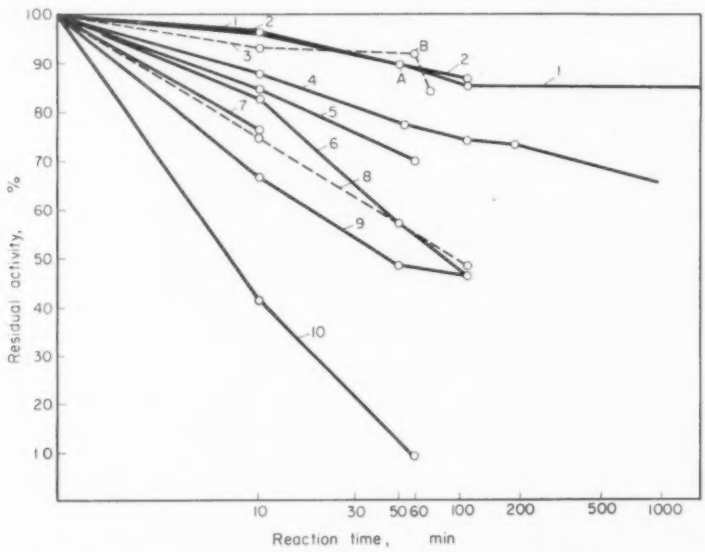

Fig. 3. The behaviour of abraded zinc (labelled by exchange with $Zn^{65}Cl_2$ solution) on immersion in electrolytes.
1, 10^{-4}M Na_2HPO_4, pH 8·1; 2, 10^{-4}M $NaNO_2$, pH 6·7;
3, H_2O; 4, 10^{-4}M sodium benzoate, pH 6·9;
5, 10^{-4}M Na_2WO_4, pH 6·9; 6, 10^{-4}M K_2CrO_4, pH 7·2;
7, 10^{-4}M K_2CrO_4, pH 7·2, saturated with ZnO;
8, 5×10^{-3}M K_2CrO_4, pH 7·6;
9, 10^{-4}M $(NH_4)_6Mo_7O_{24}$, pH 4·3;
10, 10^{-4}M K_2CrO_4, pH 4·1.
A, Transferred to fresh solution.
B, Transferred to chromate solution.

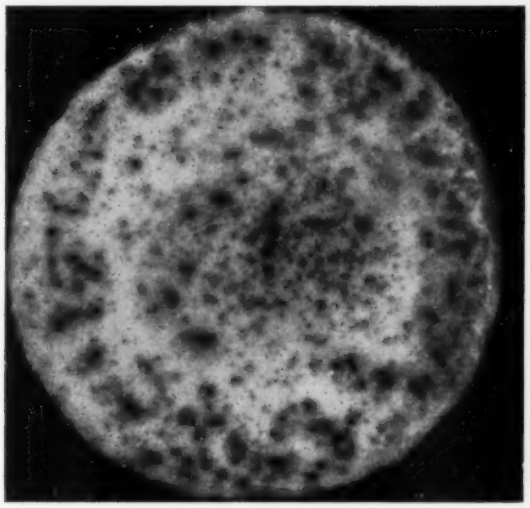

FIG. 4. Zn^{65} autoradiograph showing uneven distribution of exchanged zinc (white areas) on specimen. × 3·5.

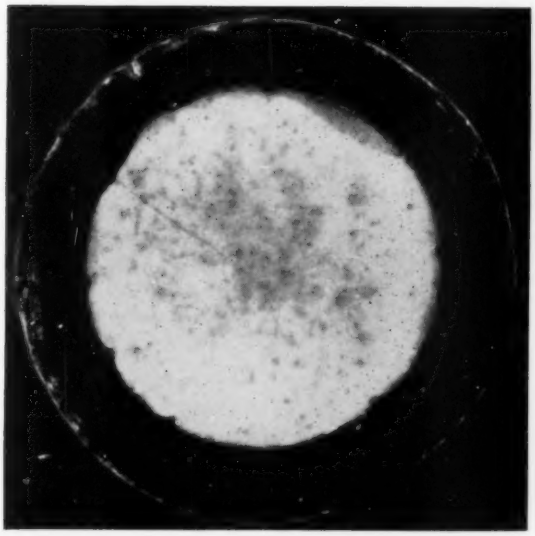

FIG. 5. Zn^{65} autoradiograph showing redeposition of zinc displaced from central area during immersion of labelled zinc in 10^{-4}M Na_2CrO_4. × 3.

gave results similar to those with pure chromate solution. In acid chromate solutions (pH 4·1) the loss of zinc was considerably accelerated. At the above concentration, only chromate solution was a satisfactory inhibitor for zinc.

3. *Abraded zinc, labelled by electrodeposited* Zn^{65}. When these specimens were immersed in 10^{-4}M chromate solution (pH 7·2) they lost no activity in 30 min. After prolonged immersion, radioactive zinc appeared in the solution, the metal losing 15–30 per cent of its activity in 44 hr and 55–78 per cent in 116 hr.

4. *Abraded zinc, labelled by evaporated* Zn^{65}. These specimens lost no activity after 70 min immersion in 10^{-4}M chromate solution (pH 7·2); after 48 hr, about 12 per cent of their activity was transferred to the solution.

DISCUSSION

De[3] recently proposed that corrosion inhibitor ions such as chromate are electrocapillary active and adsorb on cathodic areas of iron more strongly than normal ions such as chloride and sulphate, thus reducing the cathodic depolarization by oxygen. Gatos[4] subsequently reported that in line with De's theory a number of inorganic inhibitor ions including dichromate affect the positive branch of electrocapillary curves for mercury in dilute salt solutions. Gatos also examined mixed inhibitor solutions and concluded that dichromate ions were the most strongly adsorbing and could displace other inhibitor ions from the mercury surface.

The present results may be a new indication of unusual surface-active properties of chromate ions. The rapid displacement of zinc from the metal surface by chromate ions is peculiar to surfaces labelled by exchange. The apparently low bonding energy of atoms deposited by this process, compared with that of atoms electrodeposited or deposited from the vapour phase, suggests that at least part of the zinc is chemisorbed on the metal surface. However, Haissinsky[1] suggested that isotopic exchange occurring between a metal and its ions in solution disorganizes the structure of the superficial lattice planes making them looser and more permeable to a deep penetration by ions of both signs.

The process at the metal/chromate-solution interface does not appear to be simply competitive adsorption and displacement, since some of the zinc that was initially displaced by the chromate actually redeposited on the metal even though there was a large excess of chromate ions in the solution (Fig. 5).

If, as suggested, chromate ions adsorb strongly on the metal surface, there may have been some disruption of the oxide film on the labelled specimens, with zinc passing into the aqueous phase as colloidal zinc oxide, and subsequently redepositing on the metal. Such a process of disruption would be expected to have greater effect if the surface layers of the metal had previously been disorganized as pictured by Haissinsky. Since chromate solution saturated with zinc oxide gave similar results to pure chromate solution the transfer of zinc to the aqueous phase was not due to solubility of zinc oxide. Evans and Davies[5] found that when zinc corroded in distilled water colloidal particles appeared in the solution, and such a process would account for the slow loss (accompanied by some re-deposition) of zinc from labelled specimens immersed in distilled water and salt solutions. When specimens which had been corroding slowly in these solutions for several hours were transferred to chromate

solution, there was a rapid loss of zinc (Fig. 2 and 3), again consistent with a film-disruption hypothesis.

The results with specimens labelled by electrodeposited or evaporated zinc show that the barrier film formed by the reaction of the metal with chromate ions is not sufficiently impermeable to prevent zinc ions leaving the metal and passing into the solution.

When abraded zinc was immersed in stagnant 10^{-4}M ammonium molybdate solution, there was no visible corrosion for about 24hr, while the specimens developed a faint bluish tint, suggesting reduction of the molybdate. Eventually, localized corrosion developed. As indicated in Fig. 3, molybdate ions also caused rapid loss of zinc from the surface, and the temporary protective effect was probably due to strong adsorption of molybdate ions, and resultant film formation. It appears that even the combination of surface-active and oxidizing properties in an inhibitor ion will not necessarily produce long-term protection, and that under the dynamic conditions we have shown to exist at a metal/inhibitor-solution interface, permanent inhibition will not be obtained unless the film formed on the metal has inherently protective properties.

Acknowledgements—This paper is published by permission of the Chief Scientist, Australian Defence Scientific Service, Department of Supply, Melbourne. The work was carried out at the Australian Defence Scientific Service, Defence Standards Laboratories, N.S.W. Branch, Sydney, Australia.

REFERENCES

1. M. Haissinsky, *Proc. 6th Meeting CITCE, Poitiers* 1954, p. 98. Butterworths, London (1955).
2. K. G. McLaren, J. H. Green and A. H. Kingsbury, *Corrosion Sci.* **1**, 161 (1961).
3. C. P. De, *Nature, Lond.* **180**, 803 (1957).
4. H. C. Gatos, *Nature, Lond.* **181**, 1060 (1958).
5. U. R. Evans and D. E. Davies, *J. Chem. Soc.* 2607 (1951).

Corrosion Science, 1961, Vol. 1, p. 177. Pergamon Press Ltd. Printed in Great Britain.

BOOK REVIEW

Elements di Teoria Della Corrosione a Umido dei Materiali Metallici. R. PIONTELLI. 22·5 × 14·5 cm. Pp. xxiii + 452 with 3 plates. 1961. Milano: Longanesi e C. (In Italian.) 3,500 lire.

IN THE first of a series of five monographs on physico-chemical topics Professor Piontelli sets out to present "in a condensed, yet systematic and rigorous form, the ideas and theoretical methods" relating to the subject of aqueous corrosion.

A somewhat extended list of definitions (50 pp.) is followed by a discussion of the theoretical aspects. The chemical processes involved are first considered, after which a comprehensive treatment of the thermodynamics and kinetics of electrochemical systems is given. The author's aim at condensation is not fully realized.

The possible effects of the physical and chemical nature of the metal, its environment and the products of corrosion are then examined with encyclopaedic thoroughness, but the introduction to the use of potential/pH diagrams in this context is disappointing; more practical examples here would have been helful.

A very brief survey of the causes and morphology of non-uniform attack precedes a discussion of the "diagnostic approach" to corrosion problems, in which the examination of specific problems is rationalized.

The final section on prevention and protection is the shortest in the book, and mentions briefly the various alternative methods: cathodic protection is emphasized. The author wisely remarks that the best method of corrosion prevention is enlightened design.

Although this book is not a corrosion text in the conventional sense—the relative weight given to the various sections is at times surprising—the author has produced a fairly rigorous approach to the theory of the subject that should at least convince students of classical thermodynamics that the corrosion phenomena can be referred to physico-chemical laws.

The rough cream paper is not suited to the reproductions of photographs, and the extensive use of manuscript symbols is scarcely less disconcerting than the lack of logical order in the prefatory list of symbols, nor does the abbreviation of the more commonly used terms make reading any easier.

It will be interesting to compare this volume with the later titles of the series.

G. P. ROTHWELL

Corrosion Science, 1961, Vol. 1, p. 178. Pergamon Press Ltd. Printed in Great Britain.

LETTER TO THE EDITOR

SOME OBSERVATIONS ON THE MECHANISM OF STRESS-CORROSION CRACKING

HINES has pointed out[1] that one of the characteristics of stress-corrosion cracking is the relatively small number of commercial metal/electrolyte systems prone to this type of failure. No pure metals have ever been reported as stress-corrosion cracking, in the sense that their rate of corrosion is not enhanced nor its distribution altered by tensile stress. Further, there appears to be no known instances of transgranular stress-corrosion cracking in an environment containing other than chlorides, hydroxides or nitrates. Other anions have indeed appeared to be responsible for cracking, e.g. *monel*[2] has cracked transgranularly in SiF_6^{2-}, but in this and other instances the cracking is probably due to hydrogen embrittlement. Any theory of stress-corrosion cracking must, therefore, according to Hines, explain why this phenomenon is confined to a limited number of alloys and to an even more limited anionic environment.

The continuous crack propagation observed in stress corroding 18–8 steels in chloride electrolytes[3] has been shown to be basically due to the removal of activation overpotential in this material when yielding rapidly.[4,5] Thus, an advancing crack edge is enabled to corrode rapidly (*ca.* 1 A/cm^2) while substantially at the 'reversible' potential.[1,5] Hoar and West have inferred that, for this system at least, cracks can propagate transgranularly because rapid yielding at their advancing edges raises the exchange current density (i_0) to something of the order of 1 A/cm^2. I would suggest that the specificity of the *environment* may well be due to the influence of the anion upon the maximum rate at which the cation exchange reaction can proceed across the electric double layer. Likewise, the susceptibility of only particular *alloys* to stress-corrosion cracking may lie in their ability to support such high exchange currents when yielding rapidly.

It is noteworthy that the more polarizable anions are known to favour high exchange current densities on metals, chloride ion in particular.[6] It is possible that the more highly polarizable the ligands the more readily and rapidly will they deform to allow a metal cation to squeeze into and out of its solvation sheath. The fact that both chloride and hydroxyl ions are highly polarizable, and are responsible for stress-corrosion cracking in a majority of cases, lends support to the "yield-enhanced exchange rate" mechanism for crack propagation. The nitrate ion, which also causes cracking, is not very polarizable, less so than sulphate. It nonetheless leads to high exchange currents on amalgams, e.g. $i_0 > 10^{-1}$ A/cm^2 for Tl and Pb amalgams in KNO_3 as against *ca.* 10^{-4} A/cm^2 for Bi amalgam in $HClO_4$.[7] It is not clear why sulphur, either as S^{2-} or HS^-, is not perhaps the most potent agent for transgranular stress-corrosion cracking, for it is twice as polarizable as chloride.[6] Possibly, although surface-active to the extent of adsorbing into the inner Helmholtz plane,[7] it does not oust water from the *cation* solvation sheath (c.f. Cl^- and OH^-) and so does not sufficiently influence the activation energy for ion transfer.

It has been argued that for transgranular cracking to occur the applied tensile stress must operate so as to produce only *localized* yielding, concentrated at the advancing crack edge.[1] When the metal at such an edge yields rapidly in this way, a most likely result will be a large increase in the number of surface steps formed. In view of the tendency for steps to constitute active sites for anodic dissolution and cathodic deposition,[8] this factor might be expected to increase the exchange current density. Hoar and West[5] have indeed considered the possibility that yielding contributes to a lowering of the activation energy for dissolution but it is difficult to see how the yielding energy may be transferred to a solvating cation, the energies of a surface step and of a dislocation in the bulk being very similar (about 0·1–0·5 eV);[9] it is possible that it is the *excess* free energy which is required to facilitate anodic dissolution by lowering the effective activation energy for dissolution by this amount. However, when the *rate* at which surface steps are formed on rapidly yielding metals ($i \sim 0{\cdot}5$ sec^{-1}) is considered, it may be shown that, if there is concomitanta nodic dissolution at 1 A/cm^2, only metals having a slip separation of *ca.* 0·5 μ or more give rise to a stable system of surface steps. It seems not altogether fortuitous that the separation between contiguous active slip planes in 18–8 is of this order[10] whilst for nickel, for example, it is some 100 Å[11]—and nickel neither stress-corrosion cracks transgranularly nor shows any change in overpotential during yielding.[5] Pure metals all tend to deform by elementary slip, so one may presume that slip steps produced at their dissolving surfaces by yielding are insufficiently long-lived to increase the pre-exponential term contributing to i_0. Pure metals neither contain precipitates of different nobility from the matrix (c.f. $CuAl_2$ in Al-Cu alloys) nor dissolve to form a readily ruptured surface film of more noble constituent (cf. Au films in Cu-Au alloys[12]) and this would explain why they are unable to stress-corrosion crack by any known mechanism.

A coarse slip structure is often associated with low stacking fault energy and it has been suggested by Swann and Nutting[13] that stacking faults, being chemically active, may play an important part in stress-corrosion cracking. There is as yet insufficient evidence to decide whether it is the stacking faults or the coarse slip which is important in the propagation stage.

In the present communication it has been proposed that stress-corrosion cracking in any metal/electrolyte system needs to be considered from the points of view of both metal deformation and ionic solvation. There is a likelihood that the metal structure is also involved, for the electronic configuration of the metal and of its solvated cation at least partly determine the activation energy for the solvation process.[7,14] Thus, the atoms in surface steps formed during yielding may have an unusually low co-ordination and so, if their electron structure (i.e. alloy composition) is favourable, may be able to dissolve anodically with little activation energy.

J. M. West

Department of Metallurgy,
University of Sheffield.

REFERENCES

1. J. G. Hines, *Corros. Sci.* **1**, 21 (1961).
2. H. R. Copson and C. F. Cheng, *Corrosion* **12**, 71 (1956).
3. D. van Rooyen, *Corrosion* **16**, 421 (1960).

4. T. P. HOAR and J. G. HINES, *J. Iron St. Inst.* **182**, 124 (1956).
5. T. P. HOAR and J. M. WEST, submitted to *Proc. Roy. Soc.* (1961).
6. R. PIONTELLI, Proceedings of 2nd Meeting, C.I.T.C.E., Milan (1950), p. 185. Butterworths, London (1951).
7. J. E. B. RANDLES and K. W. SOMERTON, *Trans. Faraday Soc.* **48**, 951 (1952).
8. T. P. HOAR, *Industr. Chim. Belge* **19**, 931 (1954).
9. F. R. N. NABARRO, *Adv. Physics* **1**, 269 (1952).
10. P. B. HIRSCH, P. G. PARTRIDGE and R. L. SEGAL, *Phil. Mag.* **4**, 721 (1959).
11. T. NAGASHIMA and T. YAMAMOTO, *Acta Met.* **4**, 94 (1956).
12. H. GERISCHER and H. RICKERT, *Z. Metallk.* **46**, 681 (1955).
13. P. R. SWANN aqd J. NUTTING, *J. Inst. Met.* **88**, 478 (1960).
14. e.g. E. H. LYONS, Jr., *Trans. Electrochem. Soc.* **101**, 363 (1954).

LETTER TO THE EDITOR

THE EFFECT OF CO-DEPOSITED MATERIAL ON THE CORROSION BEHAVIOUR OF ELECTRODEPOSITS

THE deleterious effect of inclusions on the corrosion resistance of electrodeposited coatings has recently aroused interest as it has been demonstrated that nickel electroplating solutions containing sulphonic acids or sulphonamides as addition agents produce nickel deposits which, compared to deposits produced from a Watts bath, are inferior in their resistance to corrosion. It would appear that these addition agents result in the introduction of sulphur compounds into the deposit which release sulphide ions during corrosion of the deposit with a consequent depolarization of the reaction $Ni \rightleftarrows Ni^{2+}$ aq. In the case of copper electrodeposits previous work has shown that inclusions due to addition agents generally cause an increase in the reactivity of the metal.[1]

In view of the previous work on inclusions, the possibility of introducing corrosion inhibitors into electrodeposits has been investigated using benzotriazole, which is a specific corrosion inhibitor for copper, as an addition agent in a copper sulphate plating solution. The resulting electrodeposits (which, under suitable conditions, are fully-bright, coherent and banded) have been analysed by using the reaction $Ag_2SO_2 + Cu = CuSo_2 + 2Ag$ to dissolve the copper without decomposing the benzotriazole. It has been established that the benzotriazole is not decomposed during cathodic deposition of the copper and is included in the deposit as cuprous benzotriazolate.* The presence of a cuprous complex is probably due to the formation of cuprous ions as an intermediate in the reduction of cupric ions to copper.[2] This appears to be the first example of the deliberate introduction of a known corrosion inhibitor into an electrodeposit although previous workers have described the effect of adsorption inhibitors as addition agents.[3]

Although the present work has demonstrated that a corrosion inhibitor can be introduced into a metal it is apparent that the corrosion resistance of the deposit will not be enhanced unless the inhibitor is released from the complex by the corrosive environment. Thus cuprous benzotriazolate releases benzotriazole only if the hydronium ion concentration is very high; however, release can be achieved below pH_2 if oxidizing substances are present (e.g. oxygen) as the cupric complex is formed transiently.

Further work is clearly necessary but it is possible to suggest certain criteria for selecting corrosion inhibitors which may co-deposit in sufficient quantity to be effective. The inhibitor should form an insoluble compound of the type $M^{(m-n)+}X$, where M^{m+} is the metal ion in the plating solution and $M^{(m-n)+}$ is an intermediate valency state and X is the ligand constituting the inhibitor. If a stable complex is formed with M^{m+} then the inhibitor is likely to be retained in the plating solution. The

* The structural formula of cuprous benzotriazolate does not appear to have been established. However, some preliminary studies of the structure using PH titrations and infra-red spectroscopy indicate that the imido group of benzotriazole does not appear to take any part in the reaction with cuprous ions.

introduction of benzotriazole into a copper deposit is due to the intermediate formation of Cu^{+}aq. during the reduction of Cu^{2+}aq. to copper. This may preclude the introduction of Ni^{+} complexes into nickel deposits as the reduction of Ni^{2+}aq. to nickel probably occurs without an intermediate stage.[4] However, a further possibility of producing a deposit containing an inhibitor would exist if a complex $M^{m+}X$, which is insoluble and pH-dependent, formed only in the diffuse cathode layer where the pH may be significantly higher than that of the bulk plating solution, i.e. in unbuffered solutions where the reduction of metal and hydronium ions can occur simultaneously.

It is essential that the inhibitor is not destroyed at the cathode and it must form a stable insoluble metal complex and co-crystallize at the growing cathode surface. Finally, it should be observed that the inhibitor must be released from the metal complex during the process of corrosion for it to be effective.

Some preliminary corrosion tests on copper deposits in sulphuric amd hydrochloric acids containing oxidizing agents have shown that deposits containing benzotriazole corrode less rapidly than pure copper deposits obtained under similar conditions of electrodeposition.

J. K. PRALL and L. L. SHREIR

Metallurgy Dept. (Corrosion Section),
Battersea College of Technology,
*Battersea Park Road, London, S.W.*11.

REFERENCES

1. E. RAUB, *Z. Metallk.* **39**, 33 (1948).
2. E. MATTSSON and J. O'M. BOCKRIS, *Trans. Faraday Soc.* **55**, 1586 (1959).
   S. B. WATKINS and H. G. DENHAM, *J. Chem. Soc.* **115**, 1276 (1919).
3. J. ELZE, *Gesundheits Ing.* **76**, 193 (1955).
4. J. O'M. BOCKRIS and B. E. CONWAY, *Proc. Roy. Soc.* **A248**, 402 (1958).

EDITOR'S NOTE

PUBLICATION POLICY FOR 1962

THE prolonged time which frequently elapses between submitting a manuscript to a journal and its actual publication can be most frustrating to an author who is naturally anxious to see the results of his scientific efforts in their final form. It is the considered opinion of the editors and publishers of *Corrosion Science* that the publication of scientific work should be regarded as a matter of urgency and that this delay should be reduced to an absolute minimum, consistent with adequate refereeing and editing. To achieve this aim a more flexible publication policy will be adopted in 1962 which should result in the rapid publication of all suitable material submitted to this journal.

Delays in publication may arise from a variety of causes—refereeing, modifications of the original manuscript, printing, etc.—but a major factor is the capacity of a journal to absorb the volume of material accepted for publication.

Although this journal is still in its early stages of development it is apparent from the number and the quality of its papers already submitted for publication that its future as an international organ of Corrosion Science is assured. At the same time it is evident that the present size and quarterly appearance of *Corrosion Science* is hardly conducive to the rapid publication of manuscripts.

With this in mind the publishers have decided that, commencing in 1962, there will be complete flexibility as to the size of each quarterly issue and that all manuscripts that are available will be published in the current Journal. This should reduce delays in publishing to a minimum and it is anticipated that with the full co-operation of authors, referees and editors it should be possible to publish within 3-4 months of receipt of a manuscript.

L.L.S.

CORROSION SCIENCE SOCIETY

THE Third Meeting of the Corrosion Science Society will be held at the Battersea College of Technology, London, S.W.11 on 17–18 April, 1962. Authors who wish to present papers on work in progress and/or others who wish to attend should write to the Honorary Secretaries for further particulars.

T. P. HOAR
L. L. SHREIR
Hon. Secs.

The Editors and Editorial staff of *Corrosion Science* would like to take this opportunity to wish all readers of the Journal—**A Happy New Year.**